Charles University

Faculty of Medicine in Pilsen

Department of Surgery

DISSERTATION

MUDr. Jáchym Rosendorf

Use of Nanomaterials in Fortification of Anastomoses on the Gastrointestinal Tract

Supervisor: Prof. MUDr. Václav Liška, Ph.D.

Discipline: Surgery

2021

Originality Statement

I hereby declare that I have composed this thesis by myself and that the thesis has not been submitted, in whole or in part, in any previous application for a degree. Except where stated otherwise by reference or acknowledgment, the work presented is entirely my own.

Date: 1st March, 2021

Preface

Anastomotic leakage is a feared complication of colorectal surgical procedures, often resulting in a permanent decrease of life quality or even death. The ultimate purpose of this research is to develop an optimal nanofibrous patch for the prevention of colorectal anastomotic leakage.

The idea was born in 2015 when we started a discussion about the possible use of nanofibrous biodegradable materials in modern medicine with visiting researchers from the Faculty of Textile Engineering, Technical University of Liberec. Together, we came up with a concept of a nanofibrous patch for colorectal anastomoses. Knowing that there were many attempts to develop some kind of patch as a barrier protection against anastomotic leakage in the past (usually unsuccessful), we approached the problem differently. Our idea was to develop and produce a material structurally similar to the extracellular matrix, biodegradable, and possibly porous, to serve as a semi-permeable patch. Over the years, we got closer to our desired result, however, there is plenty of work ahead before clinical trials can be planned.

Acknowledgements

I would like to express gratitude to everyone who contributed to the following work. I am grateful to my supervisor in the first place, Prof. MUDr. Václav Liška, Ph.D. for his guidance through my both pregraduate and postgraduate education, valuable advice, and continuous support. I am grateful for support from my consulting tutor Prof. MUDr. Mgr. Zbyněk Tonar, Ph.D. whose experience was crucial for our research. My thanks belong to MVDr. Lenka Červenková for her enormous contribution to the work – mainly hours of histological evaluations and many consultations over the experimental design of our projects. My sincere gratitude belongs also to Ing. Petr Hošek, Ph.D., who provided me with critical revisions of all my manuscripts, and detail statistical evaluations for all parts of the project. I would also like to thank all my colleagues and medical students who helped during the surgical procedures and postoperative care, for they spent many hours in the theatre of the Biomedical Center taking care of the experimental animals, namely: Lukáš Bednář, MUDr. Tomáš Kříž, MUDr. Martin Dolanský, MUDr. Václav Tégl, Bc. Ondřej Brzoň, Jan Ševčík, Sima Šarčevič, Mojmír Bohanes, Lucie Kepková, Alexey Razumnyi, and especially to Mgr. Vladislava Mlejnková-Dvořáková and to Renata Michálková. My special thanks belong to MUDr. Richard Pálek, my close friend and colleague whose help and friendship I treasure. He participated mainly in surgical procedures and perioperative care during the project. The whole project could not be realized without the team from the Technical University of Liberec, Faculty of Textile Engineering, who produced (in cooperation with our team) and tested *in vitro* the nanofibrous materials used in the following experiments. Namely, my thanks belong to RNDr. Jana Horáková, Ph.D., Ing. Markéta Klíčová, Ing. Andrea Klápšťová, Prof. RNDr. David Lukáš, CSc., and Ing. Jiří Chvojka, Ph.D. Last but not least I am grateful for the opportunity to combine clinical work and the time demanding experimental research, provided to me by Prof. MUDr. Vladislav Třeška, DrSc., the head of the Department of Surgery, University Hospital in Pilsen and the guarantor of the program of study. Finally, I would like to thank my parents, my wife and my friends. It wouldn't be possible for me to complete my study without their encouragement and support.

Work with animals statement

All experimental procedures concerning the pigs were described in a protocol approved by the Commission of Work with Experimental Animals at the Faculty of Medicine in Pilsen, Charles University, and supervised by the Ministry of Education, Youth and Sports of the Czech Republic (project code: MSMT-26570/2017-2, and MSMT-30685/2019-3). All procedures were performed in compliance with the law of the Czech Republic and with the legislation of the European Union.

Abstract

Background: The main focus of the dissertation is the use of nanofibrous biodegradable materials for healing support of intestinal anastomoses in colorectal surgery. Altered healing process of an intestinal anastomosis leads to several types of local complications. Anastomotic leakage is one of the most feared ones. Severe anastomotic leakage causes peritonitis, sepsis and is a life threatening condition. Reoperation is necessary in many cases, bringing the need for intensive care, and hospital stay prolongation. Extensive peritoneal adhesions are another source of postoperative complications. These adhesions are a frequent cause of bowel obstruction and abdominal discomfort, and are the most common reason for readmission after colorectal procedures. Nanofibrous biodegradable materials showed positive effects on healing process in various locations. Our aim was to develop and perfect a biodegradable patch for both prevention of anastomotic leakage and formation of extensive peritoneal adhesions. **Methods:** We conducted 3 subsequential experiments on porcine models. In Experiment A, we managed to develop polycaprolactone and polylactic acid-polycaprolactone copolymer nanofibrous patches and applied them on anastomoses on the small porcine intestine. The animals were observed for 3 weeks. Clinical, biochemical and macroscopic signs of anastomotic leakage or intestinal obstruction were monitored, the quality of the scar tissue was assessed histologically, and a newly developed scoring system was employed to evaluate the presence of adhesions. In Experiment B, newly developed double-layered polyvinyl-alcohol/polycaprolactone patches were tested on a model of defective anastomosis on the small porcine intestine under similar conditions. Newly invented Intestine Wall Integrity Score was used to determine the quality of intestinal wall at the site of anastomosis. In Experiment C, a perfected ultrafine polycaprolactone highly porous patch was used in a model of defective anastomosis on the porcine colon under similar conditions. Experimental groups had nanofibrous patches applied over the anastomosis while Control groups had the anastomoses uncovered in each experiment. **Results:** Experiment A showed no adverse effects of the two materials. However, no positive effects on the healing process or risk of anastomotic leakage development were observed. The application of both versions of double-layered materials in Experiment B resulted in inferior healing. The application of the perfected polycaprolactone patch in Experiment C showed no adverse effects on both clinical status and histological results of the experimental animals. Higher amounts of collagen were found at the site of anastomosis in the Experimental group. **Conclusion:** Five versions of nanofibrous biodegradable patches were developed and tested on three different models of porcine intestinal anastomoses. The ultrafine polycaprolactone patch from Experiment C does not cause extensive formation of peritoneal adhesions and increases collagen levels at the site of anastomosis, which suggests higher mechanical strength. However, no direct evidence regarding the impact of these materials on the risk of anastomotic leakage was obtained. A perfected version of the polycaprolactone patch with additional antimicrobial activity was already developed and is currently being tested in vitro. A series of preclinical studies will be necessary before introduction into human medicine.

Key words: Anastomotic leakage, Colorectal surgery, Nanofibrous materials, Polycaprolactone, Animal experiment

Table of Contents

List of Abbreviations

AL – Anastomotic Leakage
ASCRS – American Society of Colon and Rectal Surgeons
COX – Cyclo-oxygenase
CT – Computed Tomography
GI – Gastro-intestinal
ERAS – Enhanced Recovery After Surgery
ESCP – European Society of Coloproctology
ESSO – European Society of Surgical Oncology
IL-6 – Interleukin 6
IWIS – Intestinal wall integrity score
MITs – Minimally invasive techniques
MMPs – Matrix metalloproteinases
PA – Peritoneal adhesion
PAAS – Perianastomotic adhesions amount score
PAI-1 – Plasminogen activator inhibitor-1
PCL – Polycaprolactone
PLCL – Polycaprolactone-polylactic acid copolymer
POD – Postoperative day
PSR – Picrosirius red
PVA – Polyvinyl alcohol
SEM – Scanning electron microscopy
SEME – Standard error of mean
TGF-β1 – Transforming growth factor-β1
TIMPs – Tissue inhibitors of metalloproteinases
TNF-α – Tumor necrosis factor α
tPA – Tissue plasminogen activator
VEGF – Vascular endothelial growth factor
vWF – von Willebrandt Factor

1 Theoretical introduction

1.1 Opening notes for anatomical introduction

The anatomical descriptions with a few notes on physiology serve only for basic explanation of the problematics discussed later in the text. There is no doubt that the anatomy, physiology and histology of the gastrointestinal tract are much more thoroughly depicted in dedicated textbooks and atlases (1–3).

1.2 Anatomy and physiology of the small intestine

The small intestine (small bowel) is the longest part of the gastrointestinal tract. It follows after the stomach as a relatively thinner tube. It is responsible for fission and extraction of nutrients from a liquid chyme. Proper intestinal function is essential for normal digestion. The small intestine consists of three main parts: the duodenum, the jejunum, and the ileum (1,4). All these parts share common anatomical signs. They are all hollow tubular organs with typical wall layers in different local variations serving different purposes.

The inner layer of the small intestine is the tunica mucosa, which is lined by cylindrical epithelium (enterocytes) with various amount of goblet cells (producing protective mucus) located on a layer of mucosal connective tissue (lamina propria mucosae) and on a fine muscular layer (lamina muscularis mucosae). The mucosa forms circular folds called plicae circulares. These can be seen mainly in the duodenum and the jejunum and they gradually disappear in the aboral direction. The inner surface of the small intestine is increased by the presence of intestinal villi, which are 0.3–1 mm tall finger-like structures lined by the epithelium. Thanks to these structural modifications, the real functional surface of the small intestine reaches up to about seven square meters. One or two little arterioles enter each of the villi and finally branch into a capillary network (rete). The venous blood is then drained via villar vein, which is usually situated centrally in the villus. Along the blood vein, a lymphatic vessel (or vessels) can be found. While the venous blood is rich in saccharides

and proteins absorbed from the luminal contents, the lymphatic drainage collects mostly fatty substances and their degradation products. A more intensive contact of the villi with the luminal contents of the small intestine is mediated by solitary smooth muscle cells in the connective tissue of the villi. Their activity produces small movements resulting in more effective absorption. Intestinal glands (glandulae intestinales) are fine tubular glands in between the villi. They were assumed to produce metabolic enzymes, but this theory actually proved wrong. They are lined by various cell types, like non-differentiated stem cells. Those are responsible for renewal of the epithelial population as the mature enterocytes do not possess a mitotic ability under normal conditions. There is also a variety of endocrine cells with either endocrine or paracrine activity. The lamina propria mucosae contains lymphatic tissue, which grows richer in the aboral direction. Both solitary lymphatic nodes and aggregated lymphatic nodes can be found there. The lamina muscularis outlines the mucosal layer and creates a thin border between the mucosa and the submucosa. Tunica submucosa is a layer of collagenous connective tissue outwards from the tunica mucosa. It is relatively less dense than the mucosal connective tissue and it contains the submucosal nervous plexus (plexus Meissneri)(2). The muscular layer, tunica muscularis, contains smooth muscle tissue in the abdominal parts of the gastrointestinal tract. It usually has two basic layers: the inner circular one (stratum circular), which forms sphincters in some anatomic locations, and the outer longitudinal layer (stratum longitudinale). The muscular layer is highly variable in terms of thickness and other local adjustments. The activity of the small intestine results in peristaltic moves, segmentation moves and swaying moves (elongations and contractions). The innervation of the muscular layer is provided by the myenteric nervous plexus (plexus Auerbachi)(2).

In the abdominal segments, the outer layer of the gastrointestinal tract is formed by either the serosa (tunica serosa, visceral peritoneum), which is a single layer of mesothelium located on subserosal connective tissues, or the adventicia (tunica adventicia), a layer of connective tissue lining the gastrointestinal tract in its extraperitoneal locations (2,5).

The duodenum is the shortest part of the three segments and it differs from the rest in its origin as it derives from both the embryonic foregut and the midgut. It is a short C-shaped tube located on the rear abdominal wall, most of which is located retroperitoneally, surrounding the head of the pancreas. It lacks a regular mesentery and it is therefore the least mobile part of the small intestine. The meaning of the name duodenum is twelve inches, referring to its length. It is not only the shortest, but also the widest segment (in physiological situations). Its oral segment (D1) starts in the midline at the level of the first lumbar vertebra and is covered with the visceral peritoneum, the descending part (D2) runs retroperitoneally right to the second lumbar vertebra in caudal direction and then back to the midline as the horizontal segment (D3) and finally the duodenum goes cranially as the last ascending segment (D4). This C-shaped structure perfectly surrounds not only the head of the pancreas, but also many other important structures. The duodenum itself is connected to the biliary system and the pancreatic duct. It has a very close relation to the coeliac trunk and its branches, superior mesenteric artery and vein – structures, which are all of vital importance. Any surgical intervention in the region can be therefore technically very demanding. Important structures on the luminal side of the duodenum are: The major duodenal papilla (papilla duodeni major seu Vateri), which is an orifice of the pancreatic duct and the bile duct, and the minor duodenal papilla (papilla duodeni minor se Santorini), which is a non-consistent orifice of the accessory pancreatic duct. Both of these are situated on the longitudinal duodenal fold, which is a mucosal fold in the D2.

The duodenal mucosa is covered with villi that are relatively flat compared to the rest of the small intestine but are developed in higher density. Another specific mucosal structures for the duodenum are the duodenal glands (glandulae duodenales), which are relatively large compared to the rest of the small intestine and branched; these reach from the mucosa to the submucosal tissue and fill the submucosal layer almost completely. They produce alkaline mucus important for the proper function of pancreatic enzymes. Arterial blood comes to the duodenum mainly via the superior and the inferior pancreaticoduodenal arteries. Venous blood is drained into the portal vein via superior and inferior pancreaticoduodenal veins and through the superior mesenteric artery. The lymphatic drainage of the duodenum

starts on the periphery as fine lymphatic veins in the sinuses of the duodenal villi forming nets that spread through the mucosal and submucosal connective tissue. Collecting lymphatic veins drain these into the regional lymphatic nodes, which are: nodi coeliaci, nodi pylorici and nodi hepatici (draining the oral parts of the duodenum), and nodi mesenterici superiores (draining the aboral segments). The innervation of the duodenum is both sympathetic and parasympathetic and it forms an autonomous nerve plexus in the intestinal wall. The parasympathetic nerves come from the nervus vagus to both the coeliac ganglion and to the intestinal wall itself, and create the plexus submucosus and plexus myentericus. The sympathetic nerves run along the arteries from ganglion coeliac and ganglion mesentericum superius as plexus coeliacus and plexus mesentericus superior. These are responsible both for the motility and secretory activity of the duodenum.

The jejunum and the ileum follow after the duodenum at the duodeno-jejunal junction as a 3–5 m long tube. Each of them has its characteristic properties that differ, but these properties change gradually in the aboral direction without any specific border. Therefore, these two parts of the gastrointestinal tract are also called the jejunoileum as a single structure. Compared to the duodenum, the jejunoileum is much more mobile. It is attached to the rear abdominal wall via mesentery which is a 5–15 cm wide (varying according to the location) peritoneal duplicature containing fatty tissue with blood vessels and lymphatic tissue supplying the intestine. The mesentery enables easy intestinal movements. The jejunum is considerably wider (3 cm outer diameter) than the ileum (2.5 cm outer diameter). The density and size of the plicae circulares decreases aborally throughout the small intestine. The amount of the lymphatic tissue in the intestinal wall grows higher in the same direction.

The vessels in the mesentery form many mutual connections (so-called arcades) and finally enter the intestinal wall as aa. rectae. The arterial arcades can be found in one or two rows in the jejunum, but they form two or three rows in the ileum. The blood supply is generally richer in the jejunum making its mucosa appear pinker. The blood supply of the jejunoileum comes through the superior mesenteric artery as arteriae jejunales and ileales (12 to 16 branches usually). The artery dedicated to the ileocecal junction is the ileocolic artery. The venous blood is collected by veins of the same anatomical names

drained respectively to the location into the superior mesenteric vein and into the portal vein afterwards. The lymphatic drainage of the jejunoileum forms mucosal and submucosal nets. The lymph is collected through lymphatic veins in the mesentery to the superior mesenteric nodes in several rows (nodi mesenterici superiores intestinales, intermediaries, and centrales), and to the celiac nodes.

Parasympathetic innervation of the jejunoileum comes from the vagus nerve. The sympathetic nerve fibers enter the celiac ganglion and superior mesenteric ganglion as splanchnic nerves (nervi splanchnici). These form nerve nets accompanying the arterial blood supply. The myenteric nerve plexus (plexus Auerbachi) regulates the motility of the intestine while the submucosal plexus Meissneri regulates mostly the activity of mucosal glands. Sensitive innervation is present as well, even though only a little information is sensed consciously (1,3,4).

1.3 Anatomy and physiology of the large intestine

The large intestine is a 1.3–1.7 m long tubular organ. It differs from the small intestine on many levels. It is a terminal part of the gastrointestinal tract and it plays an important role in many processes. It receives liquid chyme from the small intestine and contributes to the production of stool by absorbing water and minerals. Therefore, it is partially responsible for electrolyte and water regulation. The function of controllable stool disposal is important for good quality of life (1,4,6). The large intestine comprises the colon (the cecum and cecal appendix, the ascending colon, the hepatic flexure, the transverse colon, the lienal flexure, the descending colon, the sigmoid colon) and the rectum (1). Knowledge of the anatomy of the colonic blood supply and its variations and limitations is a key basis to understanding colorectal resections and colorectal surgical procedures in general (7). Sufficient blood supply is critical for vitality of the intestine and for healing of an intestinal anastomosis (8). The colonic arteries are followed by both veins and lymphatic drainage, these must be respected carefully especially when performing oncological resections (9).

The wall of the colon consists of four main layers characteristic for the gastrointestinal tract as well as for the wall of the small intestine. The mucosa is relatively pale and it lacks villi, in contrast to the small intestine. The dominant cell type is colonocytes. The mucosa contains many intestinal glands and Lieberkühn crypts. The cell types of the mucosa are similar to the small intestine. The colonic enterocytes (colonocytes) have smaller microvilli, which contain microscopic granules with A type immunoglobulins specific against the luminal microflora. Lamina propria mucosae contains lymphatic tissue in a form of solitary lymphatic nodules. The cecal appendix (the appendix vermiformis) is exceptionally rich with lymphatic tissue. Lamina muscularis is thicker compared to the small intestine. It comprises both circular and longitudinal smooth muscle fibers. The submucosa consists of connective tissue and is known for its high content of collagen. It is the most mechanically strong layer. Therefore, it is considered very important in construction of intestinal anastomoses in colorectal surgery (10). The muscle layer is represented by the circular fibers and longitudinal fibers of smooth muscle which are distributed only in three longitudinal

stripes called taeniae (10). They are responsible for bowel movements and for the mechanical strength of the intestine as well. The taeniae disappear in the sigmoideo-rectal junction and the longitudinal muscle fibers are distributed through the whole circumference (1,4). The visceral peritoneum is a smooth tissue lining the intestinal surface. It consists of a layer of simple squamous mesothelial cells covering the base membrane and of underlying extracellular matrix (2,4). The peritoneum does not cover the whole intestinal surface. Parts of the colon are attached to the abdominal wall directly and the rectum runs from the abdominal cavity and loses its peritoneal cover (1,4).

The blood is delivered to the colon through both the superior and the inferior mesenteric arteries and is specified according to the anatomical location further in the text. The ileocolic artery delivers blood mainly to the cecum, the right colic artery supplies the ascending colon up to the hepatic flexure. The middle colic artery delivers blood to the transverse colon. All these three vessels originate from the superior mesenteric artery and are connected via Haller's anastomosis to the vessels originating from the inferior mesenteric artery. The left colic artery delivers blood to the descending colon, and usually several sigmoid arteries supply the sigmoid colon. The last artery for the gastrointestinal tract coming from the inferior mesenteric artery is the superior rectal artery. The middle rectal artery and the lower rectal artery originate from iliac vessels (1,4). Venous drainage follows the arterial blood supply and the blood is drained to the portal system except for the lower rectum, which is connected to the caval system (1,4).

The cecum is the widest segment of the large intestine (usually 7–10 cm). It is situated in the right lower quadrant of the abdominal cavity. It spreads both caudally (where it ends blindly - therefore the name cecum, coming from latin "*caecum*" = blind) and cranially (where it continues as the ascending colon). It follows after the terminal ileum intestine at the ileocecal orifice. The ileocecal valve protects the small intestine against a possible reflux of bacteria-rich colonic content (1,4). The cecal appendix is a finger-like structure of variable dimensions protruding from cecum's caudal end. The role of the appendix is considered to be rudimentary, but recent studies show that it might have immune potential (11,12). The cecum has a variable level of mobility as it is partially attached directly to the rear abdominal wall

and a variable mesocecum can be found caudally. The blood supply is ensured by the ileocecal artery and its branch appendicular artery. These share the names with the venous drainage. The lymphatic drainage follows the blood vessels. We can find prececal nodes, retrocecal, appendicular and paracolic nodes, which are all drained into ileocecal lymph nodes (1,4).

The ascending colon spreads from the cecum cranially along the right side of the abdominal wall till the visceral surface of the liver, where it bends medially as the hepatic flexure. The ascending colon sits directly on the rear abdominal wall with very limited or no mesocolon. It has a smaller diameter than the cecum. The luminal contents are usually still mechanically similar to those of the small intestine but they get thicker as they move aborally. The arterial blood comes to the ascending colon from the superior mesenteric artery via the right colic artery, the venous drainage to the portal vein is ensured by the right colic vein. The lymphatic drainage follows the blood vessels through right colic nodes (1,4).

The transverse colon follows after the ascending colon after the hepatic flexure. It spreads from the right subhepatic area to the left upper abdominal quadrant just caudally to the spleen (splenic flexure) where it turns caudally again. It has a well-developed mesocolon (15–16 cm long in the midline) making it mobile. It is also attached to the large curvature of the stomach by the gastrocolic ligament, which is a part of the large omentum. The transverse colon is 50–60 cm long, which is double the diameter of the abdominal cavity. The atrial blood comes to the transverse colon mainly through the middle colic artery and its branches, the venous drainage is provided by the middle colic vein as the most aboral segment of the large intestine supplied from the superior mesenteric artery. The blood comes to the splenic flexure also via Haller's anastomosis from the left colic artery, which is a branch of the inferior mesenteric artery (Griffith’s point) (13). The colon is the most peripheral tissue at this point, so it is at the highest risk of malperfusion when the blood circulation is compromised (so-called watershed area). The parasympathetic innervation of the transverse colon, the ascending colon and cecum is provided by the vagus nerve till the distal third of the transverse colon, which is the most aboral part of the gastrointestinal tract innerved by the vagus nerve (Cannon’s point). The lymphatic drainage follows the blood vessels, we can

identify medial colic nodes, which collect the lymph from the oral two thirds of the transverse colon. The aboral end is drained through the left colic nodes (1,4).

The descending colon follows the splenic flexure caudally and runs along the left side of the abdominal cavity to the pelvis where it continues as the sigmoid colon. The descending colon is firmly attached to the abdominal wall with no mesocolon. The luminal contents are rich in microbes and already form thicker pastes in this segment (1,3,4).

The sigmoid colon is an S-shaped tube with relatively long mesocolon, the mesocolon sigmoideum. However, its total length and overall shape is inter-individually variable. The space under this part of mesocolon is called recessus intersigmoideus. It turns from the left abdominal wall to the midline and it runs in front of the sacral bone to the small pelvis where it continues as rectum. It can be either shorter and only slightly curved or long, reaching with its curve across the pelvis to the right side of the abdominal cavity. On its way to the pelvis, the sigmoid colon crosses several important structures, which must be paid attention to during surgical interventions. These are mainly the left common iliac artery, left common iliac vein, and left ureter (1,4). The arterial blood comes to the sigmoid colon via several (usually 2–4) sigmoidal arteries, which branch from the inferior mesenteric artery. There is a second point critical for the blood supply located in the rectosigmoid junction called the Sudeck's point, where the terminal sigmoid artery anastomoses with the superior rectal artery. This junction is, however, often not present. Venous blood is drained to the portal vein through the inferior mesenteric vein via sigmoid veins. The lymphatic drainage goes through sigmoid lymph nodes.

The rectum is the final segment of the gastrointestinal tract. It is 12–16 cm long. The anus is its external orifice. The boundary between the sigmoid colon and the rectum is not well defined. A clinically accepted definition of the border is the point of disappearance of taeniae in the distal sigmoid colon. The rectum is covered with peritoneum only on the superior intraperitoneal part, retroperitoneal cover of the rectum is formed by a layer of connective tissue called rectal fascia just at the point of Kohlrausch rectal valve (mentioned later in the text). The rectum has two main parts, the rectal ampulla and the anal canal. The aborally situated anal canal is narrower than the rectal ampulla, longitudinally oriented

mucosal folds can be found on its inner surface. Among other intraluminal structures, we identify three thick transverse mucosal folds (the middle one is called the Kohlrausch valve), which shape the rectum to its typical double curved shape. The arterial blood supply originates from the internal iliac artery via medial and inferior rectal artery, while the venous blood is rained via rectal venous plexus to the caval vein. There are, however, many junctions with the portal venous drainage.

The musculature of the rectum is richly formed. The circular muscle layer forms a typical sphincter structure at the aboral end called internal anal sphincter, which secures the regulatory functions of stool disposal. The internal sphincter is a smooth-muscle-based sphincter and is therefore regulated autonomously. The conscious-mind-controlled stool disposal function is secured by the external sphincter, which is derived from the muscles of the pelvic floor. The innervation comes from the pudendal nerve and straight from the sacral nervous plexus. The pelvic floor or pelvic diaphragm is a complex muscular structure securing stable position of the rectum and other pelvic organs as well as preventing fecal continence (1,4).

As written in the beginning, it is beyond the scope of this work to describe the anatomy and function of the pelvic floor.

1.4 Comparative anatomy human-versus-pig, necessary considerations in experimental conditions

Despite some differences in the anatomy, pigs (*Sus scrofa domestica*) are often used as surgical models or as models of human diseases. The small intestine of the pig shares similar anatomy to that of the human body. It begins as the duodenum, which is located partially retroperitoneally and is surrounded by the annular pancreas (Figure 1), after which it continues as the jejunoileum.

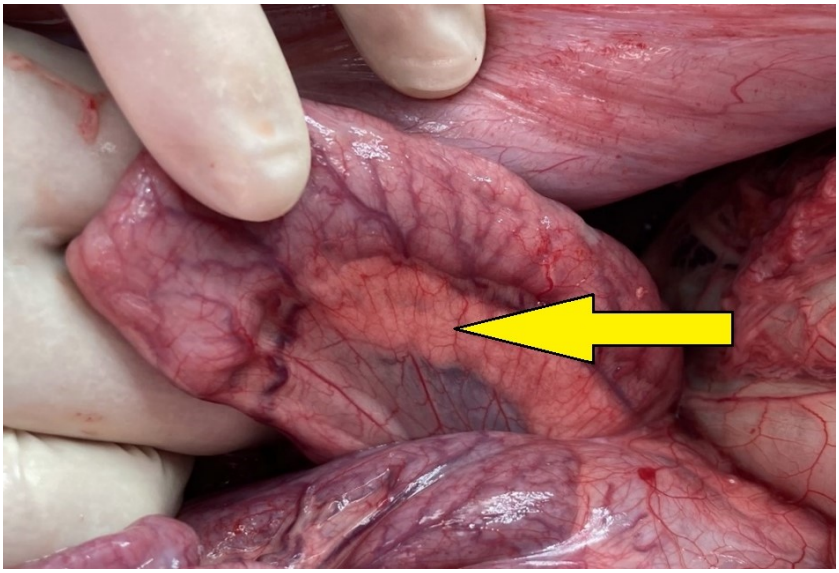

Figure 1: *The annular pancreas, the pancreatic tissue (arrow) follows the duodenum and the oral part of the jejunum situated in its mesentery, Sus scrofa domestica*

The jejunoileum lays in the peritoneal cavity, connected via the mesentery and the mesenterial radix to the rear abdominal wall. The terminal ileum enters the cecum in the right lower abdominal quadrant. The mesentery contains many relatively large lymph nodes (Figure 2). The superior mesenteric artery is the dominant blood supply for the small and the large intestine. There are no arterial arcades on the mesentery of the small intestine (Figure 3). The structure of the porcine small intestine as well as the length (in ratio to body weight) are comparable to the human small intestine. Epithelial cell population is also similar

to that of the human intestine. Unlike rodent intestinal villi, which have a leaf-like shape, the porcine ones have similar structure to the human ones (which are finger-shaped) (14).

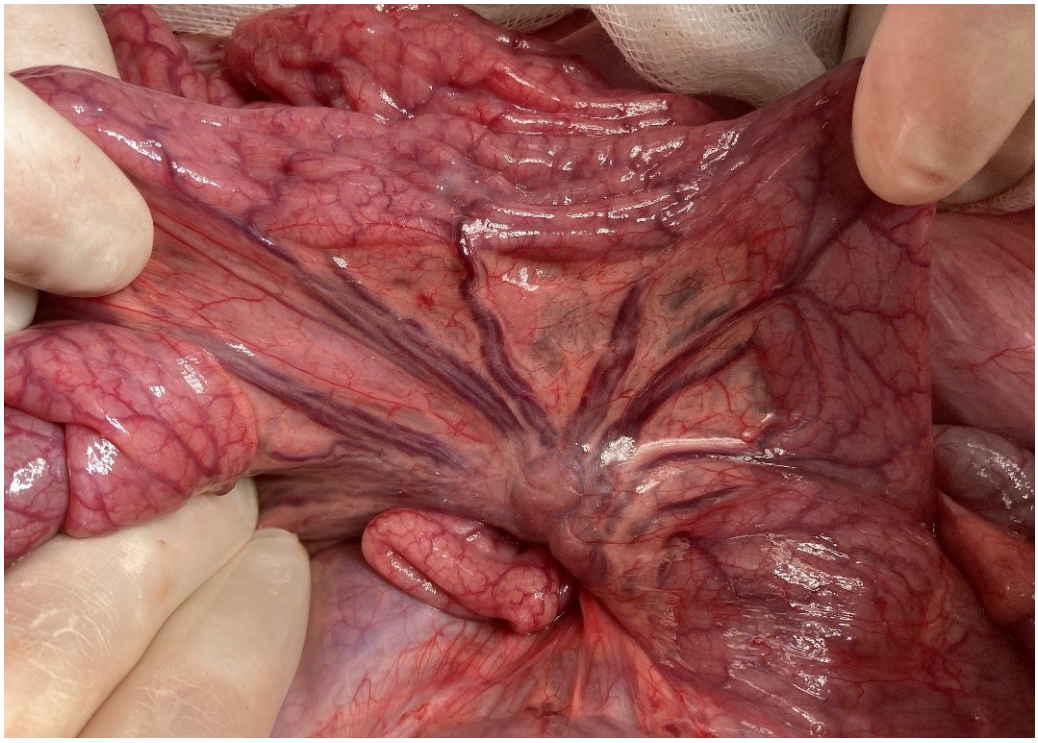

Figure 2: Oral segment of the jejunum, large lymphatic nodes in the mesentery, Sus scrofa domestica

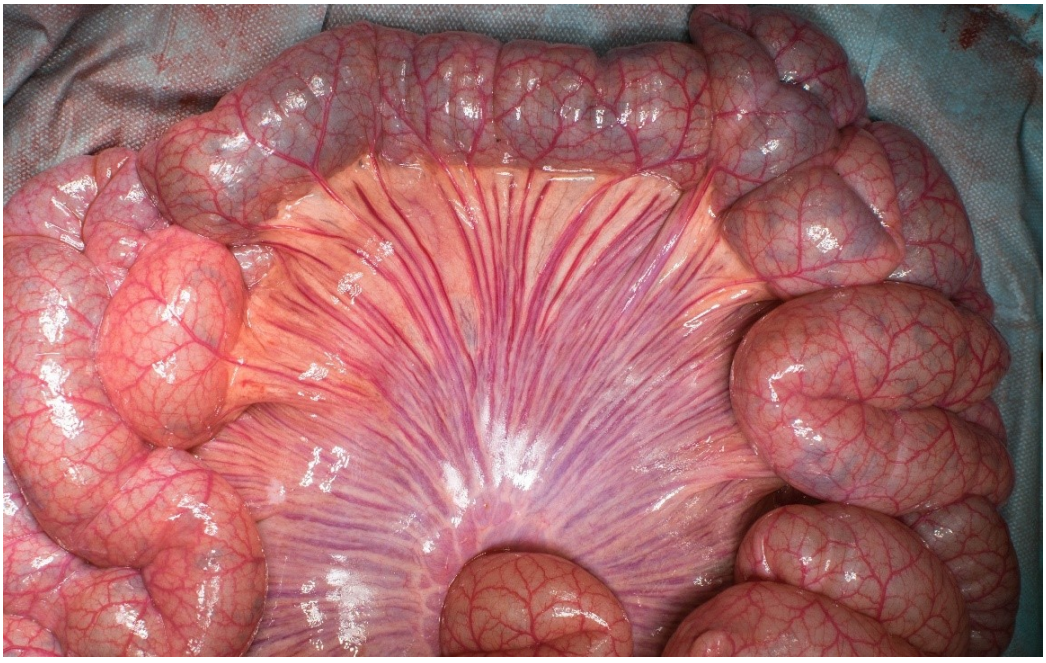

Figure 3: No arterial arcades in the mesentery of the jejunoileum, Sus scrofa domestica

The large intestine has similar morphology to the human one, yet its anatomy differs. The cecum has no appendix and has a larger diameter (relatively to the body weight). It continues as a spiral colon, which is a long, coiled segment of the large intestine with seashell-like appearance, where only the antimesenteric half of the colon is visible and the rest of the colonic tube and the mesocolon with its blood supply are hidden between the coils (Figure 4). However, the length of the colon is relatively similar to the human colon (relatively to the body weight) so the digestion times are similar as well. The microbiome of the porcine colon is significantly more similar to the human colon microbiome than the colonic microbiome of rodents. While pigs have a very similar spectrum of intestinal microbial species (15) to humans, rodents differ in about 85% of them (16). Pang et al. even performed transplantations of human gut microbiota to the colon of germ-free pigs with perfect tolerance and well-established human-like colonic flora (15).

Figure 4: The spiral colon, Sus scrofa domestica

The final segment of the colon continues as a descending colon with a short mesocolon running caudally in the midline into the pelvis as the rectum.

Because of the differences written above, it is therefore possible to create experimental models of anastomotic healing relevant to humane medicine only in the location of the free small intestine and on the descending colon and the rectum. However, the rectum lacks the typical three valves and the pelvic floor has a different anatomy.

Nevertheless, despite these differences, pigs serve as a good model for training of surgical procedures, endoscopic techniques and development of new approaches in general. The rapid development of general surgery in the 20th century was enabled (besides other factors) also by the existence of animal models. Many procedures that are currently routine in human medicine were developed using porcine experimental models. Even though the position of experimental surgery is less obvious nowadays than it was in the previous century, it is still an important preclinical step for introduction of new approaches and techniques.

1.5 Introduction to colorectal surgery

Colorectal surgery is one of the key specializations in visceral surgery dealing with disorders of the colon, rectum and anus. The variety of conditions treated by surgical approach is rather wide in this anatomical region. Many diseases of the colon and rectum can be treated conservatively. However, surgery is the first-choice treatment option for many conditions (tumors, injuries, ischemia, obstruction etc.) (17).

Surgical procedures on the gastrointestinal tract and especially on the large intestine were very limited for up until the 20th century. Even though the basic surgical techniques were developed at the beginning of the 19th century, only further development of perioperative care and invention of antibiotics etc. could transform colorectal surgical procedures into such routine state as it is nowadays (18). Similarly to other specializations, the standards of care and treatment guidelines in colorectal surgery are being continuously perfected by professional international organizations and societies such as the American Society for Surgery of Colon and Rectum, European Society of Coloproctology and others, and the recommendations given by these societies are evidence-based.

As the topic of the thesis are complications of colorectal anastomoses, the following text will mainly focus on anastomoses in colorectal surgery. Such anastomosis (a connection of two hollow viscera) is constructed either between the small intestine and colon, or between two parts of colon, between colon and rectum or the small intestine and rectum. The spectrum of techniques and approaches is broad.

1.5.1 Technique of colorectal anastomosis

Many different approaches to constructing an anastomosis on the large intestine have been invented in the past. Various materials and techniques were experimented with in an attempt to decrease the rate of postoperative complications. Many modalities survived till today as we lack enough evidence-based information. Even though a systematic review has been conducted by J. C. Slieker et al. (19) in order to establish a superior technique, only low-level evidence answers were found for most of the aspects in question. Hand-sutured and stapled

anastomoses are the two main approaches we can distinguish. Suture-less techniques, using for example magnetic rings or tissue glues, were developed lately, but they are not used in standard clinical practice. Some of these alternative methods appear safe, though.

1.5.1.1 Hand-sutured anastomosis

A hand-sutured construction is the oldest widely accepted approach. It belongs to the basic skills of both colorectal and visceral surgeons. We can find many modifications of the procedure. There are several rules that are believed to be important for a well-constructed anastomosis, like absence of axial rotation of the two ends of the intestine, preserved blood supply, no tension between the two parts of the intestine, no visible defects in the suture line. Evidence-based data exists for only a few of the many recommendations that are routinely taught. Such construction can vary in many properties.

a) Suture materials: Multiple suture materials were used for sutured anastomosis throughout the 20th century. Only a few of them remain in clinical practice nowadays. Absorbable suture materials performed superior to non-absorbable ones in several studies (19,20). Yet the anastomotic strength can be compromised when the material is resorbing too rapidly (20). Today, most anastomoses on the gastrointestinal tract are sutured with a suture material made of either polydioxanone or a copolymer of glycolide and epsilon-caprolactone (21,22). Monofilament suture lines perform better in comparison with polyfilament ones in terms of infectious complications (19,23). We can probably expect new materials to appear on the market thanks to biochemical research focusing on clinical use of new biocompatible substances. Among today's commonly used bioresorbable suture materials we can find Polydioxanone, Polyglactin 910 and Poliglecaprone 25. Poliglecaprone 25 is the most frequently used one in gastrointestinal surgery. It is a copolymer of epsilon-caprolactone and glycolide. It is usually fabricated into monofilament, violet-dyed fibers for use in visceral surgery, which are in some versions coated with antibacterial substances for prevention of infections. These materials are hypoallergenic and are usually well tolerated,

their absorption times differ according to the type of material and fiber thickness. Declared absorption time of poliglecaprone 25 fiber is between 60 and 90 days.

b) Single vs. double-layer anastomosis: A double-layer technique has been invented in the early 19th century by A. Lembert (24) and modified by his successors. It was considered the only safe technique through the rest of the 19th and a part of the 20th century. Nowadays, we have a high-level evidence showing that the single-layer anastomosis performs as well in terms of anastomotic complication rate. The single-layer technique is therefore preferred as a simpler and faster method (19). A multiple-layer anastomosis seems to be obsolete as the lumen of the intestine gets smaller with each additional layer.

c) Continuous vs. interrupted suture: A continuous suture is preferred by most surgeons over interrupted sutures for colorectal anastomosis as it is less time consuming and technically easier to perform. Yet again, any high-level evidence for the superiority of continuous suture is missing (19).

d) Depth of bite: Despite the lack of evidence, extramucosal suture is preferred by most surgeons as the mucosa produces mucus and is therefore believed to interfere with the healing process when taken into the suture. Thusly, the tendency is to create a mucosa-inverting suture (25).

e) Configuration of anastomosis: There is no evidence of a superiority of either end-to-end, side-to-side or end-to-side anastomosis on the colon (19). Each configuration is indicated depending on the type of surgical procedure, therefore there are no comparable patients. The blood supply on the site of anastomosis proved to be of the same quality in different settings in a study of microcirculation by M. Sailer et al. (26). Yet the end-to-end anastomosis is generally considered the most physiological and is favorable when possible.

f) Other criteria: There are plenty of other criteria that can be considered when constructing an anastomosis. For example the distance between two suture steps can be changed, various

amounts of tissue can be taken to the suture, and suture tension can vary. There are many hypotheses surrounding these questions, but no conclusion can be made on the basis of the available evidence (19).

1.5.1.2 Stapled colorectal anastomosis

Even though the idea of automatic mechanical devices for suturing is much older and several prototypes were developed hundreds of years ago, stapled anastomoses were introduced to the routine practice of clinical surgery in 1980s. They proved to be safe and comfortable to construct. No strict indications dictate whether to use stapler or construct a hand-sewn anastomosis, except for the low rectal anastomosis where the stapled anastomosis is obviously less technically challenging. A standard procedure mainly for aboral anastomoses on the large intestine is the so-called double stapling using circular stapler applied transanally. Straight staplers are used for anastomoses on the small intestine. Meta-analyses and systematic reviews indicate equal results to hand-sewn anastomoses (27).

1.5.2 Anastomotic healing

Wound healing is a complicated process, which can result in successfully healed wounds in optimal conditions (28,29). Skin wound healing is probably the most well-known and studied healing process (30). It is assumed that the general principles of wound healing are similar in various locations, but it is clear that the process must differ according to the location in detail. Even though there were many attempts to enhance the healing process on the small or the large intestine, the process itself has not yet been thoroughly studied. For the complexity of the process, it is supposed to be very difficult to alter it successfully and enhance the healing results (31–33). The initial phases of the healing process of a well-constructed anastomosis on both the small and large intestine take about three weeks. However, even after this period, the healing processes continue and the anastomosis matures (28,34). The risk of anastomotic leakage is highest in the very early postoperative phase (5^{th} to 8^{th} postoperative day according to the literature (35,36)), when the newly created

tissue is fragile. On the other hand, the risk of anastomotic strictures grows much later and this complication can appear years after the surgery (37).

It has been described that the following conditions are crucial for physiological healing of intestinal anastomoses: sufficient blood supply and oxygenation, defect-less suture, tension-less settings of the intestine, and a good level of contact with surrounding healthy organs (38,39).

1.5.3 Complications of colorectal anastomoses

There are several kinds of local complications of colorectal anastomoses listed below. The following text will focus mainly on the anastomotic leakage as it is the main topic of the thesis.

1.5.3.1 Bleeding

Anastomotic bleeding can occur after colorectal resections. A small amount of blood usually accompanies the first stools after the procedure as a postsurgical residue. However, intraluminal bleeding from the site of anastomosis is rather rare, and an intervention is necessary only in a very limited number of cases. Endoscopic intervention can be beneficial over a reoperation as a less invasive solution. Surgical intervention in the form of reoperation in full anesthesia is needed rarely (40).

1.5.3.2 Strictures

Anastomotic strictures are stenoses appearing at the site of anastomosis, usually months to years after the procedure. The burden of the complication lies in the fact that it is very hard to find a permanent solution for it. Anastomotic stricture leads to complete or incomplete gastrointestinal obstruction and finally in either ileus with acute need for reoperation or just chronic digestive problems of the patient. One way or the other, it decreases the patients' life quality in the long term, often for the rest of their lives (41).

1.5.3.3 Dehiscence and leakage

An insufficient healing in the early postoperative period resulting in anastomotic leakage or full-scale dehiscence is a dreadful complication and has life-threatening consequences (42). One of the most severe and feared surgical site complications in colorectal surgery is anastomotic leakage (43). There were problems in defining colorectal anastomotic leakage, though (44,45). The definition of the underlying problem, which is translocation of luminal contents into the extraluminal surroundings of the anastomosis, is clear. Yet it is a different task to identify such conditions in patients after colorectal procedure in clinical settings. The different approaches resulted in the inability of researchers to combine data from different hospitals and countries, thus making it extremely difficult to create multicentric studies on this topic and to come up with clinically valid recommendations (45). The situation has stabilized when the surgical community widely accepted the system proposed by the International Study Group of Rectal Cancer (ISGRC) in 2010 (46) (Table 1).

According to the system, we recognize three grades of severity of anastomotic leakage. The grades are defined by indicated type of treatment. Grade A leakage can be noticed as a contained leakage on the site of anastomosis using imaging methods. The patient does not manifest any symptoms and no further intervention is needed other than observation. Grade B leakage is associated with purulent drain secretion and laboratory changes (inflammatory parameters elevation). Antibiotic treatment or drainage of the collection can be employed to solve the complication, reoperation is not required though. Grade C leakage is massive and results in peritonitis, it is a life-threatening condition and it must be handled promptly. Reoperation and antibiotic treatment are indicated. It is categorized as at least Clavien-Dindo IIIb postoperative complication and thus it is a source of high morbidity and mortality (47). The duration of hospital stay is prolonged and the treatment costs grow significantly (46). The system is simple and clearly stratifies patients into three groups with different severity of the complication and treatment plan. One disadvantage of this system for leakage monitoring is that a vast majority of uncomplicated patients are not examined by additional CT scan in the early postoperative period and many grade A leakages are

therefore unnoticed. Despite its clinical merits, the scoring system is however insufficient as a sole evaluation system in experimental settings, where a more sensitive system is needed to distinguish even the slightest differences in wound healing.

Table 1: Grades of anastomotic leakage according to the ISGRC (46)

Leakage grade	Presentation	Intervention
A	Imaging methods only	No intervention
B	Imaging methods, clinical alteration	Antibiotics, drainage
C	Imaging methods, clinical alteration	Reoperation

The impact of the grade B and C anastomotic leakage is enormous both from a clinical and economical point of view. Anastomotic leaks are associated with prolonged length of stay, higher readmission rates and overall higher treatment costs (48). Adjuvant chemotherapy can no longer be used when the patient's condition worsens after severe complications. Higher local recurrence has also been found in some studies after colorectal anastomotic leakage in oncologic patients (49). Prevention of anastomotic leakage is therefore a part of a complex approach to the patients undergoing colorectal surgery. It includes both surgical intraoperative and perioperative measures. Most of the recommendations are given by national and international professional societies like American Society of Colon and Rectal Surgeons (ASCRS) (50), European Society of Coloproctology (ESCP) (51), European Society of Surgical Oncology (ESSO) (52), Enhanced Recovery After Surgery Society (ERAS)(53), and others.

Knowing the risk factors can help to stratify patients into groups with different risks of developing anastomotic leakage. This can change pre- and perioperative decision making over the operative technique and type of procedure. Significant preoperative risk factors are for example: male sex, poor physical condition (American Society of Anesthesiologists fitness

grade higher than II), renal disease or recent radiotherapy. Several risk factors are tumor-related: size of the tumor, tumor location in distal rectum, acute surgery, presence of metastases. Other risk factors were identified as adjustable: smoking, obesity, poor nutrition, alcohol abuse, immunosuppressants or bevacizumab in medication. Even though the risk factors may not be present before the surgery, some may occur during the procedure and should be therefore considered by the surgeon: blood loss or need of transfusion, duration of the surgery of more than 4 hours (42).

A proper management of clinically significant anastomotic leakage can play an important role in the postoperative period and have a major impact on the patient's future wellbeing and life quality. There is no uniform generally accepted recommendation on the type and timing of such interventions. Colorectal surgery is still developing and especially this part of the specialization goes through significant changes (54). The traditional solution for a leaky colorectal anastomosis is a reoperation with a Hartmann's procedure performed via laparotomy resulting in terminal stoma. A different approach to the problem is fecal diversion through the axial stoma of the oral intestine (diverting ileostomy, loop ileostomy). The latter is considered less invasive and can be accepted when there is no large loss of vitality of the intestinal tissue, which means that the anastomosis still has a chance to heal when it is excluded from the gastrointestinal tract passage. In a large scale dehiscence or tissue necrosis at the site of anastomosis, the non-vital tissues are resected and a Hartmann's procedure is recommended (55,56). However, after such procedures only a part of the patients manage to go through the reversal procedure to gain back the continuity of the gastrointestinal tract. The likelihood of stoma reversal is significantly higher for the diverting ileostomy than for the anastomotic resection with a Hartmann's procedure (57). Nevertheless, a second major procedure in such a short period is difficult to go through, especially for elderly or polymorbid patients. These are the patients that are originally in the highest risk of developing an anastomotic leakage in the first place. It is therefore recommended to minimize the surgical intervention and to shorten the procedure time as much as possible (58).

Results of various clinical studies showed that less aggressive intervention can suffice in some cases, yet in others the Hartmann's procedure is inevitable. The current consensus of ASCRS is that the surgical procedures should be reserved for patients with obvious purulent or feculent peritonitis or for patients with unstable vital signs (59). To decrease the severity of the surgical procedure, a laparoscopic approach can be chosen if the surgeon is capable of performing it under such conditions (60). Technical advances enabled new treatment options, especially for low colorectal leaks with pelvic collections. Some of the perianastomotic collections can be drained percutaneously using imaging methods (61). Endoscopic treatment can be chosen in selected patients as well. Endoscopic drainage, clips, stents, sealants or endo-sponges for forced luminal drainage can be used. These are, however, safe only in selected stable patients with partial anastomotic insufficiency. A small defect in the circumference of the intestine has a chance to be solved via these endoluminal approaches. When there is no viable tissue to be healed, other means must be taken. The mentioned methods can be used either alone or in a combination with a diverting stoma (59).

a) Transanal drainage: This is a relatively old technique. A foley catheter can be placed transanally through the anastomosis to drain the location. The catheter can be used to irrigate the site of the leak. The irrigation should be performed several times a day followed by removal of the catheter when the defect is decreases its size (62).

b) Endoluminal stenting: There is a large variety of types of endoluminal stents from different materials (metal, plastic or biodegradable). These have been generally accepted as a safe way to reduce the fecal contamination of the abdominal cavity (59). The stent needs to be placed over both of the anastomosed parts of the intestine and it must be more than 5 cm above the anal verge (63). Therefore, it is not a possible solution for a very low rectal anastomosis. Small studies suggest a very high success rate of the method both as an only solution or in combination with diverting ileostomy, while other ones consider stenting worthless (64,65).

c) Endoscopic clipping: Another feasible way to heal small anastomotic defects is a clip placement over the defect to bring the two intestinal edges together. It showed a high success rate (86%) in a small series of 14 patients, only two of which had protective ileostomy by the time of clip placement (66).

d) Endo-Sponge placement: This technique is a relatively new solution for contained leaks with partial intestinal wall dehiscence. A polyurethane sponge is introduced endoscopically via the anastomotic defect into the abdominal cavity (into the perianastomotic collection) and an active drainage tube is connected to the sponge, creating a negative pressure in the anastomotic defect. The sponge is then exchanged every two to three days. The goal is to gradually decrease the size of the endo sponge over time and thus decrease the defect. The success rate of the method varies among studies, however is still relatively high (50–89%). Protective ileostomy is strongly recommended prior to the procedure (59).

e) Transcutaneous drainage: Transcutaneous drainage using computed tomography is a way of solving mainly pelvic complications. A relatively rare complication of this method is a colo-cutaneous fistula development (61).

1.5.3.4 Extensive peritoneal adhesions

Peritoneal adhesions are pieces of connective tissue of various quality occurring in non-anatomic locations in the peritoneal cavity (67). They can be either thin membranes or thick and sometimes vascular bonds connecting various structures in the abdominal cavity. These appear in varying severity not only after surgical procedures, but also after injuries, irradiation, inflammations and other inflictions. Most of the patients after laparotomy (approximately 90%) develop some amount of peritoneal adhesions, treatment is needed in 5–20% of these cases as the adhesions can be a source of persisting abdominal discomfort and can be a reason of possible gastrointestinal passage blockage or other conditions. These complications can occur many years after surgical procedure. Peritoneal adhesions are also a burden in following surgical procedures in the abdominal cavity, as they prolong

the operation time and can cause technical difficulties and even injuries to the adhered organs (68,69).

A systematic review by Ellis et al. suggested that colorectal surgery is the most common surgical cause of intra-abdominal adhesions (70). A number of materials were tested as a local prevention of adhesion formation, some of which are used in current clinical practice. Frequently used local anti-adhesive barriers are hyaluronic-acid-based ones, but they are usually reserved for gynecological procedures where the gastrointestinal tract is not involved (71). It has not been proved whether it is safe to use such materials after construction of colorectal anastomosis. Questions have been raised about compromising the anastomotic healing.

1.5.3.5 Grading of peritoneal adhesions

Adhesions are classified by various systems both quantitatively and qualitatively. Some grading systems focus only on one of the modalities, some combine the two. One of the most frequently used systems is the one created by Zühlke et al. (72). Adhesions are scored according to their mechanical properties, but the evaluation is subjective (Table 2).

Table 2.: Grading of adhesions according to Zühlke (72)

Grade	**Adhesion quality**
0	No adhesion
1	Filmy adhesions, easy to separate by blunt dissection
2	Blunt dissection in combination with sharp dissection is necessary, beginning vascularization noticeable
3	Only sharp dissection usable for adhesiolysis, vascularization clearly visible
4	Only sharp dissection usable, organs are strongly attached with strong adhesions, damage of organs is hardly avoidable

Even though the system is clear and easy to use, it is insufficient as an only grading system because it does not explain anything about the extent and location of adhesions in the peritoneal cavity. Therefore, new systems were developed, the Peritoneal Adhesion Index belongs to the grading systems that score both the quantity and quality of adhesions. The quality is scored similarly to the Zühlke's system and the quantity is measured in 9 segments of the abdomen (68). The result is a single numeric score. Such scoring systems as these however do not contain information about specific organs involved. As far as we know there is no such system describing the level of involvement of each organ into peritoneal adhesions. The absence of such information does not allow to thoroughly statistically describe the amount and location of peritoneal adhesions in groups of patients.

1.5.3.6 Adhesion formation

Normal peritoneal repair is a very complex process, which is driven by many signal molecules in perfect balance and it can be destabilized easily. Some of the influencing factors are pro-adhesive some are anti-adhesive. Adhesion formation is mediated by regulated inflammation, angiogenesis, cell migration and extracellular matrix production. Well-regulated process assures normal peritoneal healing without adhesions formation (73). Adhesions develop and mature over long periods of time and the amount and mechanical character of peritoneal adhesions can change greatly in time.

As previously stated, the formation of adhesion is triggered by an injury to the peritoneal surface. The injured surface starts producing a thin fluid which is rich in many proteins and signal molecules as well as inflammatory and other cells (74). This fluid coagulates within 3 hours and thus it ensures stable contact of the two peritoneal surfaces. A process of fibrinolysis takes place at the same time and inhibits the formation of adhesion in normal peritoneal healing within the first 72 hours after the injury (74). A prolonged persistence (3-5 days) of this coagulated mass is needed for fibroblasts to migrate in it and start producing the extracellular matrix and other substances. This new scaffold is afterwards occupied by mesothelial cells (75,76). Healthy peritoneum has fibrinolytic activity, which can

be however decreased in different situations (hypoxia, injury, infection, etc.) which leads to adhesion formation (77).

1.5.3.7 Role of hypoxia

Many studies suggested local hypoxia is a strong pro-adhesive factor. Normal peritoneal healing is disrupted by hypoxia on several pathways. There are many situations not only in colorectal surgery, when the abdominal viscera are exposed to hypoxia (extensive bleeding, hypovolemia, sepsis, imperfect ventilation, comorbidities like visceral atherosclerosis etc.). Studies suggest that it doesn't matter whether the condition is transitory or prolonged for the development of adhesions. Hypoxia causes oxidative stress of the affected tissue. One of the key elements of the process are free radicals (highly reactive substances with one or more impaired electrons). These are used as a weapon against intracellular organisms and are also a part of several physiologic signaling pathways. Their production is highly regulated as they can cause tissue damage. The regulating enzymes called antioxidant enzymes are: superoxide dismutase, catalase and glutathione peroxidase.

Dysregulation of the balance of antioxidant enzymes and free radicals takes part during oxidative stress. It was observed that not only hypoxia but also exposure to CO_2 can lead to decrease of levels of antioxidant enzymes. This can be a problem during laparoscopic procedures when the abdominal cavity is filled with CO_2 gas. The longer the exposure is, the lower the levels of antioxidant enzymes get. Longer duration of CO_2 gas exposition also showed as a predisposition for adhesion formation in a clinical study (77,78).

Following molecular factors are the most important in relation to balanced peritoneal healing according to the literature:

Tissue plasminogen activator (tPA) can be found in mesothelial cells and fibroblasts of the peritoneum. It is a substance capable of converting plasminogen to plasmin and therefore decreases the formation of peritoneal adhesions. Adhesion fibroblasts show significantly lower levels of tPA in comparison to normal peritoneal fibroblasts (79). The level of tPA also decreases in normal peritoneal fibroblasts in hypoxic conditions (77,79).

Plasminogen activator inhibitor-1 (PAI-1) is responsible for inhibiting the activity of tPA. Increased levels of PAI-1 were observed in adhesion fibroblasts compared with normal peritoneal fibroblasts. The level of PAI-1 increases in hypoxic conditions both in normal peritoneal and adhesion fibroblasts (77,79).

Transforming growth factor-β1 (TGF-β1) an inflammatory signal molecule important for wound healing. A pro-adhesive character of the substance was observed as it is responsible for increased extracellular matrix production through complicated pathways (77,80).

Tumor necrosis factor α (TNF-α) is also an inflammatory signaling molecule. It interferes with tPA release in the process of peritoneal healing. Therefore, it is capable of decreasing the fibrin degradation in the coagulated peritoneal exudate. TNF-α is found in increased concentration in peritoneal adhesion fibroblasts. Hypoxic conditions also raise the level of TNF-α in normal peritoneal fibroblasts (81,82).

Interleukin 6 (IL-6) is yet another inflammatory signaling molecule found in higher concentration in normal peritoneal fibroblasts under hypoxic conditions and in adhesion fibroblasts. It is very important in the process of wound healing as it is an early marker of tissue injury and it promotes fibrin formation and thus adhesion formation (77,82).

Matrix metalloproteinases (MMPs) or matrixins are a family of endoproteases, enzymes with broad proteolytic activity. Their balanced activity plays a key role in remodeling of the extracellular matrix and therefore formation of peritoneal adhesions (83,84). Their activity is regulated by many cytokines and directly by tissue inhibitors of metalloproteinases (TIMPs) (83). There are at least 23 MMPs that have been discovered in the human extracellular matrix. Different studies proved correlations of either decreased levels of certain MMPs or their TIMPs in correlate with extensive adhesion formation (83).

Vascular endothelial growth factor (VEGF) is a signaling molecule important in formation of new blood vessels (angiogenesis). Angiogenesis is a critical process in development of peritoneal adhesions. It is necessary when the tissue is insufficiently supplied with oxygen and nutrients, when the maximum diffusion range is lower than the actual distance from the nearest blood capillary. The process is regulated by expression of angiogenic factors such as VEGF. The factor is upregulated in hypoxic conditions. It has been shown in an animal study that peritoneal injury induces an increase in VEGF expression (85). Cellular hypoxia is involved in tissue necrosis and following inflammatory reaction in any tissue trauma (86).

Cyclo-oxygenase (COX) is another agent involved in formation of peritoneal adhesions. It has been proven by Saed et al., that adhesion fibroblasts express cyclooxygenase-2 (COX-2) and normal peritoneal fibroblasts in normal conditions do not. When the normal peritoneal fibroblasts were exposed to hypoxic conditions COX-2 expression was induced to levels similar to adhesion fibroblasts (87). Wei et al. showed in an experiment on rodents that COX-2 inhibition can prevent postoperative intra-abdominal adhesions by decreasing hypoxia-induced activation of peritoneal fibroblasts (88).

1.6 Minimizing surgical site complications in present-day clinical practice

Minimization of postoperative complications should be one of the main goals of surgeons across all specializations. In this text we focus on two types of complications:

a) Extensive formation of peritoneal adhesions: Current knowledge regarding the formation of adhesions in the peritoneal cavity is still limited. As mentioned above, the causes of adhesion formation are peritoneal injury together with hypoxia, which result in an inflammatory-reaction-driven process transforming fibrin deposits into peritoneal adhesions. There are only few countermeasures available in present-day clinical practice. Surgical techniques include gentle tissue handling to prevent tissue injury, hypoxia, and drying of surfaces. Use of foreign pro-adhesive materials like silk, for example, should be avoided. Laparoscopic surgery is recommended as it minimizes the tissue manipulation and therefore also trauma. However, long laparoscopic procedures with capnoperitoneum are again a pro-adhesive factor. In reoperations, deposited fibrin should be gently removed from the abdominal cavity at the end of the surgical procedure.

A key precondition for adhesion formation is a contact of two surfaces. Building on this assumption, the process could be disrupted by keeping the tissues apart. Many materials were tested as barrier protection and several of them are currently used for adhesion prevention mainly in gynecological surgery. Their effectiveness is however limited and the safety of their usage in colorectal and gastrointestinal surgery in general is questionable. The U.S. Federal Drug Agency approved the following materials: Interceed (oxidized regenerated cellulose, Johnson & Johnson, New Jersey, USA), Seprafilm (hyaluronic acid and carboxymethylcellulose, Sanofi-Aventis, France), Adept (icodextrin solution, Baxter, Illinois, USA).

b) Defective anastomotic healing: Prevention of anastomotic leakage requires a complex approach that starts even before the procedure itself and before the patient's admission. As new data as well as new methods and techniques appear, recommendations change over

the course of time. Surgical societies argue about some precautions, while some are approved generally. The traditional conditions include: preoperative bowel preparation with laxatives, perioperative antibiotic intravenous prophylaxis, good blood perfusion of the two anastomosed intestinal ends, no axial rotation of the two anastomosed ends, no tension in the site of anastomosis, use of monofilament biodegradable suture material, careful re-alimentation in the postoperative period.

1.6.1 ERAS recommendations

The Enhanced Recovery after Surgery Society has published the fourth version of recommendations for perioperative care in colorectal surgery in November 2018 (the first version was published in 2005). The mission of the Society is to develop perioperative care and to improve recovery through research, education, audit and implementation of evidence-based practice, according to the official website. The recommendations, however, cover only planned colorectal procedures and cannot be applied to acute procedures. The current version describes many items divided into four segments: preadmission (information, optimization, prehabilitation, nutrition, anemia screening and assessment), preoperative (prevention of nausea and vomiting, selective premedication, prophylactic antibiotics, no bowel preparation, maintaining euvolemia, no fasting and carbohydrate drink), intraoperative (standard anesthetic protocol, fluid normovolemia, normothermia, minimal invasive surgery, no drainage) and postoperative (no gastric drainage, multimodal analgesia, thrombosis prophylaxis, fluid normovolemia, urinary catheter, prevent hyperglycemia, postoperative nutrition, early mobilization).

Their observations and recommendations are based on Meta-analyses, randomized controlled trials, and prospective/retrospective cohort studies. Each recommendation is valued as strong or weak depending on the level of confidence of the panel of ERAS Society. The level of evidence-based information for each item is graded as low, moderate or high. Even though the goals of ERAS protocols are complex, some of the recommendations specifically focus on anastomotic leakage:

Preoperative nutritional screening: Preoperative malnutrition has been associated with increased postoperative morbidity and mortality as well as with poor oncologic outcomes in surgery for gastrointestinal cancer. Therefore, a preoperative nutritional screening is indicated. Oral nutritional supplementation (or additional parenteral nutrition when indicated) has the best effect if started 7–10 days preoperatively and is associated with a reduction in the prevalence of infectious complications and anastomotic leaks for malnourished patients. The recommendation is valued as strong with a high level of evidence.

Bowel preparation: Oral antibiotic preparation alone proved protective of surgical site infection, anastomotic leak, ileus and major morbidity, but not mortality in a large observational study. Mechanical bowel preparation alone with systemic antibiotic prophylaxis showed no clinical advantage, it can cause dehydration and discomfort and should not be used routinely in colonic surgery. It may be used for rectal surgery when diverting a stoma. The recommendation not to use mechanical bowel preparation is valued as strong with a high level of evidence.

Minimally invasive techniques (MITs): MITs are highly recommended by surgical societies. They include laparoscopy, laparoscopically assisted procedures, transanal techniques and robotic or robotically assisted procedures. These proved valuable in decreasing the length of stay in hospital as well as infectious complication rates, wound-related complications and many more. Large multicentric studies proved their equal oncological potential.

Drainage of the peritoneal cavity and pelvis: The use of a drain in the peritoneal cavity and pelvis has been employed to prevent collections and to monitor and even prevent anastomotic leakage. The current ERAS recommendation on the topic is that the pelvic and peritoneal drains show no effect on clinical outcome (no effect on anastomotic leakage rate (clinical or radiological), mortality, wound infection, reoperation rate). They value this statement as a strong recommendation with a high level of evidence.

It is clear that some of the recommendations are controversial and are not generally accepted by wide surgical community. We took these in consideration while designing our experimental models.

1.7 Minimizing surgical site complications in experimental settings

The introduction of new surgical techniques and new drugs or medical devices to routine practice requires previous verification of their safety and efficiency via preclinical testing. Laboratory experimental animal models are still irreplaceable tools in the preclinical phase as they can easily reveal unexpected adverse reactions to foreign materials.

1.7.1 Animal models of peritoneal adhesions

Peritoneal adhesions cause many health issues in millions of patients and the interest in the research of adhesion pathophysiology is therefore significant (89,90). A reliable animal model is necessary to determine the effect of antiadhesive agents as well as to describe the pathophysiological processes behind adhesion formation. Precise assessment methods for evaluation of adhesion quality and extent are of the same importance.

Animal species: Selection of a relevant animal species is important. Rats are the most widely used animals for models of peritoneal adhesions according to the literature. Rats share with humans similar pathophysiology of the peritoneal adhesions formation (91). Larger animals like pigs can deliver more realistic models in terms of size comparability to human surgery (92). They are more expensive, though, and the perioperative care is more time consuming.

Type of model: In animal models, peritoneal adhesions are induced either by ischemia, foreign material implantation, or by mechanical injury to the peritoneal surfaces, which is the most common approach according to our literature search (93). The mechanical injury is usually achieved by abrasion of the peritoneal surfaces (Figure 5), defined peritonectomy (94,95), or by electrocautery (96). Peritoneal ischemia is reached by either ligation of peritoneal blood supply, temporary occlusion of the mesenteric artery (93), or by construction of so-called peritoneal buttons (Figure 6) (94). The last-named method is considered very reliable in terms of location and extent of adhesions (94).

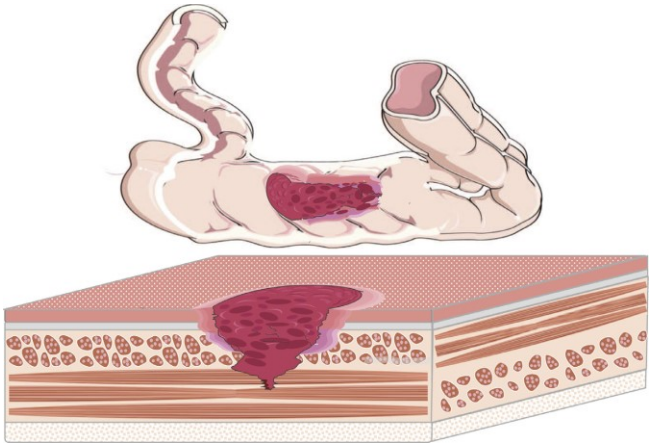

Figure 5: peritoneal abrasion of the abdominal wall and the large intestine (94)

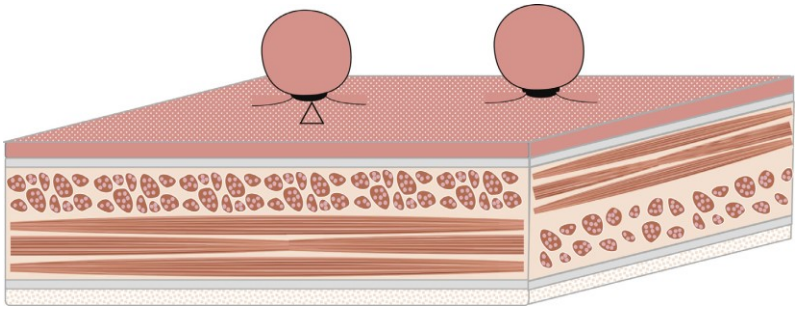

Figure 6: Peritoneal buttons with ischemic areas of peritoneal tissue (94)

Studied treatment methods and experimental design: Hundreds of agents were tested experimentally for anti-adhesive properties. Their effect is based on their anti-inflammatory, anti-coagulant, or fibrinolytic activity, a barrier mechanism, or a combination of these (97).

Assessment methods: There are two basic aspects in the evaluation of the healing process of an intestinal anastomosis:

- Macroscopic changes at the point of specimen collection, scoring of the extent and quality of adhesions according to existing systems
- Histological assessment (morphology evaluation in comprehensive overview, volume fractions of collagen, elastin, inflammatory cells, endothelial cells etc.)

1.7.2 Animal models of intestinal anastomoses and anastomotic wound healing

Most of the published research on anastomotic healing is focused on the use of different means to positively influence the anastomotic healing process, to prevent anastomotic leakage and dehiscence, or fortify the mechanical strength of intestinal anastomoses. However as stated by Bosmans et al. (98), there is an enormous lack of knowledge about the intestinal healing process. Every attempt to enhance the healing process before revealing the underlying pathophysiology is therefore uncertain. Nevertheless, such studies are very frequent. According to the systematic review by Yauw et al. over 1300 experimental studies of such kind were identified (99). The scientific quality of these studies, experimental methods and reliability of results were considered largely variable according to the same systematic review (99).

Animal species: Most of animal models of intestinal anastomoses are performed on pigs, dogs and rodents according to our literature search (99). Rodents can be used for testing new materials and their biocompatibility as they are easy to work with and the perioperative care is much less expensive. However, pigs can deliver more authentic models anatomically and functionally as their gastrointestinal tract is more similar to the human one. The size ratio is more human-like as well, and therefore the same surgical techniques can be used (100–102).

Type of model and experimental design: Anastomoses on both the large and on the small intestine appear in experimental studies, anastomoses on the rectum are not widely used for their technical difficulty. Both small intestine and large intestine of healthy experimental animals have enormous healing capacity, making the risk of anastomotic leakage rather small. For studying the effects of treatment methods on anastomotic leakage rate, extremely large samples or models simulating defective healing are therefore needed. Defective healing is reached either by ischemization of the two anastomosed intestinal ends (103), incomplete suture of the anastomosis itself (104), chemotherapy, radiotherapy, or a combination of the last two (105). Some parameters can be assessed immediately after the construction

of an anastomosis (mechanical strength (106)), while the rest is usually evaluated after varying observation time (107). The anastomotic leakage is an early postoperative complication, appearing usually in the first 10 postoperative days (108). For evaluation of anastomotic leakage occurrence, short postoperative observation periods like this are sufficient, however wound healing is a process that continues on (even though less intense) practically indefinitely (109,110). It remains a question what the ideal time point for evaluation of the healing process is, or whether multiple time points for specimen collection should be used. The large number of variables in experimental designs and assessment methods makes results of such studies difficult to compare (99).

Studied treatment methods: The most studied topics are the effects of various treatment methods: the effect of chemotherapy on intestinal anastomotic healing, the effect of fibrin glue application, the effect of various growth factors (99). Patches of some kind (collagen, bovine pericardium, fibrin, polyglycolic acid mesh) were tested in many studies (104,111–114). Some of these were meant to serve just as mechanical support, a barrier to prevent leakage of intestinal contents into the abdominal cavity, others were meant to actively stimulate the healing process.

Assessment methods: There are four basic aspects in the evaluation of the healing process of an intestinal anastomosis:

- Clinical condition in the postoperative period (signs of anastomotic leakage as sepsis, abdominal wall tenderness, activity decrease, temperature elevation, weight changes, results of biochemical assays, imaging methods etc.)
- Macroscopic changes in the abdominal cavity (signs of anastomotic leakage, visible intestinal contents in the abdominal cavity, peritoneal changes and signs of peritonitis, visible defects of the intestinal anastomosis, diameter changes of the intestinal anastomosis or of other parts of the gastrointestinal tract etc.)
- Histological evaluation of anastomotic specimens (comprehensive overview of the intestinal morphology, stereological evaluation of volume fractions

of inflammatory cells, endothelial cells volume fractions, collagen volume fractions, evaluation of microscopic integrity of the intestinal wall etc.)

- Mechanical testing of the intestinal anastomoses (Tearing strength, bursting pressure) (115,116).

Many other assessment methods can be employed, nevertheless all methods should be described in the most detailed way for better reliability and reproducibility.

1.8 Nanofibrous materials

Nanofibrous materials are non-woven fabrics with fiber diameter ranges in up to hundreds of nanometers. Their structure and properties are highly variable and their form depends on the fabrication technology. There are several methods of their creation.

Electrospinning is today's most used technique as a convenient and easily adjustable process (117). The range of source materials for their fabrication is enormous and therefore they became widely used in various fields including biomedical research and medicine. Nanofibrous materials have several advantages for tissue engineering and biomedical research (118). They have very high specific surface area and high porosity, both of which are adjustable by the fabrication process. They can be fabricated to structures similar to the fibrillar components of the extracellular matrix. Depending on the materials used, they can be both biodegradable or not. Thanks to these properties, all of which are highly adjustable, they are generally highly biocompatible (119). Many both *in vivo* and *in vitro* studies were performed, and a large variety of different materials were tested for use for a broad spectrum of purposes (120). Such materials can be cut or shaped into various forms to ease the application.

1.8.1 Fabrication of basic nanofibrous materials via electrospinning

The process of electrospinning was described by Charles Vernon Boys in 1897 (117) and the first patents appeared in 1900. The original protocols were perfected and nowadays electrospinning is a suitable technology for mass production of nanofabrics.

Electrospinning is a method utilizing electric charge to create threads from liquid polymers or polymer solutions. The liquid polymer or solution is drawn from one electrode to the other as a jetstream and the solvent is evaporated from the material before it reaches the other electrode (Figure 7).

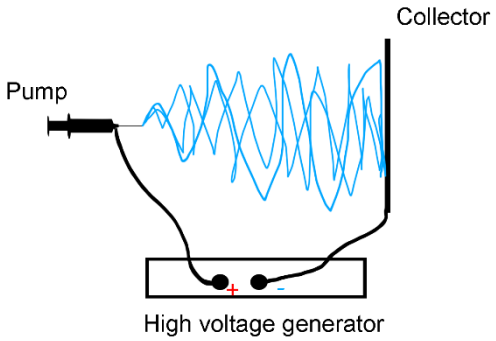

Figure 7: scheme of a basic apparatus for electrospinning

New types of fabrication apparatus use the technique of needleless electrospinning (Nanospider^{TM} 1WS500U electrospinning device, Elmarco, Czech Republic) that allow production in larger volumes (121). The final products in these cases are planar materials. The process can be adjusted by changing the character and concentrations of solvent and dissolved material, changing the electric charge or changing the distance from the pump to the collector (122). The range of source materials is enormous.

1.8.2 Drug delivery systems

Nanofibrous materials have been found useful for drug delivery systems, mainly for their high surface-to-volume ratio. There are many ways drugs can be incorporated into the materials and many ways to influence the release profile. Nanofibrous materials are also interesting for the possibility of triggered drug release, when active molecules are only released after specific stimuli (so called intelligent biomaterials).

- **Fabrication from blended solutions via electrospinning:** Drugs are dissolved together with the materials used for electrospinning in the solution used for fabrication (123). The process is however suitable only for some drugs and materials. The drugs must be dissolved in the same solvent as the fabrication material. The first condition is for the drugs

to be soluble in the specific solvent in sufficient concentrations and the second condition is for the drug to be stable enough throughout the whole process. Both hydrophobic and hydrophilic drugs, and also proteins or DNA for example, can be encapsulated into the electrospun fibers (124). It is a very convenient and technically easy method. The drug release is then achieved by biodegradation of the product, the speed of the process and therefore concentration of the released drug can be controlled by the qualities of the nanofibrous material (type of basic compound and its biodegradability, thickness and porosity of the produced nanofabrics, concentration of the drug, application site of the material) (125). Some drugs can also be used as the base substance for fabrication of such nanomaterials.

- **Surface modification of nanofabrics:** In this approach, the nanofibrous materials are produced first without the drug, which is loaded onto the product later on. There are many ways to do so. The drug can be only physically adsorbed on the surface of the fibers or covalently bound. Physical adsorption usually leads to fast release after application, while covalently bound molecules can have various release dynamics. If none of the two is suitable, alternative procedures can be chosen. Blending can be employed with different solvent or polymer then the basic nanofibrous material. The polymers are chosen to optimize the stability of the drug and its release process, the final solution can be applied to the surface of the premade drug-free nanofabric. The ways of application of such material are countless. For example, a second layer of nanofabric can be applied, or other methods like electrospraying can be employed (124).

- **Coaxial electrospinning:** Coaxial electrospinning is a modification of electrospinning that enables production of fibers with different core and shell composition. The active molecules can be incorporated either to the solution used for core fabrication or to the solution used for fabrication of the shell, depending on desired release profile, or a drug can be used for each (124,126). This variety brings in new possibilities for triggered drug release when the active substance is released after a specific stimulus,

like change of pH. The coaxial electrospinning is more technically challenging as there are two (or more) jets simultaneously producing the fiber as an inner and outer stream (Figure 8).

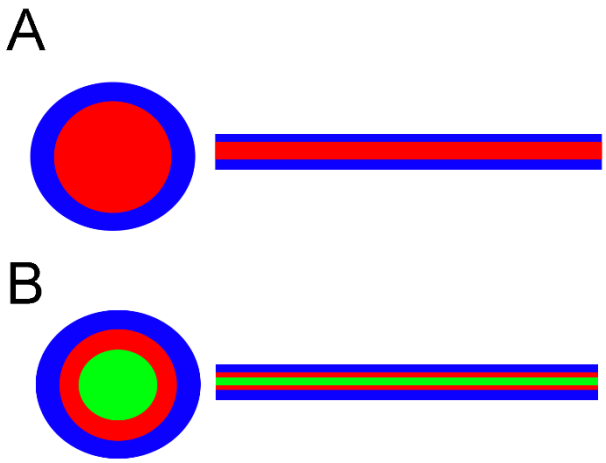

Figure 8: Co-axial electrospun fibers;
A) Co-axial fiber from two polymers; transverse cut (Left) and longitudinal cut (Right);
B) Co-axial fiber from three polymers, transverse cut (Left) and longitudinal cut (Right)

1.8.3 Nanofabrics for wound healing support

A positive effect on the wound healing process has been documented for different versions of nanomaterials in different experimental models of skin healing, bone healing and others. The effect is thought to be mediated by their structural properties as well as their composition (127). Reddy et al. state in their review that porosity and structural similarity of nanofibrous materials to actual extracellular matrix is advantageous for successful healing process (128). In normal conditions, the extracellular matrix serves as a scaffold for cells, allowing them to differentiate, grow, and multiply properly. These functions are provided by spatial, mechanical, structural and biochemical properties of the extracellular matrix. It is clear that the extracellular matrix has a complex multifactorial role in tissue regeneration, which is probably location specific. These functions will be difficult to mimic by bioengineered scaffolds

in full scale, but even current products show very promising results and can even demonstrate new properties that the extracellular matrix cannot provide (like antibacterial attributes, intelligent drug release etc.) (129). The studied materials can be divided into several groups.

- **Natural polymers:** natural polymers include collagen, gelatin, silk, hyaluronic acid and its derivatives, cellulose, chitin, and others. Collagen-based electrospun scaffolds showed excellent results and proved very effective in wound healing support (129). For example, Rho *et al.* published results of their collagen nanofibrous matrices that proved effective as wound-healing accelerators in early-stage wound healing *in vitro* simulation (130). *In vivo* experimental studies of various collagenous nanomaterials showed good results as well (129). Even though collagen has some excellent properties like high biocompatibility, compatibility with synthetic polymers, biodegradability etc., production of collagenous electrospun scaffolds is relatively expensive, it has relatively high batch-to-batch variability, and the scaffolds have tendency to swell after implantation (131) (Table 3).

Table 3: Pros and cons of collagen based electrospun scaffolds (131)

Pros	**Cons**
Highly biocompatible, non-antigenic, non-toxic	Expensive
Biodegradable, and possibility to regulate biodegradability via cross-linking	High batch-to-batch variation
Compatibility with synthetic polymers	Tendency to swell
Easily modifiable	Poor mechanical properties, low tensile strength
Promotes blood coagulation	
Easily available material	

- **Synthetic polymers:** The group of synthetic polymers offers a large variety materials suitable for electrospinning. The list of studied and tested materials is enormous. The following substances belong among the most studied ones: Polyvinyl-alcohol (PVA), Polycaprolactone (PCL), and Polylactic acid (PLA) and its derivatives etc. PVA is a non-biodegradable polymer with excellent mechanical properties (132) and a possibility of regulated drug release (133). It is traditionally used for wound dressings where it has good results in wound healing studies, however as a non-degradable material it is suitable only for external application. PCL is biodegradable polymer with high biocompatibility. It is therefore widely used in biomedical research. It served as a base material for nanofibrous scaffolds in many studies either alone or in composite scaffolds or scaffolds with regulated drug release. Both *in vitro* and *in vivo* studies suggest excellent adjustable mechanical properties, biocompatibility and tissue growth support (134–136). The advantage of synthetic polymers is their high modifiability, which provides the possibility to engineer materials with perfectly defined properties for each kind of application.

2 Experiment A

(Polycaprolactone and polylactic acid-polycaprolactone copolymer nanofibrous patches for anastomotic healing support, model of anastomosis on the small intestine of a pig)

2.1 Aims and hypotheses A

Aim 1: To create planar versions of nanofibrous material made of different polymers

Aim 2: To apply the planar materials on the anastomosis on the small intestine

Aim 3: To create a scoring system to quantitatively assess adhesions in the site of anastomosis on the gastrointestinal tract

Hypothesis 1: Polycaprolactone nanofibrous patches decrease formation of peritoneal adhesions in the site of anastomosis

Hypothesis 2: Polylactic acid-polycaprolactone copolymer nanofibrous patches decrease formation of peritoneal adhesions in the site of anastomosis.

Hypothesis 3: Polycaprolactone nanofibrous patches decrease the risk of anastomotic leakage.

Hypothesis 4: Polylactic acid-polycaprolactone copolymer nanofibrous patches decrease the risk of anastomotic leakage.

2.2 Methods A

2.2.1 Methodological background

We decided to study nanofibrous patches created form polycaprolactone and copolymer of polycaprolactone and polylactic acid. Their known biocompatibility and spinnability were the reasons to choose these substances. Previous studies already suggested pro-healing properties of similar materials. We intended to test the materials *in vivo* in an experiment after obtaining promising results *in vitro* on cell cultures. The reason to choose pigs as experimental animals was for their similar anatomy, physiology and possibility to use the same surgical techniques as in clinical human surgery. In order to study tolerance of the material, its behavior in the abdominal cavity and its effect on formation of peritoneal adhesions without other contributing factors (anastomotic, leakage, peritonitis, wound infections) we decided to create a model of non-complicated anastomotic healing on the small intestine. We also decided to construct three anastomoses per one animal to adhere to 3R rules for animal experiments (replacement, reduction, refinement).

2.2.2 Fabrication of patches

Nanomaterials for our experiment were fabricated via electrospinning on the Nanospider™ machine, which is a construct of Technical University of Liberec, Faculty of Textile Engineering, Department of Nonwovens and Nanofibrous Materials, Czech Republic.
We used two types of biocompatible polymers: PCL and PLCL. PCL (mean weight=43000 g/mol, Polysciences, Germany) and PLCL (Purasorb PLC 7015, Corbion, Netherlands) were dissolved in chloroform, acetic acid and ethanol solution (8:1:1 volume fractions) to the final concentration of 16% and 10% respectively (concentrations allowing optimal electrospinning properties based on previous research (137). The solutions were electrospun onto a spun bond (nonwoven cloth underlay) for easy manipulation and application. The material has been sterilized using ethylene oxide at 37 °C (Anprolene, H.W.Andersen Product, Inc., North

Carolina, USA). This method has been tested before to prove its safety and frugality to the nanomaterial (137).

2.2.3 Material characterization

Scanning electron microscopy was employed to obtain images of the fibers; the pictures were analyzed as described in previous work of Horakova et al. (137). Materials were also tested *in vitro* for degradability and mechanical properties (137).

2.2.4 Experimental design

Healthy male and female Prestice black-pied pigs were randomly allocated to 3 groups using simple randomization (8 animals per each group): PCL group, PLCL group and a Control group with no material applied. Each animal was given a unique code. All animals were 12-14 weeks old weighing between 19-35 kg. Power analysis was performed to estimate the sample size (Attachment 1).

2.2.5 Surgical procedure

Prior to the surgery, the animals were weighed, and intramuscularly premedicated with 10 mg/kg of ketamine (Narkamon, Spofa, Czech Republic), 5 mg/kg of azaperone (Stresnil, Jannssen Phramaceutica, Belgium) and 0,5 mg atropine (Atropin Biotika, Hoechst Biotika, Slovak Republic); general anesthesia was then induced and maintained by intravenous administration of propofol (1 % mixture 5-10 mg/kg/h Propofol, Fresenius Kabi, Norway). Fentanyl 1-2 µg/kg/h (Fentanyl Torrex, Chiesi cz, Czech Republic) was used for continuous analgesia. Augmentin 1.2 g as an antibiotic prophylaxis was administered intravenously (GlaxoSmithKline Slovakia, Slovak Republic). A ProPort Plastic Venous Access System with PolyFlow polyurethane catheter (Deltec, Smiths medical, USA) was implanted and introduced through one of the jugular veins. We entered the abdominal cavity via an upper middle laparotomy. Three end-to-end anastomoses were constructed on the small intestine in 70, 90 and 110 cm aborally from the duodeno-jejunal junction. We transected the intestine using

monopolar coagulation and constructed a hand sutured anastomosis using Monosyn 4/0 (Glycolide 72 %, Caprolactone 14 %, Trimethylencarbonate 14 %) double needled suture line (B-Braun, Germany), following a standard technique of extra-mucosal running suture (Figure 9A). A single piece of nanomaterial (2 × 5 cm) was placed in the area of the suture, covering the whole surface of the anastomosis (Figure 9B). No resection was performed. The intestine was then carefully reposed into the abdominal cavity. Wet swabs were used throughout the procedure for manipulation with the viscera.

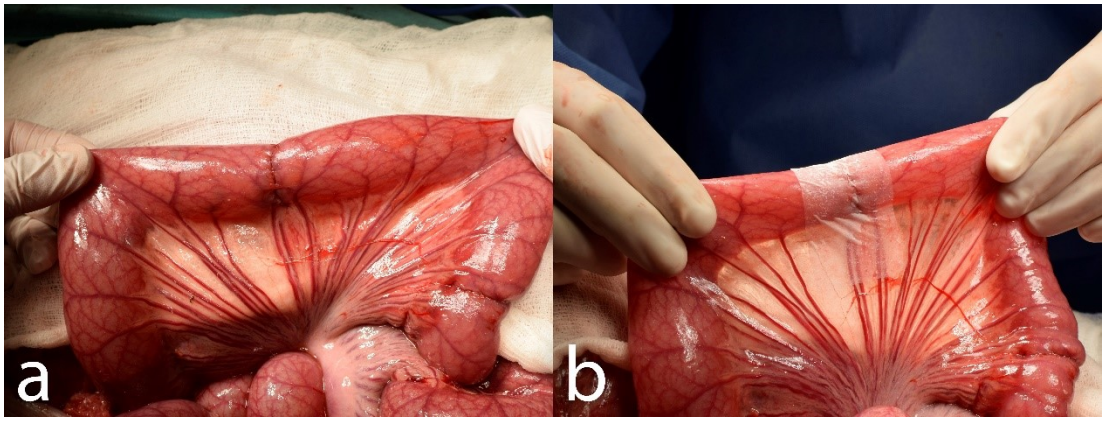

Figure 9: Reinforcing the end-to-end anastomosis on the small intestine in a pig model; a) end-to-end anastomosis before application of the material; b) the PCL nanomaterial applied to the site of anastomosis partially covering the mesentery

2.2.6 Postoperative observation and sample collection

The animals were monitored for three weeks by trained blinded caretakers. A fixed realimentation process was scheduled and the ability of the animals to feed according to the schedule was observed. Vomiting was considered as intolerance of the current food dosage. The activity of animals was also monitored. Blood samples were taken during the experiment at five time points: on day 0 before the application of the material (preoperative baseline sample), exactly two hours after the application of the nanomaterial, on day 7, on day 14, on day 21. Basic biochemical parameters were tracked in these samples (bilirubin, GGT, ALT, AST, ALP, albumin, urea, and creatinine) to see deviations in the animals' metabolism. We weighed the animals at the end of the observation period, performed

laparotomy in full anesthesia again. We inspected the abdominal cavity for changes, PAs (listed organs involved in the adhesions), checked for the presence of free GI content (signs of anastomotic leakage), intestinal strictures, and intestinal diameter growth (signs of GI passage blockage). We acquired photodocumentation, collected samples of the intestine with anastomoses and fixed them into a 10% buffered formalin (cut in the mesenterial line and pinned onto a cork underlay). The second surgery as well as the macroscopic assessment and sample collection were performed by a blinded surgeon. We sacrificed the animals after the sample collection.

2.2.7 Scoring of adhesions

None of the quantitative systems of evaluation of PAs were useful for our experiment as we performed surgery only on a small part of the abdominal cavity and the systems usually score the whole abdomen. Thus, we created a new quantitative scoring system: Perianastomotic Adhesions Amount Score (PAAS) (Attachment 2). The specimens were collected carefully together with the surrounding tissue (depending on the level of adhesions), about 4 cm of the intestine was used for each one. The quality of adhesions was evaluated according to the Zühlke's classification (72). The intestine was then *ex vivo* transected longitudinally on the mesenteric side, and pinned to a piece of cork. To evaluate the amount of PAs, we divided the area of the specimen into four equal quarters along the circumference of the intestine. Each segment was assigned zero to two points based on the level of adhesions: zero for no adhesions in the segment, one point for adhesions covering the segment partially and two points for adhesions in the whole length of the segment. This resulted in 0 to 8 points per anastomosis and 0 to 24 points for each animal. The polarity (oral and aboral part) of the intestine was respected in all measurements (Figure 10). Each sample was given random alphanumeric code for blinding during the histologic assessment.

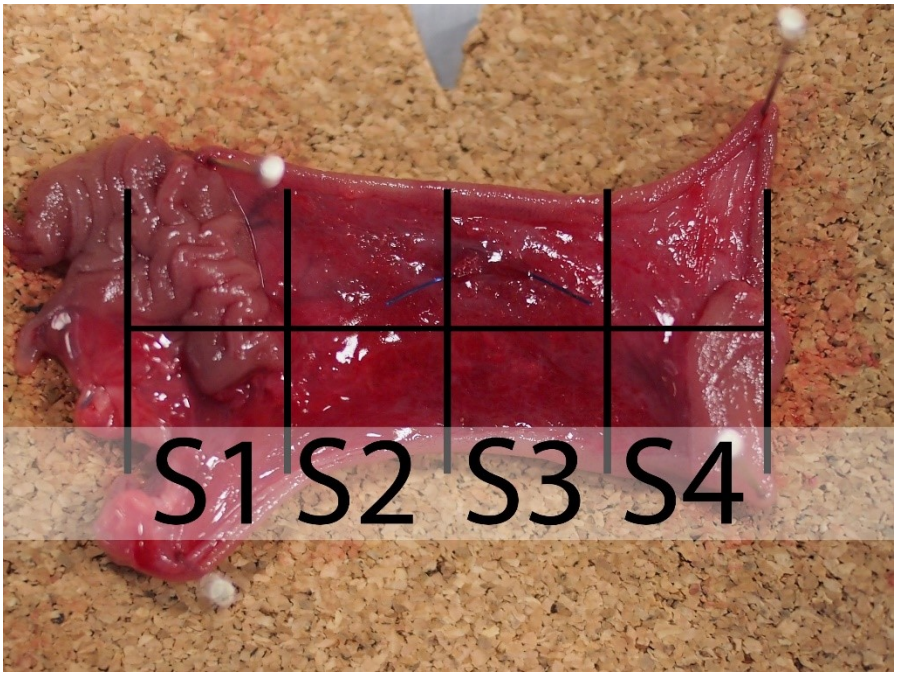

Figure 10: Perianastomotic adhesions amount scoring system for the presence of peritoneal adhesions on the intestine with an anastomosis: The sample (specimen from the Control group) was divided into 4 segments; oral part of the intestine is in the upper side of the image while the aboral part is in the lower part of the image. The area of the suture (the anastomosis itself) is located underneath the horizontal line; scoring of this sample: S1) segment no. 1 scoring 2 points; S2) segment no. 2 scoring 0 points; S3) segment no. 3 scoring 0 points; S4) segment no. 4 scoring 1 point

2.2.8 Histology

After fixing, we processed the samples by standard paraffin technique. We stained 4 µm thick sections by hematoxylin and eosin for comprehensive overview; Verhoeff's hematoxylin and green trichrome technique was used for staining connective tissues, and picrosirius red for visualization of collagen in polarized light. We used immunohistochemical methods for detection of vascular endothelium using Polyclonal Rabbit Anti-Human von Willebrand Factor (vWF) (A 0082, Dako – Agilent, dilution 1:1000); smooth muscles were detected by Monoclonal Mouse Anti-Human Smooth Muscle Actin (Clone 1A4, M0851, Dako – Agilent,

dilution 1:500); for detection of granulocytes and tissue macrophages we used S100A9 Monoclonal Antibody (MAC387, MA1-80446, ThermoFisher Scientific, dilution 1:200).

Microscopic images of IHC samples were stereologically assessed. We defined the reference space as the region of intestinal wall without mucosa located 3 mm proximally and 3 mm distally from the center of the anastomosis (contact of muscle layers); the region includes a suture line (Figure 11). We investigated samples qualitatively and quantitatively.

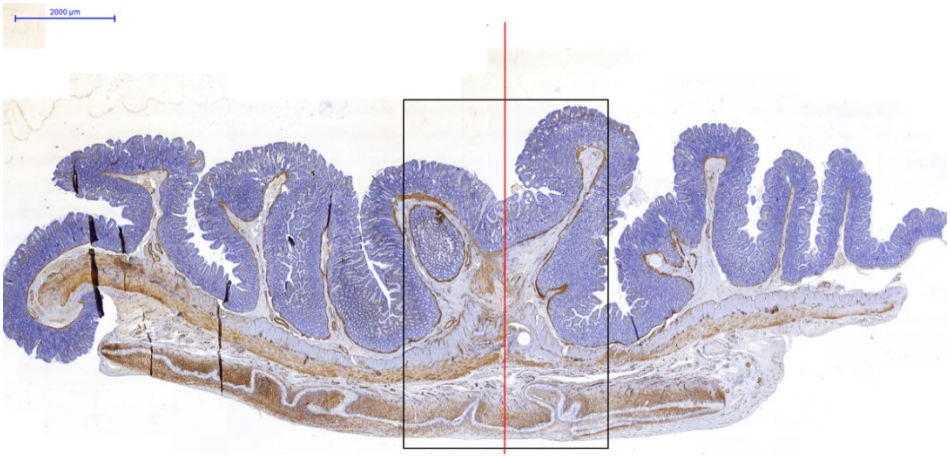

Figure 11: Blue trichrome staining of intestinal tissue in the site of anastomosis, the red line goes through the center of anastomosis, the black line marks the area where the stereological measurements were performed

Volume fractions of endothelial cells, of MAC387 positive cells and of collagen within the reference space were assessed by computerized software system (Stereologer, Stereology Resource Center). The microscope used was Nikon Eclipse Ti-U with, camera Promicra camera.

2.2.9 Statistical analysis

Standard frequency tables and descriptive statistics were used to characterize the sample data set. Adhesion scores were analyzed with respect to the group, quadrant and anastomosis position in the intestine (1st, 2nd, and 3rd) using repeated measures ANOVA, thus respecting the order and dependency of the three anastomoses sewn in each piglet. The same method was used to assess the differences between groups in collagen and von Willebrandt Factor

volume fractions. Volume fraction of MAC 387 was considerably affected by random presence of a stitch in some of the slides. Each piglet was therefore assigned one value for anastomoses with stitches (either the mean of all stitch-positive anastomoses, value of a single stitch-positive anastomosis or a missing value if no stitch-positive anastomoses were observed for that piglet) and one value for anastomoses with no stitches (defined analogically). Two-way main-effect ANOVA was then used to evaluate the differences in MAC827 in relation to group and stitch presence. All reported p values are two-tailed and the level of statistical significance was set at $\alpha = 0.05$. Statistical processing and testing were performed using STATISTICA data analysis software system (Version 12; StatSoft, Inc, 2013; www.statsoft.com).

2.3 Results A

Two types of biodegradable nanomaterials for anastomosis fortification testing were prepared by electrospinning, the PCL based sheets (Figure 12A) and the PLCL sheets (Figure 12B). The material was electrospun on the spun bond underlay that facilitated easy manipulation while using this material during the surgical procedure.

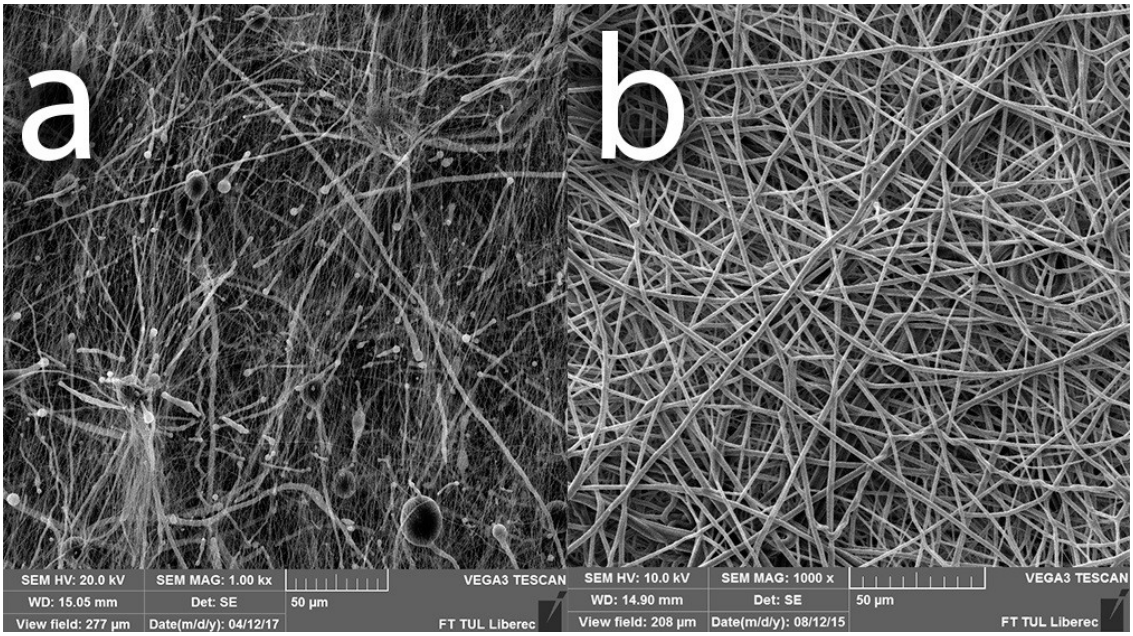

Figure 12: Scanning electron microscopy image of a) the PCL nanomaterial at 1000x magnification and b) the PLCL nanomaterial at 1000x magnification

We successfully created a model of intestinal anastomosis on pig with use of PCL and PLCL nanofibrous scaffolds. Both types of material are easy to peel of the spun bond underlay, they can be then easily manipulated with. They adhere to the intestine and hold well on the intestinal wall, yet they can also be rearranged when needed. No further fixation of the materials was necessary.

All animals survived the whole length of the experiment. None of the animals developed either ileus or sepsis. Two animals from the PCL group vomited single time, so the realimentation schedule was not respected in their case. It is worthy to note though they tolerated the feeding from then on. All animals from the Control group and the PLCL

group were able to feed according to the schedule, with daily stool and no signs of gastrointestinal passage blockage. The activity of the animals was not decreased in any of the groups throughout the postoperative observation. We did not notice any case of infection of intravenous port in the PCL group; one case of infection of the port appeared in the PLCL group, and two cases were in the Control group. We also noticed one laparotomy wound infection in one of the animals in the PLCL group in a form of an abscess. No intervention was needed.

There were no significant differences in the observed biochemical parameters between the groups and no remarkable deviations from healthy animals (baseline blood sample). All animals managed to maintain their weight within the range of 5% of their preoperative weight.

There were no signs of GI content leakage within the second surgery in any of the animals (free GI content, thick peritoneal fluid, fibrin films). All of the anastomoses could be found in the reoperation, the nanomaterial remained fixed, covering the suture line completely in all of them. It has been neither absorbed nor dislocated. All anastomoses were sufficient, no visible defects were found in any of them (Figure 13). PAs involving other organs than the small intestine were found in 3 animals from the Control group, in 5 animals from the PCL group and in 5 animals from the PLCL group. Most of these were adhesions of the left median liver lobe to the incision scar. The severity of PAs was largely variable within the groups. There was some amount of adhesions in almost all animals in the site of the surgery. Typically, the most adhesions were located within the area of the intestine we manipulated with, connecting the small intestine to the surrounding tissues, mostly only with the small intestine itself (Figure 14). The adhesions were relatively evenly spread within this area, not surrounding the intestinal circumference in the area of our material or suture line predominantly. The organs we did not manipulate with were usually adhesion-free. The perianastomotic adhesions were in all animals grade Zühlke 2 if present. The adhesions had to be separated by sharp dissection; no clear vascularization was macroscopically visible, though. Only one animal (from the PCL group) didn't develop any perianastomotic adhesions, this was recognized as grade Zühlke 0. The least adhesions according to our scoring system were found in the Control group, ranging from 2 points to 11 per animal (46 points

for 8 animals in total), then 66 points for the group PLCL in total (4-11 points per animal) and 79 points for group PCL (0-16 points per animal) (Attachment 3). Statistical analysis showed these differences between groups as non-significant (p=0.715). The position of the anastomosis (first, second or third) also proved not to be a significant factor (p=0.490) for the amount of adhesions. The most important parameter showed to be the segment of anastomosis while the inner segments (2 and 3) did not show a lot of adhesions, the segments 1 and 4 tended to be heavily adhered (p<0.001).

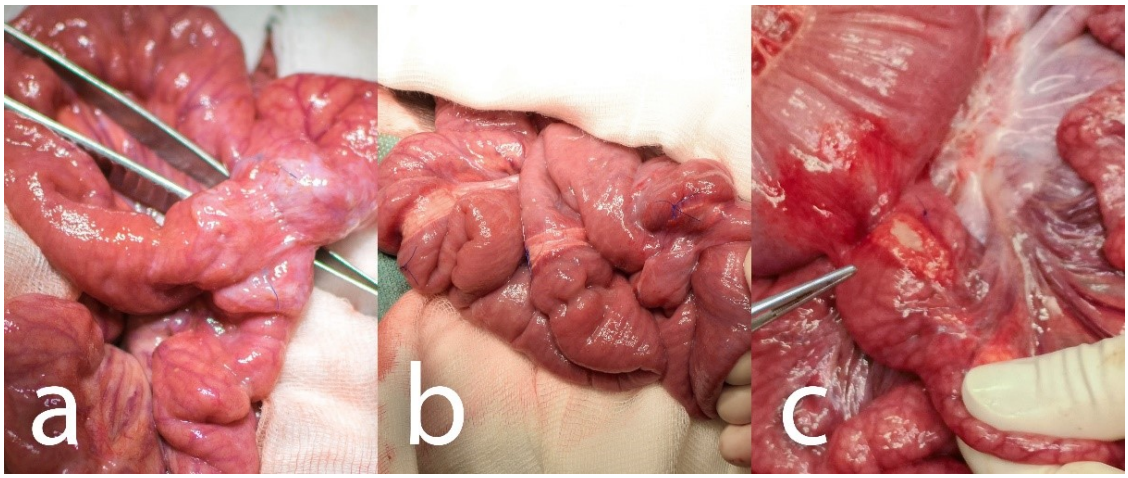

Figure 13: Macroscopic findings in animals of different groups: a) Control group, two anastomoses adhered together, oral parts are marked with a blue suture; b) PCL group, all three anastomoses are visible, the material is clearly visible in the site of application; c) PLCL group, pointing at one of the anastomoses adhering to the colon

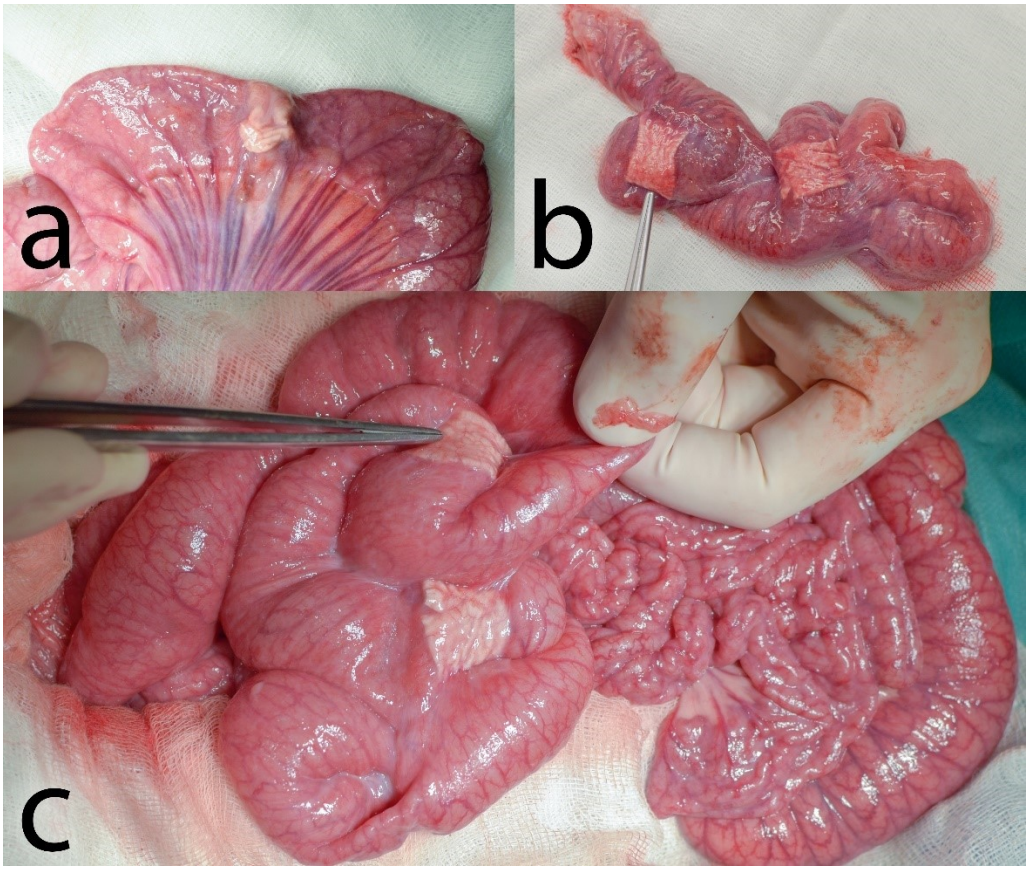

Figure 14: Anastomoses after 3 weeks: a) typical appearance of the small intestine on the 21st postoperative day (PCL group); most of the intestine seems intact with no adhesions, the segments involved in anastomoses are more or less in adhesions, the diameter of the intestine is larger in the proximal segments of the intestine; the material is clearly visible and not dislocated; b) severe adhesions in another animal from the PCL group; c) adhesion free intestine in a different animal from the PCL group

Almost all animals exhibited some level of dilation of proximal segments of the small intestine; we observed it in all 8 animals in the PLCL group, in 7 animals in the PCL group, and also in 7 animals in the Control group (Table 4). Nevertheless, the difference between the groups was not statistically significant.

*Table 4: Summary of the most important results for each group. *Each animal was assigned a score equal to the average of all segment scores in that animal (i.e. 24 segment scores per animal; result theoretically ranging from 0 to 2). Mean and Standard error of the mean (SEME) stated in the table were then calculated from these animal averages.*

	Control Group (n = 8)	**PCL Group (n = 8)**	**PLCL Group (n = 8)**	***p*-value between groups (test)**
Material fiber thickness	-	325 ± 36 nm	2047 ± 585 nm	-
Material thickness	-	49 ± 5 nm	53 ± 6 nm	-
Macroscopic signs of anastomotic stenosis (count; %)	0; 0%	0; 0%	0; 0%	-
Macroscopic signs of anastomotic leakage (count; %)	0; 0%	0; 0%	0; 0%	-
Mean PAAS score per segment (0–2) (mean ± SEME across pigs)*	0.479 ± 0.086	0.823 ± 0.171	0.688 ± 0.070	0.715 (repeated measures ANOVA)
Incomplete re-epithelisation (count; %)	0; 0%	0; 0%	0; 0%	-
Volume fraction of vWF positive cells [%] (mean ± SEME)	2.22 ± 0.10	2.16 ± 0.16	2.38 ± 0.12	0.690 (repeated measures ANOVA)
Volume fraction of collagen fibers [%] (mean ± SEME)	15.51 ± 2.10	15.67 ± 2.36	11.87 ± 1.91	0.740 (repeated measures ANOVA)
Volume fraction of MAC387 positive cells [%]: -stitch not in sample (n: mean ± SEME) -stitch in sample (n: mean ± SEM)	8: 0.38 ± 0.09 7: 0.80 ± 0.23	8: 0.46 ± 0.19 5: 0.67 ± 0.16	8: 0.21 ± 0.06 6: 0.70 ± 0.27	0.550 (two-way ANOVA)

The material was washed out of the sections during the histological staining process. The presence of the material could be detected on the sections as an empty space surrounded by granulation tissue with a borderline of tissue permeated with empty spaces in the form of single fibers (Figure 15). We observed no morphological abnormalities in standard histological stainings (Figure 16), all physiological layers were present in all samples. Also the successful reepithelization was found in all samples.

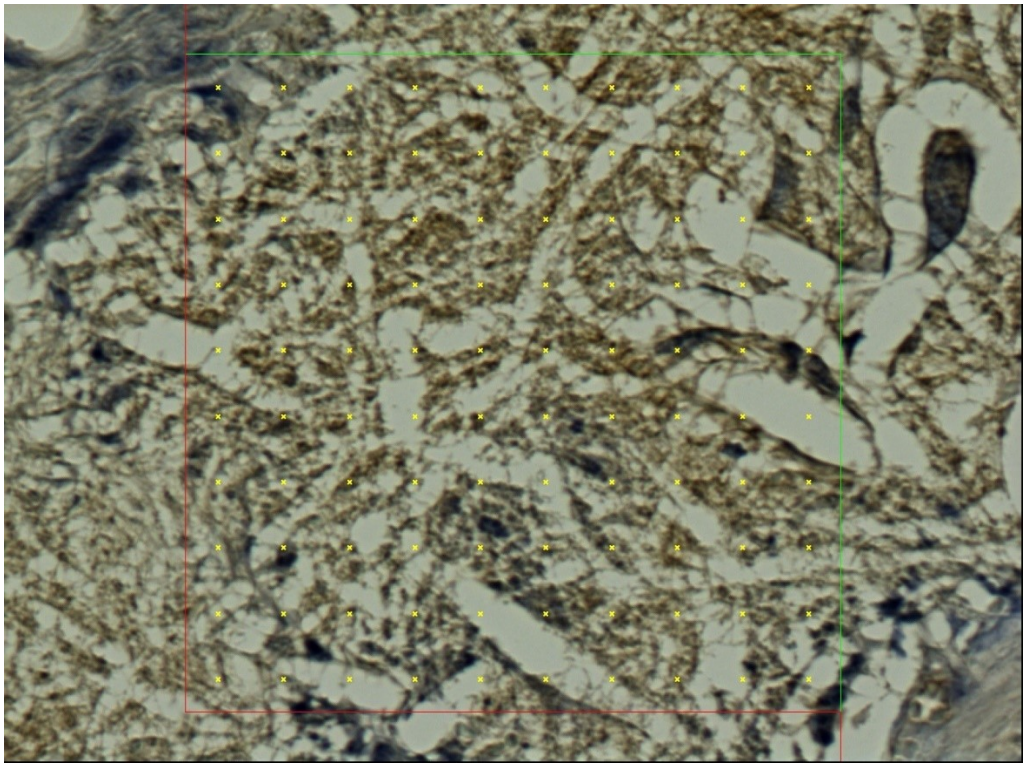

Figure 15: Histological section, PCL group, MAC387 staining: Detail of the marginal zone of the material applied, the empty spaces in the shape of the fibers (stereological grid)

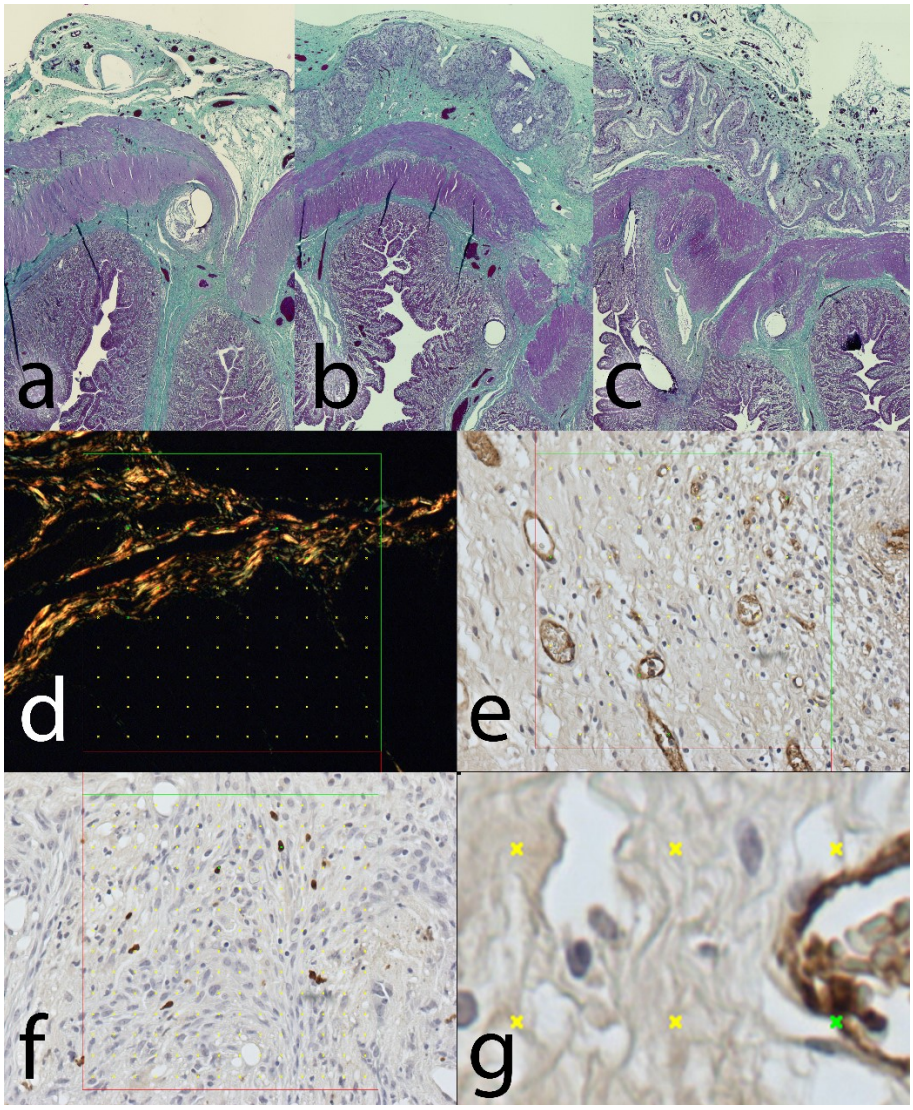

Figure 16: Histological staining of explanted anastomoses: a) Green trichrome: Control group; b) Green trichrome: PCL group, the empty space on the site of application of the nanomaterial can be seen in the upper layer, surrounded by normal granulation tissue; c) Green trichrome: PLCL group, a much thinner empty area can be seen in the upper layer, also surrounded by normal granulation tissue; d) PSR staining, collagen fibres stained yellow, stereological mesh; e) vWF factor staining, the endothelial cells stained brown, stereology grid; f) MAC 387 staining stereology, positive cells stained blue, stereological grid; g) magnification of vWF staining stereology with a positive cross in the upper right corner.

The volume fraction of von Willebrand factor positive cells (endothelial cells) did not show statistically significant differences between the groups (p=0.690) (Figure 17 b), nor did the volume fractions of collagen (p=0.740) (Figure 17c) and neutrophiles with macrophages (p=0.550) (Figure 17d).

The section areas containing suture material exhibited significantly higher level of inflammatory cells infiltration than the stitch free sections (p=0.001) (Figure 17e) (Attachment 4).

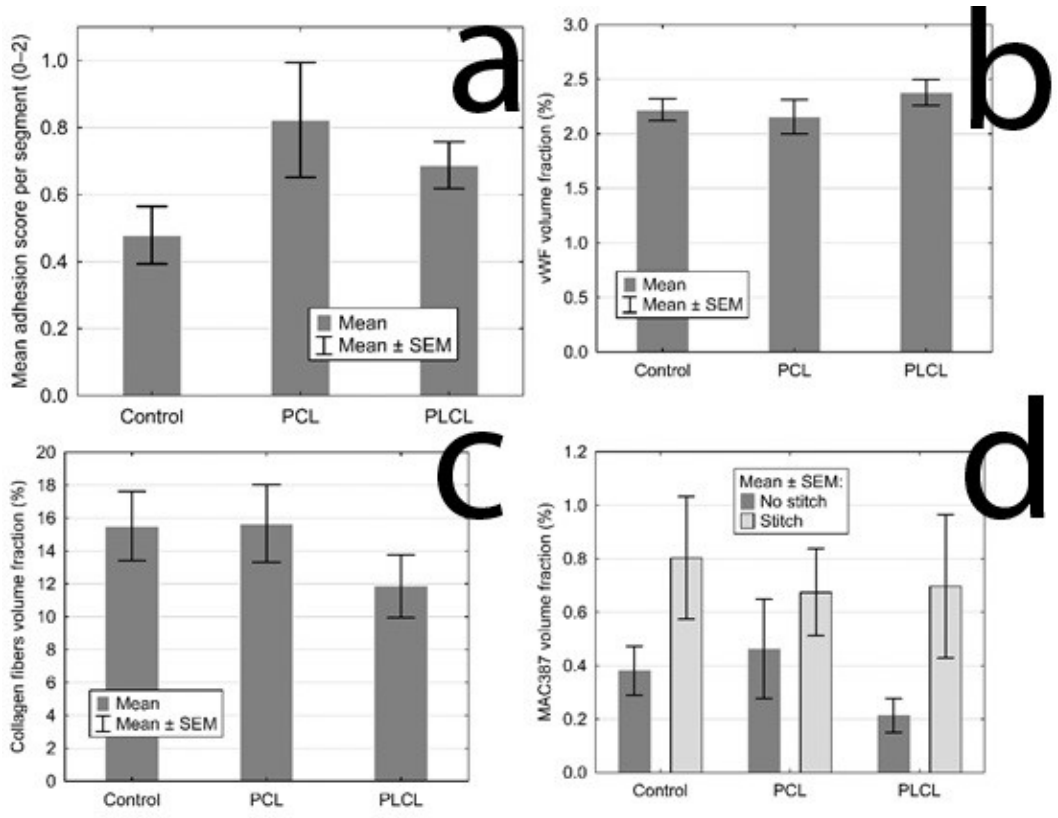

Figure 17: Statistical analysis of quantitative assessment of different parameters: a) The mean adhesion score for each group, the control group scored the lowest with no statistical significance; b) The volume fractions of vWF positively stained area for each groups showing the level of vascularisation, the three groups show the same quality of scar in this aspect; c) The volume fractions of collagen fibres for each group, the three groups show the same quality of scar in this aspect; d) The volume fractions of MAC387 positive area for each group, showing the inflammatory cells infiltration, the presence of a stitch in the section proves to be the only statistically significant factor, the three groups show the same quality of scar in this aspect as well

2.4 Discussion A

To the best of our knowledge, we were the first to use the PCL and PLCL nanofibrous scaffolds in this kind of application. We successfully designed a study to determine whether the material can be used for this purpose. There have been experimental works focusing on utilization of different locoregional types of protection in the site of intestinal anastomosis (103,106,138–143), yet no use of nanofibrous scaffolds has been described so far.

We found the material to be very easy to handle and to apply onto the intestine. The fact that there is no need of further fixation to the viscera is very positive as the application form can be a limiting factor when it comes to translation into the clinical practice. The fibrin glue could be an example of material that unnecessarily prolongs the surgery time as it needs to dry for 10 minutes before the surgeon can reinsert the viscera into the abdominal cavity (142,144).

We had no mortality in our study and also no major complications. There were also no clinical changes observed that would suggest development of sepsis or ileus, and the animals managed to maintain their weight; therefore we assume the material does not contribute to postoperative GI obstruction. Most patients develop an anastomotic leakage within the first 2 weeks after the surgery (108,145), we covered three postoperative weeks of observation.

Nordentoft experimented with fibrin coated collagen patches (TachoSil, fibrin sealant) in a pig model of intestinal anastomosis. Two anastomoses per animal were performed on the small intestine after a resection of 2 cm of the intestine. There were no significant differences between the experimental and the Control group in this study in terms of morbidity, mortality and sings of anastomotic leakage as well (138). In the second study the usage of the same material on a colonic anastomosis showed notable reduction of anastomotic leakage (146). However, when it comes to clinical use of this material, the fibrin glue does not seem to promote healing as the same authors stated in their review article including 28 studies, only 7 of which revealed a positive effect of the glue (147). Recently, a clinical study was designed to determine the effect of TachoSil patch in human patients (139). The study subjected the patients after resection surgery for colorectal cancer

to application of the patch over the constructed anastomosis on the large intestine, but was terminated after each of the first eight patients met with complications of different severity. The study concluded that the microbiome of the anastomosis is altered negatively by covering the anastomosis with any kind of material, but did not support this hypothesis with any data (139).

According to macroscopic findings we can describe the anastomoses from our experiment as well healed. Moreover, we did not observe any morphological changes either in the surrounding tissues or in the whole abdominal cavity, and thus the material seems to be safe to use. The question of the degradation speed remains unanswered at this moment as the material used was always present in the place of application at the end of the experiment. This suggests the material does not have a tendency to slip away but it is also not absorbed as fast as expected. For example a complete reabsorption of the fibrin glue has been described after variable periods ranging from 7 to 20 days (142).

We used the very new Perianastomotic adhesions amount score we developed, which accurately describes the quantity of adhesions in the site of an anastomosis on a circular hollow viscus. Some of the systems used in clinical practice consider also the quality of the adhesions, however they evaluate the whole abdominal cavity (68,72). We did not aim to evaluate the quality macroscopically and mechanically as we assessed the tissue histologically.

The differences in the amount of PAs between the groups were not significant, which can be due to a small size of our experimental groups. The absolute numbers suggest the material increases the amount of PAs in its' surroundings. This can be caused by easy infiltration

of the material by peritoneal fibroblasts from both sides of the material because of its structure similar to extracellular matrix as Srouji described earlier (148). There was also certain amount of adhesions involving different organs than the small intestine, but there was no clinical manifestation associated with those that we know about.

The amount of postoperative adhesions in the peritoneal cavity has been successfully decreased both experimentally and clinically using different substances, usually in a form

of gel. Hyaluronic acid based gels or also polycaprolactone based gels can serve as examples (69,149–151); however, the influence of such materials on the anastomotic healing has not been described and therefore cannot be considered safe in our application.

A very important factor for the formation of adhesions is the material the viscera are manipulated with. Dry swabs damage the peritoneum, cause inflammation and, consequently, adhesion formation (75). We used wet swabs throughout our experiment. The formation of adhesions should be finished by the end of the three week observation period (although their characteristic may change during the time after this period and the problems they cause can appear much later (34). To evaluate the clinical impact of all the adhesions formed a longer observation period would be needed.

Even though the materials were dissolved during the process of histological staining, the area of application was clearly visible under a microscope as a tissue-free layer. We followed a standard system of assessment of the healing of an intestinal anastomosis described in different studies (141). No morphological or any other statistically significant differences were found between the groups using this system. We value this result as positive since we assume that the healing process was not affected in a negative way and that the resulting scar is of the same quality as a physiologically healed one. The system does not evaluate peritoneal adhesions formation, though. As the peritoneal adhesions are certainly a source of many possible complications, their evaluation should be part of an anastomotic healing assessment.

A positive clinical effect could be more pronounced in different experimental settings. Fibrin glue, for example, has been tested in an animal model of complicated colonic anastomosis (severe blood loss, peritonitis), where it showed a positive effect in terms of decreasing morbidity and mortality in the period of 10 postoperative days. The histological assessment of the scar tissue however showed no significant differences between the Control group and the Experimental group on 10th postoperative day measuring also volume fractions of collagen fibers, vWF positive cells and inflammatory reaction (152) (similarly to our results).

A baseline biopsy has not been taken as no intestine was resected. It can be considered a certain limitation of this study. No clinical nor laboratory signs of any pathologies were, however, evident in our animals and no signs of pathologies were found in the final histological specimens either.

Biocompatibility of the materials used in our study was demonstrated by the presence of the granulation tissue of normal quality (according to all measured qualities) surrounding and invading the material. The level of biodegradation was not to be measured quantitatively as the degradation process of these nanomaterials was described in previous work (137).

All laboratory findings were within the physiological range, which suggests that the material does not cause any systemic disturbances. This was expected because the polymers used for the fabrication of the materials have been in use in clinical medicine for many years. For more discriminating results a study on a complicated anastomosis should be performed as shown in the works of Tebala et al. (153), Zilling et al. (144) and Adas et al. (154).

2.5 Conclusion A

We successfully demonstrated that the use of the PCL and PLCL nanofibrous scaffolds in an attempt to fortify an anastomosis on the GI tract is safe. The scaffolds did not influence the amount and quality of scar tissue in the site of anastomosis, and at the same time they did not cause any other kind of complication during our study. They seem to slightly raise the level of adhesions in the site of application, which corresponds to the statement that they promote healing. To be able to assess the adhesion level, we developed and used a novel scoring technique. The material appears to us as a practical and versatile supporting material potential of which can be further enhanced for example by adding substances supporting healing like growth factors, antibiotics etc.

The large variability of settings of the fabrication process allows further changes of the material properties. For the potentially pro-healing qualities of the material either the PCL or PLCL will be further studied by our team and used as an inner layer of a new double layered patch with an antiadhesive external layer.

3 Experiment B

(Polyvinyl alcohol-polycaprolactone double layered nanofibrous patches for prevention of anastomotic leakage and formation of extensive peritoneal adhesions in model of defective anastomosis on the small intestine of a pig)

3.1 Aims and hypotheses B

Aim 1: To create composite double-layer planar versions of nanofibrous material made

Aim 2: To apply the composite double-layer planar materials on a defective anastomosis on the small intestine

Aim 3: To create a scoring system for the level of integrity of the intestinal wall in the site of anastomosis on the gastrointestinal tract

Hypothesis 1: The PCL/PVA1 patch decreases extensive adhesions formation in the site of anastomosis

Hypothesis 2: The PCL/PVA2 patch decreases extensive adhesions formation in the site of anastomosis

Hypothesis 3: Application of the PCL/PVA1 patch to an intestinal defective anastomoses results in higher intestinal wall integrity

Hypothesis 4: Application of the PCL/PVA2 patch to an intestinal defective anastomoses results in higher intestinal wall integrity

3.2 Methods B

3.2.1 Methodological background

As the results of the previous phase of our research suggested that the polycaprolactone nanofibrous patches do not negatively alter the healing process of normal intestinal anastomoses, we intended to study similar materials further. Our general idea was to create a special patch with different properties of outer and inner layer. While the inner layer should support the healing process and serve as a cellular scaffold, the outer layer should prevent formation of peritoneal adhesions in the site of anastomosis. A barrier strategy is one of the most successful in prevention of formation of peritoneal adhesions in currently used products. Our idea was to reach low tendency to adhere to surrounding tissues by creating a hydrophobic surface on the outer layer. This strategy was successful for example in hydrophobic meshes for abdominal wall repair (155). Polyvinyl alcohol is a well-tolerated biocompatible biodegradable polymer (as written in chapter 1.6.). It was clear from our pilot test, that it would be an ideal polymer for fabrication of hydrophobic material.

The type of model limited the results of the experiment A, the intestinal healing was perfect in all anastomoses and we were not able to distinguish a positive effect on the healing process or prevention of anastomotic leakage if existing. Therefore, another goal of the second phase of our project was to study the impact of our materials in terrain of defective anastomotic healing. We created a model with small defect in the anastomotic suture that would be recognizable by the following histological assessment yet small enough to make the model clinically relevant.

3.2.2 Development of materials

Double-layered PCL/PVA nanofibrous patches were prepared in two variants differing in the degree of hydrolysis of the PVA component. The solution of PVA with high degree of hydrolysis (PVA1) was prepared by diluting the commercially available solution of 16% PVA Mowiol ® (M_w 125.000 g/mol, 98.0–98.8% hydrolysis, Sigma Aldrich, St. Louis, MO, USA)

in ethanol (Penta Chemicals, Prague, Czech Republic) and deionized water (1:4 volume fractions) in a final concentration of 10% w/w. PVA Mowiol® (M_w 130.000 g/mol, 88% hydrolysis, Merck, Germany) was used to prepare aqueous solution of the PVA with low degree of hydrolysis (PVA2) in a final concentration of 12% w/w. Polymeric granulate of PCL (M_w 43.000 g/mol, Polysciences, Germany) was dissolved in chloroform, acetic acid and ethanol solution (8:1:1 volume fractions) in a concentration of 16% w/w.

The double-layered nanofibrous mats were prepared using the needleless electrospinning device Nanospider™ 1WS500U (Elmarco, Czech Republic) by the method of sequential electrospinning. Firstly, the hydrophilic layer of PVA1 or PVA2 was created. The PCL fibers were then deposited directly on the previously electrospun PVA1/PVA2 layer. Scanning electron microscopy (PHENOM™, Fei Company, Oregon, USA) was employed to evaluate the structure of the materials. We followed the same protocols as described in Experiment A.

3.2.3 Experimental design

We randomly allocated 24 healthy male and female Prestice black-pied pigs into 3 groups, 8 animals each. A defective anastomosis on the small intestine was constructed in all animals. Animals in experimental groups PCL/PVA1 and PCL/PVA2 received one of the two types of reinforcing material (respecting the group) and the animals in the Control group remained with uncovered anastomotic defect. The animals were observed for 21 days. Sample collection, macroscopic and histologic assessments followed. Power analysis was performed to estimate the sample size (Attachment 5).

3.2.4 Surgical procedure

The animals were weighed prior to the surgery. Anesthesia was induced and maintained in the similar way as in the Experiment A including antibiotic prophylaxis.

A ProPort Plastic Venous Access System with PolyFlow polyurethane catheter (Deltec, Smiths Medical, Minnesota, USA) was implanted and introduced through one of the jugular veins as the first surgical procedure. The abdominal cavity was then approached via an upper

middle laparotomy. The small intestine was transected 70 cm from the duodenojejunal junction. All swabs used during the surgery were wet in order to prevent extensive formation of peritoneal adhesions. A hand-sutured end-to-end anastomosis was constructed with Monosyn 4/0 (Glycolide 72%, Caprolactone 14%, Trimethylencarbonate 14%) monophilament suture line (B-Braun, Germany) using seromuscular extramucosal running suture. An artificial defect on the antimesenteric side of the anastomosis with a standard diameter of 0.75 cm was created using a draining tube (Figure 18). The initial knot was always placed on the mesenteric side while the closing knot was placed about one quarter of the intestinal circumference from it. The position of the defect was marked with a single non-absorbable stitch placed orally to the anastomosis. A sheet of PCL/PVA1 or PCL/PVA2 material was placed onto the anastomosis and positioned to adhere to the intestinal wall and to cover the whole anastomosis with the defect (the hydrophilic PVA side facing the intestine) (Figure 19). The viscera were placed back to the abdominal cavity and the abdominal wall was reconstructed. All surgical procedures were performed by the same surgeon.

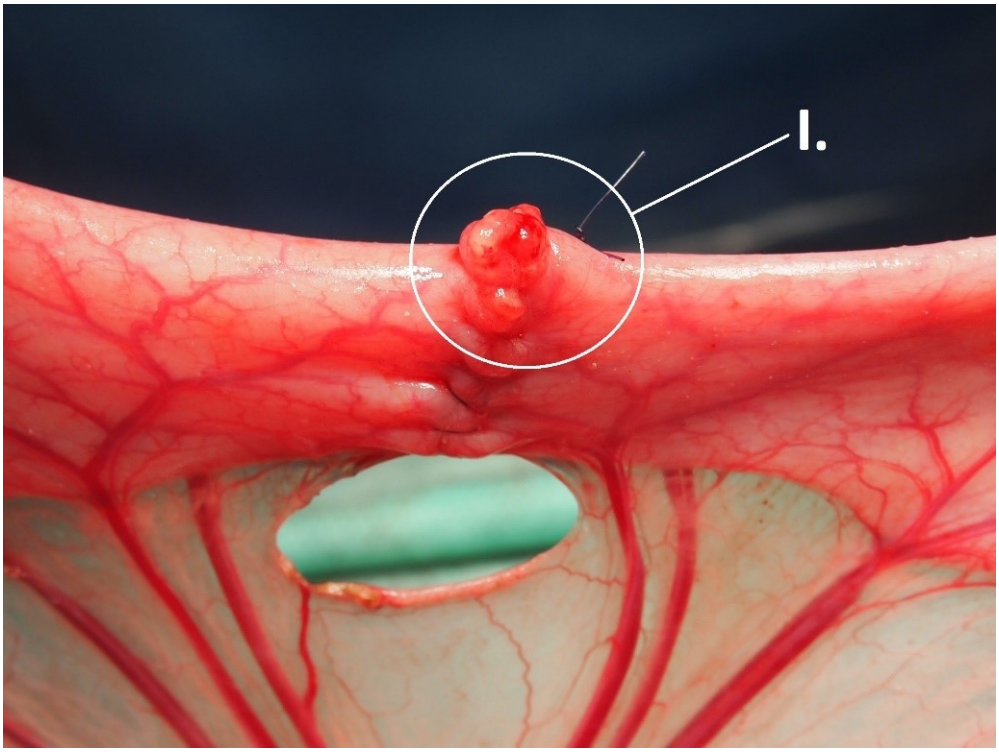

Figure 18: An intestinal anastomosis with a defect on the antimesenterial part (I.)

The animals were observed for three weeks following the surgery and fed according to pre-defined re-alimentation scheme. Their ability to feed according to the schedule was recorded alongside any clinical changes, signs of GI obstruction, abdominal diameter enlargement, stool frequency, vomiting, and body temperature elevation.

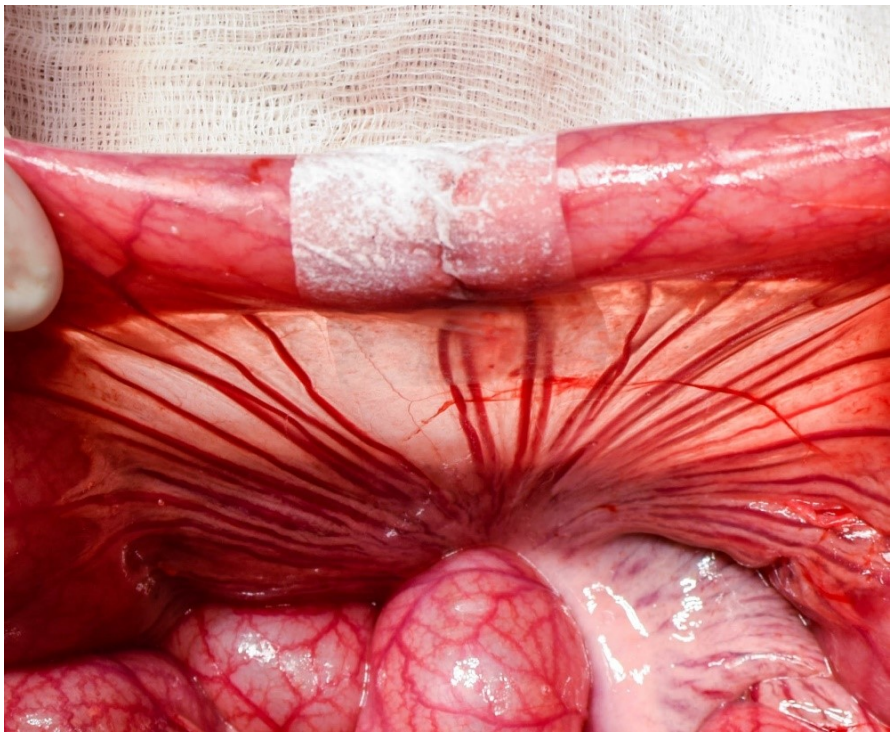

Figure 19: A defective intestinal anastomosis covered with a nanofibrous patch

3.2.5 Follow-up

Blood samples were taken during the experiment at five time points: on day 0 before the application of the material, exactly two h after the application of the nanomaterial, on the 7th POD, on the 14th POD, on the 21st POD. Basic biochemical parameters were tracked in these samples (bilirubin, GGT, ALT, AST, ALP, albumin, urea, and creatinine) to observe deviations in the animals' metabolism. The weight of the animals was also measured in defined

time points: preoperatively at the beginning of the experiment, on the 3rd, 7th, 14th, and 21st POD.

After the observation period, the following exploration and sample collection surgery was performed under general anesthesia. The abdominal cavity was searched for signs of any complications, intestinal matter, the GI tract checked for signs of obstruction (intestinal wall thickening, intestinal diameter enlargement, intestinal adhesions causing convolutes and sharp bents of the intestine, strictures of the intestine in any location and strictures of the anastomosis itself). Organs involved in adhesions in the rest of the abdominal cavity were also noted. Afterwards, the specimen of the anastomosed intestine was collected including the surrounding adhered tissues; photodocumentation was acquired. The animals were sacrificed after sample collection.

The collected intestine was transected longitudinally on the mesenteric side, pinned onto a cork underlay and the adhesions present on the site of the anastomosis were scored using the Perianastomotic adhesions amount score developed for the Experiment A. PAAS allows for the quantification of the extent of adhesions at the anastomotic circumference (156). The specimens were then fixed in 10% buffered formalin after collection.

3.2.6 Histology

Five 5 mm thick strips of tissue were cut from each specimen perpendicular to the line of the anastomosis. All specimens were processed by standard paraffin technique. Four µm thick sections were stained by hematoxylin and eosin for comprehensive overview. These samples were investigated both qualitatively and semiquantitatively. A semiquantitative scoring system has been designed to evaluate the integrity of the intestinal wall at the site of the anastomotic defect. Each layer was assessed separately using defined parameters. Each layer was assigned a score ranging from 0 to 0.25 and the scores of all four layers were then summed. The resulting sum (anastomosis integrity score) represents a measure of the deterioration of intestinal wall integrity ranging from 0 (fully defective healing) to 1 (perfect healing) (Table 5). A full-thickness defect in the intestinal wall of the specimen was considered a proof of microscopic anastomotic leakage.

Table 5: IWIS system for histological anastomotic specimens

Layer	Points	Finding
Mucosa	1/4	Completely re-epithelized
	0/4	Incompletely re-epithelized
Submucosa	1/4	Completely healed
	0/4	Purulent infiltration, necrosis
Muscularis*	3/12	Without distance (≤ 0,09 mm)
	2/12	Distance from 0,1 to 1,99 mm
	1/12	Distance from 2 to 3,99 mm
	0/12	Distance over 4 mm
Serosa	3/12	Without purulent infiltration and necrosis
	2/12	Purulent infiltration and/or necrosis from the muscular layer to area of nanomaterial**
	1/12	Purulent infiltration and/or necrosis from the area of nanomaterial to the peritoneum **
	0/12	Purulent infiltration and/or necrosis passes to the peritoneum

**Distance between the two anastomosed muscle layers*
***Samples without nanomaterial were scored: score 3/12 for no purulent infiltration and necrosis, score 2/12 purulent infiltration and/or necrosis from muscular layer to half thickness of the serosa, score 1/12 for purulent infiltration and/or necrosis from half thickness of the serosa to the peritoneum and score 0/12 for purulent infiltration or necrosis in full thickness*

The blocks with the highest semiquantitative score were analyzed quantitatively. Five µm sections were stained using picrosirius red (PSR) for the assessment of the amount of collagen. Vascularization and inflammatory infiltration in the specimens were visualized by immunohistochemical methods. We followed the standardized protocol described in our previous study (156) (Experiment A).

3.2.7 Statistical analysis

Common descriptive statistics and frequencies were used to characterize the sample data set. Due to their non-normal distributions, the PAAS values, anastomosis deficiency scores, and histologically determined volume fractions were analyzed using Kruskal-Wallis ANOVA with respect to group. In case of a significant overall finding, differences between individual group pairs were assessed post-hoc using multiple comparisons of mean ranks according to Siegel and Castellan (157), including a Bonferroni adjustment for multiple testing.

All reported *p* values are two-tailed and the level of statistical significance was set at $\alpha = 0.05$. Statistical processing and testing were performed using STATISTICA data analysis software system (Version 12; StatSoft, Inc, 2013).

3.3 Results B

Material properties: Two composite nanofibrous materials were created with mean fiber thicknesses 550 nm/344 nm for PCL/PVA 1 and 652 nm/344 nm for PCL/PVA 2 (Figure 20). Both materials were very easy to peel the spunbond underlay and to apply onto the intestinal surface. The level of their adherence to the tissue was sufficient to leave the materials attached without any further fixation.

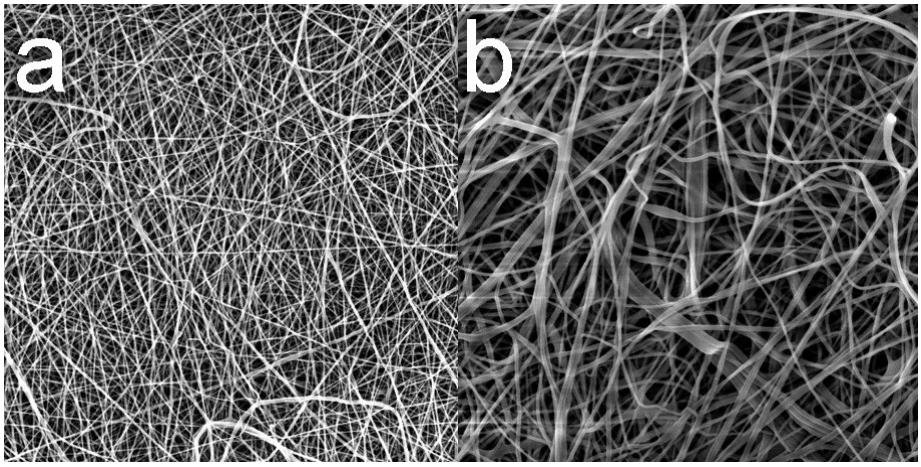

Figure 20: Scanning electron microscopy images of the two prepared materials; a) PCL/PVA 1 material; b) PCL/PVA 2 material

All animals survived through the whole experiment. Re-alimentation was unproblematic in only two animals from the Control group while all of the animals from the PCL/PVA1 and PCL/PVA2 groups were able to feed according to the schedule with no obstacles. Two animals from the Control group vomited once (on 5th POD and 11th POD).

Weight gain was achieved by 3 animals in the PCL/PVA1 group and 6 animals in the PCL/PVA2 group (Table 6). Most of the animals did pass stool daily, no animal developed gastrointestinal obstruction. No signs of sepsis or peritonitis were encountered (fevers, activity decrease, abdominal wall tenderness).

Table 6: Number of animals with weight gain and weight loss per group

Group	No. of animals having gained weight (3% tolerance)	No. of animals having lost weight (3% tolerance)
Control group (n=8)	1	5
PCL/PVA1 group (n=8)	3	4
PCL/PVA2 group (n=8)	6	1

There were no significant deviations from physiological parameters or statistically significant differences between the groups in any of the monitored parameters.

Only minor complications occurred throughout the experiment as there was no animal developing sepsis or signs of complete gastrointestinal obstruction in the whole experiment. There were two cases of infectious complications in the Control group (25%). One animal developed an abscess in the laparotomy wound without dehiscence and one animal developed infection in the tissues surrounding the central venous catheter. One of the animals in the Control group presented with abdominal diameter enlargement starting on the 17th POD and lasting for 3 days, but with no additional clinical signs, no vomiting, and no defecation problems. One animal from the PCL/PVA1 group (12.5%) developed an abscess in the laparotomy wound, no other complications were found in the group. One animal from the PCL/PVA2 group (12.5%) developed a small abscess in the laparotomy wound and another animal from the group showed a mild palpable rash on the abdominal wall from the 14th POD on. We observed no decrease in activity in any of the animals during the observation period.

All of the anastomoses in both experimental groups and the Control group were free of macroscopically visible defects on the 21st POD. There were no signs of anastomotic leak (no intraperitoneal intestinal matter, no intraperitoneal puss, no abscesses, no visible signs of peritonitis), nor signs of complete intestinal obstruction. However, some level of intestinal wall thickening was visible in the oral parts of the intestine in 2 animals from the Control group (25%), in 6 from the PCL/PVA1 group (75%) and in 5 animals from the PCL/PVA2 group (62.5%).

One animal from the PCL/PVA1 group showed a partial stenosis of the anastomosis reducing the intestinal diameter by less than one third (Table 7).

Table 7: Numbers of animals with different macroscopic findings. Proximal intestinal wall thickening value is given in numbers of positive animals. Partial anastomotic stenosis value is given in numbers of positive animals. Convolute value is also given by numbers of positive animals

Group	**Proximal intestinal wall thickening**	**Partial anastomotic stenosis**	**Mean PAAS**	**PAAS range**	**Convolute**
Control group (n=8)	2	0	2.63	0–5	3
PCL/PVA1 group (n = 8)	6	1	2.88	0–6	5
PCL/PVA2 group (n=8)	5	0	4.88	3–7	7

Small amount of clear peritoneal fluid was present in almost all animals in volumes smaller than 100ml. The nanomaterial remained fully attached at the place of application until extraction in 5 of 8 (62.5%) animals from the PCL/PVA1 group while it was partially dislocated in the remaining 3 (37.5%); it always remained covering the place of the defect though. The material was partially dislocated only in 1 of 8 animals (12.5%) in the PCL/PVA2group, also still covering the place of the defect.

We found a number of adhesions in the area of surgery in all animals except for one animal from the Control group (12.5%) and two animals from the CPL/PVA1 group (25%). The highest perianastomotic adhesions amount score (PAAS) was recorded in the PCL/PVA2 group with a mean PAAS of 4.88 points (3 to 7 points per animal), followed by the PCL/PVA1 group with a mean PAAS of 2.88 (0 to 6 points per animal) and by the Control group with

a mean PAAS of 2.63 points (0 to 5 points per animal) (Attachment 6). The adhesions were present not only at the location of the anastomosis itself, but usually also in its vicinity, both oral and aboral. An intestinal convolute (more than two segments of intestine adhered together) was present in 3 animals in the Control group (37.5%), in 5 animals from the PCL/PVA1 group (62.5%) and in 7 animals in the PCL/PVA2 group (87.5%) (Figure 21).

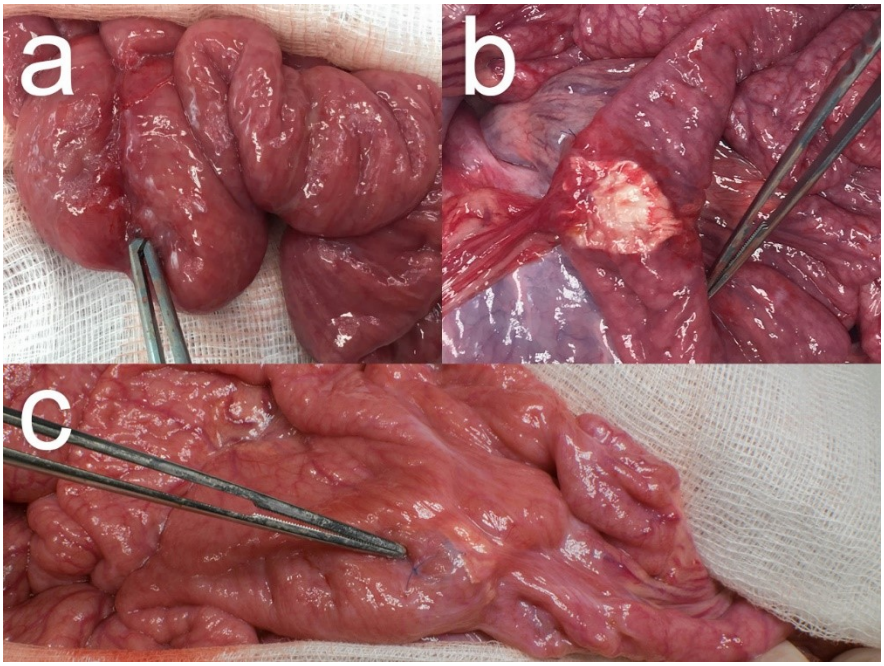

Figure 21: Examples of intraoperative findings, the forceps points to the anastomosis in all of the specimens; a) animal from Control group, well healed anastomosis, no defect is visible; b) animal from PCL/PVA1 group, the material is visible, a string of omental adhesion is attached to the anastomosis, no defect is visible; c) animal from PCL/PVA2 group, multiple adhesions of the anastomosed intestine, material is visible under a layer of peritoneum and peritoneal adhesions

No signs of full-thickness defects were visible in the comprehensive histologic assessment of the specimens. We observed complete re-epithelialization in the site of the anastomosis in 6 animals from the Control group, yet in no animal from the PCL/PVA1 group and in only one of the animals from the PCL/PVA2 group (Figure 22).

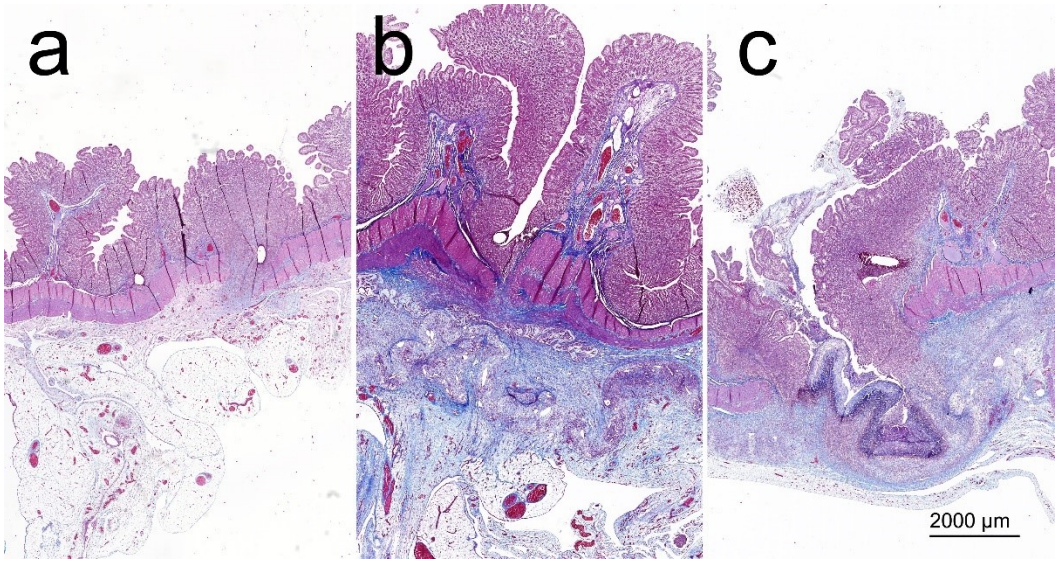

Figure 22: Specimens in blue–trichrome-stained comprehensive histological slides; a) example from the Control group; b) example from the PCL/PVA1 group; c) example from the PCL/PVA2 group

Anastomoses in the experimental groups showed significantly lower intestinal wall integrity according to our histologic evaluation system (Figure 23A)(Attachment 7).

The volume fraction of inflammatory cells (granulocytes, macrophages) in the tissue surrounding the anastomoses was highest in the PCL/PVA1 group, being significantly higher than in the Control group (p=0.0097) (Figure 23D). The volume fraction of inflammatory cells in the PCL/PVA2 group did not differ significantly from either the Control group or the PCL/PVA1 group (Figure23 D). Volume fractions of both endothelial cells (p=0.7063) and collagen fibers (p=0.6094) in the area of the anastomoses showed no significant differences between the groups (Figure 23B, Figure 23C) (Attachment 8). The applied nanomaterial was dissolved during the histological staining; however, the place of its application was visible in the histological slides. The two layers of PCL/PVA1 got separated during the follow-up period in all of the specimens (Figure 24).

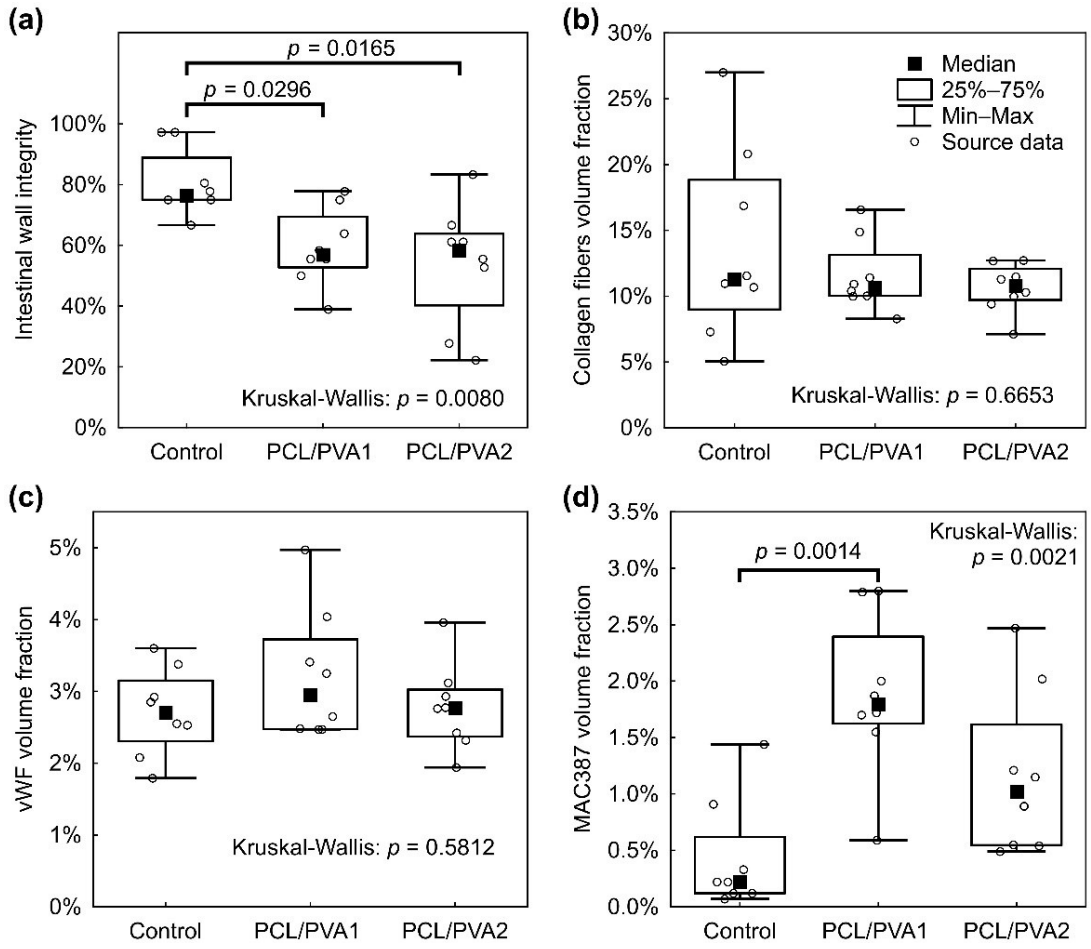

Figure 23: Results of histological evaluation in box plot graphs;
a) Anastomosis deficiency score; b) comparison of collagen fibers volume fractions;
c) comparison of vWF positive cells volume fractions; d) comparison of MAC387 positive cells volume fractions

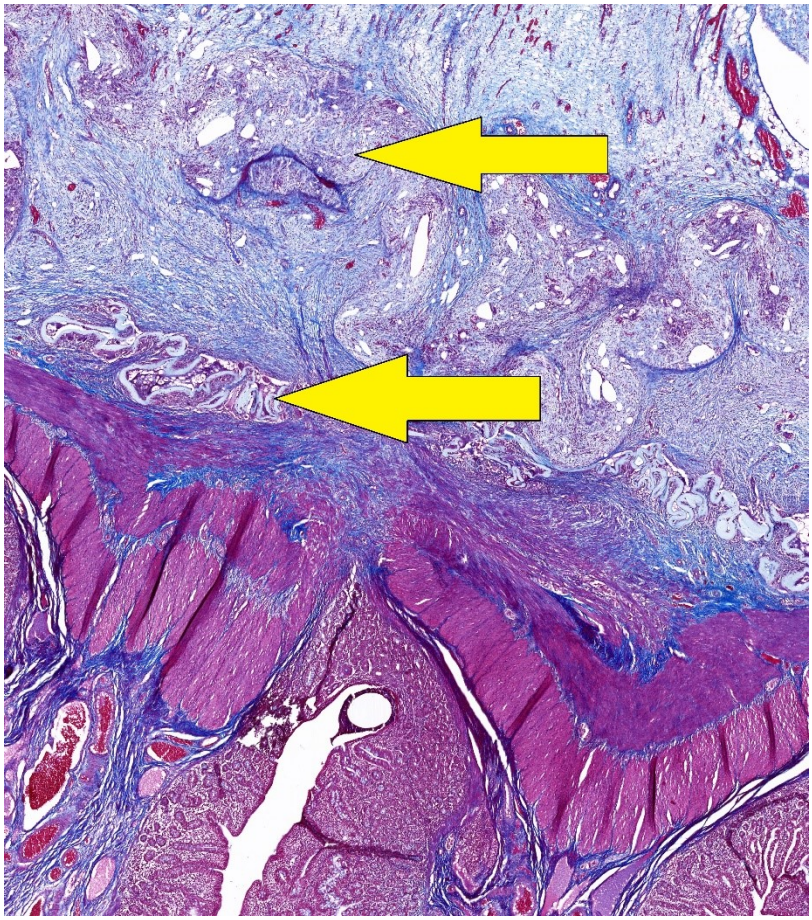

Figure 24: Washed out material imprint; A PCL/PVA1 specimen in blue trichrome staining, the two separated layers of the material are marked

3.4 Discussion B

The experiment successfully and thoroughly investigated basic features of the PCL/PVA1 and PCL/PVA2 microfibrous double-layered materials in relation to healing of a technically defective anastomosis on the small intestine of a pig. We adjusted the model of defective anastomosis designed by Testini et al. (104), where anastomotic leakage was reached by creating a 2.5 cm large defect. We, however, created rather smaller defects, which we consider to be more clinically relevant.

Polyvinyl alcohol and polycaprolactone are well-explored polymers known for their biocompatibility and biodegradability. They are routinely used as biodegradable surgical materials with no known adverse effects (158,159). Both presented materials were easy to use and their application did not require any further fixation, which is a valuable aspect not achieved by many other supporting materials (112,160).

There were no major complications and the animals from the experimental groups showed better postoperative weight gain. According to these observations, we conclude that the materials had no adverse effects on the clinical condition of the animals. It is hard to determine to what extent the rash in the one animal from the PCL/PVA2 group was associated with the application of the material (161,162).

It remains unclear whether the materials influence the risk of AL. The material remained at the application site covering the defect in all cases, however, it is questionable whether it could keep the intestinal mass contained underneath and thus prevent the manifestation of AL. A model of defective anastomosis on the large intestine would possibly bring more distinct results (112), however, we intended to test the material first in a model without bacterial contamination for easier assessment of the results. The number of bacteria in the small intestine is minimal compared to the large intestine (163,164).

We consider both materials pro-adhesive according to the obvious macroscopic findings and our scoring system (PAAS). We did not observe any clinical impact of the formed peritoneal adhesions. However, the manifestation of clinical problems due to PAs is not time-limited to the postoperative period, the 3-week observation is insufficient for definite

conclusions. A possible combination with other anti-adhesives is an option worthy of further exploration as the data regarding the safety of their use in gastrointestinal surgery is limited (165). In our study, the material of the outer layer was chosen for its hydrophobicity, which we considered a key factor for adhesion prevention as it has been presumed that the formation of peritoneal adhesions is determined by the level of contact of the two adhering surfaces (166). The materials developed by our team were tested for hydrophobicity prior to this study, and the PVA nanomaterials were shown to be hydrophobic, yet the two materials proved pro-adhesive when tested in our experiment.

We created and used a new system for the evaluation of intestinal wall integrity at the site of anastomosis on the gastrointestinal tract. It evaluates the integrity of each layer separately, thus making the evaluation of anastomotic healing more precise. In combination with stereological quantitative techniques such as PAAS and Zühlke's grading, it forms probably the most complex evaluation system for anastomotic healing according to our literature searches.

According to our intestinal wall integrity evaluation, the histological assessment suggests inferior healing quality when the material is applied. The PCL/PVA1 group showed higher inflammatory reaction, yet other parameters did not differ significantly from the Control group. The higher inflammatory infiltration could, however, suggest an ongoing healing process. Inflammation is a driving mechanism for cellular proliferation of peritoneal fibroblasts, smooth muscle cells and also intestinal epithelium (166–169). Results of the PCL/PVA2 group were not statistically different from those of the Control group in any of the three monitored aspects. No abnormal vascularization, no abnormal collagen production or inflammation were observed as a reaction to the presence of the material, which is considered normal anastomotic healing (34). Even though the integrity of the intestinal wall was significantly lower in the experimental groups, connective tissue surrounding the material residues was visible in all of the specimens, covering the place of defect. It is possible that in this way the material kept the luminal contents from leaking into the peritoneal cavity.

It is not possible in our settings to distinguish the direction of the healing process. Complete healing ad integrum or manifestation of AL seem both real possibilities for future development in the experimental groups. The same holds for possible occurrence of anastomotic strictures. Sounder results could be acquired in a longer observation period. This is a certain limitation of the study.

We decided not to perform mechanical tests to investigate bursting pressure or similar parameters as there is no evidence for the relation between the results of these and the risk of AL (170). Such tests can also compromise the quality of the samples for later histologic evaluation. Biodegradability tests were not employed in our study as this parameter was already studied for PCL and PVA (137,171).

Both materials exhibited mixed results in the study. The healing quality seems to be compromised when compared to the previous study with polycaprolactone nanofibrous material (156). It is a question whether the change of the characteristics of the material or the change of experimental settings (or possibly a combination of both) can be blamed. The materials need to be studied further after specific adjustments of their properties in new experimental settings in order to fully determine their clinical potential, probably with even more hydrophobic materials.

3.5 Conclusion B

We were the first to propose a double layered nanomaterial for prevention of both anastomotic leakage and peritoneal adhesions. Both materials tested in our study did not have negative effects on clinical results in the postoperative period. No major complications appeared. Macroscopic findings suggest that both materials are pro-adhesive. Histological assessments of the specimens confirmed no microscopic signs of anastomotic leakage. The specimens from the control group were more completely healed according to our intestinal wall integrity score. However, the material always remained covering the defect and no anastomotic leakage developed. We intend to further investigate the possibility of using nano- and microfibrous materials to determine their clinical impact.

4 Experiment C

(Ultrafine polycaprolactone nanofibrous patch for anastomotic healing support in a model of defective anastomosis on the large porcine intestine)

4.1 Aims and hypotheses C

Aim 1: To create ultra-fine planar version of nanofibrous material made of polycaprolactone

Aim 2: To study biocompatibility of such material *in vitro*

Aim 3: To apply the ultrafine nanofibrous PCL material on the anastomosis on the large intestine

Aim 4: To investigate the impact of the material on the risk of anastomotic leakage, anastomotic healing and on formation of peritoneal adhesions in the site of intestinal anastomosis

Hypothesis 1: The ultrafine polycaprolactone patches are biocompatible according to *in vitro* test

Hypothesis 2: Application of the ultrafine polycaprolactone patch to a defective large bowel anastomosis results in higher intestinal wall integrity

Hypothesis 3: The material does not support formation of extensive peritoneal adhesions when applied to a defective anastomosis on the large bowel

4.2 Methods C

4.2.1 Methodological background

A healthy peritoneum is a well-perfused metabolically active structure capable of relatively high metabolic exchange with its surroundings including both peritoneal fluid and other viscera and neighboring peritoneal surfaces (172,173). Based on the results of our previous experiments and on the presumption that a certain level of metabolic exchange between the sutured intestine and the surrounding peritoneal surfaces is needed to maintain the healing process rather than creating a sealed barrier, we decided to create a very fine porous nanofibrous patch. Such a patch should allow this metabolic exchange while maintaining the pro-healing properties of a nanofibrous mesh we proposed in the previous studies (156). The process conditions for fabricating a material with a low surface density were optimized via needleless electrospinning. According to our knowledge, our study is the first to propose the idea of a porous anastomotic patch for healing support that should not act only as a mechanical barrier, but support the healing process of the intestinal anastomosis. We intended to develop such a patch into a product that could be routinely used in colorectal surgery for healing support in either all or high risk anastomoses. In the Experiment C we aimed to develop an ultrafine porous polycaprolactone nanofibrous patch, use it in a perfected model of complicated anastomotic healing on the large intestine, and further develop current assessment methods for evaluation of anastomotic healing in experimental settings.

4.2.2 Material preparation

The mixture of 16% w/w PCL (Mw 45 000 g/mol, Sigma Aldrich, USA) in chloroform/ethanol/acetic acid in ratio 8/1/1 (Penta Chemicals, Czech Republic) was stirred 24 h until complete dissolution of the PCL granulate. Subsequently, the solution was electrospun using the needleless Nanospider^{TM} 1WS500U electrospinning device (Elmarco, Czech Republic) (Figure 25). The environmental parameters such as the relative humidity

and temperature were controlled via the climatic system NS AC150 (Elmarco, Czech Republic). The nanofibers were collected on a polypropylene spunbond substrate. The process parameters were optimized to produce a nanofibrous layer with low surface density, namely 10 g/m^2 (Table 8).

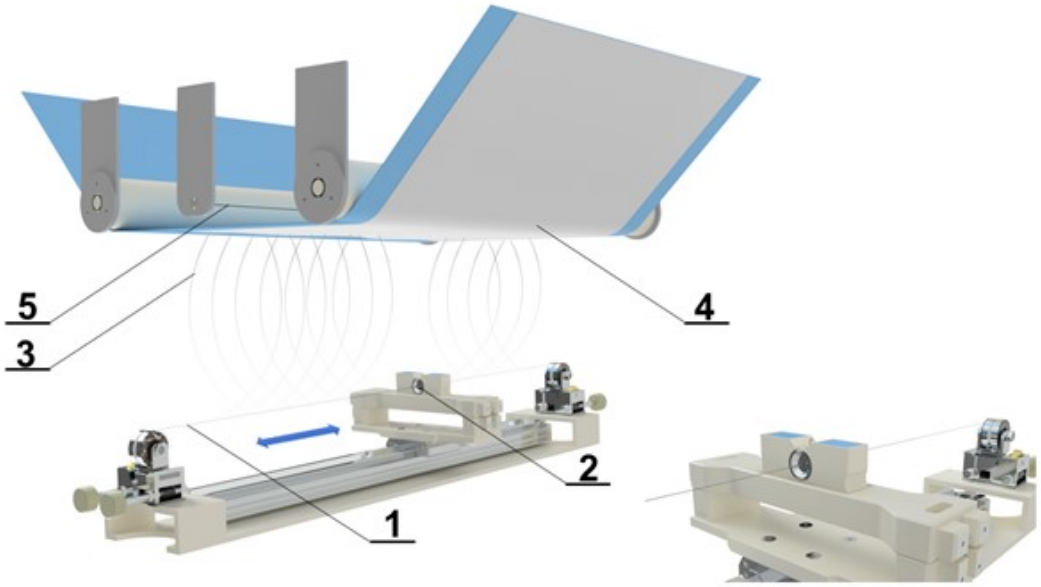

Figure 25: Nanospider^{TM} needleless electrospinning device: 1 – steel wire serves as the positive electrode, 2 – steel orifice with a reservoir for polymeric solution, 3 – nanofiber formation, 4 – created nanofibers are collected on the spunbond substrate, 5 – negative electrode

Table 8: Process parameters of the needless electrospinning via Nanospider^{TM}

Distance between the electrodes [mm]	175	
High voltage [kV]	**Electrode 1**	**Electrode 2**
	-10	40
Rewinding speed [mm/min]	60	
Cartridge movement speed [mm/s]	450–500	
Temperature [°C]	22	
Relative humidity [%]	50	

4.2.3 Material Characterization

The scanning electron microscope VEGA 3 TESCAN (SB Easy Probe, Czech Republic) was used to obtain the surface morphology of the fabricated nanofibers. Prior to scanning, the samples were sputter coated with 10 nm of gold using QUORUM Q50ES (Quorum technologies, UK). The fiber diameters were assessed by the software IMAGE J (NIH Image, USA) by randomly measuring 500 fibers in the scans. The specific weight was calculated by weighing of samples in the dimension 10 × 10 cm (n = 10).

4.2.4 Sterilization and in vitro biocompatibility tests

Before *in vitro* testing, the materials were sterilized via low temperature ethylene oxide (37 °C, Anprolene, H.W.Andersen Product, Inc., North Carolina, USA) according to the Czech norm CSN EN ISO 11135-1. The materials were tested one week after sterilisation to eliminate the effect of ethylen oxide residues in the layers. The PCL scaffolds were seeded with 3T3 mouse fibroblasts (ATCC, USA) in a concentration 7×103 cells per well. Metabolic activity was evaluated after 3, 7, 14 and 21 days via colorimetric Cell Counting Kit-8 (CCK-8) (Dojindo Laboratories, USA). During the CCK-8 assay, the scaffolds were incubated with 10% (v/v) of CCK-8 solution in full DMEM media for 3 hours at 37°C, 5% CO_2. Absorbance was measured at 450 nm (n = 5). The morphology of the cells on the PCL materials was also monitored. Fluorescence imaging was performed with Nikon Eclipse-Ti-E (Nikon Imaging, Czech Republic) on fixed cells with 2,5% v/v glutaraldehyde (Sigma Aldrich, USA) in PBS by adding DAPI (for cell nuclei visualization) and phalloidin-FITC (for staining actin cytoskeleton) after 3, 7, 14 and 21days. The MATLAB software was used to calculate the number of cells per 1 mm^2 of the scaffold from 10 random fields of view. Dehydrated samples with fixed cells were also scanned via SEM during the same time period to obtain the morphology of the cells.

4.2.5 Experimental design

We used 16 Prestice black-pied pigs in two groups, the number was chosen after consultation with a statistician (Attachment: Power analysis C). The animals were subjected to transection of the descending colon and anastomosis with a standardized defect in general anesthesia. The defect was covered with the nanomaterial in the Experimental group while it was left uncovered in the Control group. The animals were observed for 3 weeks. Sample collection and macroscopic evaluation were performed on the 21st postoperative day. Histological evaluation followed.

4.2.6 Surgical procedure

The animals were not fed on the day of the surgery, but no further intestinal preparation was applied. The premedication and perioperative general anesthesia were conducted in the same way as in the two previous experiments A and B. A Pro-Port implantable central venous catheter (Deltec, Smiths medical, USA) was introduced in general anesthesia through the right jugular vein and attached to the subcutaneous tissue on the right lateral side of the neck in each animal for easy and stress-less manipulation with the animal during the follow-up. After the implantation, we entered the abdominal cavity via a 10-cm-long transrectal incision performed in the left caudal abdominal quadrant (Figure 26, Figure 27, Figure 28). We selected this approach because of the location of the pig urethra, which is located in the midline. We pulled the descending colon up through the incision. We then transected the colon approximately 20 cm from the anus (Figure 29). We used soft intestinal clamps to prevent solid intestinal contents from contaminating the abdominal cavity. We cleaned the two ends of the transected colon using wet cotton balls. We constructed a hand-sewn end-to-end anastomosis using the standard seromuscular running suture with glyconate monofilament 4/0 suture line (Monocryl 4/0, B. Braun Medical s.r.o., Czech Republic). We intentionally left a 1-cm-large defect on the ventral side of the anastomosis, simulating a technical fault (Figure 30).

Figure 26: Pig in general anesthesia prepared for surgical procedure. The white line marks the area of skin incision

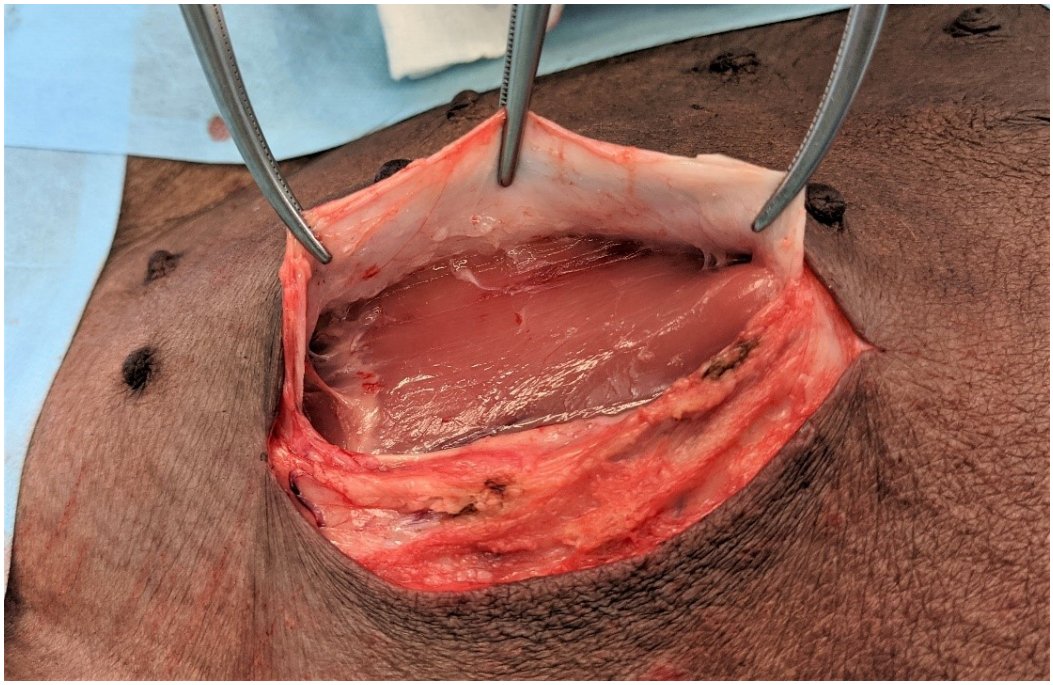

Figure 27: Transrectal incision in pig, rectus abdominis muscle revealed

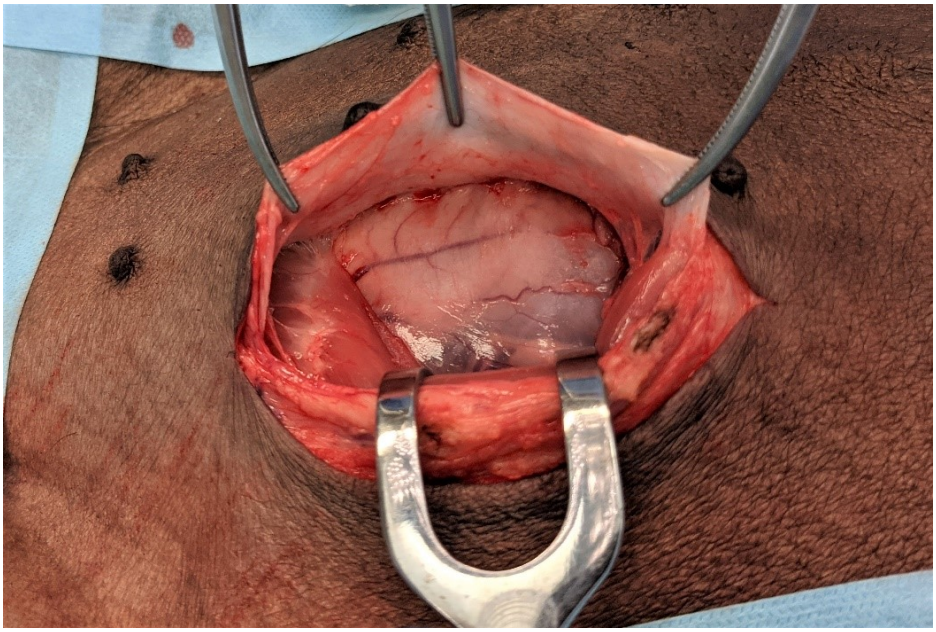

Figure 28: Transrectal incision in pig; rectus abdominis muscle pulled aside, preperitoneal fat and parietal peritoneum visible in the bottom of the wound

Figure 29: Descending colon pulled through the incision, covered in wet abdominal swabs. Intestinal clamps applied both orally and aborally

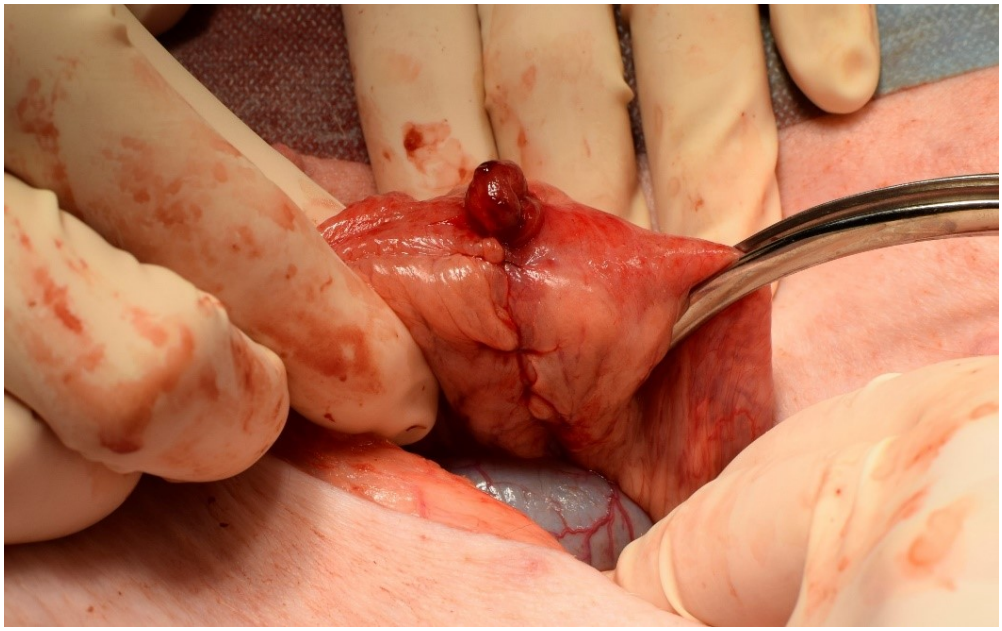

Figure 30: Construction of a defective anastomosis. Intestinal anastomosis, a defect positioned on the antimesenteric side

We placed a standard 2.5-cm-wide sheet of the nanomaterial onto the sutured intestine, covering the intestinal circumference with the defect and the neighboring parts of the mesocolon in the Experimental group (Figure 31). We left the defect uncovered in the Control group. We placed the colon back to the abdominal cavity, sutured firstly the peritoneum with an absorbable material (Vicryl 3/0, Ethicon Inc., Johnson & Johnson, New Jersey, USA) to prevent adhesions to the abdominal wall. Then we closed the muscle layer using single non-absorbable sutures (Mersilene 1, Ethicon Inc., Johnson & Johnson, New Jersey, USA). We rinsed the subcutaneous tissues with saline solution before finally suturing the skin.

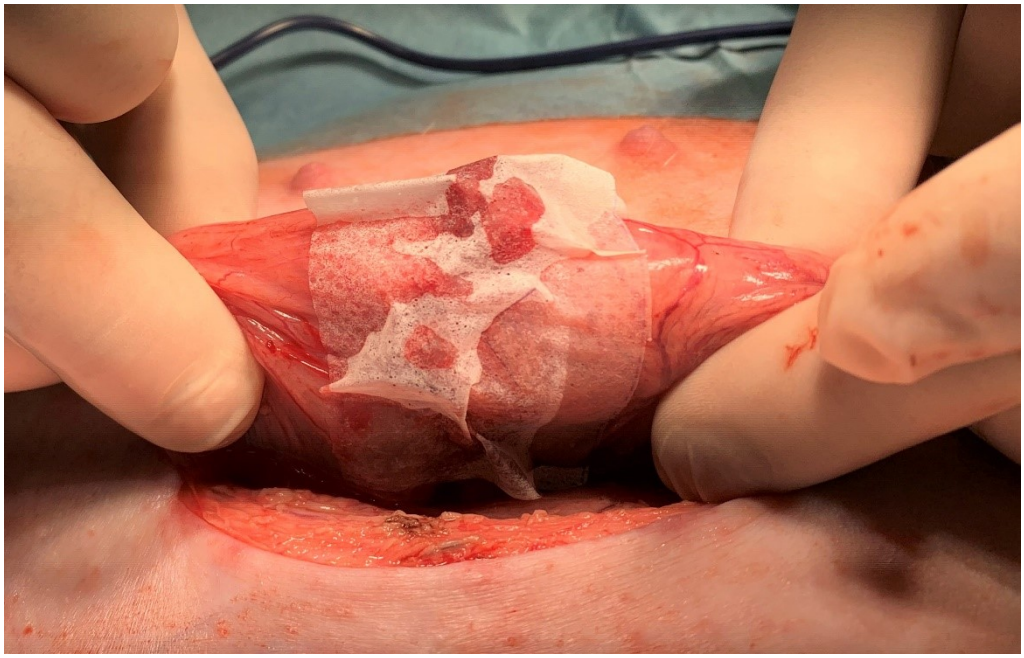

Figure 31: The PCL patch applied to the colon, the material is attached to the intestinal surface when moisted

4.2.7 Postoperative observation

The animals were observed for 3 weeks, they were checked daily for stool passage, body temperature, clinical signs of complications by both a surgeon and a veterinarian. Activity of the animals was scored using a 4-point scale (normal activity, decreased activity, little to no activity, irritated animal). Intravenous infusions of 250 ml 10% Glucose and 250 ml Hartman solution were applied intravenously once a day in the first three PODs. The animals were fed according to a re-alimentation schedule created for previous experiments A and B. When feeding intolerance occurred, intravenous infusions were administered in the same way as in the first three PODs. Blood samples were obtained in defined time points (before the surgical procedure, 2 hours after construction of colonic anastomosis, on the 1st POD, 3rd POD, 7th POD, 14th POD, 21st POD) and tested for blood count, level of bilirubin, liver enzymes, hemoglobin, urea, and creatinine to distinguish metabolic disorders. Animals were weighed each time the blood sample was taken. A 5% weight difference from the initial weight was considered a significant weight change.

4.2.8 Macroscopic evaluation

The animals were subjected to laparotomy again on the 21st POD in general anesthesia. The abdominal cavity was inspected and checked for signs of AL (visible free intestinal contents or purulent secretion, macroscopic changes of peritoneal surfaces), visible defects in the site of anastomosis, changes of the intestinal diameter (stenosis of the anastomosis, dilation of oral segments of the intestine), or any other visible postoperative changes. At same time, the extent and location of PAs (according to qualitative Zühlke's grading and quantitative PAAS (72,156)), amount and macroscopic quality of peritoneal fluid and the position and appearance of the nanofibrous material (if present) were recorded. The intestinal specimens including the anastomoses were collected together with surrounding adhering tissues, cut on the mesenteric side longitudinally, pinned onto a cork underlay and stored in 10% buffered formalin.

4.2.9 Histological evaluation

The intestinal samples were cut in 5 pieces - 5 mm thick, crosswise to the line of the anastomosis in the area of the anastomotic defect. The tissues were processed by common paraffin technique. Each sample was cut to 5µm slides and stained with hematoxylin and eosin for comprehensive overview; Gomori trichrome kit was used to stain connective tissues.

The samples were investigated semi-quantitatively and quantitatively. Epithelization, inflammatory infiltration and necrosis were assessed in a single overall semi-quantitative investigation (IWIS from the Experiment B). The inflammatory reaction to stitches and microabsceses were not included in the score. The score was determined for all 5 blocks, 3 blocks with the highest score (corresponding to the area of the anastomotic defect) were used for statistical evaluation. The blocks with the highest total score for each pig were subsequently analysed quantitatively; 5 µm sections were stained with picrosirius red (Direct red 80) for visualisation of collagen in polarized light. Immunohistochemical methods were used for detection of vascular endothelium using Anti-Von Willebrand Factor antibody

(Abcam ab6994, dilution 1:400); Calprotectin Monoclonal Antibody MAC387 (Invitrogen MA1-81381, dilution 1:200) was used for detection of granulocytes and tissue macrophages. The area for quantitative evaluation for samples without visible defect of the muscular layer was defined as the intestinal wall excluding mucosa located 3 mm orally and aborally from the center of the anastomosis. The evaluation area for samples with a defect of the muscular layer or pseudodiverticulus was defined as 2 mm orally and aborally from the defect margins. The volume of endothelial cells, volume of MAC387 positive cells and volume of collagen was assessed using stereological methods in a similar way as in the previous experiments A and B (156).

4.2.10 Statistics

Common descriptive statistics and frequencies were used to characterize the sample data set. Due to their non-normal distribution, the intestinal wall integrity scores and histologically determined volume fractions were compared between the Experimental and Control group using Mann-Whitney U test in STATISTICA data analysis software system (Version 12; StatSoft, Inc, 2013; www.statsoft.com). The material properties, presented as mean $\pm$ standard deviation (SD), were analyzed using GraphPad Prism 7 (GraphPad Software, USA). Firstly, the Shapiro-Wilk test was used to prove or reject the normal distribution of the data. For the normally distributed data, the parametric ANOVA test with Tukey's multiple comparison was performed. The nonparametric Kruskal-Wallis with Dunn's multiple comparison was chosen for the data following non-normal distribution. All reported p values are two-tailed and the level of statistical significance was set at $\alpha = 0.05$.

4.3 Results C

4.3.1 Material properties

Sheets of PCL nanofibrous material were successfully prepared and sterilized. The material appeared very subtle yet the manipulation with it was still comfortable. The material was easy to apply onto the intestinal surface and it remained adhered to the spot of application without any need of further fixation. The morphology of the fibrous material was assessed by SEM (Figure 32A). The fibers were defect less and without any dominant orientation. The fiber diameter was (385 ± 239) nm (Figure 32B). The high SD is a consequence of ultrafine fibers being present together with larger ones. The specific weight of the material was calculated as (9.67 ± 0.77) g/m^2, the data are symmetrical around mean value (Figure 32C).

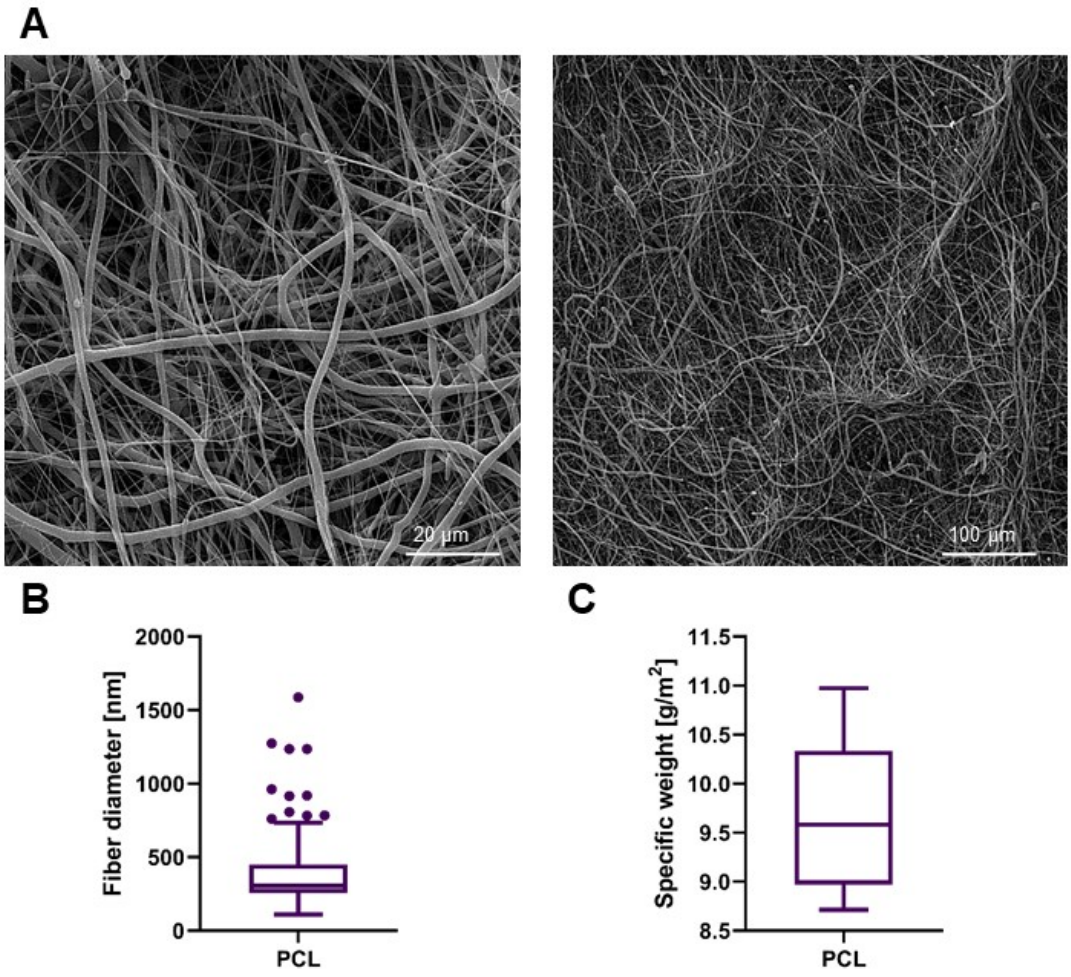

Figure 32: A) The SEM images of the electrospun PCL planar layer, scale bars 20 µm and 50 µm; B) The boxplot of fiber diameters (n=500); C) The calculated value of specific weight of the nanofibrous layer (n=10)

4.3.2 Cytocompatibility

Adhesion, proliferation and morphology of the 3T3 mouse fibroblasts on the PCL scaffolds were monitored with fluorescence microscope and the scanning electron microscope after 3, 7, 14 and 21 days (Figure 33A). The length of the experiment corresponds with the duration of the *in vivo* study. Cell viability was determined using a colorimetric assay CCK-8 after 3, 7, 14 and 21 days of incubation of 3T3 mouse fibroblasts with the tested fiber layers. The obtained mean absorbance values express the cell viability of the cultured cells (Figure 33B). According to the CCK-8 assay, the absorbance was low during the first testing day, which is in positive correlation with the microscopy observation. On the seventh day of cultivation, an increase in viability was measured. At the same time, spreading of the cells was observable on the microscopy images, the cells expanded across the material and began to form isolated cell islands. After 14 days of cultivation, there was a further increase in viability, the cells formed a sub-confluent layer. On the last testing day, the SEM image revealed 100% confluence of the cells. The number of the cells (Figure 32C) correlates with the remaining results. The highest cell density was observed during the 14^{th} day (3887 ± 539) cells/mm^2, while on the last testing day it dropped to (2735 ± 880) cells/mm^2.

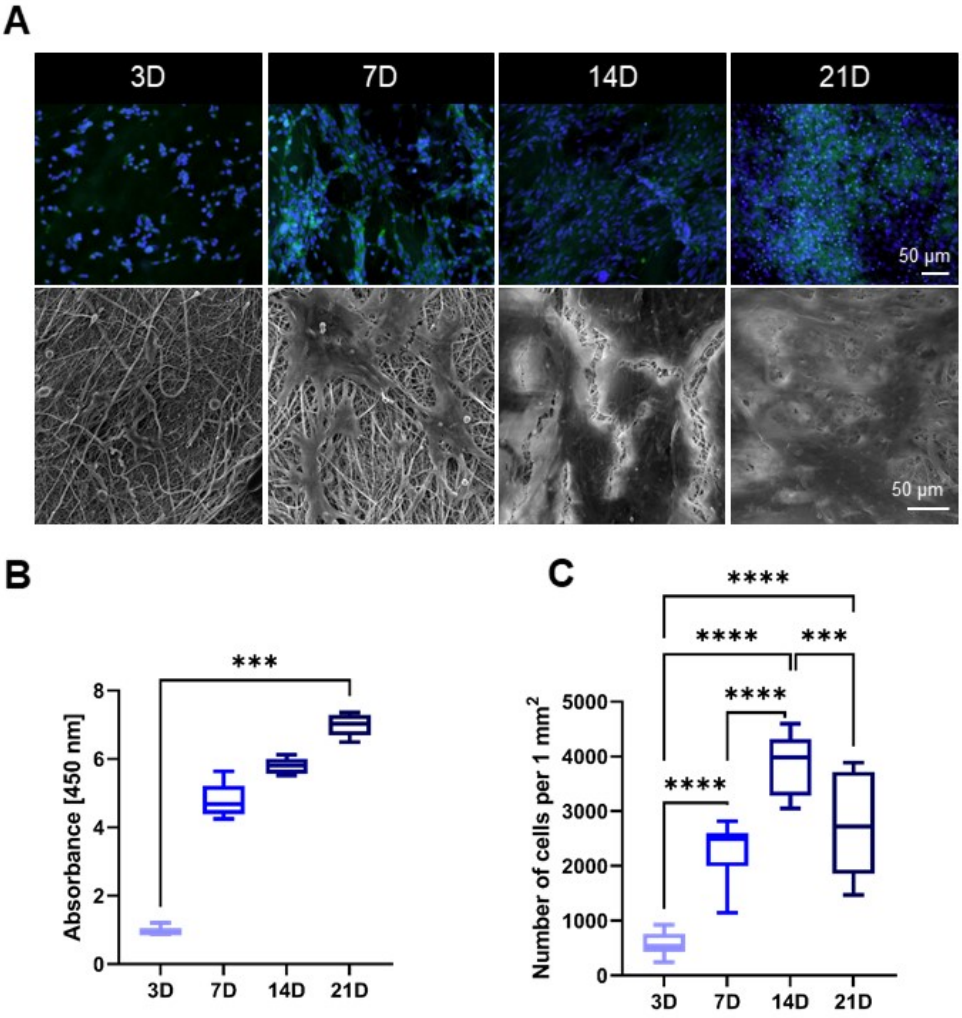

*Figure 33: A) Fluorescence microscopy images (blue cell nuclei and green actin cytoskeleton) and SEM images of the cells on the PCL scaffold after 3, 7, 14 and 21 days of the in vitro testing, scale bars 50 µm; B) The result of the colorimetric CCK-8 assay after the same time period, Kruskal-Wallis ***p=0.0004; C) Counted number of the cells on the surface of PCL materials per 1 mm^2, ordinary one-way ANOVA, ***p<0.0006, ****p=0.0001*

4.3.3 Manipulation

The material was easy to apply (subjective result) and no further fixation was needed. Procedure times were not prolonged by the usage of the material.

4.3.4 Clinical results

All animals survived the observation period in good clinical condition. Temporary activity decrease was observed in 1 animal from the Control group (12.5%) and in 3 animals from the Experimental group (37.5%). There were no major complications during the observation period. Laparotomy wound infection occurred in one animal from the Experimental group (12.5%) and one animal from the Control group (12.5%). Infection of the skin wound of the pro-port system occurred in the same animal from the Control group (12.5%). No animal developed signs of gastrointestinal obstruction (vomiting, feeding intolerance). No animal developed signs of peritonitis and sepsis (abdominal wall tenderness, significant activity decrease, significant laboratory changes). Peroral intake was tolerated by all animals, all animals were fed according to the schedule with no exceptions. Only three animals from the Control group (37.5%) gained more than 5% of weight during the experiment, while 6 animals from the Experimental group (75%) showed such weight gain.

4.3.5 Macroscopic results

There was no macroscopically visible pathological reaction to the material in abdominal cavities of the animals after 3 weeks of observation. Four animals (50%) had no PAs at the site of the anastomosis in the Control group, while 3 animals (37.5%) from the Experimental group had no PAs there. Mean PAAS value of 1 was recorded in both the Control and the Experimental group (Attachment 9). All PAs were scored 2 points according to the Zühlke's grading system in both groups (partially vascularized adhesions, possible to separate by combination of blunt and sharp dissection).

Stenosis of the anastomosis was observed in one animal from the Control group (12.5%) with low shrinkage of the intestinal diameter (less than 1/3) (Figure 34A). No stenoses were observed in the Experimental group (Figure 34B). No signs of gastrointestinal obstruction (dilation of oral segments) were observed in any of the animals. No macroscopic signs of AL were observed (no visible defect in the site of the colonic anastomosis, no free intestinal content in the abdominal cavity).

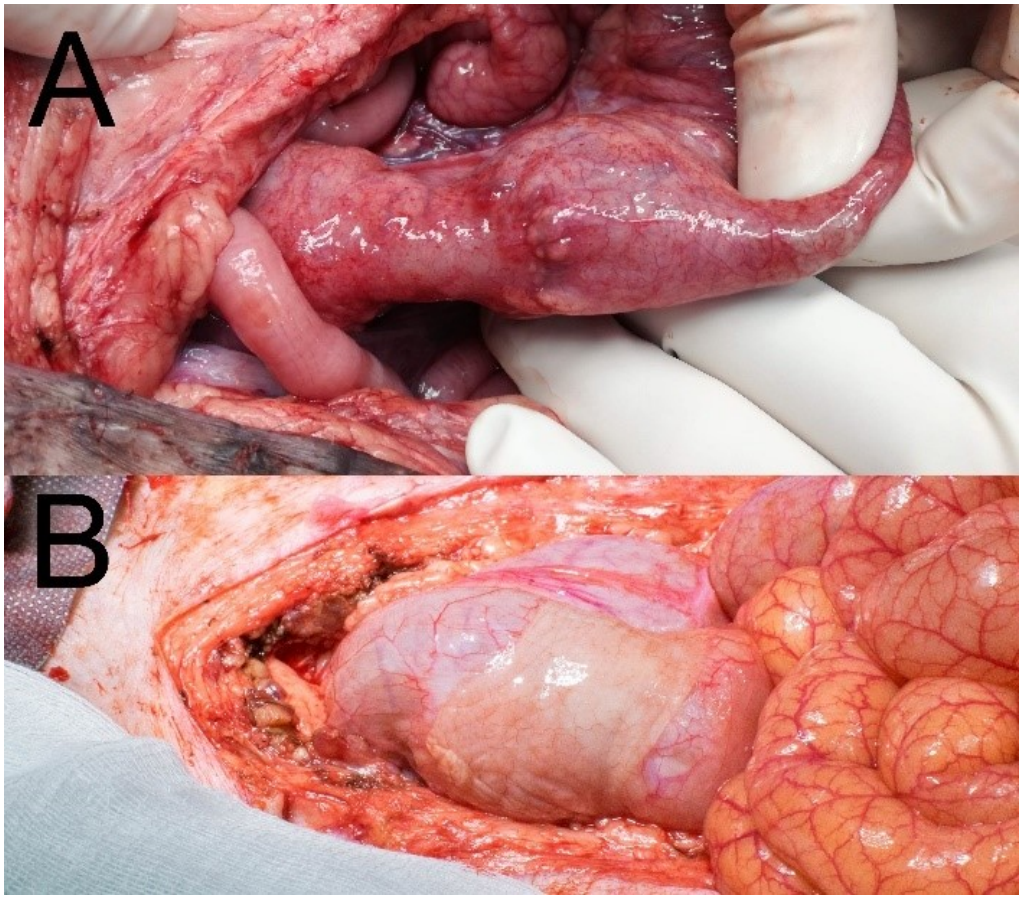

Figure 34: Macroscopic findings in situ at the end of the observation period; A) stenotic anastomosis from the Control group; B) anastomosis with attached material (Experimental group)

Complete dislocation of the material was not observed in any of the animals of the Experimental group. Partial dislocation was observed in 3 animals (37.5%), however the material always kept covering the location of the anastomotic defect (Figure35). The material was well attached in the rest of the specimens (Figure 36B). The defect was not visible in the Control specimens without a patch (Figure 36A).

Most of the adhesions in the site of the anastomosis were between the large intestine and the urinary bladder. There were no PAs observed in the rest of the abdominal cavity in any animal.

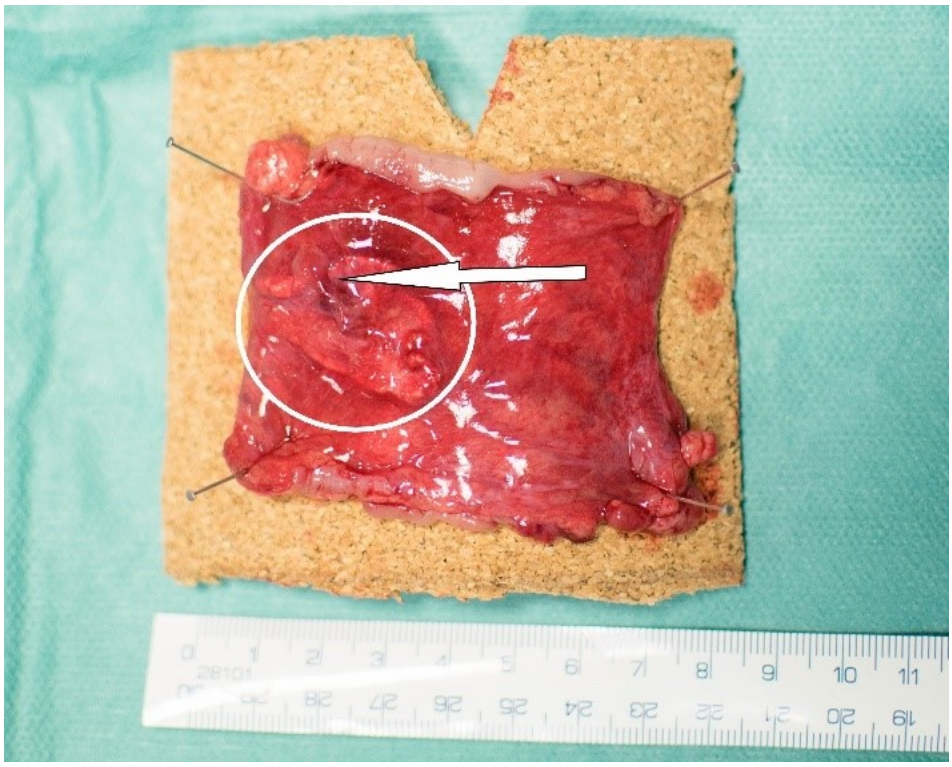

Figure 35: A specimen from the Experimental group prepared for fixation. Partial dislocation of the material (circled), residue of a PA (arrow)

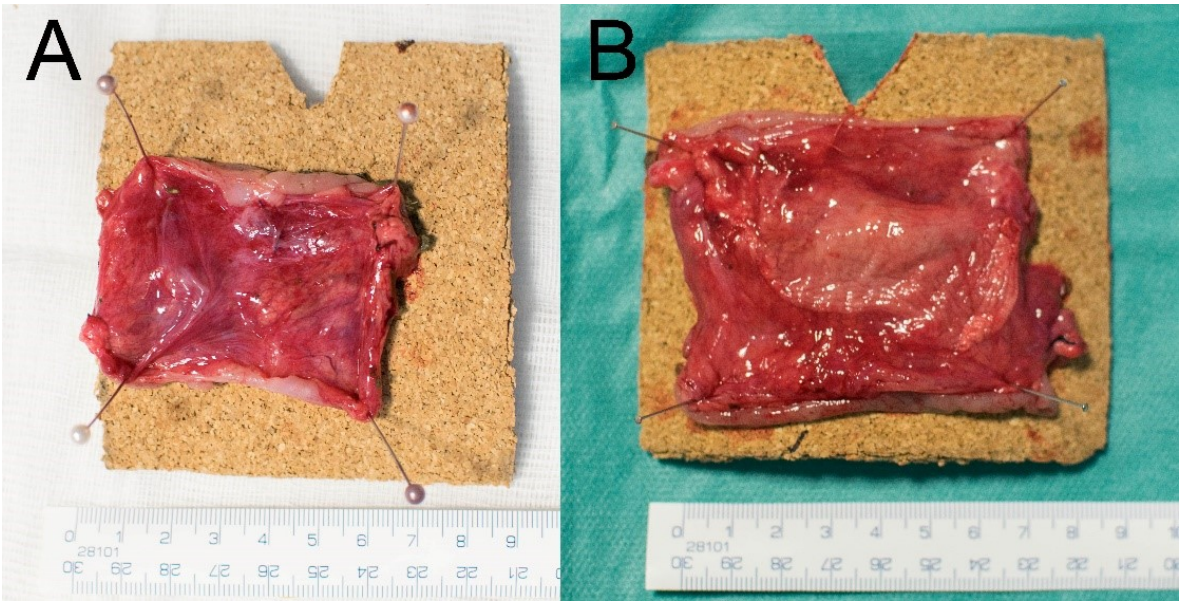

Figure 36: Specimens prepared for fixation. A) A specimen from the Control group; B) A specimen from the Experimental group. The material covers the line of anastomosis well

4.3.6 Blood sample results

There were no statistically significant differences in the measured parameters between the two groups, no significant deviations from normal levels of the parameters (Table 9).

Table 9: Leukocytosis values at different time points, values are given in number of cells times 10^9 per liter

Animal code	POD 0	POD 1	POD 5	POD 7	POD 14	POD 21
Control Group						
cg01	13,90	16,5	22,9	23,6	16	10,8
cg02	14,80	17,7	23,2	19,6	22,5	17,9
cg03	18,5	21,6	29,6	34,5	25	20,4
cg04	21,2	30,2	21,7	23,6	17,6	16,6
cg05	18,5	29,9	21	23,98	20,4	19,1
cg06	19,7	29,5	27,7	20,6	24,4	21,7
cg07	18,4	29	26,3	32,8	22	17,2
cg08	12,9	22	19,3	43,68	18,8	19,7
Experimental group						
eg01	15,4	15,4	25,4	19,5	19,2	15,4
eg02	16,4	23,4	25,9	40,5	19,9	20,7
eg03	22,2	32,3	25,2	26,8	19	15,2
eg04	16,6	18,9	20,4	19,8	18,8	16,8
eg05	18,5	20,8	22,4	19,4	17,3	16,6
eg06	22	27,4	21,4	24,2	36,5	23
eg07	24,1	35,1	33,1	26,7	19,8	21,3
eg08	18,6	33	28,6	24,5	21,1	14,3

4.3.7 Histological results

The material was washed out during the histological fixation and staining. There were no microscopic signs of AL (no full-thickness defect was found in any specimen in either the Control or the Experimental group). We found normal morphology of the intestinal wall in all specimens using the comprehensive overview (Figure 37). In some cases, the muscular layer did not heal completely and pseudodiverticuli were formed (3 cases in the Control group (37.5%) and 7 cases (87.5%) in the Experimental group; (Figure 38). There was no statistically significant difference between the groups according to our Intestinal Wall Integrity Score (Figure 39A) (Attachment 10). There were significantly higher volume fractions of collagen in the Experimental group (Figure 39B). There was no statistically significant difference between the two groups in volume fractions of endothelial cells (Figure 39C) and MAC 387 positive cells (Figure 39D) (Attachment 10).

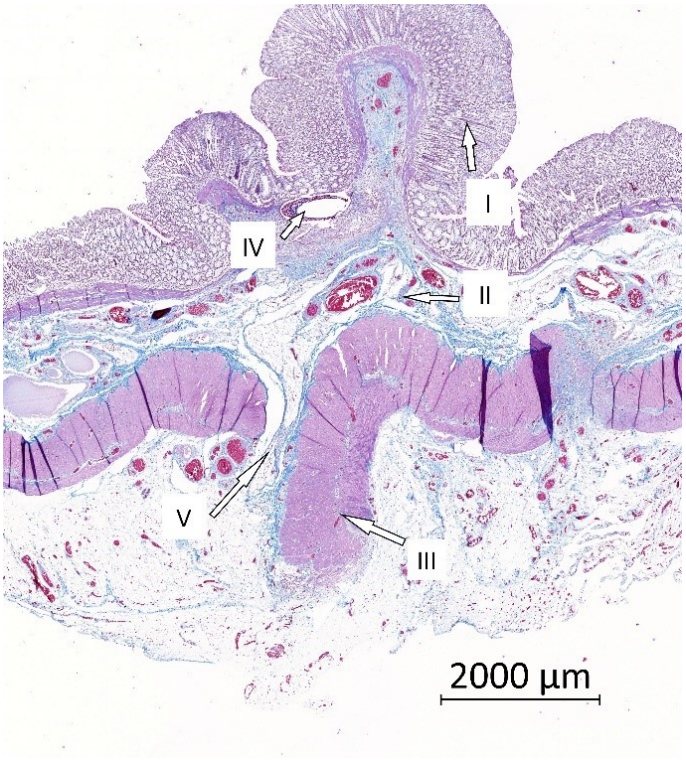

Figure 37:Example histological specimen from the Control group, Gomori trichrome staining. I) The mucosa; II) The submucosa; III) The muscular layer; IV) A defect after suture material that was washed out during histological processing; V) Location of the anastomosis with normal scar tissue

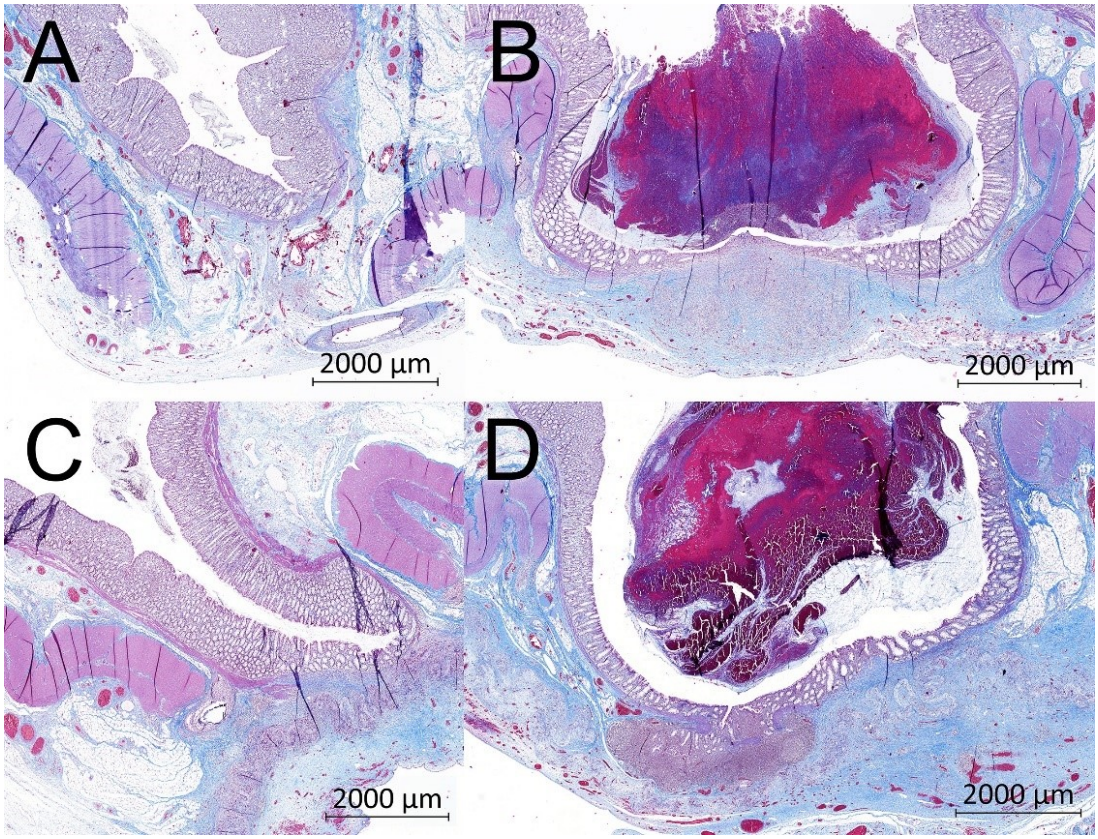

Figure 38: Example histological specimens from both groups. Gomori trichrome; A) Control group, optimal healing, normal morphology of the intestinal wall, muscular layer with normal scar tissue; B) Control group, larger defect of the muscular layer, a pseudodiverticulus; C) Experimental group, optimal healing, normal morphology of the intestinal wall, visible residues of the nanofibrous material in the bottom of the image; D) Experimental group, large defect of the muscular layer, a pseudodiverticulus, visible residues of the nanofibrous material in the bottom of the image covering the incomplete defect of the intestinal wall

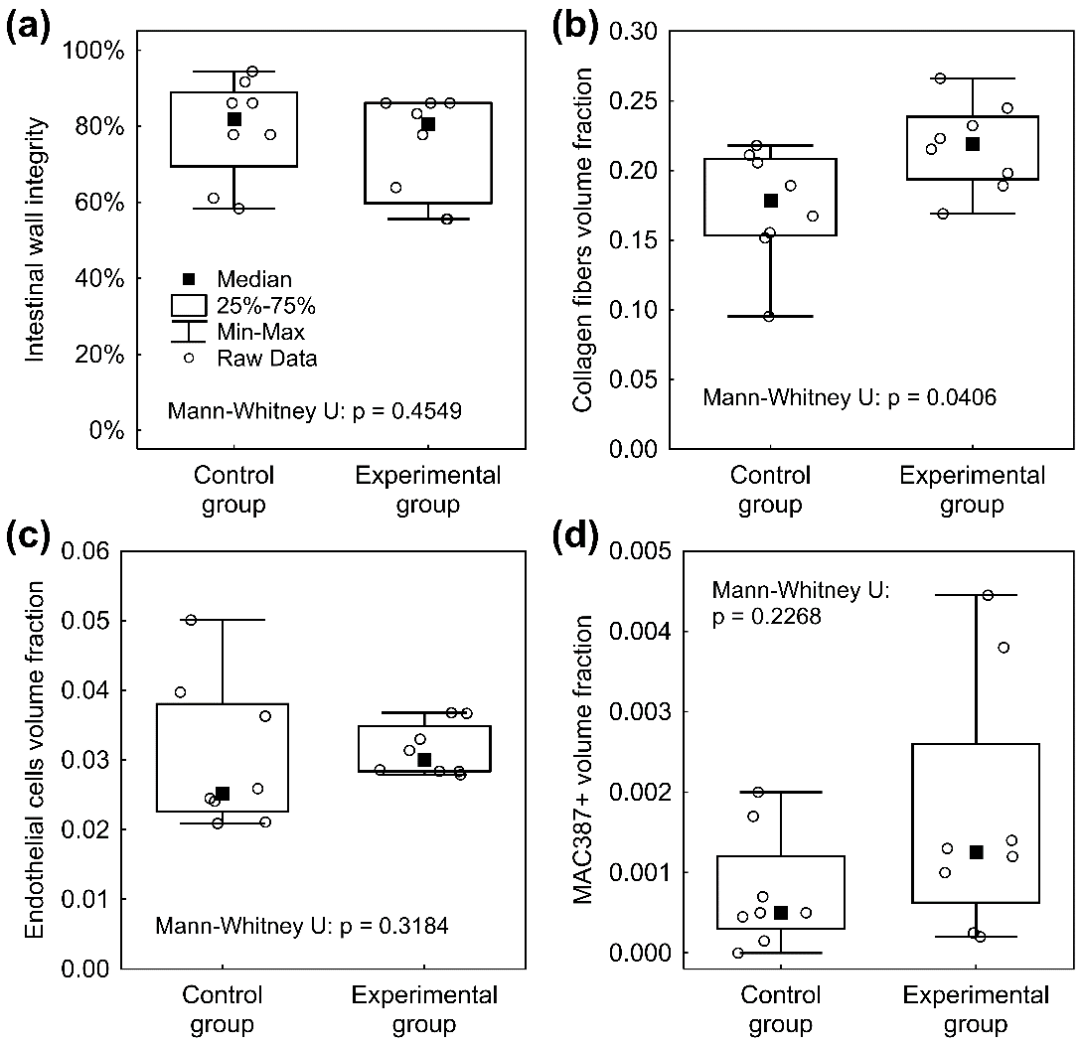

Figure 39: Graphical depiction of main histological results. A)The intestinal wall integrity score in the Control group and the Experimental group with no significant differences with median value above 80%; B) Significantly higher volume fractions of collagen at the site of anastomosis in the Experimental group; C) No significant differences between the two groups in volume fractions of endothelial cells, lower dispersion range of values in the Experimental group; D) The difference in volume fractions of inflammatory cells at the site of anastomosis between the groups is not statistically significant

4.4 Discussion C

We developed a nanofibrous material based on biodegradable polycaprolactone with very low specific weight. The material was uniquely designed for the reinforcement of GI anastomoses, and its design was based on our previous *in vitro* and *in vivo* experiments. Polycaprolactone is often used for its biocompatibility and biodegradability (159,174,175). The *in vitro* testing with 3T3 mouse fibroblasts proved the cytocompatibility of the material; the cells formed a fully confluent layer on the surface of the scaffold after 21 days. This observation is consistent with other literature resources, where the combination of micro- and nanofibers in PCL scaffolds supported the cell growth (176,177). Prior to the *in vitro* testing, the scaffolds were sterilized with low temperature ethylen oxide with respect to low melting point of PCL. The possible effect of the ethylen oxide sterilization on PCL was already examined in our previous study by Horakova et al. (178). The PCL patches are easy to apply and we value this as an important property. While the material is very subtle as its specific weight is only 10 g/m^2, it was still mechanically strong enough to be handled easily. The material always remained in the site of application during the surgical procedure and reposition of the viscera without further fixation. The convenient application together with natural fixation are key properties should this approach be used in routine clinical practice.

We successfully created a model of anastomosis with a defect on the large intestine of a pig. We used the Testini's (104) modified model from previous experiments (156) in order to move the anastomosis to a location with bacterial contamination and higher risk of healing complications. The defect was chosen small enough to simulate a technical fault (which is also one of the contributing factors of AL (179)) and large enough to induce imperfect healing. The position of the anastomosis in 20 cm from the anus was chosen for its good accessibility, no need of further preparation, possibility of small abdominal wound and therefore low non-anastomosis related complication risk. The model allowed to focus only on imperfect anastomotic healing with no other disturbing factors. Together with the assessment methodology, the model allowed reduction of number of experimental animals and what we consider statistically reliable results. A three weeks' observation period was chosen based

on our previous experience and possibility to use evaluation histologic systems from previous publications. AL is typically an early complication, appearing usually within the first 10 PODs (35,43). To verify the behavior of the material in a long term period regarding its complete absorption and impact on the risk of late complications, longer observation times would be necessary.

All of the animals in both groups survived the observation period in good clinical shape with a low complication rate. An activity decrease was observed only in the early postoperative period in both groups, which we considered as normal postoperative state. The feeding tolerance was equally good in both groups. The animals from the Experimental group gained weight in more cases than in the Control group. Weight gain is a sign of good adaption (180). No animal developed ileus or sepsis or other serious pathological reaction to the material. This contributes to our assumption that it is safe to use in this application.

We observed slight shifting of the material in a few cases, however the material always kept covering the spot of anastomotic defect. We observed this also in the last study on the small intestine with an earlier version of the material, and therefore we assume it is not a coincidence (156). This barrier was always present even in specimens with larger defect of muscular layer, and no macroscopic or microscopic AL was observed. It remains a question whether the material is able to prevent manifestation of AL. An anastomotic leakage is in experiments usually obtained by either large anastomotic defects or other negative influences (infection, radiation, devascularization). The model of small defect was chosen to study the impact of the material on imperfect anastomotic healing in highly standardized conditions.

There was one partial shrinkage of the intestinal diameter at the site of the anastomosis in one animal from the Control group (12.5%), therefore we assume the material does not cause formation of anastomotic strictures. Those can however develop in longer time periods and thus a longer observation time would be needed to verify this information (41). The level of adhesions was similarly low in both groups, suggesting the current material version to be the first in our series of polycaprolactone electrospun materials without pro-adhesive properties (156). We consider the generally low amount

of adhesions to be also a result of short procedure times with low manipulation with tissues (181). Excessive formation of PAs is considered to be a result of a healing problem (77). Visceral peritoneum is the superficial layer of the intestine, so wound healing of the peritoneum is a part of anastomotic wound healing. Therefore, we think, qualitative and quantitative assessment of PAs should be involved in the evaluation of anastomotic healing (156).

There were no statistically significant differences in vascularization and inflammatory cells infiltration according to the stereological measurements. This suggests normal healing process (34). However, the levels of collagen were found higher in the Experimental group. It was previously observed in mechanical tests of intestinal anastomoses that higher levels of collagen are associated with higher mechanical strength and higher anastomotic bursting pressure (107). Bacterial collagenases were identified as a possible contributor to development of AL. Their activity causes collagen degradation in the site of intestinal anastomosis. Intestinal colonization with several bacterial species was identified as a strong risk factor of AL due to their production of collagenases (57,107,182).

We used both traditional evaluation methods (34) with those that were developed for our purposes in previous papers (156). The intestinal wall integrity score from the previous study was adjusted for a defective model on the large intestine. Together with the rest of involved assessment methods, it forms one of the most robust and complex evaluation system of anastomotic healing in similar experiments according to our knowledge and literature search.

The above-mentioned results all suggest possible contribution to AL prevention by our material only indirectly. To obtain more distinguishable results, a model with more compromised anastomotic healing with high risk of AL manifestation would be necessary. This is certainly a limitation of this study.

Because the material was washed out during the histological processing, we cannot evaluate the level of biodegradation. However, this was studied earlier for PCL in other forms (183).

The material seems to be an ideal version for use in combination with active substances like anti-inflammatory drugs, antibacterial agents or antibiotics as an anastomotic patch. Polycaprolactone was identified as a good medium for regulated drug release (175,184); there is a broad spectrum of active molecules that could be beneficial for either AL prevention or prevention of excessive PA formation (77,185–188). Therefore, we intend to perfect the material using these substances and to study their impact on anastomotic healing and complications further to finally offer a perfect anastomotic patch for patients with high risk of AL. Possible clinical study will be planned afterwards.

4.5 Conclusion C

We succeeded in creating a unique ultrafine polycaprolactone electrospun material and in applying it in a model of complicated anastomotic healing on the pig colon. The planar PCL layer was fabricated via needleless electrospinning technique, a method suitable for eventual large scale production. The material is easy to use without any need for further fixation. The presence of the material did not cause any adverse effects *in vivo*. The PCL layer showed good cytocompatibility and biocompatibility and was well tolerated during the whole animal study. The material is also not pro-adhesive and did not cause anastomotic strictures or other complications. The anastomotic specimens showed significantly higher levels of collagen after the 3 weeks of observation, which is an indirect sign of higher mechanical strength. Impact on the risk of AL was not observed directly as no AL appeared in either group.

5 Conclusion of the dissertation, final notes and future perspectives

We conducted three subsequential experiments studying effects of nanofibrous materials on the healing process of anastomoses on the porcine intestines. The main research goals are yet to be reached. However we succeeded to create a nanofibrous patch with distinguishable positive effects on healing of defective intestinal anastomoses. We also established several models of anastomoses on the porcine GI tract that are clinically relevant, and invented and perfected several assessment methods, which are usable in similar experiments. These can be used by other research groups as they are published in full detail including standard operation procedure protocols (PAAS, IWIS).

Even though we did not manage to distinguish clearly an impact of our materials on the risk of anastomotic leakage, we can declare that the ultrafine PCL patch used in the Experiment C is biocompatible and safe to use in application on anastomoses on the large intestine with no adverse effects in the 3 weeks postoperative period. As the patch is highly porous and biodegradable, created from known biocompatible polymer, we doubt any adverse effects in the long term postoperative period.

The research regarding the topic continues on. We intend to combine the last version of the material with new active agents (antibiotics, growth factors etc.) in a version with controlled drug release. Many studies identified various bacterial species as a serious risk factor of anastomotic leakage development as written in previous chapters. A material with potent and specific antibacterial activity could be a key in decreasing the AL rate in colorectal surgery. Several versions of such prototypes of PCL patches were already prepared by our team and currently are *in vitro* tested for their specific anti-bacterial properties. These are to be tested in an *in vivo* experiment in a model of high risk colonic anastomosis.

6. References

1. Netter FH. Atlas of Human Anatomy. 6th ed. Elsevier. 2014.
2. Mescher LA. Junqueira's Basic Histology. Text and Atlas. 14th ed. Lange. 2016.
3. Trowers E, Tischler M. Gastrointestinal physiology: A clinical approach. Gastrointestinal Physiology: A Clinical Approach. 1st ed. Springer. 2014.
4. Susan Standring, PhD Ds. Gray's Anatomy 40th ed. Churchill Livingstone. 2009.
5. Lüllmann-Rauch R, Asan E. Taschenlehrbuch Histologie. 6th ed. Thieme. 2019.
6. Askari A. Anatomy and Physiology of the Large Bowel (Colon) and Pelvic Floor. In: Bowel Dysfunction. 1st ed. Springer. 2016.
7. Ong MLH, Schofield JB. Assessment of lymph node involvement in colorectal cancer. World J Gastrointest Surg. 2016 Mar 27;8(3):179-92.
8. Ogino T, Hata T, Kawada J, Okano M, Kim Y, Okuyama M, et al. The Risk Factor of Anastomotic Hypoperfusion in Colorectal Surgery. J Surg Res. 2019 Dec;244:265-271.
9. Batista VL, Iglesias ACRG, Madureira FAV, Bergmann A, Duarte RP, da Fonseca BFS. Adequate lymphadenectomy for colorectal cancer: a comparative analysis between open and laparoscopic surgery. Arq Bras Cir Dig. 2015, Apr-Jun 28(2):105-8.
10. Egorov VI, Schastlivtsev V, Turusov RA, Baranov AO. Participation of the intestinal layers in supplying of the mechanical strength of the intact and sutured gut. Eur Surg Res. 2002 Nov-Dec 34(6):425-31.
11. Girard-Madoux MJH, Gomez de Agüero M, Ganal-Vonarburg SC, Mooser C, Belz GT, Macpherson AJ, et al. The immunological functions of the Appendix: An example of redundancy? Seminars in Immunology. 2018 Apr;36:31-44.
12. Vitetta L, Chen J, Clarke S. The vermiform appendix: An immunological organ sustaining a microbiome inoculum. Clinical Science. 2019 Jan 3;133(1):1-8.
13. Meyers MA. Griffiths' point: critical anastomosis at the splenic flexure. Significance in ischemia of the colon. Am J Roengenol. 1976 Jan;126(1):77-94.
14. DeSesso JM, Jacobson CF. Anatomical and physiological parameters affecting gastrointestinal absorption in humans and rats. Food and Chemical Toxicology. 2001

Mar;39(3):209-28.

15. Pang X, Hua X, Yang Q, Ding D, Che C, Cui L, et al. Inter-species transplantation of gut microbiota from human to pigs. ISME J. 2007 Jun;1(2):156-62.
16. Ley RE, Bäckhed F, Turnbaugh P, Lozupone CA, Knight RD, Gordon JI. Obesity alters gut microbial ecology. Proc Natl Acad Sci U S A. 2005 Aug 2;102(31):11070-5.
17. Hiranyakas A, Ho YH. Surgical treatment for colorectal cancer. Int Surg. 2011 Apr-Jun;96(2):120-6.
18. Tebala GD. History of colorectal surgery: A comprehensive historical review from the ancient Egyptians to the surgical robot. International Journal of Colorectal Disease. 2015 Jun;30(6):723-48.
19. Slieker JC, Daams F, Mulder IM, Jeekel J, Lange JF. Systematic review of the technique of colorectal anastomosis. JAMA Surgery. 2013 Feb;148(2):190-201.
20. Hastings JC, Winkle W V., Barker E, Hines D, Nichols W. Effect of suture materials on healing wounds of the stomach and colon. Surg Gynecol Obstet. 1975 May;140(5):701-7.
21. Letwin ER. Evaluation of polyglycolic acid sutures in colon anastomoses. Can J Surg. 1975 1975 Jan;18(1):30-2.
22. Foresman PA, Edlich RF, Rodeheaver GT. The Effect of New Monofilament Absorbable Sutures on the Healing of Musculoaponeurotic Incisions, Gastrotomies, and Colonic Anastomoses. Arch Surg. 1989 Jun;124(6):708-10.
23. Durdey P, Bucknall TE. Assessment of sutures for use in colonic surgery: An experimental study. J R Soc Med. 1984 Jun;77(6):472-7.
24. Hardy KJ. A view of the development of intestinal suture. Part II. Principles and techniques. Aust N Z J Surg. 1990 May;60(5):377-84.
25. Carty NJ, Keating J, Campbell J, Karanjia N, Heald RJ. Prospective audit of an extramucosal technique for intestinal anastomosis. Br J Surg. 1991 Dec;78(12):1439-41.
26. Sailer M, Debus ES, Fuchs KH, Beyerlein J, Thiede A. Comparison of anastomotic microcirculation in coloanal J-pouches versus straight and side-to-end coloanal reconstruction: An experimental study in the pig. Int J Colorectal Dis. 2000

Apr;15(2):114-7.

27. MacRae HM, McLeod RS. Handsewn vs. stapled anastomoses in colon and rectal surgery: A meta- analysis. Dis Colon Rectum. 1998 Feb;41(2):180-9.
28. Wang PH, Huang BS, Horng HC, Yeh CC, Chen YJ. Wound healing. Journal of the Chinese Medical Association. 2018 Feb;81(2):94-101.
29. Reinke JM, Sorg H. Wound repair and regeneration. European Surgical Research. 2012; 49(1):35-43.
30. Zomer HD, Trentin AG. Skin wound healing in humans and mice: Challenges in translational research. Journal of Dermatological Science. 2018 Apr;90(1):3-12.
31. Ceran C, Aksoy RT, Gülbahar Ö, Öztürk F. The effects of ghrelin on colonic anastomosis healing in rats. Clinics. 2013;68(2):239-44.
32. Lyra Junior HF, de Lucca Schiavon L, Rodrigues IK, Couto Vieira DS, de Paula Martins R, Turnes BL, et al. Effects of Ghrelin on the Oxidative Stress and Healing of the Colonic Anastomosis in Rats. J Surg Res. 2019 Feb;234:167-177.
33. Despoudi K, Mantzoros I, Ioannidis O, Cheva A, Antoniou N, Konstantaras D, et al. Effects of albumin/glutaraldehyde glue on healing of colonic anastomosis in rats. World J Gastroenterol. 2017 Aug 21;23(31):5680-5691.
34. DiPietro LA, Burns AL, Williams DL, Browder IW. Murine Models of Intestinal Anastomoses. In: Wound Healing. 2003.
35. Sparreboom CL, Van Groningen JT, Lingsma HF, Wouters MWJM, Menon AG, Kleinrensink GJ, et al. Different risk factors for early and late colorectal anastomotic leakage in a nationwide audit. Dis Colon Rectum. 2018 Nov;61(11):1258-1266.
36. Hyman N, Manchester TL, Osler T, Burns B, Cataldo PA. Anastomotic leaks after intestinal anastomosis: It's later than you think. Ann Surg. 2007;245(2):254–8.
37. Luchtefeld MA, Milsom JW, Senagore A, Surrell JA, Mazier WP. Colorectal anastomotic stenosis results of a survey of the ASCRS membership. Dis Colon Rectum. 1989 Sep;32(9):733-6.
38. Kingham TP, Pachter HL. Colonic Anastomotic Leak: Risk Factors, Diagnosis, and Treatment. Journal of the American College of Surgeons. 2009 Feb;208(2):269-78.

39. Wu Z, van de Haar RCJ, Sparreboom CL, Boersema GSA, Li Z, Ji J, et al. Is the intraoperative air leak test effective in the prevention of colorectal anastomotic leakage? A systematic review and meta-analysis. International Journal of Colorectal Disease. 2016 Aug;31(8):1409-17.
40. Martínez-Serrano MA, Parés D, Pera M, Pascual M, Courtier R, Egea MJG, et al. Management of lower gastrointestinal bleeding after colorectal resection and stapled anastomosis. Tech Coloproctol. 2009 Mar;13(1):49-53.
41. Bertocchi E, Barugola G, Benini M, Bocus P, Rossini R, Ceccaroni M, et al. Colorectal Anastomotic Stenosis: Lessons Learned after 1643 Colorectal Resections for Deep Infiltrating Endometriosis. J Minim Invasive Gynecol. 2019 Jan;26(1):100-104.
42. McDermott FD, Heeney A, Kelly ME, Steele RJ, Carlson GL, Winter DC. Systematic review of preoperative, intraoperative and postoperative risk factors for colorectal anastomotic leaks. British Journal of Surgery. 2015 Apr;102(5):462-79.
43. Gessler B, Eriksson O, Angenete E. Diagnosis, treatment, and consequences of anastomotic leakage in colorectal surgery. Int J Colorectal Dis. 2017;32(4):549–56.
44. Olsen BC, Sakkestad ST, Pfeffer F, Karliczek A. Rate of Anastomotic Leakage After Rectal Anastomosis Depends on the Definition: Pelvic Abscesses are Significant. Scand J Surg. 2019 Sep;108(3):241-249.
45. Van Rooijen SJ, Jongen ACHM, Wu ZQ, Ji JF, Slooter GD, Roumen RMH, et al. Definition of colorectal anastomotic leakage: A consensus survey among Dutch and Chinese colorectal surgeons. World J Gastroenterol. 2017;23(33):6172–80.
46. Rahbari NN, Weitz J, Hohenberger W, Heald RJ, Moran B, Ulrich A, et al. Definition and grading of anastomotic leakage following anterior resection of the rectum: A proposal by the International Study Group of Rectal Cancer. Surgery. 2010;147(3):339–51.
47. Dindo D, Demartines N, Clavien PA. Classification of surgical complications: A new proposal with evaluation in a cohort of 6336 patients and results of a survey. Annals of Surgery. 2004 Aug;240(2):205-13.
48. Takahashi H, Haraguchi N, Nishimura J, Hata T, Yamamoto H, Matsuda C, et al. The severity of anastomotic leakage may negatively impact the long-term prognosis of

colorectal cancer. Anticancer Res. 2018 Jan;38(1):533-539.

49. Wang S, Liu J, Wang S, Zhao H, Ge S, Wang W. Adverse Effects of Anastomotic Leakage on Local Recurrence and Survival After Curative Anterior Resection for Rectal Cancer: A Systematic Review and Meta-analysis. World Journal of Surgery. 2017 Jan;41(1):277-284.

50. Vogel JD, Eskicioglu C, Weiser MR, Feingold DL, Steele SR. The American society of colon and rectal surgeons clinical practice guidelines for the treatment of colon cancer. Dis Colon Rectum. 2017 Oct;60(10):999-1017.

51. Schultz JK, Azhar N, Binda GA, Barbara G, Biondo S, Boermeester MA, et al. European Society of Coloproctology: guidelines for the management of diverticular disease of the colon. Color Dis. 2020 Sep;22 Suppl 2:5-28.

52. Glynne-Jones R, Nilsson PJ, Aschele C, Goh V, Peiffert D, Cervantes A, et al. Anal cancer: ESMO-ESSO-ESTRO clinical practice guidelines for diagnosis, treatment and follow-up. European Journal of Surgical Oncology. 2014 Oct;40(10):1165-76.

53. Gustafsson UO, Scott MJ, Hubner M, Nygren J, Demartines N, Francis N, et al. Guidelines for Perioperative Care in Elective Colorectal Surgery: Enhanced Recovery After Surgery (ERAS®) Society Recommendations: 2018. World Journal of Surgery. 2019 Mar;43(3):659-695.

54. Lazzar C, Currò G, Komaei I, Barbera A, Navarra G. Favorable Management of Low Colorectal Anastomotic Leakage with Transanal Conventional and Endoscopic Drainage (GelPOINT® Path Transanal Access Platform). Surg Technol Int. 2018 Nov 11;33:119-126.

55. Stafford C, Francone TD, Marcello PW, Roberts PL, Ricciardi R. Is diversion with ileostomy non-inferior to hartmann resection for left-sided colorectal anastomotic leak? J Gastrointest Surg. 2018 Mar;22(3):503-507.

56. Rickert A, Willeke F, Kienle P, Post S. Management and outcome of anastomotic leakage after colonic surgery. Color Dis. 2010 Oct;12(10 Online):e216-23.

57. Krarup PM, Jorgensen LN, Harling H. Management of anastomotic leakage in a nationwide cohort of colonic cancer patients. J Am Coll Surg. 2014 May;218(5):940-9.

58. Edden Y, Weiss EG, Edden Y, Weiss EG. Surgical considerations in anastomotic

dehiscence. In: Reconstructive Surgery of the Rectum, Anus and Perineum. 2013.

59. Blumetti J. Management of low colorectal anastomotic leak: Preserving the anastomosis. World J Gastrointest Surg [Internet]. 2015;7(12):378.

60. Joh YG, Kim SH, Hahn KY, Stulberg J, Chung CS, Lee DK. Anastomotic leakage after laparoscopic protectomy can be managed by a minimally invasive approach. Dis Colon Rectum. 2009 Jan;52(1):91-6.

61. Khurrum Baig M, Hua Zhao R, Batista O, Uriburu JP, Singh JJ, Weiss EG, et al. Percutaneous postoperative intra-abdominal abscess drainage after elective colorectal surgery. Tech Coloproctol. 2002 Dec;6(3):159-64.

62. Thorson AG, Thompson JS. Transrectal drainage of anastomotic leaks following low colonic anastomosis. Dis Colon Rectum. 1984 Jul;27(7):492-4.

63. Van Koperen PJ, Van Berge Henegouwen MI, Rosman C, Bakker CM, Heres P, Slors JFM, et al. The Dutch multicenter experience of the endo-sponge treatment for anastomotic leakage after colorectal surgery. Surg Endosc. 2009 Jun;23(6):1379-83.

64. An Y, Wang N, Yang Z, Li Y, Xu B, Guo G, et al. Efficacy of transanal drainage tube and self-expanding metallic stent in acute left malignant colorectal obstruction. Ann Palliat Med. 2020 Jul;9(4):1614-1621.

65. Bülow S, Bulut O, Christensen IJ, Harling H, Bjørn Andersen O, Bisgaard C, et al. Transanal stent in anterior resection does not prevent anastomotic leakage. Color Dis. 2006 Jul;8(6):494-6.

66. Arezzo A, Verra M, Reddavid R, Cravero F, Bonino MA, Morino M. Efficacy of the over-the-scope clip (OTSC) for treatment of colorectal postsurgical leaks and fistulas. Surgical Endoscopy. 2012 Nov;26(11):3330-3.

67. Awonuga AO, Saed GM, Diamond MP. Laparoscopy in gynecologic surgery: Adhesion development, prevention, and use of adjunctive therapies. Clin Obstet Gynecol. 2009 Sep;52(3):412-22.

68. Coccolini F, Ansaloni L, Manfredi R, Campanati L, Poiasina E, Bertoli P, et al. Peritoneal adhesion index (PAI): Proposal of a score for the “ignored iceberg” of medicine and surgery. World J Emerg Surg [Internet]. 2013;8(1):1.

69. Caglayan EK, Caglayan K, Erdogan N, Cinar H, Güngör B. Preventing intraperitoneal adhesions with ethyl pyruvate and hyaluronic acid/carboxymethylcellulose: A comparative study in an experimental model. Eur J Obstet Gynecol Reprod Biol. 2014 Oct;181:1-5.

70. Ellis H, Moran BJ, Thompson JN, Parker MC, Wilson MS, Menzies D, et al. Adhesion-related hospital readmissions after abdominal and pelvic surgery: A retrospective cohort study. Lancet. 1999 May 1;353(9163):1476-80.

71. Farag S, Padilla PF, Smith KA, Sprague ML, Zimberg SE. Management, Prevention, and Sequelae of Adhesions in Women Undergoing Laparoscopic Gynecologic Surgery: A Systematic Review. Journal of Minimally Invasive Gynecology. 2018 Nov-Dec;25(7):1194-1216.

72. Zühlke H V., Lorenz EM, Straub EM, Savvas V. Pathophysiology and classification of adhesions. Langenbecks Arch Chir Suppl II Verh Dtsch Ges Chir. 1990;1009-16.

73. Rout UK, Saed GM, Diamond MP. Transforming growth factor-β1 modulates expression of adhesion and cytoskeletal proteins in human peritoneal fibroblasts. Fertil Steril. 2002 Jul;78(1):154-61.

74. Saed GM, Diamond MP. Molecular characterization of postoperative adhesions: The adhesion phenotype. J Am Assoc Gynecol Laparosc. 2004 Aug;11(3):307-14.

75. Arung W, Meurisse M, Detry O. Pathophysiology and prevention of postoperative peritoneal adhesions. World Journal of Gastroenterology. 2011 Nov 7;17(41):4545-53.

76. Alpay Z, Saed GM, Diamond MP. Postoperative adhesions: From formation to prevention. Seminars in Reproductive Medicine. 2008 Jul;26(4):313-21.

77. Braun KM, Diamond MP. The biology of adhesion formation in the peritoneal cavity. Semin Pediatr Surg. 2014 Dec;23(6):336-43.

78. Brokelman WJA, Lensvelt M, Rinkes IHMB, Klinkenbijl JHG, Reijnen MMPJ. Peritoneal changes due to laparoscopic surgery. Surgical Endoscopy. 2011 Jan;25(1):1-9.

79. Saed GM, Diamond MP. Modulation of the expression of tissue plasminogen activator and its inhibitor by hypoxia in human peritoneal and adhesion fibroblasts. Fertil Steril. 2003 Jan;79(1):164-8.

80. Fletcher NM, Jiang ZL, Diamond MP, Abu-Soud HM, Saed GM. Hypoxia-generated superoxide induces the development of the adhesion phenotype. Free Radic Biol Med. 2008 Aug 15;45(4):530-6.

81. Ivarsson ML, Diamond MP, Falk P, Holmdahl L. Plasminogen activator/plasminogen activator inhibitor-1 and cytokine modulation by the PROACTTM System. Fertil Steril. 2003 Apr;79(4):987-92.

82. Ambler DR, Fletcher NM, Diamond MP, Saed GM. Effects of hypoxia on the expression of inflammatory markers IL-6 and TNF-a in human normal peritoneal and adhesion fibroblasts. Syst Biol Reprod Med. 2012 Dec;58(6):324-9.

83. Chegini N, Zhao Y, Kotseos K, Ma C, Bennett B, Diamond MP, et al. Differential expression of matrix metalloproteinase and tissue inhibitor of MMP in serosal tissue of intraperitoneal organs and adhesions. BJOG An Int J Obstet Gynaecol. 2002 Sep;109(9):1041-9.

84. Visse R, Nagase H. Matrix metalloproteinases and tissue inhibitors of metalloproteinases: Structure, function, and biochemistry. Circulation Research. 2003 May 2;92(8):827-39.

85. Rout UK, Oommen K, Diamond MP. Altered expressions of VEGF mRNA splice variants during progression of uterine-peritoneal adhesions in the rat. In: American Journal of Reproductive Immunology. 2000 May;43(5):299-304.

86. Diamond MP, El-Hammady E, Munkarah A, Bieber EJ, Saed G. Modulation of the expression of vascular endothelial growth factor in human fibroblasts. Fertil Steril. 2005 Feb;83(2):405-9.

87. Saed GM, Munkarah AR, Abu-Soud HM, Diamond MP. Hypoxia upregulates cyclooxygenase-2 and prostaglandin E2 levels in human peritoneal fibroblasts. Fertil Steril. 2005 Apr;83 Suppl 1:1216-9.

88. Wei G, Chen X, Wang G, Jia P, Xu Q, Ping G, et al. Inhibition of cyclooxygenase-2 prevents intra-abdominal adhesions by decreasing activity of peritoneal fibroblasts. Drug Des Devel Ther. 2015 Jun 15;9:3083-98.

89. Brüggmann D, Tchartchian G, Wallwiener M, Münstedt K, Tinneberg HR, Hackethal A.

Intra-abdominal adhesions - Definition, origin, significance in surgical practice, and treatment options. Dtsch Arztebl Int. 2010 Nov;107(44):769-75.

90. Liakakos T, Thomakos N, Fine PM, Dervenis C, Young RL. Peritoneal Adhesions: Etiology, Pathophysiology, and Clinical Significance. Dig Surg. 2001; 18(4):260-73.

91. van den Hil LCL, Vogels RRM, van Barneveld KWY, Gijbels MJJ, Peutz-Kootstra CJ, Cleutjens JPM, et al. Comparability of histological outcomes in rats and humans in a hernia model. J Surg Res. 2018 Sep;229:271-276.

92. Hu W, Zhang Z, Zhu L, Wen Y, Zhang T, Ren P, et al. Combination of Polypropylene Mesh and in Situ Injectable Mussel-Inspired Hydrogel in Laparoscopic Hernia Repair for Preventing Post-Surgical Adhesions in the Piglet Model. ACS Biomater Sci Eng. 2020 Mar 9;6(3):1735-1743.

93. Tang J, Xiang Z, Bernards MT, Chen S. Peritoneal adhesions: Occurrence, prevention and experimental models. Acta Biomater [Internet]. 2020;116:84–104.

94. Whang SH, Astudillo JA, Sporn E, Bachman SL, Miedema BW, Davis W, et al. In search of the best peritoneal adhesion model: Comparison of different techniques in a rat model. J Surg Res. 2011 May 15;167(2):245-50.

95. Poehnert D, Neubert L, Klempnauer J, Borchert P, Jonigk D, Winny M. Comparison of adhesion prevention capabilities of the modified starch powder-based medical devices 4DryField® PH and AristaTM AH in the optimized peritoneal adhesion model. Int J Med Sci. 2019 Sep 19;16(10):1350-1355.

96. Wallwiener CW, Kraemer B, Wallwiener M, Brochhausen C, Isaacson KB, Rajab TK. The extent of adhesion induction through electrocoagulation and suturing in an experimental rat study. Fertil Steril. 2010 Mar 1;93(4):1040-4.

97. Chandel AKS, Shimizu A, Hasegawa K, Ito T. Advancement of Biomaterial-Based Postoperative Adhesion Barriers. Macromol Biosci. 2021 Jan 19;e2000395.

98. Bosmans JWAM, Jongen ACHM, Bouvy ND, Derikx JPM. Colorectal anastomotic healing: Why the biological processes that lead to anastomotic leakage should be revealed prior to conducting intervention studies. BMC Gastroenterol. 2015 Dec 21;15:180.

99. Yauw STK, Wever KE, Hoesseini A, Ritskes-Hoitinga M, Van Goor H. Systematic review

of experimental studies on intestinal anastomosis. British Journal of Surgery. 2015 Jun;102(7):726-34.

100. Kararli TT. Comparison of the gastrointestinal anatomy, physiology, and biochemistry of humans and commonly used laboratory animals. Biopharmaceutics & Drug Disposition. 1995 Jul;16(5):351-80.

101. Swindle MM, Smith AC. Comparative anatomy and physiology of the pig. Scandinavian Journal of Laboratory Animal Science. 1998 Jan;25(Suppl 1):11-21.

102. Swindle MM. Comparative Anatomy of the Pig. Sinclear Res. 2003.

103. Boersema GSA, Vennix S, Wu Z, Te Lintel Hekkert M, Duncker DJGM, Lam KH, et al. Reinforcement of the colon anastomosis with cyanoacrylate glue: a porcine model. J Surg Res [Internet]. 2017;217:84–91.

104. Testini M, Gurrado A, Portincasa P, Scacco S, Marzullo A, Piccinni G, et al. Bovine pericardium patch wrapping intestinal anastomosis improves healing process and prevents leakage in a pig model. PLoS One. 2014 Jan 29;9(1):e86627.

105. Yildiz R, Can MF, Yagci G, Ozgurtas T, Guden M, Gamsizkan M, et al. The effects of hyperbaric oxygen therapy on experimental colon anastomosis after preoperative chemoradiotherapy. Int Surg. 2013 Jan-Mar;98(1):33-42.

106. Khorshidi HR, Kasraianfard A, Derakhshanfar A, Rahimi S, Sharifi A, Makarchian HR, et al. Evaluation of the effectiveness of sodium hyaluronate, sesame oil, honey, and silver nanoparticles in preventing postoperative surgical adhesion formation. An experimental study. Acta Cir Bras [Internet]. 2017;32(8):626–32.

107. Shogan BD, Belogortseva N, Luong PM, Zaborin A, Lax S, Bethel C, et al. Collagen degradation and MMP9 activation by Enterococcus faecalis contribute to intestinal anastomotic leak. Sci Transl Med. 2015 May 6;7(286):286ra68.

108. Li YW, Lian P, Huang B, Zheng HT, Wang MH, Gu WL, et al. Very Early Colorectal Anastomotic Leakage within 5 Post-operative Days: A More Severe Subtype Needs Relaparatomy. Sci Rep. 2017 Jan 13;7:39936.

109. Coger V, Million N, Rehbock C, Sures B, Nachev M, Barcikowski S, et al. Tissue Concentrations of Zinc, Iron, Copper, and Magnesium During the Phases of Full

Thickness Wound Healing in a Rodent Model. Biol Trace Elem Res. 2019 Sep;191(1):167-176.

110. Bowden LG, Byrne HM, Maini PK, Moulton DE. A morphoelastic model for dermal wound closure. Biomech Model Mechanobiol. 2016 Jun;15(3):663-81.

111. Aguilar Navarro E, Garcia Gomez De Las Heras S, Pastor Idoate C, Garcia Vasquez C, García Diego G, Fernandez Aceñero MJ. Influence of Tachosil patches on the tissue response to hypoxia in a swine model of highrisk large bowel anastomosis. Virchows Arch. 2018.

112. García-Vásquez C, Fernández-Aceñero MJ, García Gómez-Heras S, Pastor C. Fibrin patch influences the expression of hypoxia-inducible factor-1α and nuclear factor-κBp65 factors on ischemic intestinal anastomosis. Exp Biol Med. 2018 Jun;243(10):803-808.

113. Hoeppner J, Willa K, Timme S, Tittelbach-Helmrich D, Hopt UT, Keck T, et al. Reinforcement of colonic anastomoses with a collagenous double-layer matrix extracted from porcine dermis. Eur Surg Res. 2010;45(2):68-76.

114. Henne-Bruns D, Kreischer HP, Schmiegelow P, Kremer B. Reinforcement of colon anastomoses with polyglycolic acid mesh: An experimental study. Eur Surg Res. 1990 ;22(4):224-30.

115. Dogan G, Dogan G, Kayir S, Yagan O, Hanci V. Comparison of the Effects of Neostigmine and Sugammadex on Colonic Anastomotic Strength in Rats. J Surg Res. 2020 Apr;248:123-128.

116. Khoorjestan SM, Rouhi G, Toolabi K. An investigation of the effects of suture patterns on mechanical strength of intestinal anastomosis: an experimental study: Suture patterns and material for intestinal anastomosis. Biomed Tech. 2017 Aug 28;62(4):429-437.

117. Tucker N, Stanger JJ, Staiger MP, Razzaq H, Hofman K. The history of the science and technology of electrospinning from 1600 to 1995. J Eng Fiber Fabr. 2012 Jul;63-73.

118. Bölgen N, Vaseashta A. Nanofibers for tissue engineering and regenerative medicine. In: IFMBE Proceedings. 2016 Jan 08;50:319-322.

119. Nisbet DR, Forsythe JS, Shen W, Finkelstein DI, Horne MK. Review paper: A review of

the cellular response on electrospun nanofibers for tissue engineering. Journal of Biomaterials Applications. 2009 Jul;24(1):7-29.

120. Scaffaro R, Lopresti F, Botta L. Preparation, characterization and hydrolytic degradation of PLA/PCL co-mingled nanofibrous mats prepared via dual-jet electrospinning. Eur Polym J. 2017;96:266-277.
121. Jirsak O, Kalinova K, Stranska D. Nanofibre technologies and Nanospider applications. In: VDI Berichte. 2006;1940:41-46.
122. Partheniadis I, Nikolakakis I, Laidmäe I, Heinämäki J. A mini-review: Needleless electrospinning of nanofibers for pharmaceutical and biomedical applications. Processes. 2020 Jun 06; 8(6):673.
123. Kenawy ER, Abdel-Hay FI, El-Newehy MH, Wnek GE. Processing of polymer nanofibers through electrospinning as drug delivery systems. Mater Chem Phys. 2009 Aug 31;113(1):296-302.
124. Zamani M, Prabhakaran MP, Ramakrishna S. Advances in drug delivery via electrospun and electrosprayed nanomaterials. International Journal of Nanomedicine. 2013;8:2997-3017.
125. Ye K, Kuang H, You Z, Morsi Y, Mo X. Electrospun nanofibers for tissue engineering with drug loading and release. Pharmaceutics. 2019 Apr 15;11(4):182.
126. Luu YK, Kim K, Hsiao BS, Chu B, Hadjiargyrou M. Development of a nanostructured DNA delivery scaffold via electrospinning of PLGA and PLA-PEG block copolymers. J Control Release. 2003 Apr 29;89(2):341-53.
127. Dong Y, Zheng Y, Zhang K, Yao Y, Wang L, Li X, et al. Electrospun Nanofibrous Materials for Wound Healing. Adv Fiber Mater. 2020 Mar 21; 2:212–227.
128. Jayarama Reddy V, Radhakrishnan S, Ravichandran R, Mukherjee S, Balamurugan R, Sundarrajan S, et al. Nanofibrous structured biomimetic strategies for skin tissue regeneration. Wound Repair and Regeneration. 2013 Jan-Feb 2013;21(1):1-16.
129. Zhong W, Xing MMQ, Maibach HI. Nanofibrous materials for wound care. Cutaneous and Ocular Toxicology. 2010 Sep;29(3):143-52.
130. Rho KS, Jeong L, Lee G, Seo BM, Park YJ, Hong SD, et al. Electrospinning of collagen

nanofibers: Effects on the behavior of normal human keratinocytes and early-stage wound healing. Biomaterials. 2006 Mar;27(8):1452-61.

131. Lee CH, Singla A, Lee Y. Biomedical applications of collagen. Int J Pharm. 2001 Jun 19;221(1-2):1-22.
132. Hong KH. Preparation and properties of electrospun poly (vinyl alcohol)/silver fiber web as wound dressings. Polym Eng Sci. 2007; 47: 43-49.
133. Taepaiboon P, Rungsardthong U, Supaphol P. Drug-loaded electrospun mats of poly(vinyl alcohol) fibres and their release characteristics of four model drugs. Nanotechnology. 2006 Apr 11;17:2317.
134. Contreras-Cáceres R, Cabeza L, Perazzoli G, Díaz A, López-Romero JM, Melguizo C, et al. Electrospun nanofibers: Recent applications in drug delivery and cancer therapy. Nanomaterials. 2019 Apr 24;9(4):656.
135. Ong CT, Zhang Y, Lim R, Samsonraj R, Masilamani J, Phan THH, et al. Preclinical Evaluation of TegadermTM Supported Nanofibrous Wound Matrix Dressing on Porcine Wound Healing Model. Adv Wound Care. 2015 Feb 1; 4(2): 110–118.
136. Zarei F, Soleimaninejad M. Role of growth factors and biomaterials in wound healing. Artificial Cells, Nanomedicine and Biotechnology. 2018 2018;46(sup1):906-911.
137. Horakova J, Mikes P, Saman A, Jencova V, Klapstova A, Svarcova T, et al. The effect of ethylene oxide sterilization on electrospun vascular grafts made from biodegradable polyesters. Mater Sci Eng C. 2018 Jun 27;92:132-142.
138. Nordentoft T, Rømer J, Sørensen M. Sealing of gastrointestinal anastomoses with a fibrin glue-coated collagen patch: A safety study. J Investig Surg. 2007 Nov-Dec;20(6):363–9.
139. Nordentoft T, Holte K. Preventing Clinical Leakage of Colonic Anastomoses with A Fibrin-Coated Collagen Patch Sealing - An Experimental Study. Arch Clin Exp Surg. 2014;3:201-206.
140. Trotter J, Onos L, McNaught C, Peter M, Gatt M, Maude K, et al. The use of a novel adhesive tissue patch as an aid to anastomotic healing. Ann R Coll Surg Engl. 2018 Mar; 100(3): 230–234.

141. Aznan MI, Khan OH, Unar AO, Tuan Sharif SE, Khan AH, Syed SH, et al. Effect of Tualang honey on the anastomotic wound healing in large bowel anastomosis in rats-A randomized controlled trial. BMC Complement Altern Med [Internet]. 2016;16(1):1–7.
142. Bonanomi G, Prince JM, McSteen F, Schauer PR, Hamad GG. Sealing effect of fibrin glue on the healing of gastrointestinal anastomoses: Implications for the endoscopic treatment of leaks. Surg Endosc Other Interv Tech. 2004 Nov;18(11):1620–4.
143. Fajardo AD, Amador-Ortiz C, Chun J, Stewart D, Fleshman JW. Evaluation of bioabsorbable seamguard for staple line reinforcement in stapled rectal anastomoses. Surg Innov. 2012 Sep;19(3):288–94.
144. Zilling TL, Jansson O, Walther BS, Ottosson A. Sutureless small bowel anastomoses: Experimental study in pigs. Eur J Surg. 1999 Jan;165(1):61–8.
145. Kosmidis C, Efthimiadis C, Anthimidis G, Basdanis G, Apostolidis S, Hytiroglou P, et al. Myofibroblasts and colonic anastomosis healing in Wistar rats. BMC Surg [Internet]. 2011 Mar 2;11(1):6.
146. Nordentoft T, Sørensen M. Leakage of colon anastomoses: Development of an experimental model in pigs. Eur Surg Res. 2007;39(1):14–6.
147. Nordentoft T, Pommergaard HC, Rosenberg J, Achiam MP. Fibrin glue does not improve healing of gastrointestinal anastomoses: A systematic review. Eur Surg Res. 2015;54(1–2):1–13.
148. Srouji S, Kizhner T, Suss-Tobi E, Livne E, Zussman E. 3-D Nanofibrous electrospun multilayered construct is an alternative ECM mimicking scaffold. J Mater Sci Mater Med. 2008;19(3):1249–55.
149. Ditzel M, Deerenberg EB, Komen N, Mulder IM, Jeekel H, Lange JF. Postoperative adhesion prevention with a new barrier: An experimental study. Eur Surg Res. 2012;48(4):187–93.
150. Gao X, Deng X, Wei X, Shi H, Wang F, Ye T, et al. Novel thermosensitive hydrogel for preventing formation of abdominal adhesions. Int J Nanomedicine. 2013;8:2453–63.
151. Kataria H, Singh VP. Liquid Paraffin vs Hyaluronic Acid in Preventing Intraperitoneal Adhesions. Indian J Surg. 2017;79(6):539–43.

152. Wang P, Gong G, Li Y, Li J. Hydroxyethyl starch 130/0.4 augments healing of colonic anastomosis in a rat model of peritonitis. Am J Surg. 2010 Feb;199(2):232-9.
153. Tebala GD, Ceriati F, Ceriati E, Vecchioli A, Nori S. The use of cyanoacrylate tissue adhesive in high-risk intestinal anastomoses. Surg Today. 1995;25(12):1069–72.
154. Adas G, Kemik O, Eryasar B, Okcu A, Adas M, Arikan S, et al. Treatment of ischemic colonic anastomoses with systemic transplanted bone marrow derived mesenchymal stem cells. Eur Rev Med Pharmacol Sci. 2013;17(17):2275–85.
155. Emans PJ, Schreinemacher MHF, Gijbels MJJ, Beets GL, Greve JWM, Koole LH, et al. Polypropylene meshes to prevent abdominal herniation. Can stable coatings prevent adhesions in the long term? Ann Biomed Eng. 2009 Feb 2;37(2):410-418.
156. Rosendorf J, Horakova J, Klicova M, Palek R, Cervenkova L, Kural T, et al. Experimental fortification of intestinal anastomoses with nanofibrous materials in a large animal model. Sci Rep. 2020 Jan 24;10(1):1134.
157. Siegel S, Castellan Jr. NJ. Nonparametric statistics for the behavioral sciences, 2nd ed. Nonparametric Stat Behav Sci 2nd ed. 1988.
158. Baker MI, Walsh SP, Schwartz Z, Boyan BD. A review of polyvinyl alcohol and its uses in cartilage and orthopedic applications. Journal of Biomedical Materials Research - Part B Applied Biomaterials. 2012 Jul;100(5):1451-7.
159. Cai EZ, Teo EY, Jing L, Koh YP, Qian TS, Wen F, et al. Bio-conjugated polycaprolactone membranes: A novel wound dressing. Arch Plast Surg. 2014 Nov; 41(6): 638–646.
160. Kwon TR, Han SW, Yeo IK, Kim JH, Kim JM, Hong JY, et al. Biostimulatory effects of polydioxanone, poly-d, l lactic acid, and polycaprolactone fillers in mouse model. J Cosmet Dermatol. 2019 Aug;18(4):1002-1008.
161. McLoughlin CE, Smith MJ, Auttachoat W, Bowlin GL, White KL. Evaluation of innate, humoral and cell-mediated immunity in mice following in vivo implantation of electrospun polycaprolactone. Biomed Mater. 2012 Apr 27;7(3):035015.
162. Yao N zhao, Huang C, Jin D di. Evaluation of biocompatibility of a pectin/polyvinyl alcohol composite hydrogel as a new nucleus material. Orthop Surg. 2009 Aug; 1(3): 231–237.

163. Duvallet C, Gibbons SM, Gurry T, Irizarry RA, Alm EJ. Meta-analysis of gut microbiome studies identifies disease-specific and shared responses. Nat Commun. 2017 Dec 5;8(1):1784.
164. Mancabelli L, Milani C, Lugli GA, Turroni F, Ferrario C, van Sinderen D, et al. Meta-analysis of the human gut microbiome from urbanized and pre-agricultural populations. Environmental Microbiology. 2017 Apr;19(4):1379-1390.
165. Ouaïssi M, Gaujoux S, Veyrie N, Denève E, Brigand C, Castel B, et al. Post-operative adhesions after digestive surgery: Their incidence and prevention: Review of the literature. Journal de Chirurgie Viscerale. 2012 Apr;149(2):e104-14.
166. Chen Y, Hills BA. Surgical adhesions: Evidence for adsorption of surfactant to peritoneal mesothelium. Aust N Z J Surg. 2000 Jun;70(6):443-7.
167. Fletcher NM, Awonuga AO, Abusamaan MS, Saed MG, Diamond MP, Saed GM. Adhesion phenotype manifests an altered metabolic profile favoring glycolysis. Fertil Steril. 2016 Jun 1;105(6):1628-1637
168. Fortin CN, Saed GM, Diamond MP. Predisposing factors to post-operative adhesion development. Hum Reprod Update. 2014 Jul-Aug 2015;21(4):536-51.
169. Lovisa S, Genovese G, Danese S. Role of Epithelial-to-Mesenchymal Transition in Inflammatory Bowel Disease. Journal of Crohn's and Colitis. 2019 Apr 26;13(5):659-668.
170. Wu Z, Vakalopoulos KA, Kroese LF, Boersema GSA, Kleinrensink GJ, Jeekel J, et al. Reducing anastomotic leakage by reinforcement of colorectal anastomosis with cyanoacrylate glue. Eur Surg Res. 2013;50(3–4):255–61.
171. Klicova M, Klapstova A, Chvojka J, Koprivova B, Jencova V, Horakova J. Novel double-layered planar scaffold combining electrospun PCL fibers and PVA hydrogels with high shape integrity and water stability. Mater Lett. 2020 March15;127281.
172. Mehrotra R, Devuyst O, Davies SJ, Johnson DW. The current state of peritoneal dialysis. Journal of the American Society of Nephrology. 2016 Nov;27(11):3238-3252.
173. Giffin DM, Gow KW, Warriner CB, Walley KR, Phang PT. Oxygen uptake during peritoneal ventilation in a porcine model of hypoxemia. Crit Care Med. 1998 Sep;26(9):1564-8.
174. Hashemi H, Asgari S, Shahhoseini S, Mahbod M, Atyabi F, Bakhshandeh H, et al.

Application of polycaprolactone nanofibers as patch graft in ophthalmology. Indian J Ophthalmol. 2018 Feb; 66(2): 225–228.

175. García-Salinas S, Evangelopoulos M, Gámez-Herrera E, Arruebo M, Irusta S, Taraballi F, et al. Electrospun anti-inflammatory patch loaded with essential oils for wound healing. Int J Pharm. 2020 22 Jan;577:119067.
176. Gunatillake PA, Adhikari R, Gadegaard N. Biodegradable synthetic polymers for tissue engineering. European Cells and Materials. 2003 May 20;5:1-16.
177. Luo L, He Y, Chang Q, Xie G, Zhan W, Wang X, et al. Polycaprolactone nanofibrous mesh reduces foreign body reaction and induces adipose flap expansion in tissue engineering chamber. Int J Nanomedicine. 2016 11: 6471–6483.
178. Horakova J, Klicova M, Erben J, Klapstova A, Novotny V, Behalek L, et al. Impact of Various Sterilization and Disinfection Techniques on Electrospun Poly-ϵ-caprolactone. ACS Omega. 2020 Apr 21; 5(15): 8885–8892.
179. Ricciardi R, Roberts PL, Marcello PW, Hall JF, Read TE, Schoetz DJ. Anastomotic leak testing after colorectal resection: What are the data? Arch Surg. 2009 May;144(5):407-11.
180. Špinka M, editor. Advances in pig welfare. 1st ed. United Kingdom. Elsevier/ Woodhead Publishing. 2017 Nov 10.
181. Ergul E, Korukluoglu B. Peritoneal adhesions: Facing the enemy. International Journal of Surgery. 2008;6(3):253-260.
182. Guyton KL, Levine ZC, Lowry AC, Lambert L, Gribovskaja-Rupp I, Hyman N, et al. Identification of Collagenolytic Bacteria in Human Samples: Screening Methods and Clinical Implications for Resolving and Preventing Anastomotic Leaks and Wound Complications. Dis Colon Rectum. 2019 Aug;62(8):972-979.
183. Huang J, Xia X, Zou Q, Ma J, Jin S, Li J, et al. The long-term behaviors and differences in bone reconstruction of three polymer-based scaffolds with different degradability. J Mater Chem B. 2019 Nov 5;7:7690-7703.
184. Ranjbar-Mohammadi M, Bahrami SH. Electrospun curcumin loaded poly(ε-caprolactone)/gum tragacanth nanofibers for biomedical application. Int J Biol

Macromol. 2016 Mar;84:448-56.

185. Wirth U, Rogers S, Haubensak K, Schopf S, von Ahnen T, Schardey HM. Local antibiotic decontamination to prevent anastomotic leakage short-term outcome in rectal cancer surgery. Int J Colorectal Dis. 2018.

186. Oh J, Kuan KG, Tiong LU, Trochsler MI, Jay G, Schmidt TA, et al. Recombinant human lubricin for prevention of postoperative intra-abdominal adhesions in a rat model. J Surg Res. 2017 Feb;208:20-25.

187. Hirai K, Tabata Y, Hasegawa S, Sakai Y. Enhanced intestinal anastomotic healing with gelatin hydrogel incorporating basic fibroblast growth factor. J Tissue Eng Regen Med. 2016 Oct;10(10):E433-E442.

188. Landes LC, Drescher D, Tagkalos E, Grimminger PP, Thieme R, Jansen-Winkeln B, et al. Upregulation of VEGFR1 in a rat model of esophagogastric anastomotic healing. Acta Chir Belg. 2018 Jun;118(3):161-166.

7. List of authors' scientific outputs during the postgraduate study

Articles (22)

Rosendorf J, Klicova M, Cervenkova L, Horakova J, Klapstova A, Hosek P, Palek R, Sevcik J, Polak R, Treska V, Chvojka J, Liska V. Reinforcement of Colonic Anastomosis with Improved Ultrafine Nanofibrous Patch: Experiment on Pig. Biomedicines. 2021; 9(2):102. **Q1, IF = 4.717**

Rosendorf J, Horakova J, Klicova M, Palek R, Cervenkova L, Kural T, Hosek P, Kriz T, Tegl V, Moulisova V, Tonar Z, Treska V, Lukas D, Liska V: Experimental fortification of intestinal anastomoses with nanofibrous materials in a large animal model. Sci Rep. 2020 Jan 24;10(1):1134. **Q1, IF = 4.180**

Rosendorf J, Klicova M, Cervenkova L, Palek R, Horakova J, Klapstova A, Hosek P, Moulisova V, Bednar L, Tegl V, Brzon O, Tonar Z, Treska V, Lukas D, Liska V. Double-layered Nanofibrous Patch for Prevention of Anastomotic Leakage and Peritoneal Adhesions, Experimental Study. In Vivo. 2021 Mar-Apr;35(2):731-741. **Q2, IF = 1.586**

Jirik M, Gruber I, Moulisova V, Schindler C, Cervenkova L, Palek R, Rosendorf J, Arlt J, Bolek L, Dejmek J, Dahmen U, Zelezny M, Liska V. Semantic Segmentation of Intralobular and Extralobular Tissue from Liver Scaffold H&E Images. Sensors. 2020; 20(24):7063. **Q1, IF = 3.215**

Bendova P, Pardini B, Susova S, Rosendorf J, Levy M, Skrobanek P, Buchler T, Kral J, Liska V, Vodickova L, Landi S, Soucek P, Naccarati A, Vodicka P, Vymetalkova V. Genetic variations in microRNA binding sites of solute carrier transporter genes as predictors of clinical outcome in colorectal cancer. Carcinogenesis. 2020 Dec 15:bgaa136. **Q1, IF = 4.546**

Palek R, Rosendorf J, Maleckova A, Vistejnova L, Bajcurova K, Mirka H, Tegl V, Brzon O, Kumar A, Bednar L, Tonar Z, Hosek P, Moulisova V, Eberlova L, Treska V, Liska V. Influence of Mesenchymal Stem Cell Administration on The Outcome of Partial Liver Resection in a Porcine Model of Sinusoidal Obstruction Syndrome. Anticancer Res. 2020 Dec;40(12):6817-6833. **Q2, IF = 2.036**

Treska V, Skala M, Prochazkova K, Svejdova A, Petrakova T, Sebek J, Riha I, Rosendorf J, Polak R, Skalicky T, Liska V. Long-term Results of Surgery for Colorectal Liver Metastases in Terms of Primary Tumour Location and Clinical Risk Factors. In Vivo. 2020 Sep-Oct;34(5):2675-2685. **Q2, IF = 1.586**

Rosendorf J, Mirka H, Michal M, Palek R, Sleisova G, Treska V, Liska V: Benign liver angiomyolipoma: a case study. Rozhl Chir 2020;99:91–94.

Rosendorf J, Liska V, Palek R, Treska V: Acute Abdomen in Pregnancy: A Retrospective Study of Pregnant Patients Hospitalised for Abdominal Pain. Rozhl Chir. Winter 2020;99(3):131-135.

Moulisova V, Jirik M, Schindler C, Cervenkova L, Palek R, Rosendorf J, Arlt J, Bolek L: Novel morphological multi-scale evaluation system for quality assessment of decellularized liver scaffolds. J Tissue Eng. 2020 Jan-Dec; 11: 2041731420921121. **Q1, IF = 3.140**

Rosendorf J, Palek R, Mirka H, Treska V, Liska V. Injuries of the small and large intestine. Rozhl Chir. 2019 Summer;98(8):315-320. **Awarded by the Czech Surgical Society as the best publication of the journal of the year 2019 (Niederle's Prize)**

Vycital O, Horsky O, Rosendorf J, Liska V, Skalicky T, Treska V. Treatment of liver injuries at the Trauma Centre of the University Hospital in Pilsen. Rozhl Chir. 2019 Winter;98(12):488-491. doi: 10.33699/PIS.2019.98.12.488-491.

Rosendorf J, Mirka H, Boudova L, Liska V, Treska V. Hepatic pseudolymphoma: a surprising finding in a case with suspected generalisation of lung cancer. Rozhl Chir. 2019 Winter;98(11):469-472. doi: 10.33699/PIS.2019.98.11.469-472.

Cervenkova L, Vycital O, Bruha J, Rosendorf J, Palek R, Liska V, Daum O, Mohelnikova-Duchonova B, Soucek P. Protein expression of ABCC2 and SLC22A3 associates with prognosis of pancreatic adenocarcinoma. Sci Rep. 2019 Dec 24;9(1):19782. **Q1, IF = 4.180**

Liska V, Moulisova V, Palek R, Rosendorf J, Cervenková L, Bolek L, Treska V. Repopulation of decellularized pig scaffolds: Promising approach for liver tissue engineering. Rozhl Chir. 2019 Fall;98(10):388-393.

Palek R, Jonasova A, Rosendorf J, Mik P, Bajcurova K, Hosek P, Moulisova V, Eberlova L, Haidingerova L, Brzon O, Bednar L, Kriz T, Dolansky M, Treska V, Tonar Z, Vimmr J, Liska V. Allogeneic Venous Grafts of Different Origin Used for Portal Vein Reconstruction After Pancreaticoduodenectomy - Experimental Study. Anticancer Res. 2019 Dec;39(12):6603-6620. **Q2, IF = 2.036**

Maleckova A, Tonar Z, Mik P, Michalova K, Liska V, Palek R, Rosendorf J, Kralickova M, Treska V. Animal models of liver diseases and their application in experimental surgery. Rozhl Chir. 2019 Winter;98(3):100-109.

Thiele JA, Hosek P, Kralovcova E, Ostasov P, Liska V, Bruha J, Vycital O, Rosendorf J, Kralickova M, Pitule P: lncRNAs in healthy tissue have prognostic value in colorectal cancer. Int J Mol Sci. 2018 Sep 8;19(9). **Q1, IF = 4.602**

Mik P, Tonar Z, Maleckova A, Eberlova L, Liska V, Palek R, Rosendorf J, Jirik M, Mírka H, Kralickova M, Witter K: Distribution of connective tissue in the male and female porcine liver: Histological mapping and recommendations for sampling of tissue probes. J Comp Pathol. 2018 Jul;162:1-13. **Q2, IF = 1.063**

Palek R, Liska V, Treska V, Rosendorf J, Emingr M, Tegl V, Kralickova A, Bajcurova K, Jirik M, Tonar Z: Sinusoidal obstruction syndrome induced by monocrotaline in experiment on large animal model - a pilot study. Rozhl Chir. 2018; 214-221.

Liska V, Treska V, Mirka H, Vycital O, Bruha J, Haidingerova L, Benes J, Tonar Z, Palek R, Rosendorf J. Experimental promotion of liver regeneration after portal vein branch ligation. Rozhl Chir. Spring 2018;97(5):239-245.

Liska V, Treska V, Skalicky T, Fichtl J, Bruha J, Vycital O, Topolcan O, Palek R, Rosendorf J, Polivka J, Holubec L: Evaluation of Tumor Markers and Their Impact on Prognosis in Gallbladder, Bile Duct and Cholangiocellular Carcinomas - A Pilot Study. Anticancer Res., 2017, 37(4): 2003-2009. **Q2, IF = 2.036**

Eberlova L, Liska V, Mirka H, Tonar Z, Haviar S, Svoboda M, Benes J, Palek R, Emingr M, Rosendorf J, Mik P, Lametschwandtner A.: The use of porcine corrosion casts for teaching human anatomy. Ann Anat. 2017 Sep;213:69-77. doi: 10.1016/j.aanat.2017.05.005. Epub 2017 Jun 1. **Q2, IF = 2.553**

Chapters in books (2)

Liska V, Treska V, Novak P, Vycital O, Bruha J, Palek R, Rosendorf J.: Impact of complications of colorectal anastomosis on oncological results. In: Antos F., Hoch J.: Coloproctology – selected chapters, Mlada fronta, Praha, 2017, ISBN: 9788020441799.

Liska V, Treska V, Mirka H, Vycital O, Bruha J, Haidingerova L, Tegl V, Benes J, Mlejnkova V, Tonar Z, Palek R, Rosendorf J, Bajcurova K: Liver regeneration in experiment. In: Rokyta R., Höschl C.: The most important innovations in medicine, Axonite, 2018, ISBN: 978-80-88046-16-5.

Invited lectures (1)

Rosendorf J., Palek R., Cervenkova L., Klicova M., Horakova J., Hosek P., Bednar L., Tegl V., Brzon O., Lukas D., Treska V., Liska V. Modern Trends in Colorectal Surgery, 3rd annual Im gonna be a scientist! Conference in Lodz, Poland, 1/2020

Posters and lectures (examples)

Rosendorf J, Palek R, Tegl V, Brzon O, Kriz T, Dolansky M, Tonar Z., Cervenkova L, Maleckova A, Lukas D, Horakova J, Treska V, Liska V: Fortification of gastrointestinal anastomoses using nanofibrous materials. 8th congress of hepato-pancreato-biliary surgery, Pilsen, Czech Republic, 9/2018, **3rd place award in young authors section**

Rosendorf J, Liska V, Cervenkova L, Hosek P, Palek R, Kriz T, Dolansky M, Bednar L, Lukas D, Horakova J, Klicova M, Treska V: Fortification of gastrointestinal anastomoses with nanomaterials. The 15th International Medical Postgraduate Conference, Hradec Kralove, Czech Republic, 11/2018

Rosendorf J, Cervenkova L, Klicova M, Horakova J, Palek R, Lukas D, Hosek P, Bednar L, Kriz T, Dolanska M, Liska V: Experimental enhancement of anastomotic healing, 4th annual conference of the Biomedical Center in Pilsen, Czech Republic, 7/2018

Rosendorf J, Liska V, Palek R, Treska V: Intestinal and bowel injury in abdominal trauma, 20th European Congress of Trauma and Emergency Surgery, Prague, Czech Republic, 5/2019

Rosendorf J, Liska V, Palek R, Treska V: Intestinal and bowel injury in abdominal trauma, 13thEuropean Colorectal Congress of St.Gallen, Switzerland, 12/2019

Rosendorf J, Horakova J, Klicova M, Palek R, Cervenkova L, Kural T, Hosek P, Treska V, Lukas D, Liska V: Fortification of intestinal anastomoses using nanofibrous materials, 13thEuropean Colorectal Congress of St.Gallen, Switzerland, 12/2019

Rosendorf J, Kural T, Horakova J, Klicova M, Palek R, Cervenkova L, Hosek P, Kriz T, Tegl V, Moulisova V, Tonar Z, Treska V, Lukas D, Liska V: Fortification of intestinal anastomoses using biomaterials and its histological reaction in a large animal model, 23. Chirurgische forschungstage in Aachen, Germany, 9/2019

Rosendorf J, Palek R, Cervenkova L, Klicova M, Horakova J, Hosek P, Bednar L, Tegl V, Brzon O, Lukas D, Treska V, Liska V: Fortification of gastrointestinal anastomoses with nanomaterials. The International Colorectal Disease Symposium 2020, Jerusalem, Israel, 1/2020

Rosendorf J, Cervenkova L, Hosek P, Palek R, Bednar L, Sevcik J, Bohanes M, Sarcevic S, Lukas D, Horakova J, KlicovaM, Treska V, Liska V: Double-layered nanofibrous patch for prevention of anastomotic leakage and peritoneal adhesions, 6/2020. **Awarded by Albert Schweitzer 3rd Prize of the French Institute in Prague, Czech Republic**

8. Attachments

1. Experiment A, Power analysis
2. Experiment A, PAAS standard operating protocol
3. Experiment A, PAAS results
4. Experiment A, Stereology results
5. Experiment B and C, Power analysis
6. Experiment B, PAAS results
7. Experiment B, IWIS results
8. Experiment B, Stereology results
9. Experiment C, PAAS results
10. Experiment C, Stereology and IWIS results
11. Article A: Rosendorf J et al. Experimental fortification of intestinal anastomoses with nanofibrous materials in a large animal model. 2020
12. Article B: Rosendorf J et al. Double-layered Nanofibrous Patch for Prevention of Anastomotic Leakage and Peritoneal Adhesions, Experimental Study. 2021
13. Article C: Rosendorf J et al. Reinforcement of Colonic Anastomosis with Improved Ultrafine Nanofibrous Patch: Experiment on Pig. 2021

Attachment 1: Experiment A, Power analysis

Sample size estimation: We decided to construct 3 intestinal anastomoses per animal to reduce the number of used animals according to the RRR policy. We consider these anastomoses independent for the purpose of the sample size estimation. The sample size was determined by the total number of anastomoses. A suitable number of anastomoses for sufficient results must be divisible by three to result in a whole number of animal subjects.

We assumed the same sample size for both experimental and control group.

We assumed peritoneal adhesions to occur at about 93 % of anastomoses according to literature search. We also assumed about 50 % decrease of peritoneal adhesions occurrence in experimental groups as an effect of our nanomaterials

Sample sizes 21 (3 anastomoses x 7 animals, power level 81,4 %) and 24 (3 anastomoses x 8 animals, power level 87,7 %) are within the desired power range.

We prefer the higher test power for both rough estimate of the results and also a possible influence of grouping the anastomoses. Therefore we chose 24 anastomoses in 8 animals per group.

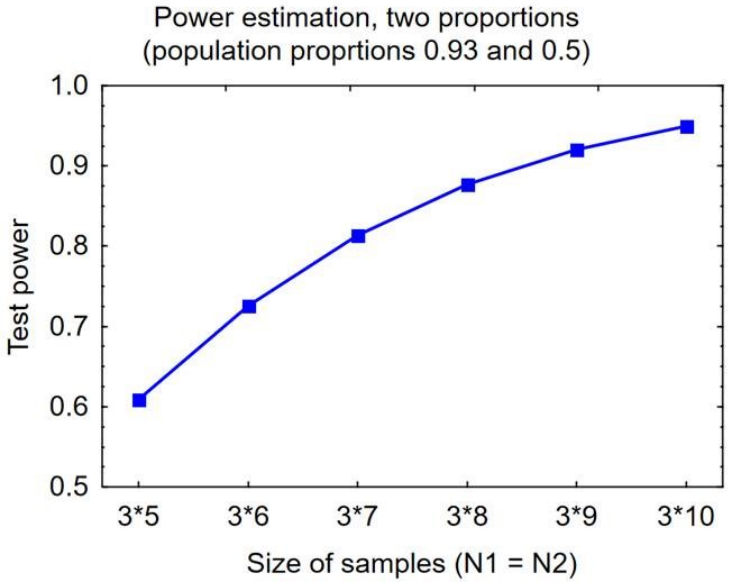

Figure A 1: Power estimation graph

Attachment 2: Experiment A, PAAS standard operating protocol

Title: Standard operating procedure for peritoneal adhesions quality and quantity assessment, sample collection

Created by: Rosendorf J., Biomedical Center, Faculty of Medicine in Pilsen, Charles University, Czech Republic; verified by Liska V. (Head of the laboratory)

Date of creation: 10/2017, translated to English 10/2019

Purpose: Created for the project 'Experimental fortification of intestinal anastomoses with nanofibrous materials in a large animal model'. Project code: MSMT-26570/2017-2. The aim of this protocol is standardization of sample collection and documentation, peritoneal adhesions qualitative and quantitative assessment (Zühlke grading, Perianastomotic adhesions amount score). The experimental animals are subjected to laparotomy in full anesthesia prior to this procedure.

Steps: Take a picture of each anastomosis in situ as well as of the whole abdominal cavity to be archived. Release each anastomosis from peritoneal adhesions if present; leave as much adhesion tissue as possible on the intestine while doing so. Evaluate the quality of adhesions for each anastomosis while performing the step number 2 according to Zühlke's grading system for peritoneal adhesions (Table A1). Resect each anastomosis together with 2 cm of oral and aboral intestine. Cut the collected sample of intestine immediately after collection longitudinally along the mesentery. Treat the specimens carefully. Pin the sample to a cork underlay with a V-shaped incision in one of its sides (Figure A2). Mucosa faces the cork. Oral part faces a marked side of the cork underlay. Assign a random alphanumeric code to the anastomosis sample. Take a picture of the anastomosis on the cork underlay with both animal code/number of anastomosis (1/2/3 starting orally) and the new alphanumeric code to be archived. Measure the specimen and divide its circumference into four parts along the suture line. Assign to each quadrant (starting from left to right to respect the polarity of the intestine) a number of points according to the extent of adhesions (Figure A2). Zero points for no

adhesions in the segment, One point for a segment being partially covered by adhesions, Two points for a fully adhered segment Put the samples of the intestine into 300 ml storing containers filled with 10 % buffered formalin. Mark the containers with the newly created alphanumeric code (for blinding during the histologic evaluation).

Table A 1: Zühlke's adhesions grading system

Grade	**Quality**
0	No adhesions
1	filmy adhesions easy to separate by blunt dissection
2	blunt dissection is possible for the most of adhesions but some sharp dissection is needed, beginning vascularization
3	adhesiolysis is possible by sharp dissection, clear vascularization and bleeding from adhesions during sharp dissection
4	adhesiolysis is possible by sharp dissection but is very challenging. Organs are strongly attached and damage is hardly preventable.

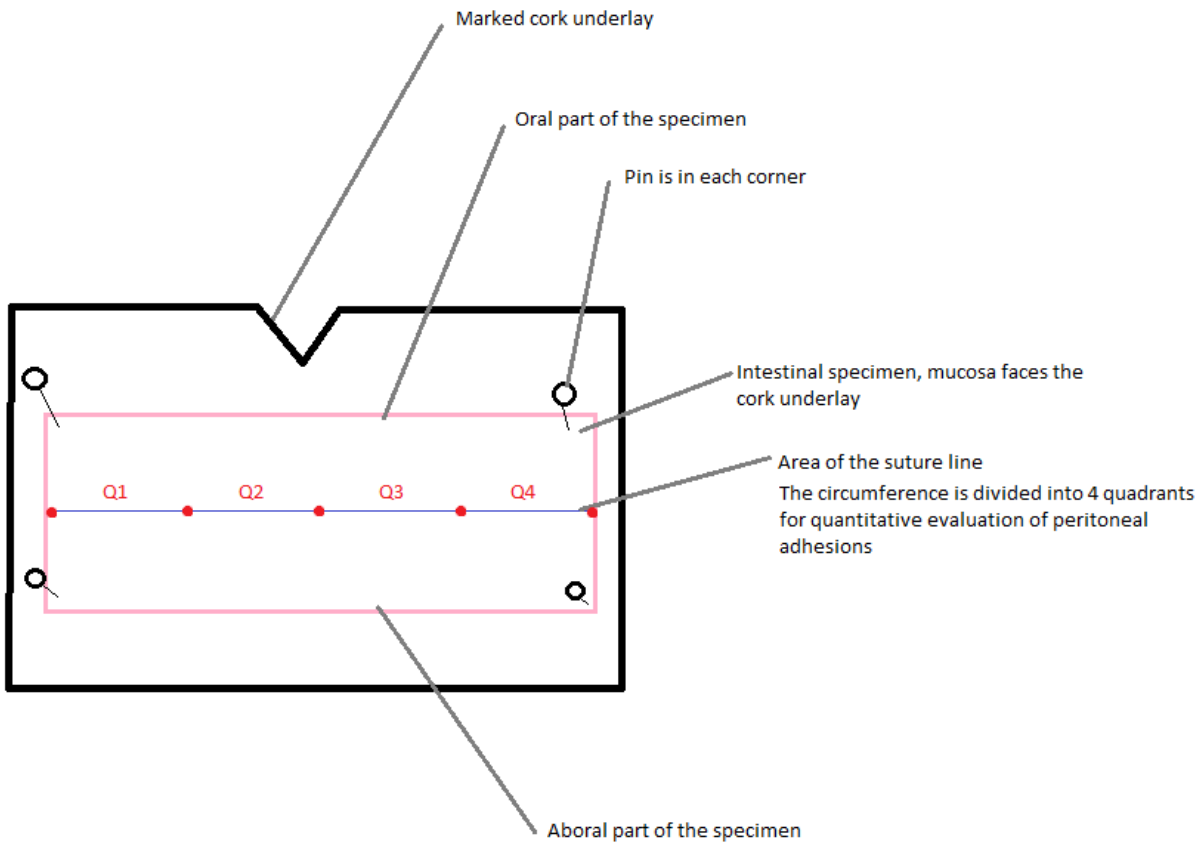

Figure A 2: PAAS grading in 4 quadrants of an instesine pinned onto a cork underlay

Attachment 3: Experiment A, PAAS results

PAAS scores for each quadrant of each anastomosis. Anastomosis is named as animal/number of anastomosis in oral to aboral direction (for example C2/1 means first anastomosis in animal C1). Quadrants are numbered Q1 to Q4 from the right mesenteric quadrant to left mesenteric quadrant. Sum gives the total for each anastomosis (Table A2 – Table A10).

Table A 2: PAAS results Control Group, anastomosis 1

anastomosis	Q1	Q2	Q3	Q4	Sum
C1/1	1	0	0	2	3
C2/1	0	0	0	0	0
C3/1	0	1	0	0	1
C4/1	2	2	0	0	4
C5/1	2	0	0	1	3
C6/1	0	0	1	2	3
C7/1	2	1	0	0	3
C8/1	0	0	0	0	0

Table A 3: PAAS results Control Group, anastomosis 2

anastomosis	Q1	Q2	Q3	Q4	Sum
C1/2	1	0	0	1	2
C2/2	0	0	1	2	3
C3/2	0	0	1	2	3
C4/2	0	0	1	2	3
C5/2	0	0	2	2	4
C6/2	0	0	0	0	0
C7/2	1	0	0	1	2
C8/2	1	1	0	0	2

Table A 4: PAAS results Control Group, anastomosis 3

anastomosis	Q1	Q2	Q3	Q4	Sum
C1/3	0	0	0	0	0
C2/3	0	1	2	1	4
C3/3	0	0	0	0	0
C4/3	1	0	0	0	1
C5/3	0	1	2	1	4
C6/3	0	0	0	0	0
C7/3	0	0	1	0	1
C8/3	0	0	0	0	0

Table A 5: PAAS results PCL Group, anastomosis 1

anastomosis	Q1	Q2	Q3	Q4	Sum
PCL1/1	2	2	0	1	5
PCL2/1	2	0	0	2	4
PCL3/1	0	1	1	0	2
PCL4/1	1	1	1	2	5
PCL5/1	1	0	1	1	3
PCL6/1	2	1	1	1	5
PCL7/1	0	0	0	0	0
PCL8/1	0	0	0	0	0

Table A 6: PAAS results PCL Group, anastomosis 2

anastomosis	Q1	Q2	Q3	Q4	Sum
PCL1/2	2	1	1	2	6
PCL2/2	2	0	0	2	4
PCL3/2	0	0	0	1	1
PCL4/2	2	1	0	2	5
PCL5/2	1	1	0	0	2
PCL6/2	0	0	2	2	4
PCL7/2	0	0	0	0	0
PCL8/2	0	0	0	0	0

Table A 7: PAAS results PCL Group, anastomosis 3

anastomosis	Q1	Q2	Q3	Q4	Sum
PCL1/3	2	1	0	1	4
PCL2/3	2	1	1	2	6
PCL3/3	2	0	1	2	5
PCL4/3	2	1	0	1	4
PCL5/3	2	1	0	0	3
PCL6/3	2	2	1	2	7
PCL7/3	0	0	0	0	0
PCL8/3	2	1	0	1	4

Table A 8: PAAS results PLCL Group, anastomosis 1

anastomosis	Q1	Q2	Q3	Q4	Sum
PLCL1/1	2	0	0	2	4
PLCL2/1	2	0	0	0	2
PLCL3/1	1	0	2	1	4
PLCL4/1	2	2	2	0	6
PLCL5/1	2	2	0	2	6
PLCL6/1	2	0	0	1	3
PLCL7/1	0	0	2	1	3
PLCL8/1	1	1	0	0	2

Table A 9: PAAS results PLCL Group, anastomosis 2

anastomosis	Q1	Q2	Q3	Q4	Sum
PLCL1/2	2	1	0	1	4
PLCL2/2	0	1	2	0	3
PLCL3/2	0	0	0	0	0
PLCL4/2	0	0	0	2	2
PLCL5/2	2	2	1	0	5
PLCL6/2	0	0	0	0	0
PLCL7/2	0	1	1	0	2
PLCL8/2	1	2	0	0	3

Table A 10: PAAS results PLCL Group, anastomosis 3

anastomosis	Q1	Q2	Q3	Q4	Sum
PLCL1/3	0	1	2	0	3
PLCL2/3	2	1	0	0	3
PLCL3/3	0	0	0	0	0
PLCL4/3	2	0	0	0	2
PLCL5/3	0	0	0	0	0
PLCL6/3	2	1	0	1	4
PLCL7/3	0	0	1	2	3
PLCL8/3	2	0	0	0	2

Attachment 4: Experiment A, Stereology results

Results of stereological measurements from Experiment B are listed below. Thickness means the thickness of histological slide. Volume Region Point Counting gives value of the total volume of tissue where our measurements were taken in. Area Fraction stands for volume fraction positive in given parameter (vWF, collagen, MAC387). Value + or – for surgical stich presence was assigned to slides where MAC387 positivity was measured as the presence of stich was associated with higher inflammatory cells infiltration.

Table A 11: Volume fractions of vWF positive area, Control Group

Anastomosis	Thickness (µm)	Volume Region Point Counting (μm^3)	Area Fraction
C 8_1	9,8800	75761963,9016	0,0203
C 8_2	9,6800	86439040,3643	0,0316
C 8_3	9,4800	73324069,0645	0,0339
C 6_1	9,6800	173199415,4512	0,0192
C 6_2	9,1400	174763598,5221	0,0186
C 6_3	9,2300	134201728,9481	0,0214
C 7_1	9,0300	85430885,8681	0,03
C 7_2	9,2900	116262421,3644	0,0155
C 7_3	9,0900	110440221,2625	0,0196
C 1_1	9,0800	81081248,6062	0,0218
C 1_2	9,1800	59728423,5102	0,0185
C 1_3	9,2400	104287723,5893	0,0287
C 2_1	9,0300	80934523,4540	0,018
C 2_2	9,0400	79223615,2308	0,0245
C 2_3	9,3300	101586918,5246	0,0189
C 3_1	9,0800	90123767,0381	0,027
C 3_2	9,1400	61592032,1180	0,0217
C 3_3	9,6800	72621647,2949	0,0195
C 4_1	9,3800	82826016,4799	0,0231
C 4_2	9,1800	116409478,4740	0,019
C 4_3	9,1400	130162471,8159	0,018
C 5_1	9,4900	91673012,0279	0,0221
C 5_2	9,1300	187907782,0695	0,0172
C 5_3	9,2400	87110922,0569	0,0249
Mean	**9,2858**	**102378871,9599**	**0,0222**

Table A 12: Volume fractions of vWF positive area, PCL Group

Anastomosis	Thickness (µm)	Volume Region Point Counting (µm^3)	Area Fraction
PCL 1_1	9,0400	139241505,5572	0,0284
PCL 1_2	9,4800	159235961,1443	0,0216
PCL 1_3	9,1900	463399525,4310	0,0155
PCL 2_1	9,4300	136483603,8270	0,0208
PCL 2_2	9,0400	116434707,2332	0,0229
PCL 2_3	9,2400	116250138,9422	0,0257
PCL 3_1	9,0800	150105805,9699	0,0153
PCL 3_2	9,3500	210127347,8272	0,0229
PCL 3_3	9,2600	121420042,8357	0,0284
PCL 4_1	11,3300	122987213,5228	0,0245
PCL 4_2	9,3500	107701905,0163	0,0238
PCL 4_3	9,1500	105398120,9518	0,0228
PCL 5_1	9,2800	141705956,9830	0,0148
PCL 5_2	9,2900	172389107,5403	0,0166
PCL 5_3	9,1000	144092730,3871	0,014
PCL 6_2	9,2900	101459778,8565	0,0232
PCL 6_3	9,6800	182839457,1275	0,0132
PCL 6_1	9,1500	142454520,8253	0,0227
PCL 7_1	9,2900	218030588,6065	0,0107
PCL 7_3	9,2800	273134514,1624	0,0181
PCL 7_2	9,6800	127294914,9058	0,0224
PCL 8_1	9,5628	144434646,4658	0,0324
PCL 8_2	9,5000	151478117,6878	0,0319
PCL 8_3	9,0900	120807249,5528	0,0246
Mean	**9,3755**	**161204477,5566**	**0,0215**

Table A 13: Volume fractions of vWF positive area, PLCL Group

Anastomosis	Thickness (µm)	Volume Region Point Counting (μm^3)	Area Fraction
PLCL 7_1	9,3400	210522709,0406	0,0229
PLCL 7_2	9,8800	290912822,4274	0,023
PLCL 7_3	9,0200	256008834,0632	0,0263
PLCL 8_1	9,0900	228725922,7239	0,0273
PLCL 8_2	9,0400	135640432,1377	0,0232
PLCL 8_3	9,1700	122066363,8117	0,0286
PLCL 1_1	9,2800	140781787,6984	0,0238
PLCL 1_2	9,1800	92944740,6664	0,0223
PLCL 1_3	9,1900	113790666,8767	0,0171
PLCL 2_1	9,3300	168795337,1826	0,021
PLCL 2_2	9,0900	267048076,0035	0,0171
PLCL 2_3	9,1800	226419483,0005	0,015
PLCL 3_1	9,4900	318807863,1349	0,0239
PLCL 3_2	9,1700	131807320,5248	0,0268
PLCL 3_3	9,1800	123418426,1308	0,0209
PLCL 4_2	9,5400	231181743,2584	0,0221
PLCL 4_3	9,4400	146969472,8515	0,0238
PLCL 5_1	9,4800	131857446,0859	0,0183
PLCL 5_2	9,0700	206845617,3860	0,02
PLCL 5_3	11,8800	171548923,4672	0,0259
PLCL 6_1	9,1000	153759328,6520	0,0358
PLCL 6_2	9,0200	200615109,5328	0,0237
PLCL 6_3	9,0900	271876063,5460	0,0239
PLCL 4_1	9,3400	113409911,6736	0,0289
Mean	**9,3633**	**185656433,4115**	**0,0234**

Table A 14: Volume fractions of Collagen, Control Group

Anastomosis	Area Fraction	Area Fraction (%)
C1_1	0,2077	20,77
C1_2	0,1385	13,85
C1_3	0,1692	16,92
C2_1	0,0538	5,38
C2_2	0,1077	10,77
C2_3	0,2154	21,54
C3_1	0,0692	6,92
C3_2	0,0769	7,69
C3_3	0,0692	6,92
C4_1	0,1154	11,54
C4_2	0,2154	21,54
C4_3	0,1308	13,08
C5_1	0,3077	30,77
C5_2	0,3385	33,85
C5_3	0,2000	20,00
C6_1	0,0846	8,46
C6_2	0,1538	15,38
C6_3	0,1692	16,92
C7_1	0,1615	16,15
C7_2	0,2000	20,00
C7_3	0,0769	7,69
C9_1	0,0769	7,69
C9_2	0,1692	16,92
C9_3	0,2154	21,54
Mean	**0,16**	**15,51**

Table A 15: Volume fractions of Collagen, PCL Group

Anastomosis	Area Fraction	Area Fraction (%)
PCL 1_1	0,2462	24,62
PCL 1_2	0,0077	0,77
PCL 1_3	0,1385	13,85
PCL 2_1	0,0231	2,31
PCL 2_2	0,0846	8,46
PCL 2_3	0,0077	0,77
PCL 3_1	0,2154	21,54
PCL 3_2	0,0692	6,92
PCL 3_3	0,1077	10,77
PCL 4_1	0,1769	17,69
PCL 4_2	0,2462	24,62
PCL 4_3	0,0769	7,69
PCL 5_1	0,0769	7,69
PCL 5_2	0,1923	19,23
PCL 5_3	0,2385	23,85
PCL 6_1	0,1231	12,31
PCL 6_2	0,1692	16,92
PCL 6_3	0,1231	12,31
PCL 7_1	0,1692	16,92
PCL 7_2	0,2385	23,85
PCL 7_3	0,2308	23,08
PCL 8_1	0,1923	19,23
PCL 8_2	0,3923	39,23
PCL 8_3	0,2154	21,54
Mean	**0,16**	**15,67**

Table A 16: Volume fractions of Collagen, PLCL Group

Anastomosis	Area Fraction	Area Fraction (%)
PLCL 1_1	0,1154	11,54
PLCL 1_2	0,0769	7,69
PLCL 1_3	0,0308	3,08
PLCL 2_1	0,0077	0,77
PLCL 2_2	0,0923	9,23
PLCL 2_3	0,2385	23,85
PLCL 3_1	0,1000	10,00
PLCL 3_2	0,0692	6,92
PLCL 3_3	0,1308	13,08
PLCL 4_1	0,0769	7,69
PLCL 4_2	0,0231	2,31
PLCL 4_3	0,0769	7,69
PLCL 5_1	0,0385	3,85
PLCL 5_2	0,2846	28,46
PLCL 5_3	0,0462	4,62
PLCL 6_1	0,1769	17,69
PLCL 6_2	0,0692	6,92
PLCL 6_3	0,1846	18,46
PLCL 7_1	0,2538	25,38
PLCL 7_2	0,1000	10,00
PLCL 7_3	0,3846	38,46
PLCL 8_1	0,1308	13,08
PLCL 8_2	0,0308	3,08
PLCL 8_3	0,2615	26,15
Mean	**0,13**	**12,50**

Table A 17: Volume fractions of Inflammatory cells (MAC387 positive areas), Control Group

Anastomosis	Thickness (µm)	Volume Region Point Counting (µm^3)	Area Fraction	Stitch (+/-)
C5_2	9.4900	204602039.5020	**0.0020**	+
C5_3	9.2900	75530269.3464	**0.0075**	-
C1_1	9.7900	98072912.9752	**0.0019**	-
C1_3	9.5300	123140297.8463	**0.0003**	-
C2_1	9.2800	78817224.0174	**0.0086**	+
C2_2	9.3300	74500918.2591	**0.0050**	+
C2_3	9.1800	112620300.6972	**0.0026**	-
C3_1	9.1800	101291631.3963	**0.0111**	-
C3_2	9.2300	62982058.5599	**0.0200**	+
C3_3	9.3300	70437231.8086	**0.0020**	-
C4_2	9.1200	109236073.0745	**0.0079**	-
C5_1	9.0800	79095976.3592	**0.0033**	-
C4_3	9.8800	127662764.1927	**0.0102**	+
C1_2	9.0300	60961830.0154	**0.0013**	-
C6_1	9.2900	158478690.1466	**0.0085**	+
C6_2	9.9600	180753470.1990	**0.0026**	-
C6_3	9.2400	114697876.7282	**0.0016**	-
C7_1	9.4000	70965699.7858	**0.0028**	+
C7_2	9.2400	96587685.6659	**0.0007**	-
C7_3	9.4200	114196993.6180	**0.0020**	+
C9_1	9.0400	65622946.6104	**0.0042**	-
C9_2	9.8200	90532081.4554	**0.0063**	+
C9_3	9.3200	73744512.1710	**0.0039**	-
Mean	**9.3683**	**101936151.4967**	**0.0051**	X

Table A 18: Volume fractions of Inflammatory cells (MAC387 positive areas), PCL Group

Anastomosis	Thickness (µm)	Volume Region Point Counting ($µm^3$)	Area Fraction	Stitch (+/-)
PCL 4_2	9.3400	98989020.9246	**0.0033**	-
PCL 2_2	9.5300	135592687.5162	**0.0053**	-
PCL 2_1	9.2100	144411133.9257	**0.0112**	+
PCL 4_3	9.2300	115243766.7266	**0.0036**	+
PCL 1_1	9.2000	120211946.4456	**0.0038**	+
PCL 1_2	9.2300	169515540.5920	**0.0019**	-
PCL 5_3	9.1400	122081910.0570	**0.0169**	+
PCL 6_1	8.4900	132505360.1718	**0.0018**	-
PCL 5_1	9.0300	140933262.9389	**0.0033**	+
PCL 5_2	9.3300	138165339.3169	**0.0175**	-
PCL 4_1	9.4400	95937263.5429	**0.0036**	-
PCL 2_3	9.2800	111152495.4122	**0.0021**	-
PCL 1_3	9.2800	483008116.4142	**0.0036**	+
PCL 3_1	9.4300	141699831.8728	**0.0051**	+
PCL 3_2	9.0400	206712281.8228	**0.0037**	-
PCL 3_3	9.7400	114541078.5372	**0.0021**	-
PCL 6_3	9.1300	167678969.1879	**0.0010**	-
PCL 6_2	9.8300	77779887.8370	**0.0018**	-
PCL 7_1	9.8400	284292542.3332	**0.0046**	-
PCL 7_2	9.2900	116667291.0441	**0.0022**	-
PCL 7_3	9.7900	270055847.3230	**0.0027**	-
PCL 8_1	9.5900	143407915.8703	**0.0050**	-
PCL 8_2	9.3800	155247631.1271	**0.0013**	-
PCL 8_3	9.4300	121848164.6056	**0.0021**	-
Mean	**9.3425**	**158653303.5641**	**0.0046**	

Table A 19: Volume fractions of Inflammatory cells (MAC387 positive areas), PLCL Group

Anastomosis	**Thickness (µm)**	**Volume Region Point Counting (µm^3)**	**Area Fraction**	Stitch (+/-)
PLCL 6_2	9.7300	223196417.5709	**0.0025**	-
PLCL 5_1	9.4100	137300771.5137	**0.0009**	-
PLCL 1_2	9.3800	110307527.3798	**0.0034**	+
PLCL 6_1	9.1900	166112439.1129	**0.0020**	-
PLCL 1_1	9.0300	147488298.4244	**0.0008**	+
PLCL 6_3	9.6400	290410575.4531	**0.0193**	+
PLCL 4_2	9.2800	210852915.5337	**0.0013**	-
PLCL 5_2	9.8400	205719226.6130	**0.0045**	+
PLCL 5_3	9.7800	133470104.5971	**0.0017**	-
PLCL 1_3	9.3300	103624004.4906	**0.0023**	-
PLCL 2_1	9.4300	270393398.9918	**0.0050**	-
PLCL 3_1	9.4000	317980924.0490	**0.0010**	-
PLCL 2_3	9.2300	263988628.4318	**0.0089**	-
PLCL 2_2	9.2900	297400435.5516	**0.0092**	+
PLCL 3_2	9.0300	144866284.2302	**0.0033**	+
PLCL 3_3	9.0800	124576162.7622	**0.0063**	+
PLCL 4_1	9.3900	167000962.1953	**0.0013**	-
PLCL 4_3	9.7300	144088826.5331	**0.0009**	-
PLCL 7_1	9.3800	202911377.5314	**0.0018**	-
PLCL 7_2	9.2900	356745647.1910	**0.0024**	-
PLCL 7_3	9.4300	260125295.2327	**0.0019**	-
PLCL 8_1	9.2300	198996504.1788	**0.0007**	-
PLCL 8_2	9.0300	135689234.5543	**0.0019**	+
PLCL 8_3	9.4800	135569458.1584	**0.0013**	-
Mean	**9.3762**	**197867309.1775**	**0.0035**	

Attachment 5: Experiment B and C, Power analysis

Sample size estimation: We decided to construct one intestinal anastomosis with artificial defect per animal. We assumed the same sample size for both experimental and control group. We considered the Intestinal Wall Integrity Score (IWIS) as the most valuable result of the study. We anticipated a very low IWIS of 30% in the Control group with an uncovered anastomotic defect and a substantially higher IWIS of 60% in the Experimental group as an effect of our nanomaterial patch. Standard deviation of 20 percentage points was assumed in both groups. After performing power analysis for two-tailed two-sample t-test, sample sizes of 7 (1 anastomosis x 7 animals, test power 73.13%) and 8 (1 anastomosis x 8 animals, test power 79.65%) were considered. Finally, the power close to 80% provided by the 8-animal group size was preferred.

Attachment 6: Experiment B, PAAS results

PAAS scores for each quadrant of each anastomosis. Anastomosis is named after animal. Quadrants are numbered Q1 to Q4 from the right mesenteric quadrant to left mesenteric quadrant. Sum gives the total for each anastomosis.

Table A 20: PAAS results Control Group

anastomosis	Q1	Q2	Q3	Q4	Sum
C1	0	0	0	0	0
C2	2	2	0	0	4
C3	0	1	1	0	2
C4	2	1	0	0	3
C5	0	1	1	0	2
C6	2	1	0	0	3
C7	0	1	1	0	2
C8	2	2	1	0	5

Table A 21: PAAS result PCL/PVA1 Group

anastomosis	Q1	Q2	Q3	Q4	Sum
PCL/PVA1 1	0	2	2	2	6
PCL/PVA1 2	2	1	1	2	6
PCL/PVA1 3	0	1	0	2	3
PCL/PVA1 4	1	1	1	0	3
PCL/PVA1 5	0	1	2	0	3
PCL/PVA1 6	0	0	0	0	0
PCL/PVA1 7	0	1	1	0	2
PCL/PVA1 8	0	0	0	0	0

Table A 22: PAAS result PCL/PVA2 Group

anastomosis	Q1	Q2	Q3	Q4	Sum
PCL/PVA2 1	2	2	1	0	5
PCL/PVA2 2	1	1	2	2	6
PCL/PVA2 3	1	2	2	2	7
PCL/PVA2 4	2	1	0	2	5
PCL/PVA2 5	1	0	0	2	3
PCL/PVA2 6	1	0	1	1	3
PCL/PVA2 7	1	2	2	2	7
PCL/PVA2 8	2	1	0	0	3

Attachment 7: Experiment B, IWIS input data

Input data for Experiment B IWIS are listed below. Three specimens from each animal were scored, values of non-weighted partial scores are given in the table. Range for mucosa is 0-1 point, range for submucosa is 0-1 point, range for muscularis is 0-3 points, range for serosa is 1-3 points, as explained in the methods of Experiment B.

Table A 23: IWIS input data, Control Group

Animal	specimen code	mucosa	submucosa	muscularis	serosa
C1	**2**	0	0	1	0
C1	**3**	0	1	1	0
C1	**4**	0	0	1	0
C2	**1**	1	0	1	0
C2	**2**	1	0	1	0
C2	**3**	0	0	1	0
C3	**1**	0	0	0	0
C3	**2**	1	1	2	1
C3	**3**	0	0	0	0
C4	**1**	0	0	0	0
C4	**2**	0	0	1	0
C4	**3**	0	0	0	0
C5	**1**	0	0	0	0
C5	**2**	0	0	1	0
C5	**3**	0	0	0	0
C6	**2**	0	1	0	0
C6	**3**	0	1	1	0
C6	**4**	0	0	0	0
C7	**3**	0	0	1	0
C7	**4**	0	1	2	1
C7	**5**	0	0	1	0
C8	**3**	0	1	1	0
C8	**4**	0	1	2	0
C8	**5**	0	0	0	0

Table A 24: IWIS input data, PCL/PVA1 Group

Animal	specimen code	mucosa	submucosa	muscularis	serosa
PCL/PVA1 1	**2**	0	1	2	1
PCL/PVA1 1	**3**	0	0	1	0
PCL/PVA1 1	**4**	0	0	1	0
PCL/PVA1 2	**2**	0	0	0	0
PCL/PVA1 2	**3**	1	1	2	1
PCL/PVA1 2	**4**	0	0	0	0
PCL/PVA1 3	**2**	0	0	0	0
PCL/PVA1 3	**3**	1	1	2	2
PCL/PVA1 3	**4**	0	0	1	2
PCL/PVA1 4	**2**	0	1	0	2
PCL/PVA1 4	**3**	1	1	2	2
PCL/PVA1 4	**4**	0	0	1	2
PCL/PVA1 5	**2**	0	0	0	0
PCL/PVA1 5	**3**	1	1	2	1
PCL/PVA1 5	**4**	1	1	1	0
PCL/PVA1 6	**2**	1	1	2	2
PCL/PVA1 6	**3**	1	1	2	1
PCL/PVA1 6	**5**	0	1	0	0
PCL/PVA1 7	**3**	1	1	2	1
PCL/PVA1 7	**4**	0	1	2	0
PCL/PVA1 7	**5**	0	0	1	0
PCL/PVA1 8	**2**	0	0	0	0
PCL/PVA1 8	**3**	1	1	2	2
PCL/PVA1 8	**4**	0	1	1	2

Table A 25: IWIS input data, PCL/PVA2 Group

Animal	specimen code	mucosa	submucosa	muscularis	serosa
PCL/PVA2 1	**1**	0	0	0	0
PCL/PVA2 1	**2**	1	1	1	1
PCL/PVA2 1	**3**	0	1	1	0
PCL/PVA2 2	**3**	0	0	1	0
PCL/PVA2 2	**4**	1	1	2	2
PCL/PVA2 2	**5**	0	1	0	0
PCL/PVA2 3	**2**	0	1	1	2
PCL/PVA2 3	**3**	1	1	2	2
PCL/PVA2 3	**4**	1	1	2	2
PCL/PVA2 4	**1**	1	1	2	2
PCL/PVA2 4	**2**	0	1	1	0
PCL/PVA2 4	**3**	0	0	0	0
PCL/PVA2 5	**2**	0	0	2	0
PCL/PVA2 5	**3**	0	1	1	0
PCL/PVA2 5	**4**	0	0	0	0
PCL/PVA2 6	**2**	0	1	0	0
PCL/PVA2 6	**4**	0	1	1	0
PCL/PVA2 6	**5**	1	1	2	2
PCL/PVA2 7	**2**	0	1	1	2
PCL/PVA2 7	**3**	1	1	3	2
PCL/PVA2 7	**4**	1	1	3	2
PCL/PVA2 8	**2**	1	1	0	0
PCL/PVA2 8	**3**	1	1	2	1
PCL/PVA2 8	**4**	0	0	1	0

Attachment 8: Experiment B, Stereology results

Results of stereological measurements from Experiment B are listed below. Thickness means the thickness of histological slide. Volume Region Point Counting gives value of the total volume of tissue where our measurements were taken in. Area Fraction stands for volume fraction positive in given parameter (vWF, collagen, MAC387).

Table A 26: Volume fractions of vWF positive area, Control Group

Animal	Thickness (µm)	Volume Region Point Counting (μm^3)	Area Fraction
C1	9.0300	116024128.0971	**0.0292**
C2	9.5300	503629982.2171	**0.0179**
C3	9.9300	214088330.0645	**0.0360**
C4	9.6200	159918184.6547	**0.0338**
C5	9.6200	217879797.4335	**0.0253**
C6	8.9900	238198955.6041	**0.0285**
C7	9.3400	357309685.1282	**0.0208**
C8	9.4300	451112025.1535	**0.0255**

Table A 27: Volume fractions of vWF positive area, PCL/PVA1 Group

Animal	Thickness (µm)	Volume Region Point Counting (μm^3)	Area Fraction
PCL/PVA1 1	9.6800	411775278.9812	**0.0341**
PCL/PVA1 2	8.5800	450934175.3535	**0.0247**
PCL/PVA1 3	9.5300	403319065.4294	**0.0325**
PCL/PVA1 4	9.3300	521506427.8286	**0.0404**
PCL/PVA1 5	9.4900	322403213.7698	**0.0497**
PCL/PVA1 6	9.1400	289944536.3935	**0.0247**
PCL/PVA1 7	9.1300	258477462.3918	**0.0248**
PCL/PVA1 8	9.1400	380842480.2971	**0.0265**

Table A 28: Volume fractions of vWF positive area, PCL/PVA2 Group

Animal	Thickness (µm)	Volume Region Point Counting (µm³)	Area Fraction
PCL/PVA2 1	9.8700	242170450.5257	**0.0293**
PCL/PVA2 2	9.7200	282942335.6963	**0.0276**
PCL/PVA2 3	9.0400	305146701.7469	**0.0201**
PCL/PVA2 4	9.0400	229680313.1429	**0.0396**
PCL/PVA2 5	9.1300	147796087.4702	**0.0232**
PCL/PVA2 6	9.2800	174475735.2229	**0.0194**
PCL/PVA2 7	9.4300	332686561.7976	**0.0247**
PCL/PVA2 8	8.5400	270291044.6171	**0.0312**

Table A 29: Volume fractions of Collagen, Control Group

Animal	Thickness (µm)	Volume Region Point Counting (µm³)	Area Fraction
C1	9.4700	113428246.9347	**0.2700**
C2	9.2300	460975066.9192	**0.0506**
C3	9.3400	198656048.8473	**0.1096**
C4	9.6800	191131187.5135	**0.1068**
C5	9.1400	153929364.8588	**0.1688**
C6	9.9400	273472015.3257	**0.1156**
C7	9.1400	317147570.7004	**0.2081**
C8	8.9500	346937775.1592	**0.0728**

Table A 30: Volume fractions of Collagen, PCL/PVA1 Group

Animal	Thickness (µm)	Volume Region Point Counting (µm³)	Area Fraction
PCL/PVA1 1	8.9800	476519865.3567	**0.1092**
PCL/PVA1 2	9.2300	495146183.7984	**0.1141**
PCL/PVA1 3	9.4500	492542317.5429	**0.1042**
PCL/PVA1 4	9.6300	580218639.3551	**0.0829**
PCL/PVA1 5	9.0200	543465433.7469	**0.1487**
PCL/PVA1 6	9.0900	309473896.2686	**0.1003**
PCL/PVA1 7	9.6300	364209531.4506	**0.1000**
PCL/PVA1 8	10.4900	431001931.2376	**0.1656**

Table A 31: Volume fractions of Collagen, PCL/PVA2 Group

Animal	Thickness (µm)	Volume Region Point Counting (µm^3)	Area Fraction
PCL/PVA2 1	9.7300	233084866.4571	**0.1029**
PCL/PVA2 2	9.5800	487495738.7282	**0.1149**
PCL/PVA2 3	9.4300	407985989.3649	**0.1007**
PCL/PVA2 4	9.4800	341332239.8302	**0.0712**
PCL/PVA2 5	9.8900	165124465.3306	**0.1129**
PCL/PVA2 6	9.9900	230610939.4433	**0.1267**
PCL/PVA2 7	9.0300	361182455.2629	**0.0946**
PCL/PVA2 8	9.1200	309833225.4563	**0.1272**

Table A 32: Volume fractions of MAC387 positive area, Control Group

Animal	Thickness (µm)	Volume Region Point Counting (µm^3)	Area Fraction
C1	9.2000	94166024.7184	**0.0022**
C2	9.4400	408418636.2253	**0.0012**
C3	9.1800	221908639.8416	**0.0144**
C4	9.0800	146327556.2645	**0.0022**
C5	9.0400	293990800.8229	**0.0007**
C6	9.7900	231679490.0784	**0.0033**
C7	9.2800	377918484.4016	**0.0012**
C8	9.4800	387439619.0008	**0.0091**

Table A 33: Volume fractions of MAC387 positive area, PCL/PVA1 Group

Animal	Thickness (µm)	Volume Region Point Counting (µm^3)	Area Fraction
PCL/PVA1 1	9.6800	471503775.0792	**0.0280**
PCL/PVA1 2	9.5819	500112877.1149	**0.0172**
PCL/PVA1 3	9.6900	464956724.6865	**0.0155**
PCL/PVA1 4	9.9900	681680135.4612	**0.0279**
PCL/PVA1 5	9.6169	441901256.9362	**0.0200**
PCL/PVA1 6	9.9800	536829095.4955	**0.0170**
PCL/PVA1 7	9.1800	302542109.5739	**0.0059**
PCL/PVA1 8	9.2100	423204850.8220	**0.0187**

Table A 34: Volume fractions of MAC387 positive area, PCL/PVA2 Group

Animal	Thickness (µm)	Volume Region Point Counting (μm^3)	Area Fraction
PCL/PVA2 1	9.8200	206726800.1796	**0.0089**
PCL/PVA2 2	9.9800	459311263.8922	**0.0049**
PCL/PVA2 3	9.9200	396780726.0473	**0.0149**
PCL/PVA2 4	9.1800	312537994.2514	**0.0055**
PCL/PVA2 5	9.4200	151122967.6065	**0.0054**
PCL/PVA2 6	9.2400	181772658.4457	**0.0202**
PCL/PVA2 7	9.6700	465400986.2278	**0.0320**
PCL/PVA2 8	9.8200	444106194.8686	**0.0115**

Attachment 9: Experiment C, PAAS results

Table A 35: PAAS results, Control Group

anastomosis	Q1	Q2	Q3	Q4	Sum
C1	0	1	0	0	1
C2	0	1	0	0	1
C3	0	0	0	0	0
C4	0	2	2	1	5
C5	0	0	0	0	0
C6	0	0	0	0	0
C7	0	1	0	0	1
C8	0	0	0	0	0

Table A 36: PAAS results, PCL Group

anastomosis	Q1	Q2	Q3	Q4	Sum
PCL1	0	1	0	0	1
PCL2	0	1	0	0	1
PCL3	0	0	0	0	0
PCL4	0	1	0	0	1
PCL5	0	0	0	0	0
PCL6	0	0	0	0	0
PCL7	1	1	0	0	2
PCL8	2	1	0	0	3

Attachment 10: Experiment C, Stereology results and IWIS input data

Input data for Experiment C IWIS are listed below. Five specimens from each animal were scored. Specimens with the highest IWIS were used for Stereology measurements and only their IWIS values are in the following tables. When the score was equally high for several samples, all of them were used for stereology. Values of non-weighted partial scores are given in the table. Range for mucosa is 0-1 point, range for submucosa is 0-1 point, range for muscularis is 0-3 points, range for serosa is 1-3 points, as explained in the methods of Experiment B.

Table A 37: IWIS input data, Control Group

Animal	specimen	mucosa	submucosa	muscularis	serosa
C1	3	1	1	3	2
C2	1	1	1	0	0
C3	2	0	0	1	0
C3	3	0	0	1	0
C3	5	0	0	1	0
C4	2	0	1	2	0
C5	1	0	0	2	0
C5	3	0	0	2	0
C6	1	0	0	1	0
C6	2	0	0	1	0
C6	3	0	0	1	0
C6	4	0	0	1	0
C6	5	0	0	1	0
C7	1	0	0	3	0
C8	4	0	1	3	0
C8	5	0	1	3	0

Table A 38: IWIS input data, PCL Group

Animal	specimen	mucosa	submucosa	muscularis	serosa
PCL1	2	0	1	2	0
PCL2	2	0	0	3	0
PCL3	1	0	0	2	0
PCL3	2	0	0	2	0
PCL4	4	1	1	3	1
PCL5	2	0	0	2	0
PCL5	3	0	0	2	0
PCL6	1	0	0	2	0
PCL6	2	0	0	2	0
PCL6	3	0	0	2	0
PCL7	2	1	1	3	1
PCL8	3	0	0	3	0
PCL8	4	0	0	3	0

Table A 39: Stereology results, Control Group

Animal	specimen	Collagen volume fraction	endothelial cells volume fraction	MAC387 positive cells volume fraction
C1	3	0,1516	0,0363	0,002
C2	1	0,2111	0,0211	0,0005
C3	2	0,1435	0,0204	0,0002
C3	3	0,1675	0,0286	0,0007
C4	2	0,1892	0,0209	0,0007
C5	3	0,218	0,0259	0
C6	3	0,0952	0,0241	0,0005
C7	1	0,2057	0,0501	0,0017
C8	4	0,2077	0,0394	0,0002
C8	5	0,127	0,0401	0,0001

Table A 40: Stereology results, PCL Group

Animal	Specimen	Collagen volume fraction	endothelial cells volume fraction	MAC387 positive cells volume fraction
PCL1	2	0,2662	0,0368	0,0014
PCL2	2	0,1982	0,0314	0,0002
PCL3	1	0,191	0,0305	0,0014
PCL3	2	0,1471	0,0267	0,0012
PCL4	4	0,2153	0,033	0,0012
PCL5	2	0,2405	0,0288	0,0004
PCL5	3	0,2056	0,0279	0,0001
PCL6	2	0,2031	0,027	0,0016
PCL6	3	0,1751	0,0298	0,0073
PCL7	2	0,2323	0,0367	0,0038
PCL8	4	0,2449	0,0251	0,0015

Attachment 11: Article A

Rosendorf J, Horakova J, Klicova M, Palek R, Cervenkova L, Kural T, Hosek P, Kriz T, Tegl V, Moulisova V, Tonar Z, Treska V, Lukas D, Liska V. Experimental fortification of intestinal anastomoses with nanofibrous materials in a large animal model. Sci Rep. 2020 Jan 24;10(1):1134.

Q1, IF=4.180

SCIENTIFIC REPORTS
nature research

OPEN

Experimental fortification of intestinal anastomoses with nanofibrous materials in a large animal model

Jachym Rosendorf[1,2*], Jana Horakova[4], Marketa Klicova[4], Richard Palek[1,2], Lenka Cervenkova[2], Tomas Kural[3,5], Petr Hosek[2], Tomas Kriz[2], Vaclav Tegl[2,6], Vladimira Moulisova[2], Zbynek Tonar[2,5], Vladislav Treska[1], David Lukas[4] & Vaclav Liska[1,2]

Anastomotic leakage is a severe complication in gastrointestinal surgery. It is often a reason for reoperation together with intestinal passage blockage due to formation of peritoneal adhesions. Different materials as local prevention of these complications have been studied, none of which are nowadays routinely used in clinical practice. Nanofabrics created proved to promote healing with their structure similar to extracellular matrix. We decided to study their impact on anastomotic healing and formation of peritoneal adhesions. We performed an experiment on 24 piglets. We constructed 3 hand sutured end-to-end anastomoses on the small intestine of each pig. We covered the anastomoses with a sheet of polycaprolactone nanomaterial in the first experimental group, with a sheet of copolymer of polylactic acid with polycaprolactone in the second one and no fortifying material was used in the Control group. The animals were sacrificed after 3 weeks of observation. Clinical, biochemical and macroscopic signs of anastomotic leakage or intestinal obstruction were monitored, the quality of the scar tissue was assessed histologically, and a newly developed scoring system was employed to evaluate the presence of adhesions. The material is easy to manipulate with. There was no mortality or major morbidity in our groups. No statistical difference was found inbetween the groups in the matter of level of peritoneal adhesions or the quality of the anastomoses. We created a new adhesion scoring system. The material appears to be safe however needs to be studied further to prove its' positive effects.

Anastomotic leakage remains one of the major problems in gastrointestinal (GI) surgery[1,2]. It occurs in 3–19% of colorectal surgeries depending on many factors some of which can and some of which cannot be influenced[3–6]. For rectal anastomoses, the reported risk factors include, besides others, male gender, preoperative radiotherapy and so-called low anastomosis[7], i.e. an anastomosis within 5 cm from the anus. One of the most important factors influencing the anastomotic healing has proven to be the oxygenation on the site of the anastomosis. Correct oxygen levels are needed for leukocytes activation, fibroblasts production and angiogenesis, which are essential for wound healing[8]. The technique of construction of GI anastomoses is also very important. Although it has been modified and improved repeatedly throughout the history of modern surgery, the mentioned anastomotic leakage as well as other kinds of complications have not been eradicated completely so far (though their frequency has been lowered noticeably). Various sealing techniques and materials were tested both experimentally and clinically including fibrin patches, fibrin glue, collagen patches, hyaluronic acid derivatives and many others[9–16] as a local barrier protection, while other experiments included systemic administration of various substances[17,18]. The anastomotic leakage occurs in different severity, prolonging the patients' stay in the hospital. Minimal leakage can stay

[1]Department of Surgery, Faculty of Medicine in Pilsen, Charles University, Prague, Czech Republic. [2]Biomedical Center, Faculty of Medicine in Pilsen, Charles University, Prague, Czech Republic. [3]Department of Surgery, University Hospital Regensburg, Regensburg, Germany. [4]Department of Nonwovens, Faculty of Textile Engineering, Technical University in Liberec, Liberec, Czech Republic. [5]Department of Histology and Embryology, Faculty of Medicine in Pilsen, Charles University, Prague, Czech Republic. [6]Department of Anesthesiology and Intensive Care Medicine, Faculty of Medicine in Plzen, Pilsen, Czech Republic. *email: jachymrosendorf@gmail.com

clinically invisible, being detectable only by laboratory markers[19]. The incomplete dehiscence can be approached conservatively by administering antibiotics and parenteral nutrition until the anastomosis is sealed[20–23]. It is usually associated with abdominal drain secretion, abdominal discomfort, temperature elevation, elevation of C-reactive protein and other inflammatory markers[24]. The worst cases need to be approached more radically with relaparotomy bringing a high risk of stomy and higher morbidity and mortality[25,26].

Peritoneal adhesions (PAs) are bonds between peritoneal surfaces of different abdominal organs. They can range from thin films to thick fibrous bonds containing vessels[27]. Some amount of PAs appears after almost every intraabdominal surgical procedure, but also after inflammations, radiotherapy or chemotherapy[28,29]. PAs can be a source of other complications as they cause abdominal discomfort in many patients, decreasing their quality of life in the long term follow-up. Even more serious problem is abdominal passage blockage, which can appear due to PAs in any time of the patients' life from the surgery onwards[29,30]. There are various products on the market designed to decrease the level of postoperative adhesions, none of which is commonly used nowadays in GI surgery to successfully prevent the formation of adhesions while maintaining the GI anastomoses healing process intact. Specific inflammatory responses are crucial for both tissue healing after surgical interventions and adhesion formation; so it is therefore a very difficult task to influence the anastomotic healing positively while trying to decrease the amount of newly formed adhesions. To influence one part of the process in one way while the other one in the opposite way seems to be easier by using some kind of barrier protection rather than a systemic treatment[31].

There are several systems of PA evaluation that focus both on quantity and quality of the adhesions. Coccolini's peritoneal adhesion index divides the abdominal cavity into segments and evaluates the amount of adhesions in each of them separately, while the other systems evaluate adhesions based on their mechanical properties[32–34]; nevertheless, none of these systems grade regional adhesions in the site of anastomosis in the GI tract.

According to the literature, nanomaterials have never been used in attempts to resolve these complications, therefore we decided to test their ability to reinforce GI anastomoses and investigate their effect on the formation of PAs. In our study we focused on non-woven nanofibrous scaffolds. These structures are considered as very interesting in recent years in the field of tissue engineering thanks to their similar morphology to extracellular matrix[17,18]. Srouji S *et al.*[35] have noticed their ability to accelerate tissue regeneration in the site of surgery.

There are several ways how to produce nanofibers. The most appealing method for mass production seems to be electrospinning, which is a method with highly adjustable settings allowing to create a large variety of different products with different shapes and thicknesses of the fibers. It is also a method suitable for high volume production[36]. In the process of electrospinning a liquid polymer solution is dosed to an electrode (spinneret) charged with electric potential, while a collector either grounded or oppositely charged is placed on the opposite side of the apparatus. In the presence of electric field, the drop of the polymer shapes into a so called Taylor's cone from which the material is dragged to the collector. The stream of the solution gets unstable in the process and the solvent evaporates before the polymer hits the collector. The polymer solution forms different types of structures depending on individual settings. The needle-less spinning has been developed lately, allowing production in larger volumes[36,37].

Nanomaterials have been experimentally used in numerous surgical applications to fortify various anatomical structures[38–40]. However, the impact of the nanomaterials on healing in the abdominal cavity and on the formation of PAs has not been described yet. The right material for fabrication must be chosen according to the parameters needed. Biodegradability is a crucial quality. Biodegradable polymers are widely used in human medicine; they have been successfully used even as nanofibrous cloths having the best results when the speed of degradation is similar to the speed of tissue regeneration[41]. The wound healing of an anastomosis on the GI tract takes about 3 weeks, from this point on the scar tissue only matures and remodelation of connective tissue continues for much longer[42]. Polycaprolactone and polylactic acid are approved biocompatible polymers with good mechanical properties and cytocompatibility[43] that are also used for production of different surgical sutures.

Our aim was to investigate whether it is possible to use the nanomaterials in abdominal surgery to determine their influence of the nanomaterials on the healing process of GI anastomosis, and on the formation of PAs. We also aimed to develop a new scoring system for PAs specific for the site of surgery.

Materials and Methods

Nanomaterial preparation. Nanomaterials for our experiment were fabricated via electrospinning on the Nanospider™ machine which is a construct of Technical University of Liberec, Faculty of Textile Enigineering, Department of Nonwovens and Nanofibrous Materials, Czech Republic. Electrospinning has been selected as a method for fabrication of planar fibrous scaffolds as this technique allows large scale production of nanofibers; our team has also wide experience with this technique[39].

We used two types of biocompatible polymers: polycaprolactone (PCL), and a polylactic acid-polycaprolactone copolymer (PLCL). PCL (mean weight = 43000 g/mol, Polysciences) and PLCL (Purasorb PLC 7015, Corbion) were dissolved in chloroform, acetic acid and ethanol solution (8:1:1 volume fractions) to the final concentration of 16% and 10% respectively (concentrations allowing optimal electrospinning properties based on previous research[41]). The solutions were electrospun onto a spun bond (nonwoven cloth underlay) for easy manipulation and application. The material has been sterilised using ethylene oxide (37 °C, Anprolene). This method has been tested before to prove its safety and frugality to the nanomaterial[41].

Material characterization. Scanning electron microscopy (SEM) was employed to obtain images of the fibers; the pictures were analyzed as described in previous work of Horakova *et al.*[41]. Materials were also tested *in vitro* for degradability and mechanical properties[41].

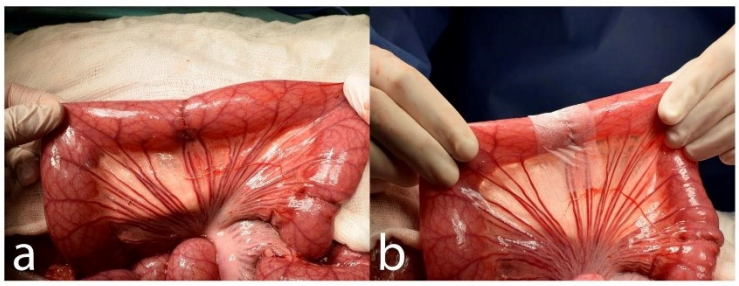

Figure 1. Reinforcing the end-to-end anastomosis on the small intestine in a pig model: (**a**) constructed anastomosis; (**b**) the PCL nanomaterial applied to the site of anastomosis partially covering the mesentery.

Experimental design. All experimental procedures with the use of piglets were described in an experimental protocol approved by the Commission of Work with Experimental Animals at the Medical Faculty of Pilsen, Charles University, and were under control of the Ministry of Education, Youth and Sports of the Czech Republic (project code: MSMT-26570/2017-2). All procedures were performed in compliance to the law of the Czech Republic, which is compatible with the legislation of the European Union.

Healthy male and female Prestice black-pied pigs were randomly allocated to 3 groups using simple randomization (8 animals per each group): PCL group, PLCL group and a control group with no material applied. Each animal was given a unique code. All animals were 12–14 weeks old weighing between 19–35 kg.

Prior to the surgery, the animals were weighed, and intramuscularly premedicated with 10 mg/kg of ketamine (Narkamon, Spofa, Czech Republic), 5 mg/kg of azaperone (Stresnil, Jannssen Phramaceutica, Belgium) and 0,5 mg atropine (Atropin Biotika, Hoechst Biotika, Slovak Republic); general anesthesia was then induced and maintained by intravenous administration of propofol (1% mixture 5–10 mg/kg/h Propofol, Fresenius Kabi, Norway). Fentanyl 1–2 μg/kg/h (Fentanyl Torrex, Chiesi cz, Czech Republic) was used for continuous analgesia. Augmentin 1.2 g as an antibiotic prophylaxis was administered intravenously (GlaxoSmithKline Slovakia, Slovak Republic). A ProPort Plastic Venous Access System with PolyFlow polyurethane catheter (Deltec, Smiths medical, U.S.A.) was implanted and introduced through one of the jugular veins.

We entered the abdominal cavity via an upper middle laparotomy. Three end-to-end anastomoses were constructed on the small intestine in 70, 90 and 110 cm aborally from the duodeno-jejunal junction. We transsected the intestine using monopolar coagulation and constructed a hand sutured anastomosis using MONOSYN 4/0 (Glycolide 72%, Caprolactone 14%, Trimethylencarbonate 14%) double needled polycaprone suture line (B-Braun, Germany), following a standard technique of extramucosal running suture (Fig. 1a). No intestinal resection was performed. A 2 × 5 cm large piece of PCL or PLCL nanomaterial (respecting the group) was placed in the area of the suture, covering the whole surface of the anastomosis (Fig. 1b). No fortifying material was used in the Control group. The intestine was then carefully reposed into the abdominal cavity. Wet swabs were used throughout the procedure for manipulation with the viscera.

The animals were monitored for three weeks by trained blinded caretakers. A fixed realimentation process was scheduled and the ability of the animals to feed according to the schedule was observed. Vomiting was considered as intolerance of the current food dosage. The activity of animals was also monitored.

Blood samples were taken during the experiment at five time points: on day 0 before the application of the material (preoperative baseline sample), exactly two hours after the application of the nanomaterial, on day 7, on day 14, on day 21. Basic biochemical parameters were tracked in these samples (bilirubin, GGT, ALT, AST, ALP, albumin, urea, and creatinine) to see deviations in the animals' metabolism.

We weighed the animals at the end of the observation period, performed laparotomy in full anesthesia again. We inspected the abdominal cavity for changes, PAs (listed organs involved in the adhesions), checked for the presence of free GI content (signs of anastomotic leakage), intestinal strictures, and intestinal diameter growth (signs of GI passage blockage). We acquired photodocumentation, collected samples of the intestine with anastomoses and fixed them into a 10% buffered formalin (cut in the mesenterial line and pinned onto a cork underlay). The second surgery as well as the macroscopic assessment and sample collection were performed by a blinded surgeon. We sacrificed the animals after the sample collection.

Scoring of adhesions. None of the quantitative systems of evaluation of PAs were useful for our experiment as we performed surgery only on a small part of the abdominal cavity and the systems usually score the whole abdomen. Thus we created a new quantitative scoring system for our purposes - a *Perianastomotic adhesions amount score* (PAAS). To evaluate the amount of PAs, we divided the area of the specimen into four equal quarters along the circumference of the intestine. Each segment was assigned zero to two points based on the level of adhesions: zero for no adhesions in the segment, one point for adhesions covering the segment partially and two points for adhesions in the whole length of the segment. This resulted in zero to eight points per anastomosis and zero to twenty four points for one animal (in 12 evaluated segments per animal). The specimen were collected carefully together with the surrounding tissue (depending on the level of adhesions), about 4 cm of the intestine was used for each one. The quality of adhesions was evaluated according to the Zühlke's classification[33]. The

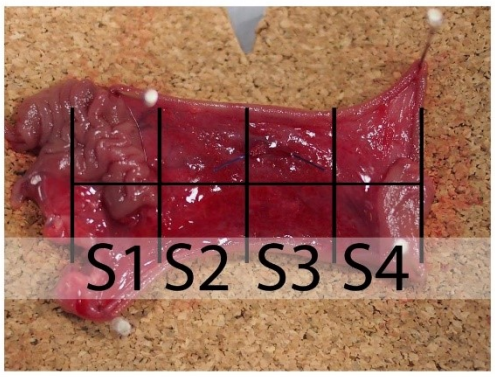

Figure 2. Perianastomotic adhesions amount scoring system for the presence of peritoneal adhesions on the intestine with an anastomosis: The sample (specimen from the Control group) was divided into 4 segments; oral part of the intestine is in the upper side of the image while the aboral part is in the lower part of the image. The area of the suture (the anastomosis itself) is located underneath the horizontal line; scoring of this sample: S1) segment no. 1 scoring 2 points; S2) segment no. 2 scoring 0 points; S3) segment no. 3 scoring 0 points; S4) segment no. 4 scoring 1 point.

intestine was then *ex vivo* transected longitudinally on the mesenteric side, and pinned to a piece of cork. The polarity (oral and aboral part) of the intestine was respected in all measurements (Fig. 2). Each sample was given random alphanumeric code for blinding during the histologic assessment.

Histology. After fixing, we processed the samples by standard paraffin technique. We stained 4 µm thick sections by hematoxylin and eosin for comprehensive overview; Verhoeff's hematoxylin and green trichrome technique was used for staining connective tissues and picrosirius red for visualization of collagen in polarized light. We used immunohistochemical methods for detection of vascular endothelium using Polyclonal Rabbit Anti-Human von Willebrad Factor (A 0082, Dako – Agilent, dilution 1:1000); smooth muscles were detected by Monoclonal Mouse Anti-Human Smooth Muscle Actin (Clone 1A4, M0851, Dako – Agilent, dilution 1:500); for detection of granulocytes and tissue macrophages we used S100A9 Monoclonal Antibody (MAC387, MA1-80446, ThermoFisher Scientific, dilution 1:200).

Stereology. Microscopic images of IHC samples were stereologically assessed. We defined the reference space as the region of intestinal wall without mucosa located 3 mm proximally and 3 mm distally from the center of the anastomosis (contact of muscle layers); the region includes a suture line. We investigated samples qualitatively and quantitatively.

Volume fractions of endothelial cells, of MAC387 positive cells and of collagen within the reference space were assessed by computerized software system (Stereologer, Stereology Resource Center). The microscope used was Nikon Eclipse Ti-U with, camera Promicra camera.

Statistical analysis. Standard frequency tables and descriptive statistics were used to characterize the sample data set. Adhesion scores were analyzed with respect to the group, quadrant and anastomosis position in the intestine (1st, 2nd, and 3rd) using repeated measures ANOVA, thus respecting the order and dependency of the three anastomoses sewn in each piglet. The same method was used to assess the differences between groups in collagen and vWF volume fractions. Volume fraction of MAC 387 was considerably affected by random presence of a stitch in some of the slides. Each piglet was therefore assigned one value for anastomoses with stitches (either the mean of all stitch-positive anastomoses, value of a single stitch-positive anastomosis or a missing value if no stitch-positive anastomoses were observed for that piglet) and one value for anastomoses with no stitches (defined analogically). Two-way main-effect ANOVA was then used to evaluate the differences in MAC827 in relation to group and stitch presence. All reported p values are two-tailed and the level of statistical significance was set at $\alpha = 0.05$. Statistical processing and testing were performed using STATISTICA data analysis software system (Version 12; StatSoft, Inc, 2013; www.statsoft.com).

Results

Two types of biodegradable nanomaterials for anastomosis fortification testing were prepared by electrospinning, the PCL based sheets (Fig. 3a) and the PLCL sheets (Fig. 3b) (Table 1). The material was electrospun on the spun bond underlay that facilitated easy manipulation while using this material during the surgical procedure.

We successfully created a model of intestinal anastomosis on pig with use of PCL and PLCL nanofibrous scaffolds.

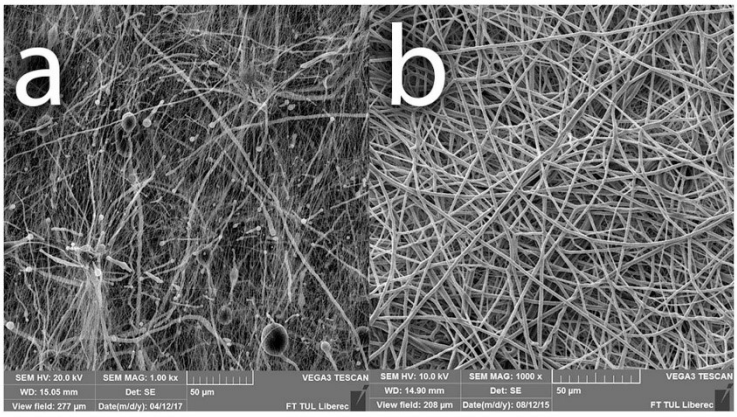

Figure 3. Scanning electron microscopy image of (**a**) the PCL nanomaterial at 1000x magnification and (**b**) the PLCL nanomaterial at 1000x magnification.

	Control Group (n = 8)	PCL Group (n = 8)	PLCL Group (n = 8)	*p*-value between groups (test)
Material fibre thickness	—	325 ± 36 nm	2047 ± 585 nm	—
Material thickness	—	49 ± 5 nm	53 ± 6 nm	—
Macroscopic signs of anastomotic stenosis (count; %)	0; 0%	0; 0%	0; 0%	—
Macroscopic signs of anastomotic leakage (count; %)	0; 0%	0; 0%	0; 0%	—
Mean PAAS score per segment (0–2) (mean ± SEM across pigs)*	0.479 ± 0.086	0.823 ± 0.171	0.688 ± 0.070	0.715 (repeated measures ANOVA)
Incomplete re-epithelisation (count; %)	0; 0%	0; 0%	0; 0%	—
Volume fraction of vWF positive cells [%] (mean ± SEM)	2.22 ± 0.10	2.16 ± 0.16	2.38 ± 0.12	0.690 (repeated measures ANOVA)
Volume fraction of collagen fibres [%] (mean ± SEM)	15.51 ± 2.10	15.67 ± 2.36	11.87 ± 1.91	0.740 (repeated measures ANOVA)
Volume fraction of MAC387 positive cells [%]:				0.550 (two-way ANOVA)
• stitch not in sample (n: mean ± SEM)	8: 0.38 ± 0.09	8: 0.46 ± 0.19	8: 0.21 ± 0.06	
• stitch in sample (n: mean ± SEM)	7: 0.80 ± 0.23	5: 0.67 ± 0.16	6: 0.70 ± 0.27	

Table 1. Summary of the most important results for each group. *Each animal was assigned a score equal to the average of all segment scores in that animal (i.e. 24 segment scores per animal; result theoretically ranging from 0 to 2). Mean and Standard error of the mean (SEM) stated in the table were then calculated from these animal averages.

Both types of material are easy to peel of the spun bond underlay, they can be then easily manipulated with. They adhere to the intestine and hold well on the intestinal wall, yet they can also be rearranged when needed. No further fixation of the materials was necessary.

All animals survived the whole length of the experiment. None of the animals developed either ileus or sepsis. Two animals from the PCL group vomited single time, so the realimentation schedule was not respected in their case. It is worthy to note though they tolerated the feeding from then on. All animals from the Control group and the PLCL group were able to feed according to the schedule, with daily stool and no signs of gastrointestinal passage blockage. The activity of the animals was not decreased in any of the groups throughout the postoperative observation. We did not notice any case of infection of intravenous port in the PCL group; one case of infection of the port appeared in the PLCL group, and two cases were in the Control group. We also noticed one laparotomy wound infection in one of the animals in the PLCL group in a form of an abscess. No intervention was needed.

There were no significant differences in the observed biochemical parameters between the groups and no remarkable deviations from healthy animals (baseline blood sample).

All animals managed to maintain their weight within the range of 5% of their preoperative weight.

There were no signs of GI content leakage within the second surgery in any of the animals (free GI content, thick peritoneal fluid, fibrin films) (Table 1). All of the anastomoses could be found in the reoperation, the nanomaterial remained fixed, covering the suture line completely in all of them. It has been neither absorbed nor dislocated. All anastomoses were sufficient, no visible defects were found in any of them (Fig. 4a–c). PAs involving other organs than the small intestine were found in 3 animals from the Control group, in 5 animals from the PCL

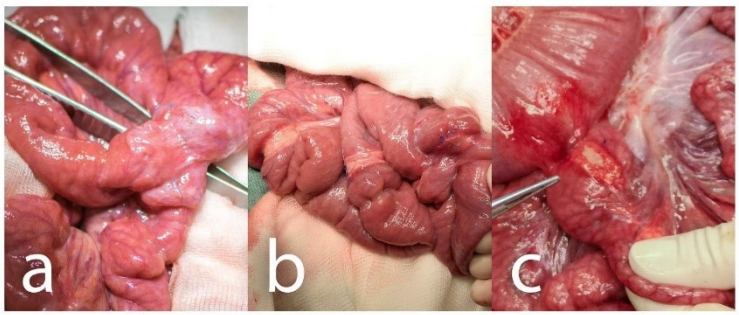

Figure 4. Macroscopic findings in animals of different groups: (**a**) Control group, two anastomoses adhered together, oral parts are marked with a blue suture; (**b**) PCL group, all three anastomoses are visible, the material is clearly visible in the site of application; (**c**) PLCL group, pointing at one of the anastomoses adhering to the colon, oral part is marked with a blue stitch.

group and in 5 animals from the PLCL group. Most of these were adhesions of the left median liver lobe to the incision scar.

The severity of PAs was largely variable within the groups. There was some amount of adhesions in almost all animals in the site of the surgery. Typically, the most adhesions were located within the area of the intestine we manipulated with, connecting the small intestine to the surrounding tissues, mostly only with the small intestine itself (Fig. 5a–c). The adhesions were relatively evenly spread within this area, not surrounding the intestinal circumference in the area of our material or suture line predominantly. The organs we did not manipulate with were usually adhesion-free. The perianastomotic adhesions were in all animals grade Zühlke 2 if present. The adhesions had to be separated by sharp dissection; no clear vascularization was macroscopically visible, though. Only one animal (from the PCL group) didn't develop any perianastomotic adhesions, this was recognized as grade Zühlke 0. The least adhesions according to our scoring system were found in the Control group, ranging from 2 points to 11 per animal (46 points for 8 animals in total), then 66 points for the group PLCL in total (4–11 points per animal) and 79 points for group PCL (0–16 points per animal). Statistical analysis showed these differences between groups as non-significant ($p = 0.715$) (Fig. 6a) (Table 1). The position of the anastomosis (first, second or third) also proved not to be a significant factor ($p = 0.490$) for the amount of adhesions. The most important parameter showed to be the segment of anastomosis while the inner segments (2 and 3) did not show a lot of adhesions, the segments 1 and 4 tended to be heavily adhered ($p < 0.001$).

Almost all animals exhibited some level of dilatation of the proximal segments of the small intestine; we observed it in all 8 animals in the PLCL group, in 7 animals in the PCL group, and also in 7 animals in the Control group. Nevertheless, the difference between the groups was not statistically significant.

The material was washed out of the sections during the histological staining process. The presence of the material could be detected on the sections as an empty space surrounded by granulation tissue with a borderline of tissue permeated with empty spaces in the form of single fibers (Fig. 7). We observed no morphological abnormalities in standard histological stainings (Fig. 8), all physiological layers were present in all samples. Also the successful reepithelisation was found in all samples (Table 1). The volume fraction of von Willebrand factor positive cells (endothelial cells) did not show statistically significant differences between the groups ($p = 0.690$) (Fig. 6b), nor did the volume fractions of collagen ($p = 0.740$) (Fig. 6c) and neutrophiles with macrophages ($p = 0.550$) (Fig. 6d) (Table 1).

The section areas containing suture material exhibited significantly higher level of inflammatory cells infiltration than the stitch free sections ($p = 0.001$) (Fig. 6e).

Discussion

To the best of our knowledge, we were the first to use the PCL and PLCL nanofibrous scaffolds in this kind of application. We successfully designed a study to determine whether the material can be used for this purpose. There have been experimental works focusing on utilization of different locoregional types of protection in the site of intestinal anastomosis[9–16], yet no use of nanofibrous scaffolds has been described so far.

We found the material to be very easy to handle and to apply onto the intestine. The fact that there is no need of further fixation to the viscera is very positive as the application form can be a limiting factor when it comes to translation into the clinical practice. The fibrin glue could be an example of material that unnecessarily prolongs the surgery time as it needs to dry for 10 minutes before the surgeon can reinsert the viscera into the abdominal cavity[14,44].

We had no mortality in our study and also no major complications. There were also no clinical changes observed that would suggest development of sepsis or ileus, and the animals managed to maintain their weight; therefore we assume the material does not contribute to postoperative GI obstruction. Most patients develop an anastomotic leakage within the first 2 weeks after the surgery[45,46], we covered three postoperative weeks of observation.

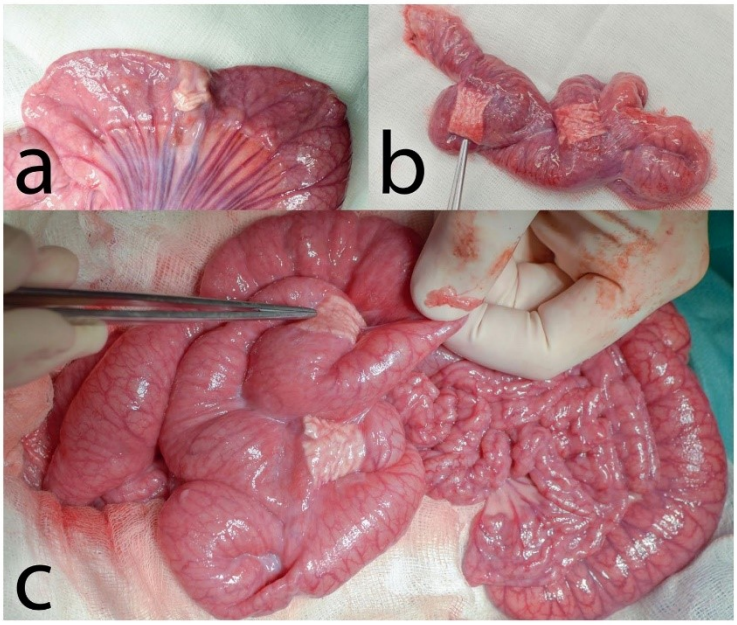

Figure 5. Anastomoses after 3 weeks: (**a**) typical appearance of the small intestine on the 21st postoperative day (PCL group); most of the intestine seems intact with no adhesions, the segments involved in anastomoses are more or less in adhesions, the diameter of the intestine is larger in the proximal segments of the intestine; the material is clearly visible and not dislocated; (**b**) severe adhesions in another animal from the PCL group; (**c**) adhesion free intestine in a different animal from the PCL group.

Nordentoft *et al.* experimented with fibrin coated collagen patches (TachoSil, fibrin sealant) in a pig model of intestinal anastomosis. Two anastomoses per animal were performed on the small intestine after a resection of 2 cm of the intestine. There were no significant differences between the experimental and the Control group in this study in terms of morbidity, mortality and sings of anastomotic leakage as well[10]. In the second study the usage of the same material on a colonic anastomosis showed notable reduction of anastomotic leakage[47]. However, when it comes to clinical use of this material, the fibrin glue does not seem to promote healing as the same authors stated in their review article including 28 studies, only 7 of which revealed a positive effect of the glue[48]. Recently, a clinical study was designed to determine the effect of TachoSil patch in human patients[12]. The study subjected the patients after resection surgery for colorectal cancer to application of the patch over the constructed anastomosis on the large intestine, but was terminated after each of the first eight patients met with complications of different severity. The study concluded that the microbiome of the anastomosis is altered negatively by covering the anastomosis with any kind of material, but did not support this hypothesis with any data.

According to macroscopic findings we can describe the anastomoses from our experiment as well healed. Moreover, we did not observe any morphological changes either in the surrounding tissues or in the whole abdominal cavity, and thus the material seems to be safe to use. The question of the degradation speed remains unanswered at this moment as the material used was always present in the place of application at the end of the experiment. This suggests the material does not have a tendency to slip away but it is also not absorbed as fast as expected. For example a complete reabsorption of the fibrin glue has been described after variable periods ranging from 7 to 20 days[14].

We used the very new *Perianastomotic adhesions amount score* we developed, which accurately describes the quantity of adhesions in the site of an anastomosis on a circular hollow viscus. Some of the systems used in clinical practice consider also the quality of the adhesions, however they evaluate the whole abdominal cavity[32,33]. We did not aim to evaluate the quality macroscopically and mechanically as we assessed the tissue histologically.

The differences in the amount of PAs between the groups were not significant, which can be due to a small size of our experimental groups. The absolute numbers suggest the material increases the amount of PAs in its′ surroundings. This can be caused by easy infiltration of the material by peritoneal fibroblasts from both sides of the material because of its structure similar to extracellular matrix as Srouji described earlier[35]. There was also certain amount of adhesions involving different organs than the small intestine, but there was no clinical manifestation associated with those that we know about.

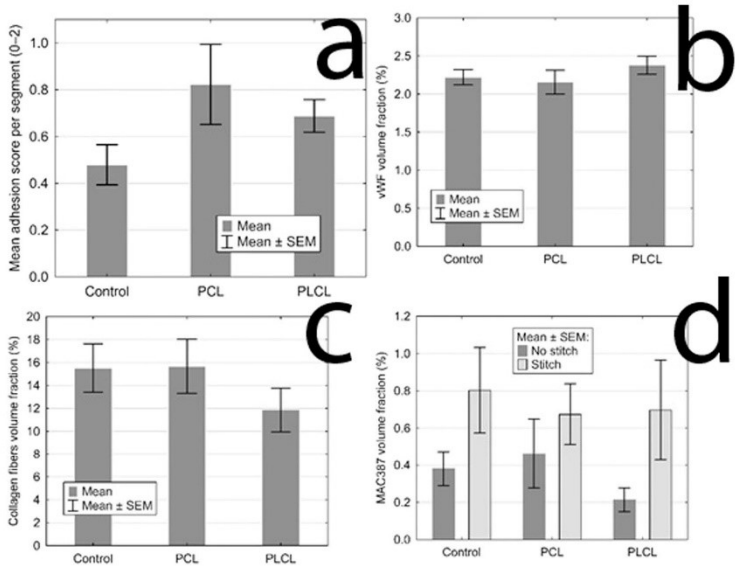

Figure 6. Statistical analysis of quantitative assessment of different parameters: (**a**) The mean adhesion score for each group, the control group scored the lowest with no statistical significance; (**b**) The volume fractions of vWF positively stained area for each groups showing the level of vascularisation, the three groups show the same quality of scar in this aspect; (**c**) The volume fractions of collagen fibres for each group, the three groups show the same quality of scar in this aspect; (**d**) The volume fractions of MAC387 positive area for each group, showing the inflammatory cells infiltration, the presence of a stitch in the section proves to be the only statistically significant factor, the three groups show the same quality of scar in this aspect as well.

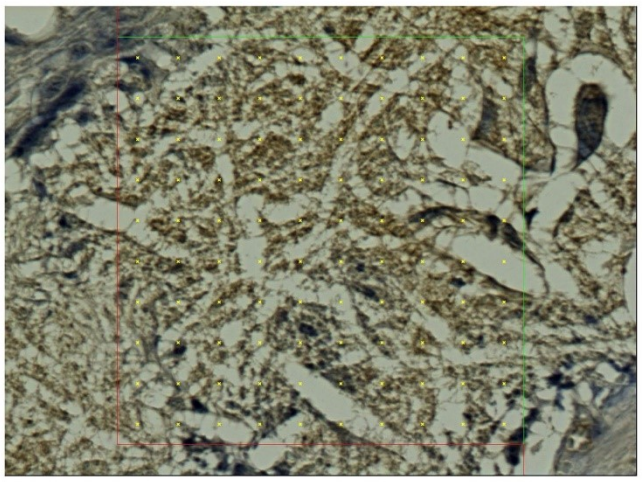

Figure 7. Histological section, PCL group, MAC387 staining: Detail of the marginal zone of the material applied, the empty spaces in the shape of the fibres (stereological grid).

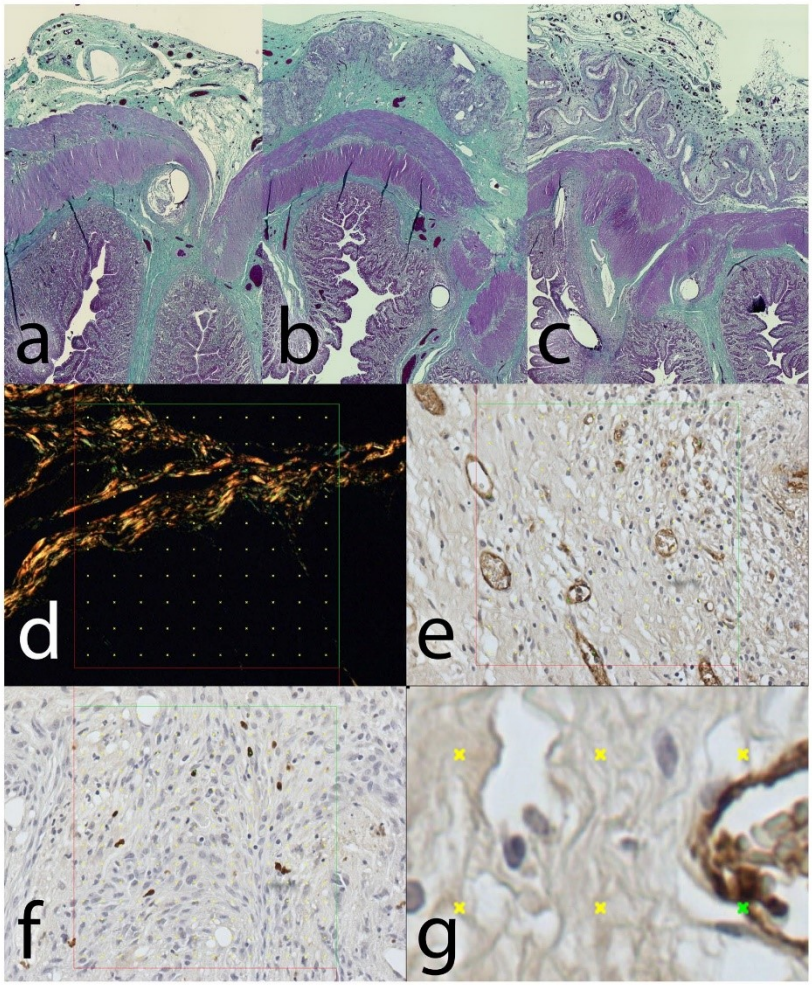

Figure 8. Histological staining of explanted anastomoses: (**a**) Green trichrome: Control group; (**b**) Green trichrome: PCL group, the empty space on the site of application of the nanomaterial can be seen in the upper layer, surrounded by normal granulation tissue; (**c**) Green trichrome: PLCL group, a much thinner empty area can be seen in the upper layer, also surrounded by normal granulation tissue; (**d**) PSR staining, collagen fibres stained yellow, stereological mesh; (**e**) vWF factor staining, the endothelial cells stained brown, stereological grid; (**f**) MAC 387 staining stereology, positive cells stained blue, stereological grid; (**g**) magnification of vWF staining stereology with a positive cross in the upper right corner.

The amount of postoperative adhesions in the peritoneal cavity has been successfully decreased both experimentally and clinically using different substances, usually in a form of gel. Hyaluronic acid based gels or also polycaprolactone based gels can serve as examples[31,49–51]; however, the influence of such materials on the anastomotic healing has not been described and therefore cannot be considered safe in our application.

A very important factor for the formation of adhesions is the material the viscera are manipulated with. Dry swabs damage the peritoneum, cause inflammation and, consequently, adhesion formation[52]. We used wet swabs throughout our experiment. The formation of adhesions should be finished by the end of the three week observation period (although their characteristic may change during the time after this period and the problems they cause can appear much later[42]. To evaluate the clinical impact of all the adhesions formed a longer observation period would be needed.

Even though the materials were dissolved during the process of histological staining, the area of application was clearly visible under a microscope as a tissue-free layer. We followed a standard system of assessment of the healing of an intestinal anastomosis described in different studies[12]. No morphological or any other statistically significant differences were found between the groups using this system. We value this result as positive since we assume that the healing process was not affected in a negative way and that the resulting scar is of the same quality as a physiologically healed one. The system does not evaluate peritoneal adhesions formation, though. As the peritoneal adhesions are certainly a source of many possible complications, their evaluation should be part of an anastomotic healing assessment.

A positive clinical effect could be more pronounced in different experimental settings. Fibrin glue, for example, has been tested in an animal model of complicated colonic anastomosis (severe blood loss, peritonitis), where it showed a positive effect in terms of decreasing morbidity and mortality in the period of 10 postoperative days[52]. The histological assessment of the scar tissue however showed no significant differences between the Control group and the Experimental group on 10th postoperative day measuring also volume fractions of collagen fibers, vWF positive cells and inflammatory reaction[52] (similarly to our results).

A baseline biopsy has not been taken as no intestine was resected. It can be considered a certain limitation of this study. No clinical nor laboratory signs of any pathologies were, however, evident in our animals and no signs of pathologies were found in the final histological specimens either.

Biocompatibility of the materials used in our study was demonstrated by the presence of the granulation tissue of normal quality (according to all measured qualities) surrounding and invading the material.

The level of biodegradation was not to be measured quantitatively as the degradation process of these nanomaterials was described in previous work[41].

All laboratory findings were within the physiological range, which suggests that the material does not cause any systemic disturbances. This was expected because the polymers used for the fabrication of the materials have been in use in clinical medicine for many years.

For more discriminating results a study on a complicated anastomosis should be performed as shown in the works of Tebala *et al.*[53], Zilling *et al.*[44] and Adas *et al.*[17].

Conclusion

We successfully demonstrated that the use of the PCL and PLCL nanofibrous scaffolds in an attempt to fortify an anastomosis on the GI tract is safe. The scaffolds did not influence the amount and quality of scar tissue in the site of anastomosis, and at the same time they did not cause any other kind of complication during our study. From the macroscopic finding they seem to slightly raise the level of adhesions in the site of application, which corresponds to the statement that they promote healing. To be able to assess the adhesion level, we developed and used a novel scoring technique. The material appears to us as a practical and versatile Supporting Material potential of which can be further enhanced for example by adding substances supporting healing like growth factors, antibiotics etc.

The large variability of settings of the fabrication process allows further changes of the material properties.

For the potentially pro-healing qualities of the material, either the PCL or PLCL will be further studied by our team and used as an inner layer of a new double layered patch with an antiadhesive external layer.

Data availability

The authors declare they will supply any existing additional data as soon as possible when requested.

Received: 31 July 2019; Accepted: 9 January 2020;
Published online: 24 January 2020

References

1. Jex, R. K., van Heerden, J. A., Wolff, B. G., Ready, R. L., Ilstrup, D. M. Gastrointestinal Anastomoses Factors Affecting Early Complications, *Ann. Surg.* Aug, **206**(2), 138–41 (1987).
2. Hyman, N., Manchester, T. L., Osler, T., Burns, B. & Cataldo, P. A. Anastomotic Leaks After Intestinal Anastomosis It's Later Than You Think. *Ann. Surg. Feb* **245**(2), 254–8 (2007).
3. Yo, L. S., Consten, E. C., Quarles van Ufford, H. M., Gooszen, H. G. & Gagner, M. Buttressing of the staple line in gastrointestinal anastomoses: overview of new technology designed to reduce perioperative complications. *Dig. Surg.* **23**(5-6), 283–91 (2006).
4. van Rooijen, S. J. *et al.* Definition of colorectal anastomotic leakage: A consensus survey among Dutch and Chinese colorectal surgeons. *World J. Gastroenterol.* **23**(33), 6172–6180 (2017).
5. Slieker, J. C., Daams, F., Mulder, I. M., Jeekel, J. & Lange, J. F. Systematic review of the technique of colorectal anastomosis. *JAMA Surg.* **148**(2), 190–201 (2013).
6. Golub, R., Golub, R. W., Cantu, R. Jr. & Stein, H. D. A multivariate analysis of factors contributing to leakage of intestinal anastomoses. *J. Am. Coll. Surg.* **184**(4), 364–72 (1997).
7. Pommergaard, H. C. *et al.* Preoperative risk factors for anastomotic leakage after resection for colorectal cancer: a systematic review and meta-analysis. *Colorectal Dis.* **16**(9), 662–71 (2014).
8. Boersema, G. S. A. *et al.* Hyperbaric oxygen therapy improves colorectal anastomotic healing. *Int. J. Colorectal Dis.* **31**, 1031–1038 (2016).
9. Khorshidi, H. R. *et al.* Evaluation of the effectiveness of sodium hyaluronate, sesame oil, honey, and silver nanoparticles in preventing postoperative surgical adhesion formation. An experimental study. *Acta Cir. Bras.* **32**(8), 626–632 (2017).
10. Nordentoft, T., Rømer, J. & Sørensen, M. Sealing of gastrointestinal anastomoses with a fibrin glue-coated collagen patch: a safety study. *J. Invest. Surg.* **20**(6), 363–9 (2007).
11. Nordentoft, T. & Holte, K. Preventing Clinical Leakage of Colonic Anastomoses with A Fibrin - Coated Collagen Patch Sealing - An Experimental Study. *Arch Clin Exp Surg.* **3**(4), 201–206.
12. Trotter, J. *et al.* (2018) The use of a novel adhesive tissue patch as an aid to anastomotic healing. *Ann. R. Coll. Surg. Engl.* **100**(3), 230–234 (2014).
13. Aznan, M. I. *et al.* Effect of Tualang honey on the anastomotic wound healing in large bowel anastomosis in rats-A randomized controlled trial. *BMC Complement. Altern. Med.* **23**, 16–28 (2016).

14. Bonanomi, G., Prince, J. M., McSteen, F., Schauer, P. R. & Hamad, G. G. Sealing effect of fibrin glue on the healing of gastrointestinal anastomoses: implications for the endoscopic treatment of leaks. *Surg. Endosc.* **18**(11), 1620–4 (2004).
15. Fajardo, D. A., Amador-Ortiz, C., Chun, J., Stewart, D. & Fleshman, J. W. Evaluation of Bioabsorbable Seamguard for Staple Line Reinforcement in Stapled Rectal Anastomoses. *Surg. Innov.* **19**(3), 288–94 (2012).
16. Boersema, G. S. A. *et al.* Reinforcement of the colon anastomosis with cyanoacrylate glue: a porcine model. *J. Surg. Res.* **217**, 84–91 (2017).
17. Adas, G. *et al.* Treatment of ischemic colonic anastomoses with systemic transplanted bone marrow derived mesenchymal stem cells. *Eur. Rev. Med. Pharmacol. Sci.* **17**(17), 2275–85 (2013).
18. Hirst, N. A. *et al.* Systematic review of methods to predict and detect anastomotic leakage in colorectal surgery. *Colorectal Dis.* **16**(2), 95–109 (2014).
19. Mileski, W. J., Joehl, R. J., Rege, R. V. & Nahrwold, D. L. Treatment of anastomotic leakage following low anterior colon resection. *Arch. Surg.* **123**(8), 968–71 (1988).
20. Sevim, Y., Celik, S. U., Yavarifar, H. & Akyol, C. Minimally invasive management of anastomotic leaks in colorectal surgery. *World J. Gastrointest. Surg. 27* **8**(9), 621–626 (2016).
21. Chadi, S. A. *et al.* Emerging Trends in the Etiology, Prevention, and Treatment of Gastrointestinal Anastomotic Leakage. *J. Gastrointest. Surg.* **20**(12), 2035–2051 (2016).
22. Thomas, M. S. & Margolin, D. A. Management of Colorectal Anastomotic Leak. *Clin. Colon. Rectal Surg.* **29**(2), 138–44 (2016).
23. Blumetti, J. & Abcarian, H. Management of low colorectal anastomotic leak: Preserving the anastomosis. *World J. Gastrointest. Surg. 27* **7**(12), 378–83 (2015).
24. Gessler, B., Eriksson, O. & Angenete, E. Diagnosis, treatment, and consequences of anastomotic leakage in colorectal surgery. *Int. J. Colorectal Dis.* **32**(4), 549–556 (2017).
25. Paliogiannis, P. *et al.* Conservative management of minor anastomotic leakage after open elective colorectal surgery. *Ann. Ital. Chir.* **83**(1), 25–8 (2012).
26. Zhao, R., Li, K., Shen, C. & Zheng, S. The outcome of conservative treatment for anastomotic leakage after surgical repair of esophageal atresia. *J. Pediatr. Surg.* **46**(12), 2274–8 (2011).
27. Beyene, R. T., Kavalukas, S. L. & Barbul, A. Intra-abdominal adhesions. Anatomy, physiology, pathophysiology, and treatment. *Curr. Probl. Surg.* **52**(7), 271–319 (2015).
28. Diamond, M. P. & Freeman, M. L. Clinical implications of postsurgical adhesions. *Hum. Reprod. Update.* **7**(6), 567–76 (2001).
29. van Goor, H. Consequences and complications of peritoneal adhesions. *Colorectal Dis.* **9**(Suppl 2), 25–34 (2007).
30. Ellis, H. The clinical significance of adhesions: focus on intestinal obstruction. *Eur. J. Surg. Suppl.* **577**, 5–9 (1997).
31. Ditzel, M. *et al.* Postoperative adhesion prevention with a new barrier: an experimental study. *Eur. Surg. Res.* **48**(4), 187–93 (2012).
32. Coccolini, F. *et al.* Peritoneal adhesion index (PAI): proposal of a score for the "ignored iceberg" of medicine and surgery. World J. Emerg. Surg. 31;8(1):6 (2013).
33. Zühlke, H. V., Lorenz, E. M., Straub, E. M. & Savvas, V. Pathophysiology and classification of adhesions. *Langenbecks Arch. Chir. Suppl. II Verh. Dtsch. Ges. Chir.* **1990**, 1009–16 (1990).
34. Nair, S. K., Bhat, I. K. & Aurora, A. L. Role of proteolytic enzyme in the prevention of postoperative intraperitoneal adhesions. *Arch Surg.* **108**(6), 849–53 (1974).
35. Srouji, S., Kizhner, T., Suss-Tobi, E., Livne, E. & Zussman, E. 3-D Nanofibrous electrospun multilayered construct is an alternative ECM mimicking scaffold. *J. Mater. Sci. Mater Med.* **19**(3), 1249–55 (2008).
36. Yu, M. *et al.* Recent advances in needleless electrospinning of ultrathin fibers: From academia to industrial production. *Marcomol. Mater. Eng.* **1**, 1–19 (2017).
37. Pokorny, P. *et al.* Effective AC needleless and collectorless electrospinning for yarn production. *Phys. Chem. Chem Phys.* **16**(48), 26816–22 (2014).
38. Dahlin, R. L., Kasper, F. K. & Mikos, A. G. Polymeric nanofibers in tissue engineering. *Tissue Eng. Part. B Rev.* **17**(5), 349–64 (2011).
39. Krchova, S. *et al.* Nanofibers for the wound healing. *Czech Dermatology.* **4**, 234–240 (2014).
40. Yalcin, I. *et al.* Design of polycaprolactone vascular grafts. *J. Ind. Text.* **45**, 1–21 (2014).
41. Horakova, J. *et al.* The effect of ethylene oxide sterilization on electrospun vascular grafts made from biodegradable polyesters. *Mater. Sci. Eng. C. Mater Biol. Appl.* **1**(92), 132–142 (2018).
42. Williams, D. L. & Browder, I. W. Murine models of intestinal anastomoses. In: DiPietro, L. A. & Burns, A. L., (ed) *Wound healing: Methods and protocols.*, vol. 10, 1st ed. New Jersey: Humana Press Inc., pp 133–140 (2010).
43. Gunatillake, P. A. & Adhikari, R. Biodegradable synthetic polymers for tissue engineering. *Eur. Cell Mater.* **5**, 1–16 (2003).
44. Zilling, T. L., Jansson, O., Walther, B. S. & Ottosson, A. Sutureless small bowel anastomoses: experimental study in pigs. *Eur. J. Surg.* **165**(1), 61–8 (1999).
45. Li, Y. W. *et al.* Very Early Colorectal Anastomotic Leakage within 5 Post-operative Days: a More Severe Subtype Needs Relaparatomy. *Sci. Rep.* **7**, 39936 (2017).
46. Kosmidis, C. *et al.* Myofibroblasts and colonic anastomosis healing in Wistar rats. *BMC Surg.* **11**, 6 (2011).
47. Nordentoft, T. & Sørensen, M. Leakage of Colon Anastomoses: Development of an Experimental Model in Pigs. *Eur. Surg. Res.* **39**, 14–16 (2007).
48. Nordentoft, T., Pommergaard, H. C., Rosenberg, J. & Achiam, M. P. Fibrin glue does not improve healing of gastrointestinal anastomoses: a systematic review. *Eur. Surg. Res.* **54**(1-2), 1–13 (2015).
49. Gao, X. *et al.* Novel thermosensitive hydrogel for preventing formation of abdominal adhesions. **8**, 2453–63 (2013).
50. Caglayan, E. K., Caglayan, K., Erdogan, N., Cinar, H. & Güngör, B. Preventing intraperitoneal adhesions with ethyl pyruvate and hyaluronic acid/carboxymethylcellulose: a comparative study in an experimental model. *Eur. J. Obstet. Gynecol. Reprod. Biol.* **181**, 1–5 (2014).
51. Kataria, H. & Singh, V. P. Liquid Paraffin vs Hyaluronic Acid in Preventing Intraperitoneal Adhesions. *Indian. J. Surg.* **79**(6), 539–543 (2017).
52. Arung, W., Meurisse, M. & Detry, O. Pathophysiology and prevention of postoperative peritoneal adhesions. *World J. Gastroenterol.* **17**(41), 4545–4553 (2011).
53. Tebala, G. D., Ceriati, F., Ceriati, E., Vecchioli, A. & Nori, S. The use of cyanoacrylate tissue adhesive in high-risk intestinal anastomoses. *Surg. Today.* **25**(12), 1069–72 (1995).

Acknowledgements

This study was supported by the Centrum of Clinical and Experimental liver surgery (UNCE/MED/006), the National Sustainability Program I (NPU I) Nr. LO1503 provided by the Ministry of Education Youth and Sports of the Czech Republic (V.L.).

Author contributions

J. Rosendorf: Acquisition of data, Analysis and interpretation of data, Drafting of manuscript, J. Horakova: Study conception and design, Critical revision of manuscript, M. Klicova: Study conception and design, Critical revision of manuscript, R. Palek: Acquisition of data, L. Cervenkova: Acquisition of data, Analysis and interpretation of data, Drafting of manuscript, T. Kural: Acquisition of data, P. Hosek: Analysis and interpretation of data, Drafting of manuscript, T. Kriz: Acquisition of data, V. Tegl: Acquisition of data, V. Moulisova: Analysis and interpretation of data, Critical revision of manuscript, Z. Tonar: Critical revision of manuscript, V. Treska: Critical revision of manuscript D. Lukas: Study conception and design, V. Liska: Study conception and design, Critical revision of manuscript.

Competing interests

All authors certify they have no affiliations with or involvement in any organization or entity with any financial interest or non-financial interest in the subject of matter or materials in this manuscript.

Additional information

Supplementary information is available for this paper at https://doi.org/10.1038/s41598-020-58113-4.

Correspondence and requests for materials should be addressed to J.R.

Reprints and permissions information is available at www.nature.com/reprints.

Publisher's note Springer Nature remains neutral with regard to jurisdictional claims in published maps and institutional affiliations.

Attachment 12: Article B

Rosendorf J, Klicova M, Cervenkova L, Palek R, Horakova J, Klapstova A, Hosek P, Moulisova V, Bednar L, Tegl V, Brzon O, Tonar Z, Treska V, Lukas D, Liska V. Double-layered Nanofibrous Patch for Prevention of Anastomotic Leakage and Peritoneal Adhesions, Experimental Study. In Vivo. 2021 Mar-Apr;35(2):731-741.

Q2, IF=1.586

in vivo *35*: 731-741 (2021)
doi:10.21873/invivo.12314

Double-layered Nanofibrous Patch for Prevention of Anastomotic Leakage and Peritoneal Adhesions, Experimental Study

JACHYM ROSENDORF[1,2], MARKETA KLICOVA[3], LENKA CERVENKOVA[2,4], RICHARD PALEK[1,2], JANA HORAKOVA[3], ANDREA KLAPSTOVA[3], PETR HOSEK[2], VLADIMIRA MOULISOVA[2], LUKAS BEDNAR[2], VACLAV TEGL[2,5], ONDREJ BRZON[2], ZBYNEK TONAR[2,6], VLADISLAV TRESKA[1], DAVID LUKAS[3,7] and VACLAV LISKA[1,2]

[1]*Department of Surgery, Faculty of Medicine in Pilsen, Charles University, Prague, Czech Republic;*
[2]*Biomedical Center, Faculty of Medicine in Pilsen, Charles University, Prague, Czech Republic;*
[3]*Department of Nonwovens and Nanofibrous Materials, Faculty of Textile Engineering, Technical University of Liberec, Liberec, Czech Republic;*
[4]*Department of Pathology, Third Faculty of Medicine, Charles University, Prague, Czech Republic;*
[5]*Department of Anesthesiology and Intensive Care Medicine, Faculty of Medicine in Plzen, Pilsen, Czech Republic;*
[6]*Department of Histology and Embryology, Faculty of Medicine in Pilsen, Charles University, Prague, Czech Republic;*
[7]*Department of Chemistry, Faculty of Science, Humanities and Education, Technical University of Liberec, Liberec, Czech Republic*

Abstract. *Background/Aim: Anastomotic leakage is a feared complication in colorectal surgery. Postoperative peritoneal adhesions can also cause life-threatening conditions. Nanofibrous materials showed their pro-healing properties in various studies. The aim of the study was to evaluate the impact of double-layered nanofibrous materials on anastomotic healing and peritoneal adhesions formation. Materials and Methods: Two versions of double-layered materials from polycaprolactone and polyvinyl alcohol were applied on defective anastomosis on the small intestine of healthy pigs. The control group remained with uncovered defect. Tissue specimens were subjected to histological analysis and adhesion scoring after 3 weeks of observation. Results: The wound healing was inferior in the experimental groups, however, no anastomotic leakage was observed and the applied material always kept covering the defect. The extent of adhesions was larger in the experimental groups. Conclusion: Nanofibrous materials may prevent anastomotic leakage but delay healing.*

Correspondence to: Jachym Rosendorf, MD, Biomedical Center, Alej Svobody 80, Plzen, 32 600, Czech Republic. Tel: +420 377103642, e-mail: jachymrosendorf@gmail.com

Key Words: Anastomotic leak, colorectal surgery, anastomotic reinforcement, nanofibrous materials, polycaprolactone.

Anastomotic leakage (AL) is a result of partial or total dehiscence of an anastomosis on the gastrointestinal (GI) tract. It is a feared complication especially in colorectal surgery that usually appears in the early postoperative period (1-4). The reported rates of AL in colorectal surgery in general are between 6 and 7% (5-7). In rectal cancer surgery in particular, the rate reaches up to 11% or even higher according to some studies (8-10). The numbers differ as the definitions of leakage are variable (11).

There are three clinical grades of AL following anterior resection of the rectum according to the system proposed by the International Study Group of Rectal Cancer (12, 13). Grade A presents with no symptoms, no laboratory deviations and is detectable only by radiologic evaluation as a contained leak. No intervention is needed. Grade B manifests with discomfort of the patient, possible purulent drain secretion and laboratory changes. Grade B ALs can be approached by application of antibiotics or drainage in some cases; reoperation is not required. A grade C AL results in peritonitis. It is a life-threatening condition and requires reoperation. Grade B and especially grade C ALs are associated with generally higher morbidity and mortality, worse clinical outcome, prolonged stay in hospital, higher risk of stoma and higher treatment costs (14). Higher local

malignancy recurrence has been observed in several studies after AL alongside shorter overall survival of the patients suffering from AL (15-17). AL is therefore to be considered as an enormous socio-economic burden in colorectal surgery.

Only little is known about anastomotic healing and the processes involved in anastomotic failure. A thorough description of the results of the healing process should therefore be implemented in any experimental work focusing on the anastomotic healing. A standard histological evaluation comprises (i) intestinal wall morphology assessment by comprehensive staining, (ii) re-epithelization assessment, and (iii) stereological evaluation of volume fractions of collagen, endothelial cells and inflammatory cells (18). To the best of our knowledge, there are currently no complex histological scoring systems for evaluation of the integrity of intestinal wall focusing on each intestinal wall layer separately.

Many studies have been conducted to identify the risk factors associated with the occurrence of AL in colorectal surgery. Patient-specific factors, perioperative care, surgical treatment and technique were analyzed. It is clear from these studies that the occurrence of AL is determined by many factors. Some studies list the experience of the performing surgeon among these factors. This observation may suggest that a technical fault can be involved in the development of AL (19-21).

Another adverse effect of intra-abdominal surgical procedures is the formation of peritoneal adhesions (PAs). PAs can develop in various amounts and in different forms ranging from thin fragile connections to thick vascular bonds (22, 23). PAs can often cause abdominal discomfort or even more serious complications including ileus. Besides that, subsequent surgical procedures are more technically challenging due to PAs. No routine use of currently sold anti-adhesives is recommended because of lack of clinical data (23). One of the conditions for the formation of peritoneal adhesions is the contact of the two peritoneal surfaces. Hydrophobicity is suspected to belong among the factors determining the pro- or anti-adhesive properties of surgical materials.

Over the recent decades, various materials have been tested both for reinforcement of intestinal anastomoses and for prevention of the formation of peritoneal postoperative adhesions. Experimental studies on new supporting materials and techniques in general often show positive results of reinforcing materials in animal models according to a systematic review conducted by Yauw *et al.* (24). The quality of such studies is however highly variable, as are also their experimental settings including species, location of anastomosis, perioperative treatment and, most importantly, methodology of the assessment of the healing quality (24). Furthermore, none of the reinforcing materials is currently recommended for use in colorectal surgery (25).

Nanofibrous and microfibrous materials are nonwoven fabrics created from various polymer solutions. They have been proved to have a positive influence in experimental studies of wound healing (26). However, their impact on anastomotic healing, formation of peritoneal adhesions and on the risk of AL has not been studied thoroughly yet. To the best of our knowledge, the only study focusing on nanofibrous patches has been performed by our research group (27). In this study, the material consisting of polycaprolactone appeared safe and easy to use with no negative clinical and histological effects in an experimental porcine model of anastomosis on the small intestine. However, in the experimental settings with no complications, the possible positive effect of the material on the risk of AL development was not distinguishable. To address this shortcoming, the experimental design was modified for the current study by including a standardized defect in all of the performed anastomoses. A new nanofibrous patch from polyvinyl alcohol (PVA) and polycaprolactone (PCL) was developed by our team and tested *in vitro* for its physical properties and biocompatibility (28).

The aims of this study were: 1) To assess the impact of the developed composite microfibrous materials on anastomotic healing in an experimental model of a technically defective intestinal anastomosis in pig. 2) To develop and use a new semiquantitative system for the evaluation of intestinal integrity in the site of anastomosis for more complex anastomotic healing assessment.

Materials and Methods

Development of materials. Double-layered PCL/PVA nanofibrous mats were prepared in two variants differing in the degree of hydrolysis of the PVA component. The solution of PVA with high degree of hydrolysis (PVA1) was prepared by diluting the commercially available solution of 16% PVA Mowiol® (M_w 125.000 g/mol, 98.0-98.8% hydrolysis, Sigma Aldrich, St. Louis, MO, USA) in ethanol (Penta Chemicals, Prague, Czech Republic) and deionized water (1:4 volume fractions) in a final concentration of 10% w/w. PVA Mowiol® (M_w 130.000 g/mol, 88% hydrolysis, Merck, Darmstadt, Germany) was used to prepare aqueous solution of the PVA with low degree of hydrolysis (PVA2) in a final concentration of 12% w/w. Polymeric granulate of PCL (M_w 43.000 g/mol, Polysciences, Hirschberg an der Bergstrasse, Germany) was dissolved in chloroform, acetic acid and ethanol solution (8:1:1 volume fractions) in a concentration of 16% w/w.

The double-layered nanofibrous mats were prepared using the needleless electrospinning device Nanospider™ 1WS500U (Elmarco, Liberec, Czech Republic) by the method of sequential electrospinning. Firstly, the hydrophilic layer of PVA1 or PVA2 was created. The PCL fibres were then deposited directly on the previously electrospun PVA1/PVA2 layer. Scanning electron microscopy (PHENOMTM, Fei Company, Hillsboro, OR, USA) was employed to evaluate the structure of the materials. We followed the same protocols as in our recent publication (28).

Experimental design. We randomly allocated 24 healthy male and female Prestice black-pied pigs into 3 groups, 8 animals each. A

defective anastomosis on the small intestine was constructed in all animals. Animals in experimental groups PCL/PVA1 and PCL/PVA2 received one of the two types of reinforcing material (respecting the group) and the animals in the Control group remained with uncovered anastomotic defect. The animals were observed for 21 days. Sample collection, macroscopic and histologic assessments followed.

Surgery. The animals were weighed prior to the surgery. Anesthesia was induced by intramuscular application of 10 mg/kg of ketamine (Narkamon, Spofa, Prague, Czech Republic), 5 mg/kg of azaperone (Stresnil, Jannssen Phramaceutica, Beerse, Belgium) and 0.5 mg atropine (Atropin Biotika, Hoechst Biotika, Martin, Slovak Republic). Laryngeal tube was then inserted while maintaining general anaesthesia using intravenous propofol administration (1% mixture 5-10 mg/kg/h Propofol, Fresenius Kabi, Oslo, Norway) in combination with Fentanyl 1-2 μg/kg/h (Fentanyl Torrex, Chiesi cz, Prague, Czech Republic) for analgesia. 1.2 g of Augmentin (GlaxoSmithKline Slovakia, Bratislava, Slovak Republic) was used for antibiotic prophylaxis; half of the dose was administered prior to surgery and the other half two h after its beginning.

A ProPort Plastic Venous Access System with PolyFlow polyurethane catheter (Deltec, Smiths Medical, Minneapolis, MN, USA) was implanted and introduced through one of the jugular veins as the first surgical procedure. The abdominal cavity was then approached via an upper middle laparotomy. The small intestine was transected 70 cm from the duodenojejunal junction. All swabs used during the surgery were wet in order to prevent extensive formation of peritoneal adhesions. A hand-sutured end-to-end anastomosis was constructed with MONOSYN 4/0 (Glycolide 72%, Caprolactone 14%, Trimethylencarbonate 14%) monophilament suture line (B-Braun, Germany) using seromuscular extramucosal running suture. An artificial defect on the antimesenteric side of the anastomosis with a standard diameter of 0.75 cm was created using a draining tube (Figure 1). The initial knot was always placed on the mesenteric side while the closing knot was placed about one quarter of the intestinal circumference from it. The position of the defect was marked with a single non-absorbable stitch placed orally to the anastomosis. A sheet of PCL/PVA1 or PCL/PVA2 material was placed onto the anastomosis and positioned to adhere to the intestinal wall and to cover the whole anastomosis with the defect (the hydrophilic PVA side facing the intestine). The viscera were placed back to the abdominal cavity and the abdominal wall was reconstructed. All surgical procedures were performed by the same surgeon.

The animals were observed for three weeks following the surgery and fed according to pre-defined re-alimentation scheme. Their ability to feed according to the schedule was recorded alongside any clinical changes, signs of GI obstruction, abdominal diameter enlargement, stool frequency, vomiting, and body temperature elevation.

Follow-up. Blood samples were taken during the experiment at five time points: on day 0 before the application of the material, exactly two h after the application of the nanomaterial, on the 7th postoperative day (POD), on the 14th POD, on the 21st POD. Basic biochemical parameters were tracked in these samples (bilirubin, GGT, ALT, AST, ALP, albumin, urea, and creatinine) to observe deviations in the animals' metabolism. The weight of the animals was also measured in defined time points: preoperatively at the beginning of the experiment, on the 3rd, 7th, 14th, 21st POD.

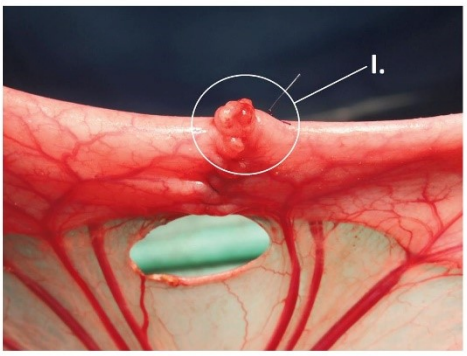

Figure 1. *Construction of anastomosis. An intestinal anastomosis with defect on the antimesenteric side (I.), the size of the defect is standardized using a drain tube.*

After the observation period, the following exploration and sample collection surgery was performed under general anaesthesia. The abdominal cavity was searched for signs of any complications, intestinal matter, the GI tract checked for signs of obstruction (intestinal wall thickening, intestinal diameter enlargement, intestinal adhesions causing convolutes and sharp bents of the intestine, strictures of the intestine in any location and strictures of the anastomosis itself). Organs involved in adhesions in the rest of the abdominal cavity were also noted. Afterwards, the specimen of the anastomosed intestine was collected including the surrounding adhered tissues; photodocumentation was acquired. The animals were sacrificed after sample collection.

The collected intestine was transected longitudinally on the mesenteric side, pinned onto a cork underlay and the adhesions present on the site of the anastomosis were scored using the perianastomotic adhesions amount score (PAAS) developed previously by our team. PAAS allows for the quantification of the extent of adhesions at the anastomotic circumference (27). The specimens were then fixed in 10% buffered formalin.

All experimental procedures concerning the pigs were described in a protocol approved by the Commission of Work with Experimental Animals at the Faculty of Medicine in Pilsen, Charles University, and supervised by the Ministry of Education, Youth and Sports of the Czech Republic (project code: MSMT-26570/2017-2). All procedures were performed in compliance with the law of the Czech Republic and with the legislation of the European Union.

Histology. Five 5 mm thick strips of tissue were cut from each specimen perpendicular to the line of the anastomosis. All specimens were processed by standard paraffin technique. Four μm thick sections were stained by hematoxylin and eosin for comprehensive overview. These samples were investigated both qualitatively and semi-quantitatively. A semiquantitative scoring system has been designed to evaluate the integrity of the intestinal wall at the site of the anastomotic defect. Each layer was assessed separately using defined parameters. Each layer was assigned a

Table I. *Parameters for semiquantitative assessment of anastomotic healing.*

Layer	Absolute score	Weighted score	Parameter
Mucosa	1	3/12	Completely re-epithelized
	0	0/12	Incompletely re-epithelized
Submucosa	1	3/12	Completely healed
	0	0/12	Purulent infiltration, necrosis
Muscularis	3	3/12	Distance ≤0.09 mm
	2	2/12	Distance 0.1-1.99 mm
	1	1/12	Distance 2-3.99 mm
	0	0/12	Distance ≥ 4 mm
Serosa	3	3/12	No purulent infiltration or necrosis
	2	2/12	Purulent infiltration and/or necrosis from muscular layer to area of nanomaterial*
	1	1/12	Purulent infiltration and/or necrosis from area of nanomaterial to peritoneum*
	0	0/12	Purulent infiltration and/or necrosis passing to peritoneum

The absolute score focuses only on the level of integrity of a selected intestinal wall layer, while the weighted score corrects this result to make each layer have the same impact in the total score. *Samples without nanomaterial were scored: score 2 for no necrosis, score 1 (2/12) for purulent infiltration and/or necrosis from muscular layer to ½ thickness of serosa and score 0 (1/12) for purulent infiltration and/or necrosis reaching more than ½ thickness of serosa to peritoneum.

score ranging from 0 to 0.25 and the scores of all four layers were then summed. The resulting sum (anastomosis integrity score) represents a measure of the deterioration of intestinal wall integrity ranging from 0 (fully defective healing) to 1 (perfect healing) (Table I). A full-thickness defect in the intestinal wall of the specimen was considered a proof of microscopic anastomotic leakage.

The blocks with the highest semiquantitative score were analyzed quantitatively. Five μm sections were stained using picrosirius red (PSR) for the assessment of the amount of collagen. Vascularization and inflammatory infiltration were visualized by immunohistochemical methods. We followed the standardized protocol described in our previous study (27).

Statistical analysis. Common descriptive statistics and frequencies were used to characterize the sample data set. Due to their non-normal distributions, the PAAS values, anastomosis deficiency scores, and histologically determined volume fractions were analyzed using Kruskal-Wallis ANOVA with respect to group. In case of a significant overall finding, differences between individual group pairs were assessed *post-hoc* using multiple comparisons of mean ranks according to Siegel and Castellan (28), including a Bonferroni adjustment for multiple testing. All reported *p*-values are two-tailed and the level of statistical significance was set at α=0.05. Statistical processing and testing were performed using STATISTICA data analysis software system [Version 12; StatSoft, Inc, 2013; (29)].

Results

Material properties. Two composite nanofibrous materials were created with mean fibre thicknesses 550 nm/344 nm for PCL/PVA 1 and 652 nm/344 nm for PCL/PVA 2 (Figure 2). Both materials were very easy to peel the spunbond underlay and to apply onto the intestinal surface. The level of their adherence to the tissue was sufficient to leave the materials attached without any further fixation.

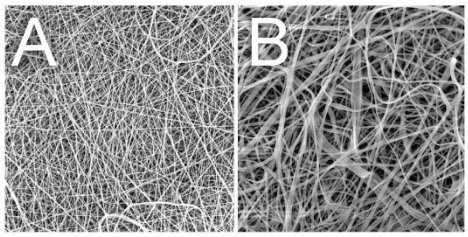

Figure 2. *Scanning electron microscopy. Scanning electron microscopy images of the two prepared materials; A) PCL/PVA 1 material; B) PCL/PVA 2 material.*

Clinical results. All animals survived through the whole experiment. Re-alimentation was unproblematic in only two animals from the Control group while all of the animals from the PCL/PVA1 and PCL/PVA2 groups were able to feed according to the schedule with no obstacles. Two animals from the Control group vomited once (on 5th POD and 11th POD).

Weight gain was achieved by 3 animals in the PCL/PVA1 group and 6 animals in the PCL/PVA2 group (Table II). Most of the animals did pass stool daily, no animal developed gastrointestinal obstruction. No signs of sepsis or peritonitis were encountered (fevers, activity decrease, abdominal wall tenderness).

Biochemical results. There were no significant deviations from physiological parameters or statistically significant differences between the groups in any of the monitored parameters.

Table II. *Number of animals with weight gain and weight loss per group.*

Group	Number of animals having gained weight (3% tolerance)	Number of animals having lost weight (3% tolerance)
Control group (n=8)	1	5
PCL/PVA1 group (n=8)	3	4
PCL/PVA2 group (n=8)	6	1

Table III. *Intraoperative macroscopic findings.*

Group	Proximal intestinal wall thickening (number of animals)	Partial anastomotic stenosis (number of animals)	Mean PAAS (points)	PAAS range (points per animal)	Convolute (number of animals)
Control group (n=8)	2	0	2.63	0-5	3
PCL/PVA1 group (n=8)	6	1	2.88	0-6	5
PCL/PVA2 group (n=8)	5	0	4.88	3-7	7

PAAS: Perianastomotic adhesions amount score.

Complications. Only minor complications occurred throughout the experiment as there was no animal developing sepsis or signs of complete gastrointestinal obstruction in the whole experiment. There were two cases of infectious complications in the Control group (25%). One animal developed an abscess in the laparotomy wound without dehiscence and one animal developed infection in the tissues surrounding the central venous catheter. One of the animals in the Control group presented with abdominal diameter enlargement starting on the 17th POD and lasting for 3 days, but with no additional clinical signs, no vomiting, and no defecation problems. One animal from the PCL/PVA1 group (12.5%) developed an abscess in the laparotomy wound, no other complications were found in the group. One animal from the PCL/PVA2 group (12.5%) developed a small abscess in the laparotomy wound and another animal from the group showed a mild palpable rash on the abdominal wall from the 14th POD on.

We observed no decrease in activity in any of the animals during the observation period.

Macroscopic findings. All of the anastomoses in both experimental groups and the Control group were free of macroscopically visible defects on the 21st POD. There were no signs of anastomotic leak (no intraperitoneal intestinal matter, no intraperitoneal puss, no abscesses, no visible signs of peritonitis), nor signs of complete intestinal obstruction. However, some level of intestinal wall thickening was visible in the oral parts of the intestine in 2 animals from the Control group (25%), in 6 from the PCL/PVA1 group (75%) and in 5 animals from the PCL/PVA2 group (62.5%). One animal from the PCL/PVA1 group showed a partial stenosis of the anastomosis reducing the intestinal diameter by less than one third (Table III).

Small amount of clear peritoneal fluid was present in almost all animals in volumes smaller than 100 ml. The nanomaterial remained fully attached at the place of application until extraction in 5 of 8 (62.5%) animals from the PCL/PVA1 group while it was partially dislocated in the remaining 3 (37.5%); it always remained covering the place of the defect though. The material was partially dislocated only in 1 of 8 animals (12.5%) in the PCL/PVA2group, also still covering the place of the defect.

We found a number of adhesions in the area of surgery in all animals except for one animal from the Control group (12.5%) and two animals from the CPL/PVA1 group (25%). The highest perianastomotic adhesions amount score (PAAS) was recorded in the PCL/PVA2 group with a mean PAAS of 4.88 points (3 to 7 points per animal), followed by the PCL/PVA1 group with a mean PAAS of 2.88 (0 to 6 points per animal) and by the Control group with a mean PAAS of 2.63 points (0 to 5 points per animal). The adhesions were present not only at the location of the anastomosis itself, but usually also in its vicinity, both oral and aboral. An intestinal convolute (more than two segments of intestine adhered together) was present in 3 animals in the Control group (37.5%), in 5 animals from the PCL/PVA1 group (62.5%) and in 7 animals in the PCL/PVA2 group (87.5%) (Figure 3).

Histology. No signs of full-thickness defects were visible in the comprehensive histologic assessment of the specimens. We observed complete re-epithelialization in the site of the

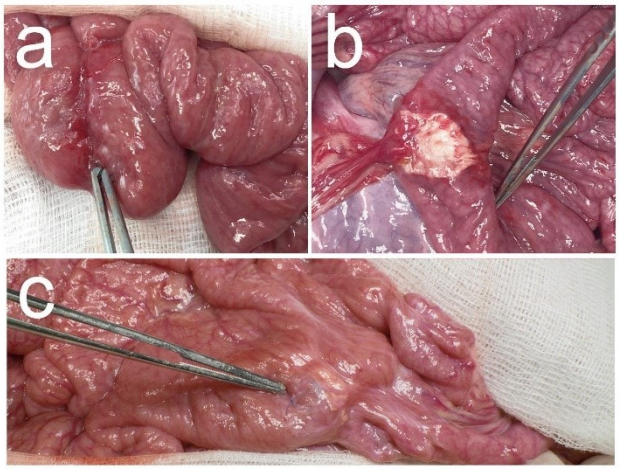

Figure 3. *Intraoperative findings. Examples of intraoperative findings, the forceps point to the anastomosis in all of the specimens; A) animal from Control group, well healed anastomosis, no defect is visible; B) animal from PCL/PVA1 group, the material is visible, a string of omental adhesion is attached to the anastomosis, no defect is visible; C) animal from PCL/PVA2 group, multiple adhesions of the anastomosed intestine, material is visible under a layer of peritoneum and peritoneal adhesions.*

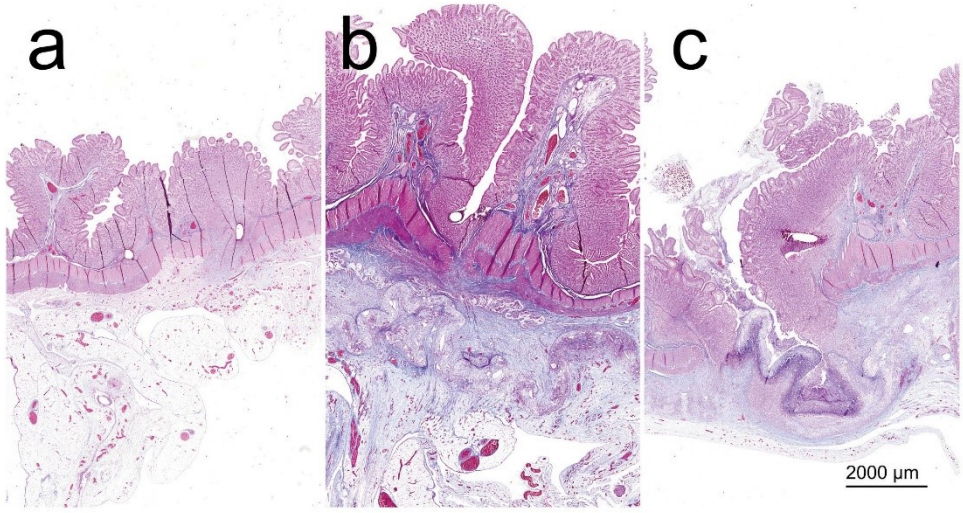

Figure 4. *Specimens in blue–trichrome-stained comprehensive histological slides. A) example from the Control group; B) example from the PCL/PVA1 group; C) example from the PCL/PVA2 group.*

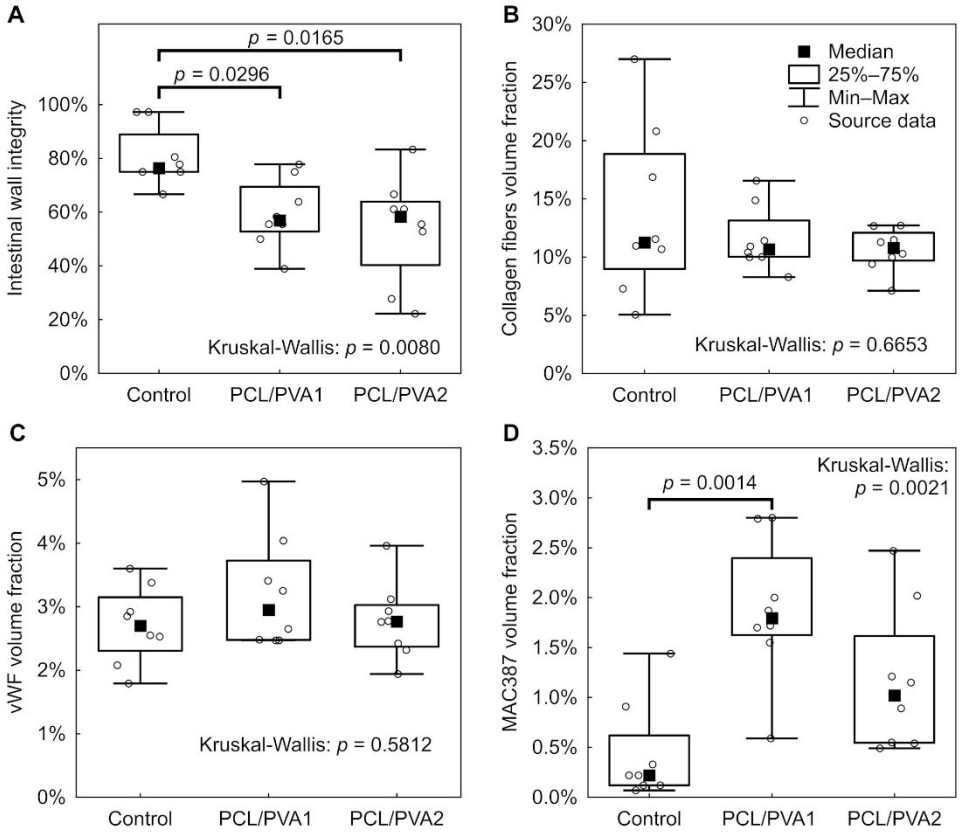

Figure 5. *Results of histological evaluation in box plot graphs. A) Anastomosis deficiency score; B) comparison of collagen fibers volume fractions; C) comparison of vWF positive cells volume fractions; D) comparison of MAC387 positive cells volume fractions.*

anastomosis in 6 animals from the Control group, yet in no animal from the PCL/PVA1 group and in only one of the animals from the PCL/PVA2 group (Figure 4).

Anastomoses in the experimental groups showed significantly lower intestinal wall integrity according to our histologic evaluation system (Figure 5A).

The volume fraction of inflammatory cells (granulocytes, macrophages) in the tissue surrounding the anastomoses was highest in the PCL/PVA1 group, being significantly higher than in the Control group (p=0.0097) (Figure 5D). The volume fraction of inflammatory cells in the PCL/PVA2 group did not differ significantly from either the Control group or the PCL/PVA1 group (Figure 5D). Volume fractions of both endothelial cells (p=0.7063) and collagen fibers (p=0.6094) in the area of the anastomoses showed no significant differences between the groups (Figure 5B and C).

The applied nanomaterial was dissolved during the histological staining; however, the place of its application was visible in the histological slides. The two layers of PCL/PVA1 got separated during the follow-up period in all of the specimens (Figure 6).

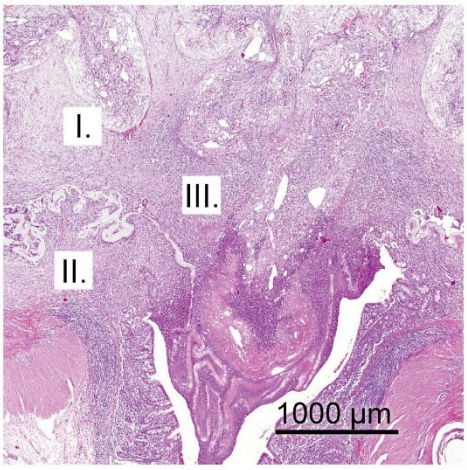

Figure 6. *Washed out material imprint. A PCL/PVA1 specimen in blue trichrome staining, the two separated layers of the material are clearly visible.*

Discussion

The experiment successfully and thoroughly investigated basic features of the PCL/PVA1 and PCL/PVA2 microfibrous double-layered materials in relation to healing of a technically defective anastomosis on the small intestine of a pig. We adjusted the model of defective anastomosis designed by Testiti *et al.* (30), where anastomotic leakage was reached by creating a 2.5 cm large defect. We, however, created rather smaller defects, which we consider to be more clinically relevant.

Polyvinyl alcohol and polycaprolactone are well-explored polymers known for their biocompatibility and biodegradability. They are routinely used as biodegradable surgical materials with no known adverse effects (31, 32). Both presented materials were easy to use and their application did not require any further fixation, which is a valuable aspect not achieved by many other supporting materials (33, 34).

There were no major complications and the animals from the experimental groups showed better postoperative weight gain. According to these observations, we conclude that the materials had no adverse effects on the clinical condition of the animals. It is hard to determine to what extent the rash in the one animal from the PCL/PVA2 group was associated with the application of the material (35, 36).

It remains unclear whether the materials influence the risk of AL. The material remained at the application site covering the defect in all cases, however, it is questionable whether it could keep the intestinal mass contained underneath and thus prevent the manifestation of AL. A model of defective anastomosis on the large intestine would possibly bring more distinct results (34), however, we intended to test the material first in a model without bacterial contamination for easier assessment of the results. The number of bacteria in the small intestine is minimal compared to the large intestine (37, 38).

We consider both materials pro-adhesive according to the obvious macroscopic findings and our scoring system (PAAS). We did not observe any clinical impact of the formed peritoneal adhesions. However, the manifestation of clinical problems due to PAs is not time-limited to the postoperative period, the 3-week observation is insufficient for definite conclusions. A possible combination with other anti-adhesives is an option worthy of further exploration as the data regarding the safety of their use in gastrointestinal surgery is limited (23). In our study, the material of the outer layer was chosen for its hydrophobicity, which we considered a key factor for adhesion prevention as it has been presumed that the formation of peritoneal adhesions is determined by the level of contact of the two adhering surfaces (39). The materials developed by our team were tested for hydrophobicity prior to this study, and the PVA nanomaterials were shown to be hydrophobic (28), yet the two materials proved pro-adhesive when tested in our experiment.

We created and used a new system for the evaluation of intestinal wall integrity at the site of anastomosis on the gastrointestinal tract. It evaluates the integrity of each layer separately, thus making the evaluation of anastomotic healing more precise. In combination with stereological quantitative techniques such as PAAS and Zühlke's grading, it forms probably the most complex evaluation system for anastomotic healing compared to the literature (40-43).

According to our intestinal wall integrity evaluation, the histological assessment suggests inferior healing quality when the material is applied. The PCL/PVA1 group showed higher inflammatory reaction, yet other parameters did not differ significantly from the Control group. The higher inflammatory infiltration could, however, suggest an ongoing healing process. Inflammation is a driving mechanism for cellular proliferation of peritoneal fibroblasts, smooth muscle cells and also intestinal epithelium (44-46). Results of the PCL/PVA2 group were not statistically different from those of the Control group in any of the three monitored aspects. No abnormal vascularization, no abnormal collagen production or inflammation were observed as a reaction to the presence of the material, which is considered normal anastomotic healing (18). Even though the integrity of the intestinal wall was significantly lower in the experimental groups, connective tissue surrounding the material residues was visible in all of the specimens, covering the place of defect. It is possible that in this way the material kept the luminal contents from leaking into the peritoneal cavity.

It is not possible in our settings to distinguish the direction of the healing process. Complete healing ad integrum or manifestation of AL seem both real possibilities for future development in the experimental groups. The same holds for possible occurrence of anastomotic strictures. Sounder results could be acquired in a longer observation period (47, 48). This is a certain limitation of the study.

We decided not to perform mechanical tests to investigate bursting pressure or similar parameters as there is no evidence for the relation between the results of these and the risk of AL (49). Such tests can also compromise the quality of the samples for later histologic evaluation. Biodegradability tests were not employed in our study as this parameter was already studied for PCL and PVA (50, 51).

Both materials exhibited mixed results in the study. The healing quality seems to be compromised when compared to the previous study with polycaprolactone nanofibrous material (27). It is a question whether the change of the characteristics of the material or the change of experimental settings (or possibly a combination of both) can be blamed. The materials need to be studied further after specific adjustments of their properties in new experimental settings in order to fully determine their clinical potential, probably with even more hydrophobic materials.

Conclusion

We were the first to propose a double layered nanomaterial for prevention of both anastomotic leakage and peritoneal adhesions. Both materials tested in our study did not have negative effects on clinical results in the postoperative period. No major complications appeared. Macroscopic findings suggest that both materials are pro-adhesive. Histological assessments of the specimens confirmed no microscopic signs of anastomotic leakage. The specimens from the control group were more completely healed according to our intestinal wall integrity score. However, the material always remained covering the defect and no anastomotic leakage developed. We intend to further investigate the possibility of using nano- and microfibrous materials to determine their clinical impact.

Conflicts of Interest

The Authors certify that they have no affiliations with or involvement in any organization or entity with any financial interest, or non-financial interest in the subject matter or materials discussed in this manuscript.

Authors' Contributions

Conceptualization: J. R., V. L., M. K.; methodology: J. R., J. H., P. H., O. B., Z. T., A. K., L. B., V. T., R. P.; supervision: V. L., V. T., D. L., writing original draft: J. R., M. K., original draft review and editing: V. M., formal analysis: P. H.

Acknowledgements

The research was funded by the project Czech health research council project AZV NU20J-08-00009 Prevention of intestinal anastomotic leakage and postoperative adhesions by using nanofibrous biodegradable materials, and by Charles University Grant Agency project number 1612319: Double-layer nanomaterials as a solution for gastrointestinal anastomoses leakage in a piglet experimental model.

References

1 Qu H, Liu Y and Bi DS: Clinical risk factors for anastomotic leakage after laparoscopic anterior resection for rectal cancer: a systematic review and meta-analysis. Surg Endosc *29(12)*: 3608-3617, 2015. PMID: 25743996. DOI: 10.1007/s00464-015-4117-x

2 Meyer J, Naiken S, Christou N, Liot E, Toso CH, Buchs NCH and Ris F: Reducing anastomotic leak in colorectal surgery: The old dogmas and the new challenges. World J Gastroenterol *25(34)*: 5017-5025, 2019. PMID: 25743996. DOI: 10.3748/wjg.v25.i34.5017

3 Sciuto A, Merola G, De Palma GD, Sodo M, Pirozzi F, Bracale UM and Bracale U: Predictive factors for anastomotic leakage after laparoscopic colorectal surgery. World J Gastroenterol *24(21)*: 2247-2260, 2018. PMID: 29881234. DOI: 10.3748/wjg.v24.i21.2247

4 Bouassida M, Charrada H, Chtourou MF, Hamzaoui L, Mighri MM, Sassi S, Azzouz MM and Touinsi H: Surgery for colorectal cancer in elderly patients: How could we improve early outcomes? J Clin Diagn Res *9(5)*: PC04-8, 2015. PMID: 26155516. DOI: 10.7860/JCDR/2015/12213.5973

5 Paun BC, Cassie S, MacLean AR, Dixon E and Buie WD: Postoperative complications following surgery for rectal cancer. Ann Surg *251*: 807-818, 2010. PMID: 20395841. DOI: 10.1097/SLA.0b013e3181dae4ed

6 2015 European Society of Coloproctology collaborating group: The relationship between method of anastomosis and anastomotic failure after right hemicolectomy and ileo-caecal resection: An international snapshot audit. Colorectal Dis *19(8)*: e296-e311, 2017. PMID: 28263043. DOI: 10.1111/codi.13646

7 Krarup PM, Jorgensen LN, Andreasen AH, Harling H and Danish Colorectal Cancer Group: A nationwide study on anastomotic leakage after colonic cancer surgery. Colorectal Dis *14*: e661-e667, 2012. PMID: 22564292. DOI: 10.1111/j.1463-1318.2012.03079.x

8 Yun JA, Cho YB, Park YA, Huh JW, Yun SH, Kim HC and Lee WY: Clinical manifestations and risk factors of anastomotic leakage after low anterior resection for rectal cancer. ANZ J Surg *87(11)*: 908-914, 2017. PMID: 25925005. DOI: 10.1111/ans.13143

9 Platell C, Barwood N, Dorfmann G and Makin G: The incidence of anastomotic leaks in patients undergoing colorectal surgery. Colorectal Dis *9(1)*: 71, 2007. PMID: 17181849. DOI: 10.1111/j.1463-1318.2006.01002.x

10 Kingham TP and Pachter HL: Colonic anastomotic leak: risk factors, diagnosis, and treatment. J Am Coll Surg *208(2)*: 269, 2009. PMID: 19228539. DOI: 10.1016/j.jamcollsurg.2008.10.015

11 Bruce J, Krukowski ZH, Al-Khairy G, Russell EM and Park KG: Systematic review of the definition and measurement of anastomotic leak after gastrointestinal surgery. Br J Surg *88*: 1157-1168, 2001. PMID: 11531861. DOI: 10.1046/j.0007-1323.2001.01829.x

12 Rahbari NN, Weitz J, Hohenberger W, Heald RJ, Moran B, Ulrich A, Holm T, Wong WD, Tiret E, Moriya Y, Laurberg S, den Dulk M, van de Velde C and Büchler MW: Definition and grading of anastomotic leakage following anterior resection of the rectum: a proposal by the International Study Group of Rectal Cancer. Surgery *147(3)*: 339-351, 2010. PMID: 20004450. DOI: 10.1016/j.surg.2009.10.012

13 Vallance A, Wexner S, Berho M, Cahill R, Coleman M, Haboubi N, Heald RJ, Kennedy RH, Moran B, Mortensen N, Motson RW, Novell R, O'Connell PR, Ris F, Rockall T, Senapati A, Windsor A and Jayne DG: A collaborative review of the current concepts and challenges of anastomotic leaks in colorectal surgery. Colorectal Dis *19*: O1-O12, 2017. PMID: 27671222. DOI: 10.1111/codi.13534

14 Ashraf SQ, Burns EM, Jani A, Altman S, Young JD, Cunningham C, Faiz O and Mortensen NJ: The economic impact of anastomotic leakage after anterior resections in English NHS hospitals: Are we adequately remunerating them? Colorectal Dis *15*: e190-e198, 2013. PMID: 23331871. DOI: 10.1111/codi.12125

15 Wang S, Liu J, Wang S, Zhao H, Ge S and Wang W: Adverse effects of anastomotic leakage on local recurrence and survival after curative anterior resection for rectal Cancer: A systematic review and meta-analysis. World J Surg *41*: 277-284, 2017. PMID: 27743072. DOI: 10.1007/s00268-016-3761-1

16 Ha GW, Kim JH and Lee MR: Oncologic impact of anastomotic leakage following colorectal cancer surgery: a systematic review and meta-analysis. Ann Surg Oncol *24*: 3289-3299, 2017. PMID: 28608118. DOI: 10.1245/s10434-017-5881-8

17 Smith JD, Paty PB, Guillem JG, Temple LK, Weiser MR and Nash GM: Anastomotic leak is not associated with oncologic outcome in patients undergoing low anterior resection for rectal cancer. Ann Surg *256*: 1034-1038, 2012. PMID: 22584695. DOI: 10.1097/SLA.0b013e318257d2c1

18 Williams DL and Browder IW: Murine models of intestinal anastomoses. *In*: Wound healing: Methods and protocols, 1st edition. DiPietro LA, Burns AL (eds.), New Jersey: Humana Press Inc. pp. 133-140, 2010.

19 Marinello FG, Baguena G, Lucas E, Frasson M, Hervás D, Flor-Lorente B, Esclapez P, Espí A and García-Granero E: Anastomotic leakage after colon cancer resection: does the individual surgeon matter? Colorectal Dis *18*: 562-569, 2016. PMID: 26558741. DOI: 10.1111/codi.13212

20 García-Granero E, Navarro F, Cerdán Santacruz C, Frasson M, García-Granero A, Marinello F, Flor-Lorente B and Espí A: Individual surgeon is an independent risk factor for leak after double-stapled colorectal anastomosis: An institutional analysis of 800 patients. Surgery *162*: 1006-1016, 2017. PMID: 28739093. DOI: 10.1016/j.surg.2017.05.023

21 Nikolian VC, Kamdar NS, Regenbogen SE, Morris AM, Byrn JC, Suwanabol PA and Campbell DA Jr: Anastomotic leak after colorectal resection: A population-based study of risk factors and hospital variation. Surgery *161*: 1619-1627, 2017. PMID: 28238345. DOI: 10.1016/j.surg.2016.12.033

22 van Goor H: Consequences and complications of peritoneal adhesions. Colorectal Dis *9*: 25-34, 2007. PMID: 17824967. DOI: 10.1111/j.1463-1318.2007.01358.x

23 Ouaïssi M, Gaujoux S, Veyrie N, Denève E, Brigand C, Castel B, Duron JJ, Rault A, Slim K and Nocca D: Post-operative adhesions after digestive surgery: their incidence and prevention: review of the literature. J Visc Surg *149(2)*: e104-14, 2012. PMID: 22261580. DOI: 10.1016/j.jviscsurg.2011.11.006

24 Yauw ST, Wever KE, Hoesseini A, Ritskes-Hoitinga M and van Goor H: Systematic review of experimental studies on intestinal anastomosis. Br J Surg *102(7)*: 726-734, 2015. PMID: 25846745. DOI: 10.1002/bjs.9776

25 Hunt SL and Silviera ML: Anastomotic construction. *In*: The ASCRS Textbook of Colon and Rectal Surgery, 3rd edition. Steele SR, Hull TL, Hyman N, Maykel JA, Read ThE, Whitlow CB (eds.), New York: Springer, pp. 141-160, 2016.

26 Gholipour-Kanani A, Bahrami SH, Joghataie MT, Samadikuchaksaraei A, Ahmadi-Taftie H, Rabbani S, Kororian A and Erfani E: Tissue engineered poly(caprolactone)-chitosan-poly(vinyl alcohol) nanofibrous scaffolds for burn and cutting wound healing. IET Nanobiotechnol *8(2)*: 123-131, 2014. PMID: 25014084. DOI: 10.1049/iet-nbt.2012.0050

27 Rosendorf J., Horakov J., Klicova M., Palek R., Cervenkova L, Kural T, Hosek P, Kriz T, Tegl V, Moulisova V, Tonar Z, Treska V, Lukas D and Liska V: Experimental fortification of intestinal anastomoses with nanofibrous materials in a large animal model. Sci Rep *10*: 1134, 2020. PMID: 31980716. DOI: 10.1038/s41598-020-58113-4

28 Siegel S and Castellan Jr. NJ: Nonparametric Statistics for the Behavioral Sciences. McGraw-Hill, New York. pp. 213-215, 1988. DOI: 10.1177/014662168901300212

29 StatSoft Europe. Available at: https://www.statsoft.de/en/home [Last accessed on January 21 2021]

30 Testini M, Gurrado A, Portincasa P, Scacco S, Marzullo A, Piccinni G, Lissidini G, Greco L, De Salvia MA, Bonfrate L, Debellis L, Sardaro N, Staffieri F, Carratù MR and Crovace A: Bovine pericardium patch wrapping intestinal anastomosis improves healing process and prevents leakage in a pig model. PLoS One *9(1)*: e86627, 2014. PMID: 24489752. DOI: 10.1371/journal.pone.0086627

31 Baker MI, Walsh SP, Schwartz Z and Boyan BD: A review of polyvinyl alcohol and its uses in cartilage and orthopedic applications. J Biomed Mater Res B Appl Biomater *100(5)*: 1451-1457, 2012. PMID: 22514196. DOI: 10.1002/jbm.b.32694

32 Cai EZ, Teo EY, Jing L, Koh YP, Qian TS, Wen F, Lee JW, Hing EC, Yap YL, Lee H, Lee CN, Teoh SH, Lim J and Lim TC: Bio-conjugated polycaprolactone membranes: a novel wound dressing. Arch Plast Surg *41(6)*: 638-646, 2014. DOI: 10.5999/aps.2014.41.6.638

33 Kwon TR, Han SW, Yeo IK, Kim JH, Kim JM, Hong JY, Lee BC, Lee SE, Moon HS, Kwon HJ and Kim BJ: Biostimulatory effects of polydioxanone, poly-d, l lactic acid, and polycaprolactone fillers in mouse model. J Cosmet Dermatol *18(4)*: 1002-1008, 2019. PMID: 30985064. DOI: 10.1111/jocd.12950

34 García-Vásquez C, Fernández-Aceñero MJ, García Gómez-Heras S and Pastor C: Fibrin patch influences the expression of hypoxia-inducible factor-1α and nuclear factor-κBp65 factors on ischemic intestinal anastomosis. Exp Biol Med (Maywood) *243(10)*: 803-808, 2018. PMID: 29932372. DOI: 10.1177/1535370218777216

35 McLoughlin CE, Smith MJ, Auttachoat W, Bowlin GL and White KL Jr: Evaluation of innate, humoral and cell-mediated immunity in mice following *in vivo* implantation of electrospun polycaprolactone. Biomed Mater *7(3)*: 035015, 2017. PMID: 22539041. DOI: 10.1088/1748-6041/7/3/035015

36 Yao NZ, Huang C and Jin DD: Evaluation of biocompatibility of a pectin/polyvinyl alcohol composite hydrogel as a new nucleus material. Orthop Surg *1(3)*: 231-237, 2009. PMID: 22009848. DOI: 10.1111/j.1757-7861.2009.00036.x

37 Mancabelli L, Milani C, Lugli GA, Turroni F, Ferrario C, van Sinderen D and Ventura M: Meta-analysis of the human gut microbiome from urbanized and pre-agricultural populations. Environ Microbiol *19(4)*: 1379-1390, 2017. PMID: 28198087. DOI: 10.1111/1462-2920.13692

38 Duvallet C, Gibbons SM, Gurry T, Irizarry RA and Alm EJ: Meta-analysis of gut microbiome studies identifies disease-specific and shared responses. Nat Commun *8(1)*: 1784, 2017. PMID: 29209090. DOI: 10.1038/s41467-017-01973-8

39 Chen Y and Hills BA: Surgical adhesions: evidence for adsorption of surfactant to peritoneal mesothelium. Aust N Z J Surg *70(6)*: 443-447, 2000. PMID: 10843402. DOI: 10.1046/j.1440-1622.2000.01841.x

40 Fletcher NM, Awonuga AO, Abusamaan MS, Saed MG, Diamond MP and Saed GM: Adhesion phenotype manifests an altered metabolic profile favoring glycolysis. Fertil Steril *105(6)*: 1628-1637.e1, 2016. PMID: 26947752. DOI: 10.1016/j.fertnstert.2016.02.009

41 Fortin CN, Saed GM and Diamond MP: Predisposing factors to post-operative adhesion development. Hum Reprod Update *21(4)*: 536-551, 2015. PMID: 25935859. DOI: 10.1093/humupd/dmv021

42 Lovisa S, Genovese G and Danese S: Role of Epithelial-to-Mesenchymal Transition in Inflammatory Bowel Disease. J Crohns Colitis *13(5)*: 659-668, 2019. PMID: 30520951. DOI: 10.1093/ecco-jcc/jjy201

43 Boersema GSA, Vennix S, Wu Z, Te Lintel Hekkert M, Duncker DGM, Lam KH, Menon AG, Kleinrensink GJ and Lange JF: Reinforcement of the colon anastomosis with cyanoacrylate glue: a porcine model. J Surg Res *217*: 84-91, 2017. PMID: 28595813. DOI: 10.1016/j.jss.2017.05.001

44 Naito M, Sato T, Nakamura T, Yamanashi T, Miura H, Tsutsui A, Yamashita K and Watanabe M: Secure overlap stapling using a linear stapler with bioabsorbable polyglycolic acid felt. Asian J Endosc Surg *10(3)*: 308-312, 2017. PMID: 28224709. DOI: 10.1111/ases.12364

45 Ikeda T, Kumashiro R, Oki E, Taketani K, Ando K, Aishima S, Akahoshi T and Morita M, Maehara Y: Evaluation of techniques to prevent colorectal anastomotic leakage. World J Gastrointest Surg *7(12)*: 378-383, 2015. PMID: 26730283. DOI: 10.4240/wjgs.v7.i12.378

46 Nordentoft T: Sealing of gastrointestinal anastomoses with fibrin glue coated collagen patch. Dan Med J *62(5)*: B5081, 2015. PMID: 26050838.

47 Hyman N, Manchester TL, Osler T, Burns B and Cataldo PA: Anastomotic leaks after intestinal anastomosis: it's later than you think. Ann Surg *245(2)*: 254, 2007. PMID: 17245179. DOI: 10.1097/01.sla.0000225083.27182.85

48 Strik C, Stommel MW, Schipper LJ, van Goor H and Ten Broek RP: Long-term impact of adhesions on bowel obstruction. Surgery *159(5)*: 1351-1359, 2016. PMID: 26767310. DOI: 10.1016/j.surg.2015.11.016

49 Vakalopoulos KA, Wu Z, Kroese L, Kleinrensink GJ, Jeekel J, Vendamme R, Dodou D and Lange JF: Mechanical strength and rheological properties of tissue adhesives with regard to colorectal anastomosis: an ex vivo study. Ann Surg *261(2)*: 323-331, 2015. PMID: 24670843. DOI: 10.1097/SLA.0000000000000599

50 Horakova J, Mikes P, Saman A, Jencova V, Klapstova A, Svarcova T, Ackermann M, Novotny V, Suchy T and Lukas D: The effect of ethylene oxide sterilization on electrospun vascular grafts made from biodegradable polyesters. Mater Sci Eng C Mater Biol Appl *92*: 132-142, 2018. PMID: 30184736. DOI: 10.1016/j.msec.2018.06.041

51 Klicova M, Klapstova A, Chvojka J, Koprivova B, Jencova V and Horakova J. Novel double-layered planar scaffold combining electrospun PCL fibers and PVA hydrogels with high shape integrity and water stability. Mater Lett 263, 2020. DOI: 10.1016/j.matlet.2019.127281

Received December 24, 2020
Revised January 17, 2021
Accepted January 21, 2021

Attachment 13: Article C

Rosendorf J, Klicova M, Cervenkova L, Horakova J, Klapstova A, Hosek P, Palek R, Sevcik J, Polak R, Treska V, Chvojka J, Liska V. Reinforcement of Colonic Anastomosis with Improved Ultrafine Nanofibrous Patch: Experiment on Pig. Biomedicines. 2021 Jan 21;9(2):102.

Q1, IF=4.757

biomedicines

MDPI

Article

Reinforcement of Colonic Anastomosis with Improved Ultrafine Nanofibrous Patch: Experiment on Pig

Jachym Rosendorf [1,2,*], Marketa Klicova [3], Lenka Cervenkova [1], Jana Horakova [3], Andrea Klapstova [3], Petr Hosek [1], Richard Palek [1,2], Jan Sevcik [1], Robert Polak [1,2], Vladislav Treska [2], Jiri Chvojka [3] and Vaclav Liska [1,2,*]

[1] Biomedical Center, Faculty of Medicine in Pilsen, Charles University, 301 00 Pilsen, Czech Republic; lenka.cervenkova@lfp.cuni.cz (L.C.); petr.hosek@lfp.cuni.cz (P.H.); palekr@fnplzen.cz (R.P.); sevcik.jan97@seznam.cz (J.S.); polakr@fnplzen.cz (R.P.)

[2] Department of Surgery, Faculty of Medicine in Pilsen, Charles University, 301 00 Pilsen, Czech Republic; treska@fnplzen.cz

[3] Department of Nonwovens and Nanofibrous Materials, Faculty of Textile Engineering, Technical University of Liberec, 460 01 Liberec, Czech Republic; marketa.klicova@seznam.cz (M.K.); horakova2222@gmail.com (J.H.); a.klapstova@centrum.cz (A.K.); jiri.chvojka@tul.cz (J.C.)

* Correspondence: jachymrosendorf@gmail.com (J.R.); vena.liska@skaut.cz (V.L.)

Abstract: Anastomotic leakage is a dreadful complication in colorectal surgery. It has a negative impact on postoperative mortality, long term life quality and oncological results. Nanofibrous polycaprolactone materials have shown pro-healing properties in various applications before. Our team developed several versions of these for healing support of colorectal anastomoses with promising results in previous years. In this study, we developed highly porous biocompatible polycaprolactone nanofibrous patches. We constructed a defective anastomosis on the large intestine of 16 pigs, covered the anastomoses with the patch in 8 animals (Experimental group) and left the rest uncovered (Control group). After 21 days of observation we evaluated postoperative changes, signs of leakage and other complications. The samples were assessed histologically according to standardized protocols. The material was easy to work with. All animals survived with no major complication. There were no differences in intestinal wall integrity between the groups and there were no signs of anastomotic leakage in any animal. The levels of collagen were significantly higher in the Experimental group, which we consider to be an indirect sign of higher mechanical strength. The material shall be further perfected in the future and possibly combined with active molecules to specifically influence the healing process.

Keywords: colorectal surgery; nanofibrous materials; anastomotic leakage; intestinal anastomosis; anastomotic patch; polycaprolactone; electrospinning; experiment; peritoneal adhesions

Citation: Rosendorf, J.; Klicova, M.; Cervenkova, L.; Horakova, J.; Klapstova, A.; Hosek, P.; Palek, R.; Sevcik, J.; Polak, R.; Treska, V.; et al. Reinforcement of Colonic Anastomosis with Improved Ultrafine Nanofibrous Patch: Experiment on Pig. *Biomedicines* **2021**, *9*, 102. https://doi.org/10.3390/biomedicines9020102

Academic Editor: Valeria Barresi
Received: 31 December 2020
Accepted: 19 January 2021
Published: 21 January 2021

1. Introduction

Anastomotic leakage (AL) is a severe and feared complication in colorectal surgery. There used to be a lack of consensus over the classification of such conditions in the past, making it difficult to compare complication rates after specific types of procedures. Rahbari et al. [1] created a clear classification of the leaks depending on the type of approach to the complication, which is generally accepted by the wider medical community. However, different hospitals have different approaches and what could be treated conservatively in one department (classified as grade A or B [1]), could also end up with an anastomosis resection and a Hartmann procedure in another (classified as grade C [1]). It is therefore very difficult to assess the real incidence of AL, however it is usually reported to be as high as 5 to 19% [2–4]. The majority of colorectal procedures are performed for colorectal cancer and the number of performed procedures is enormous. Therefore, these complications form a great medical problem [5,6].

Many risk factors have been identified and one of the strongest is the position of anastomosis. Especially low anastomoses (within 5 or 6 cm from the anal verge [7,8]) show high risk of AL [9,10]. Other known factors are age, gender, smoking, steroid therapy and more [9–11]. All of the risk conditions are assumed to decrease the patient's healing abilities generally or locally. However, the specific pathophysiological mechanisms are not well described. As postoperative life quality is often terribly compromised after such complications and the complication itself is in many cases (especially grade C) fatal, AL is considered a large socioeconomic burden [12,13].

Peritoneal adhesions (PAs) are a common problem in abdominal surgery. They are formed in various extents after all surgical procedures and also other damage to the peritoneal cavity. Their purpose is protective, however they are in many cases a source of long term postoperative complications such as gastrointestinal obstruction, infertility or abdominal discomfort [14].

Some kind of patch seems to be a promising solution for local prevention of AL (and possibly PAs). Many materials have been tested for these purposes yet none of them are currently accepted in routine clinical practice [15–17]. There also has not been any material developed and tested for prevention of both PAs and AL according to our knowledge and a literature search.

Nanofibrous materials are nonwoven fabrics created by different techniques, usually from polymeric biomaterials. The variety of source materials and range of fabrication protocols offer an enormous spectrum of such fabrics, naturally resulting in novel applications in medical use. Some versions of nanofibrous planar biodegradable materials have been described to have a positive effect on wound healing by several authors [18–20]. It is assumed to be caused, among other factors, by its structural similarities to collagenous extracellular matrix [19]. There are a variety of synthetic biodegradable materials suitable for fabrication of nanofibrous scaffolds such as polycaprolactone (PCL), polylactide, polyglycolide, polydioxanone, polyhydroxybutyrate and others [21]. PCL is among the most used for implantable devices because of its good mechanical and biological properties and for the fact that it is a substance already in use in clinical medicine [22–24].

Electrospinning is one of the most commonly used approaches for scaffold production. The versatility of the process together with easily controlled parameters has led to wide use of electrospun scaffolds in the field of regenerative medicine and tissue engineering [25]. In our study, the planar nanofibrous PCL layers were fabricated via a needleless electrospinning technique called Nanospider^{TM}. The chosen method contrasts with commonly used needle electrospinning by allowing large-scale industrial production, thus supporting further introduction of the material to the market.

Our team developed and tested several versions of these materials [26,27]. A complex histological, clinical and macroscopic evaluation system has been perfected in recent works [26].

The healing process of both a skin wound or an anastomosis on the small or the large intestine is a complicated process that is yet to be fully explored and understood [28]. However, some parts of the process are known and it is certain that this process must remain well balanced for a successful outcome. A healthy peritoneum is a well-perfused metabolically active structure capable of relatively high metabolic exchange with its surroundings including both peritoneal fluid and other viscera and neighboring peritoneal surfaces [29,30]. Based on the results of our previous experiments and on the presumption that a certain level of metabolic exchange between the sutured intestine and the surrounding peritoneal surfaces is needed to maintain the healing process rather than creating a sealed barrier, we decided to create a very fine porous nanofibrous patch. Such a patch should allow this metabolic exchange while maintaining the pro-healing properties of a nanofibrous mesh we proposed in the previous studies [26,27]. The process conditions for fabricating a material with a low surface density were optimized via needleless electrospinning.

According to our knowledge, our study is the first to propose the idea of a porous anastomotic patch for healing support that should not act only as a mechanical barrier, but

support the healing process of the intestinal anastomosis. We intend to develop such a patch into a product that could be routinely used in colorectal surgery for healing support in either all or high risk anastomoses.

In this study we aimed to develop an ultrafine porous polycaprolactone nanofibrous patch, use it in a perfected model of complicated anastomotic healing on the large intestine, and further develop current assessment methods for evaluation of anastomotic healing in experimental settings.

2. Materials and Methods

2.1. Material Preparation (Electrospinning Method)

A mixture of 16% w/w PCL (Mw 45,000 g/mol, Sigma Aldrich, St. Louis, MI, USA) in chloroform/ethanol/acetic acid in ratio 8/1/1 (Penta Chemicals, Prague, Czech Republic) was stirred 24 h until complete dissolution of the PCL granulate. Subsequently, the solution was electrospun using the needleless NanospiderTM 1WS500U electrospinning device (Elmarco, Liberec, Czech Republic) (scheme in Supplementary Figure S1). The environmental parameters such as the relative humidity and temperature were controlled via the climatic system NS AC150 (Elmarco). The nanofibers were collected on a polypropylene spunbond substrate. The process parameters were optimized to produce a nanofibrous layer with low surface density, namely 10 g/m^2 (listed in Appendix A, Table A1).

2.2. Material Characterization

A scanning electron microscope (SEM) VEGA 3 TESCAN (SB Easy Probe, Brno, Czech Republic) was used to obtain the surface morphology of the fabricated nanofibers. Prior to scanning, the samples were sputter coated with 10 nm of gold using QUORUM Q50ES (Quorum technologies, Lewes, UK). The fiber diameters were assessed by the software IMAGE J (NIH Image, Bethesda, MD, USA) by randomly measuring 500 fibers in the scans. The specific weight was calculated by weighing of samples in the dimension 10 $\times$ 10 cm (n = 10).

Sterilization and in vitro biocompatibility tests: Before in vitro testing, the materials were sterilized via low temperature ethylene oxide (Anprolene, Andersen Sterilizers, Haw River, NC, USA) according to the Czech norm CSN EN ISO 11135-1. The materials were tested one week after sterilization to eliminate the effect of ethylene oxide residues in the layers. The PCL scaffolds were seeded with 3T3 mouse fibroblasts (ATCC, Manassas, VA, USA) in a concentration 7 $\times$ 10^3 cells per well. Metabolic activity was evaluated after 3, 7, 14 and 21 days via colorimetric Cell Counting Kit-8 (CCK-8) (Dojindo Laboratories, Rockville, MD, USA). During the CCK-8 assay, the scaffolds were incubated with 10% (v/v) of CCK-8 solution in full DMEM media for 3 h at 37 °C, 5% CO_2. Absorbance was measured at 450 nm (n = 5). The morphology of the cells on the PCL materials was also monitored. Fluorescence imaging was performed with Nikon Eclipse-Ti-E (Nikon Imaging, Prague, Czech Republic) on fixed cells with 2.5% v/v glutaraldehyde (Sigma Aldrich, St. Louis, MI, USA) in PBS by adding DAPI (for cell nuclei visualization) and phalloidin-FITC (for staining actin cytoskeleton) after 3, 7, 14 and 21 days. The MATLAB software (MATLAB Student R2020b, Mathworks, Natick, MA, USA) was used to calculate the number of cells per 1 mm^2 of the scaffold from 10 random fields of view. Dehydrated samples with fixed cells were also scanned via SEM during the same time period to obtain the morphology of the cells.

2.3. Experimental Design

We used 16 Prestice black-pied pigs in two groups; this number was chosen after consultation with a statistician (Supplementary Document S1). The animals were subjected to transection of the descending colon and anastomosis with a standardized defect under general anesthesia (Figure 1).

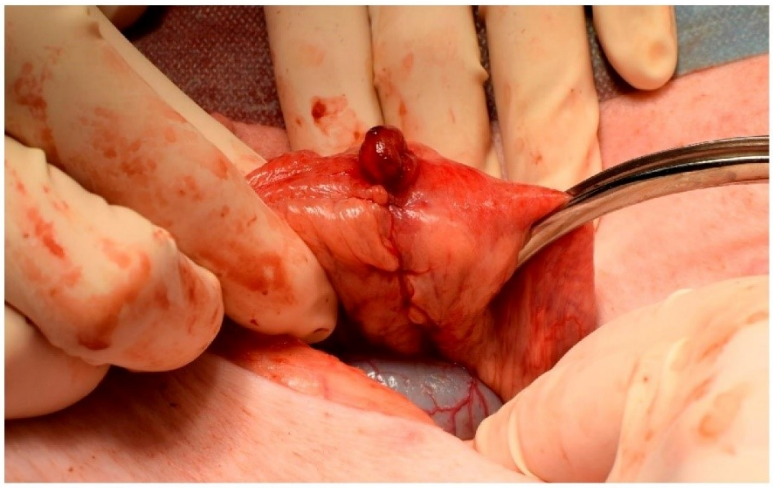

Figure 1. Construction of a defective anastomosis. Intestinal anastomosis with a defect on antimesenteric side pulled through a small incision.

The defect was covered with the nanomaterial in the Experimental group while it was left uncovered in the Control group. The animals were observed for 3 weeks. Sample collection and macroscopic evaluation were performed on the 21st postoperative day (POD). Histological evaluation followed.

2.4. Surgical Procedure

The animals were not fed on the day of the surgery, but no further intestinal preparation was applied. They were premedicated with ketamine (Narkamon 100 mg/mL, BioVeta a.s., Ivanovice na Hané, Czech Republic) and azaperone (Stresnil 40 mg/mL, Elanco AH, Prague, Czech Republic) administered intramuscularly. The animals were weighed prior to the surgical procedure. General anesthesia was maintained by continual application of propofolum MCT/LCT (Propofol 2% MCT/LCT Fresenius Medical Care a.s.). Nalbuphin (Nalbuphin, Torrex Chiesi CZ s.r.o., Prague, Czech Republic) was used for analgesia. A single dose of 0.6 g Amoksiklav (Amoksiklav 1.2 g, Sandoz s.r.o., Prague, Czech Republic) was administered intravenously 30 min before the skin incision, a second 0.6 g dose was administered 2 h later.

A Pro-Port implantable central venous catheter (Deltec, Smiths medical, Minneapolis, MN, USA) was introduced in general anesthesia through the right jugular vein and attached to the subcutaneous tissue on the right lateral side of the neck in each animal for easy and stress-less manipulation with the animal during the follow-up. After the implantation, we entered the abdominal cavity via a 10-cm-long transrectal incision performed in the left caudal abdominal quadrant. We pulled the descending colon up through the incision. We then transected the colon approximately 20 cm from the anus. We used soft intestinal clamps to prevent solid intestinal contents from contaminating the abdominal cavity. We cleaned the two ends of the transected colon using wet cotton balls. We constructed a hand-sewn end-to-end anastomosis using the standard seromuscular running suture using glyconate monofilament 4/0 suture line (Monocryl 4/0, B. Braun Medical s.r.o., Prague, Czech Republic). We intentionally left a 1-cm-large defect on the ventral side of the anastomosis, simulating a technical fault. We placed a standard 2.5-cm-wide sheet of the nanomaterial onto the sutured intestine, covering the intestinal circumference with the defect and the neighboring parts of the mesocolon in the Experimental group. We left the defect uncovered in the Control group. We placed the colon back to the abdominal cavity

and sutured the peritoneum with an absorbable material (Vicryl 3/0, Ethicon Inc., Johnson & Johnson, s.r.o., Prague, Czech Republic) to prevent adhesions to the abdominal wall. Then we closed the muscle layer using single non-absorbable sutures (Mersilene 1, Ethicon Inc., Johnson & Johnson, s.r.o., Prague, Czech Republic). We rinsed the subcutaneous tissue with saline solution before finally suturing the skin.

2.5. Postoperative Observation

The animals were observed for 3 weeks and they were checked daily for stool passage, body temperature and clinical signs of complications by both a surgeon and a veterinarian. Activity of the animals was scored using a 4-point scale (normal activity, decreased activity, little to no activity, irritated animal). Intravenous infusions of 250 mL 10% glucose and 250 mL Hartmann solution were applied daily in the first 3 Postoperative days (PODs). The animals were fed according to a re-alimentation schedule created for previous experiments. When feeding intolerance occurred, intravenous infusions were administered in the same way as in the first three PODs. Blood samples were obtained in defined time points (before the surgical procedure, 2 h after construction of colonic anastomosis, on the 1st POD, 3rd POD, 7th POD, 14th POD, 21st POD) and tested for blood count, level of bilirubin, liver enzymes, hemoglobin, urea and creatinine to distinguish metabolic disorders. Animals were weighed each time the blood sample was taken. A 5% weight difference from the initial weight was considered a significant weight change.

2.6. Macroscopic Evaluation

The animals were subjected to laparotomy again on the 21st POD under general anesthesia. The abdominal cavity was inspected and checked for signs of AL (visible free intestinal contents or purulent secretion, macroscopic changes of peritoneal surfaces), visible defects in the site of anastomosis, changes in the intestinal diameter (stenosis of the anastomosis, dilation of oral segments of the intestine) or any other visible postoperative changes. At same time, the extent and location of PAs (according to qualitative Zühlke's grading and quantitative Peritoneal Adhesions Amount Score (PAAS) (Supplementary Figure S2) [26]), amount and macroscopic quality of peritoneal fluid and the position and appearance of the nanofibrous material (if present) were recorded.

The intestinal specimens including the anastomoses were collected together with surrounding adhering tissues, cut on the mesenteric side longitudinally, pinned onto a cork underlay and stored in 10% buffered formalin.

2.7. Histological Evaluation

The intestinal samples were cut into 5 pieces, 5 mm thick, crosswise to the line of the anastomosis in the area of the anastomotic defect. The tissues were processed by common paraffin technique. Each sample was cut to 5 µm slides and stained with hematoxylin and eosin for comprehensive overview; a Gomori trichrom kit was used to stain connective tissues.

The samples were investigated semi-quantitatively and quantitatively. Epithelization, inflammatory infiltration and necrosis were assessed in a single overall semi-quantitative investigation (Intestinal Wall Integrity Score (Appendix B, Table A2)). The inflammatory reaction to stitches and microabscesses were not included in the score. The score was determined for all five blocks, and the three blocks with the highest score (corresponding to the area of the anastomotic defect) were used for statistical evaluation.

The blocks with the highest total score for each pig were subsequently analyzed quantitatively; 5 µm sections were stained with picrosirius red (Direct red 80) for visualization of collagen in polarized light. Immunohistochemical methods were used for detection of the vascular endothelium using Anti-Von Willebrand Factor antibody (Abcam ab6994, dilution 1:400); Calprotectin Monoclonal Antibody MAC387 (Invitrogen MA1-81381, dilution 1:200) was used for detection of granulocytes and tissue macrophages.

The area for quantitative evaluation for samples without visible defect of the muscular layer was defined as the intestinal wall excluding mucosa located 3 mm orally and aborally from the center of the anastomosis. The evaluation area for samples with a defect of the muscular layer or pseudodiverticulum was defined as 2 mm orally and aborally from the defect margins. The volume of endothelial cells, volume of MAC387 positive cells and volume of collagen was assessed using stereological methods in a similar way as in a previous study [26].

2.8. Statistics

Common descriptive statistics and frequencies were used to characterize the sample data set. Due to their non-normal distribution, the intestinal wall integrity scores and histologically determined volume fractions were compared between the Experimental and Control group using Mann–Whitney U test in STATISTICA data analysis software (Version 12, StatSoft, Inc., Tulsa, OK, USA). The material properties, presented as mean ± standard deviation (SD), were analyzed using GraphPad Prism (Version 7, GraphPad Software, San Diego, CA, USA). Firstly, the Shapiro–Wilk test was used to prove or reject the normal distribution of the data. For the normally distributed data, a parametric ANOVA test with Tukey's multiple comparison was performed. The nonparametric Kruskal–Wallis with Dunn's multiple comparison was chosen for the data following non-normal distribution. All reported p values are two-tailed and the level of statistical significance was set at $\alpha = 0.05$.

3. Results

3.1. Material Properties

Sheets of PCL nanofibrous material were successfully prepared and sterilized. The material appeared very subtle yet the manipulation with it was still comfortable. The material was easy to apply onto the intestinal surface and it remained adhered to the spot of application without any need of further fixation. The morphology of the fibrous material was assessed by SEM (Figure 2A). The fibers had no defects and were without any dominant orientation. The fiber diameter was (385 ± 239) nm (Figure 2B). The high SD is a consequence of ultrafine fibers being present together with larger ones. The specific weight of the material was calculated as (9.67 ± 0.77) g/m^2; the data are symmetrical around the mean value (Figure 2C).

3.2. Cytocompatibility

Adhesion, proliferation and morphology of the 3T3 mouse fibroblasts on the PCL scaffolds were monitored with fluorescence microscope and the scanning electron microscope after 3, 7, 14 and 21 days (Figure 3A). The length of the experiment corresponds with the duration of the in vivo study. Cell viability was determined using a colorimetric assay CCK-8 after 3, 7, 14 and 21 days of incubation of 3T3 mouse fibroblasts with the tested fiber layers. The obtained mean absorbance values express the cell viability of the cultured cells (Figure 3B). According to the CCK-8 assay, the absorbance was low during the first testing day, which is in positive correlation with the microscopy observation. On the seventh day of cultivation, an increase in viability was measured. At the same time, spreading of the cells was observable on the microscopy images, as the cells expanded across the material and began to form isolated cell islands. After 14 days of cultivation, there was a further increase in viability and the cells formed a sub-confluent layer. On the last testing day, the SEM image revealed 100% confluence of the cells. The number of the cells (Figure 3C) correlates with the remaining results. The highest cell density was observed during the 14th day (3887 ± 539) cells/mm^2, while on the last testing day it dropped to (2735 ± 880) cells/mm^2.

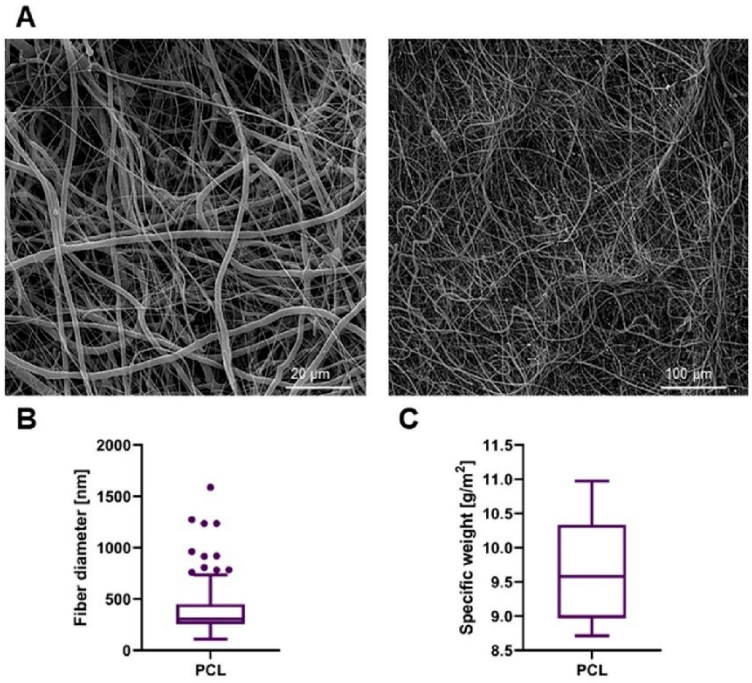

Figure 2. The SEM (scanning electron microscopy) images of the electrospun PCL (polycaprolactone) planar layer, scale bars 20 µm and 50 µm (**A**). The boxplot of fiber diameters (n = 500) (**B**). The calculated value of specific weight of the nanofibrous layer (n = 10) (**C**).

3.3. Manipulation

The material was easy to apply and no further fixation was needed. Procedure times were not prolonged by the usage of the material.

3.4. Clinical Results

All animals survived the observation period in good clinical condition. A temporary activity decrease was observed in one animal from the Control group (12.5%) and in three animals from the Experimental group (37.5%).

There were no major complications during the observation period. Laparotomy wound infection occurred in one animal from the Experimental group (12.5%) and one animal from the Control group (12.5%). Infection of the skin wound of the pro-port system occurred in the same animal from the Control group (12.5%).

No animal developed signs of gastrointestinal obstruction (vomiting, feeding intolerance). No animal developed signs of peritonitis and sepsis (abdominal wall tenderness, significant activity decrease, significant laboratory changes). Peroral intake was tolerated by all animals, all animals were fed according to the schedule with no exceptions. Only three animals from the Control group (37.5%) gained more than 5% of weight during the experiment, while six animals from the Experimental group (75%) showed such weight gain (Appendix C, Table A3).

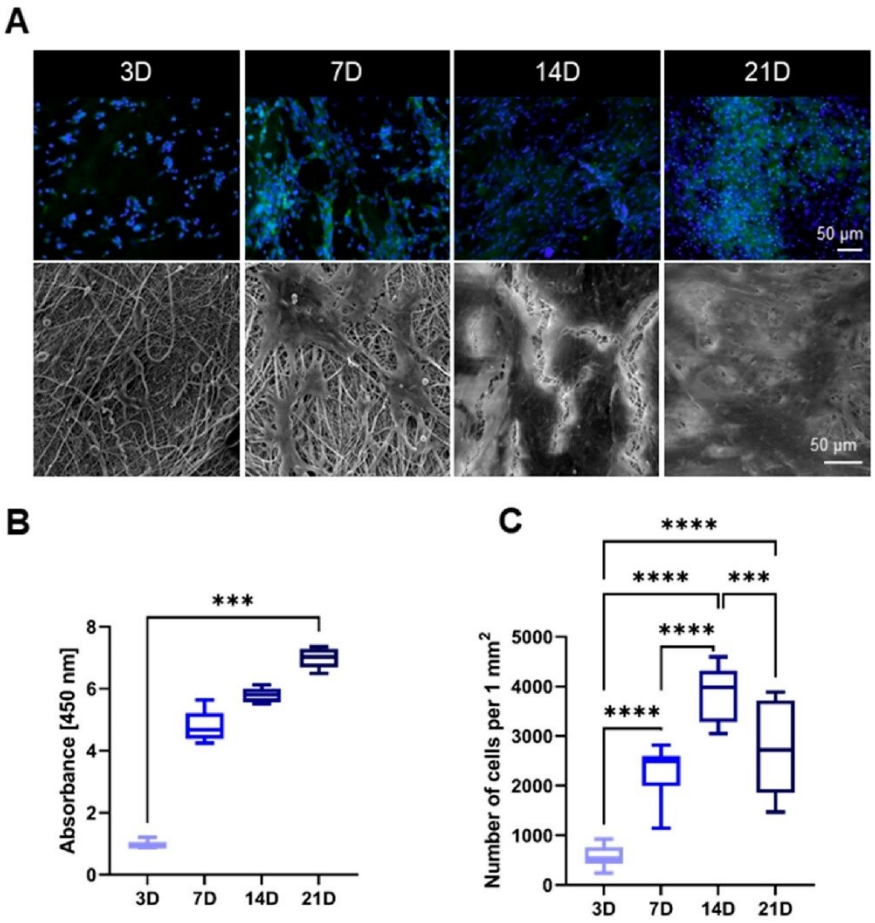

Figure 3. Fluorescence microscopy images (blue cell nuclei and green actin cytoskeleton) and SEM images of the cells on the PCL scaffold after 3, 7, 14 and 21 days of the in vitro testing, scale bars 50 µm (**A**). The result of the colorimetric CCK-8 assay after the same time period, Kruskal–Wallis *** $p = 0.0004$. (**B**). Counted number of the cells on the surface of PCL materials per 1 mm^2, ordinary one-way ANOVA, *** $p < 0.0006$, **** $p = 0.0001$ (**C**).

3.5. Macroscopic Results

There was no macroscopically visible pathological reactions to the material in theabdominal cavities of the animals after 3 weeks of observation. Four animals (50%) had no PAs at the site of the anastomosis in the Control group, while three animals (37.5%) from the Experimental group had no PAs there. A mean PAAS value of 1 was recorded in both the Control and the Experimental group (Tab). All PAs were scored 2 points according to the Zühlke's grading system in both groups (partially vascularized adhesions, possible to separate by combination of blunt and sharp dissection). Stenosis of the anastomosis was observed in one animal from the Control group (12.5%) with low shrinkage of the intestinal diameter (less than 1/3) (Figure 4A). No stenoses were observed in the Experimental group (Figure 4B). No signs of gastrointestinal obstruction (dilatation of oral segments) were ob-

served in any of the animals. No macroscopic signs of AL were observed (no visible defect in the site of the colonic anastomosis, no free intestinal content in the abdominal cavity).

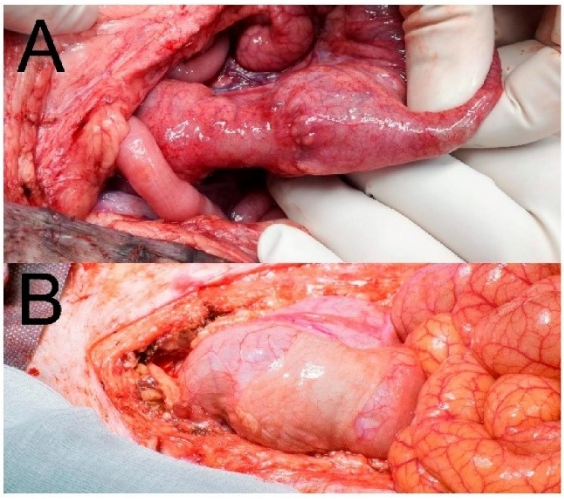

Figure 4. Macroscopic findings in situ at the end of the observation period; (**A**) stenotic anastomosis from the Control group; (**B**) anastomosis with attached material (Experimental group).

Complete dislocation of the material was not observed in any of the animals of the Experimental group. Partial dislocation was observed in three animals (37.5%), however the material always kept covering the location of the anastomotic defect (Figure 5). The defect was not visible in the Control specimens without a patch (Figure 6A). The material was well attached in the most of the specimens (Figure 6B).

Most of the adhesions in the site of the anastomosis were between the large intestine and the urinary bladder. There were no PAs observed in the rest of the abdominal cavity in any animal.

3.6. Blood Sample Results

There were no statistically significant differences in the measured parameters between the two groups and no significant deviations from normal levels of the parameters (see Supplementary Table S1).

3.7. Histological Results

The material was washed out during the histological fixation and staining. There were no microscopic signs of AL (no full-thickness defect was found in any specimen in either the Control or the Experimental group). We found normal morphology of the intestinal wall in all specimens using a comprehensive overview (Figure 7). In some cases, the muscular layer did not heal completely and pseudodiverticula were formed (three cases in the Control group (37.5%) and seven cases (87.5%) in the Experimental group; Figure 8)). There was no statistically significant difference between the groups according to our Intestinal Wall Integrity Score (Figure 9A). There were significantly higher volume fractions of collagen in the Experimental group (Figure 9B). There was no statistically significant difference between the two groups in volume fractions of MAC 387 positive cells (Figure 9D) and endothelial cells (Figure 9C).

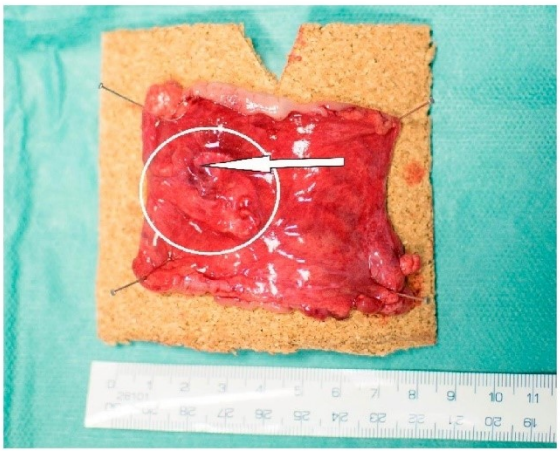

Figure 5. A specimen from the Experimental group prepared for fixation. Partial dislocation of the material (circled), residue of a PA (arrow).

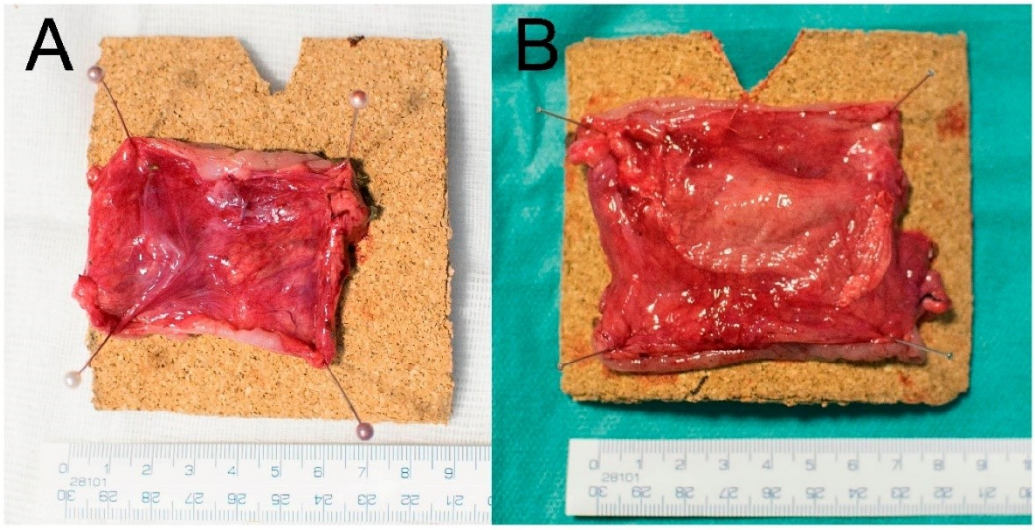

Figure 6. Specimens prepared for fixation. (**A**) A specimen from the Control group; (**B**) a specimen from the Experimental group. The material covers the line of anastomosis well.

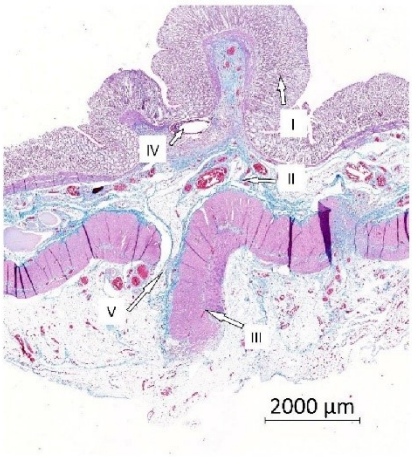

Figure 7. Example histological specimen from the Control group, Gomori trichrome staining. (I) The mucosa; (II) the submucosa; (III) the muscular layer; (IV) a defect after suture material that was washed out during histological processing; (V) location of the anastomosis with normal scar tissue.

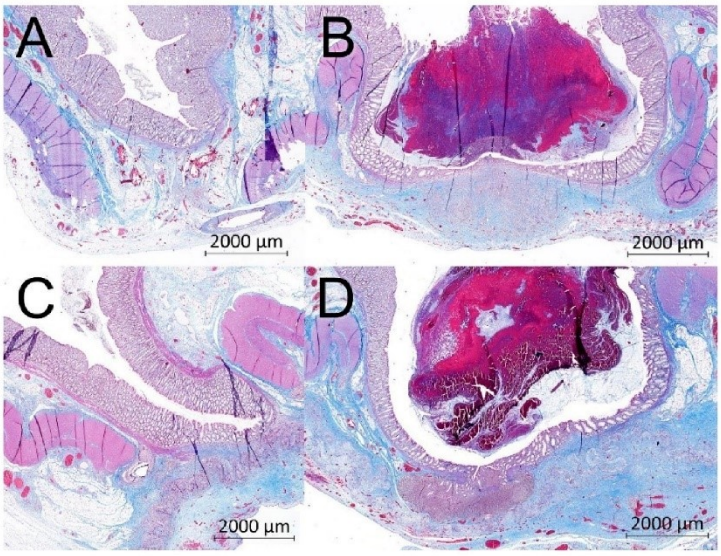

Figure 8. Example histological specimens from both groups. Gomori trichrome (**A**) Control group, optimal healing, normal morphology of the intestinal wall, muscular layer with normal scar tissue; (**B**) Control group, larger defect of the muscular layer, a pseudodiverticulus; (**C**) Experimental group, optimal healing, normal morphology of the intestinal wall, visible residues of the nanofibrous material in the bottom of the image; (**D**) Experimental group, large defect of the muscular layer, a pseudodiverticulus, visible residues of the nanofibrous material in the bottom of the image covering the incomplete defect of the intestinal wall.

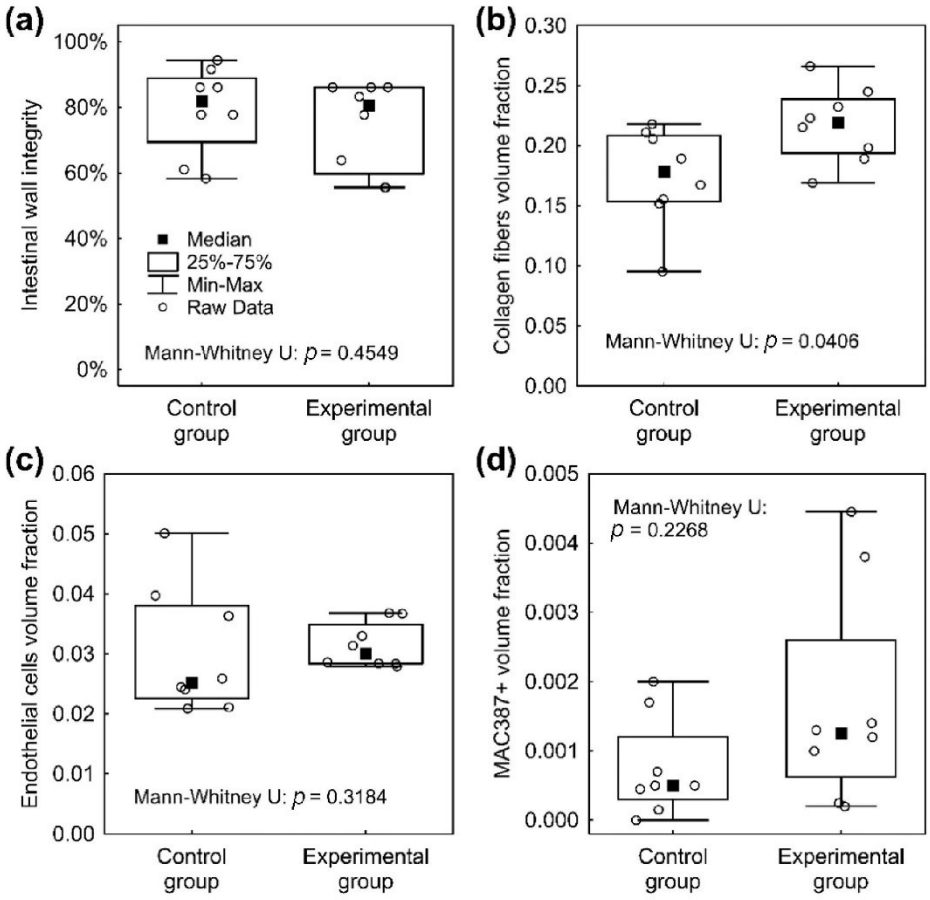

Figure 9. Graphical depiction of main histological results. (**a**) The intestinal wall integrity score in the Control group and the Experimental group with no significant differences with median value above 80%. (**b**) Significantly higher volume fractions of collagen at the site of anastomosis in the Experimental group. (**c**) No significant differences between the two groups in volume fractions of endothelial cells, lower dispersion range of values in the Experimental group. (**d**) The difference in volume fractions of inflammatory cells at the site of anastomosis between the groups is not statistically significant.

4. Discussion

We developed a nanofibrous material based on biodegradable polycaprolactone with very low specific weight. The material was uniquely designed for the reinforcement of GI anastomoses and its design was based on our previous in vitro and in vivo experiments. Polycaprolactone is often used for its biocompatibility and biodegradability [31–33]. The in vitro testing with 3T3 mouse fibroblasts proved the cytocompatibility of the material; the cells formed a fully confluent layer on the surface of the scaffold after 21 days. This observation is consistent with other literature resources, where the combination of micro- and nanofibers in PCL scaffolds supported cell growth [21,22]. Prior to the in vitro testing, the scaffolds were sterilized with low temperature ethylene oxide with respect to the low melting point of PCL. The possible effect of the ethylene oxide sterilization on PCL was

already examined in our previous study by Horakova et al. [27]. The PCL patches are easy to apply and we value this as an important property. While the material is very subtle as its specific weight is only 10 g/m^2, it was still mechanically strong enough to be handled easily. The material always remained in the site of application during the surgical procedure and during reposition of the viscera without further fixation. The convenient application together with natural fixation are key properties should this approach be used in routine clinical practice.

We successfully created a model of anastomosis with a defect on the large intestine of a pig. We used the Testini's [16] modified model from previous experiments [26] in order to move the anastomosis to a location with bacterial contamination and higher risk of healing complications. The defect was chosen to be small enough to simulate a technical fault (which is also one of the contributing factors of AL [34]) and large enough to induce imperfect healing. The position of the anastomosis 20 cm from the anus was chosen for its good accessibility, no need for further preparation, possibility of small abdominal wound and therefore low non-anastomosis related complication risk. The model allowed us to focus only on imperfect anastomotic healing with no other disturbing factors. Together with the assessment methodology, the model allowed a reduction in the number of experimental animals and gave what we consider statistically reliable results. A three-week observation period was chosen based on our previous experience and the possibility of using evaluation histologic systems from previous publications. AL is typically an early complication, usually appearing within the first 10 PODs [2,35]. To verify the behavior of the material in a long term period regarding its complete absorption and impact on the risk of late complications, longer observation times would be necessary.

All of the animals in both groups survived the observation period in good clinical shape with a low complication rate. An activity decrease was observed only in the early postoperative period in both groups, which we considered as normal postoperative state. The feeding tolerance was equally good in both groups. The animals from the Experimental group gained weight in more cases than in the Control group. Weight gain is a sign of good postoperative adaption [36]. No animal developed ileus or sepsis or other serious pathological reaction to the material. This contributes to our assumption that it is safe to use in this application.

We observed slight shifting of the material in a few cases, however the material always remained covering the spot of anastomotic defect. We observed this also in the last study on the small intestine with an earlier version of the material, and therefore we assume it is not a coincidence [26]. This barrier was always present even in specimens with larger defect of muscular layer, and no macroscopic or microscopic AL was observed. It remains a question whether the material is able to prevent manifestation of AL. An anastomotic leakage is in experiments usually obtained by either large anastomotic defects or other negative influences (infection, radiation, devascularization). The model of a small defect was chosen to study the impact of the material on imperfect anastomotic healing in highly standardized conditions.

There was one partial shrinkage of the intestinal diameter at the site of the anastomosis in one animal from the Control group (12.5%), therefore we assume the material does not cause formation of anastomotic strictures. Those can however develop in longer time periods and thus a longer observation time would be needed to verify this information [37].

The level of adhesions was similarly low in both groups, suggesting the current material version to be the first in our series of polycaprolactone electrospun materials without pro-adhesive properties [26]. We consider the generally low amount of adhesions to be also a result of short procedure times with low manipulation with tissues [38]. Excessive formation of PAs is considered to be a result of a healing problem [39]. The visceral peritoneum is the superficial layer of the intestine, so wound healing of the peritoneum is a part of anastomotic wound healing. Therefore, we think, qualitative and quantitative assessment of PAs should be involved in the evaluation of anastomotic healing [26].

There were no statistically significant differences in vascularization and inflammatory cells infiltration according to the stereological measurements. This suggests a normal healing process [40]. However, the levels of collagen were found higher in the Experimental group. It was previously observed in mechanical tests of intestinal anastomoses that higher levels of collagen are associated with higher mechanical strength and higher anastomotic bursting pressure [41]. Bacterial collagenases were identified as a possible contributor to development of AL. Their activity causes collagen degradation in the site of intestinal anastomosis. Intestinal colonization with several bacterial species was identified as a strong risk factor of AL due to their production of collagenases [41–43].

We used both traditional evaluation methods [40] with those that were developed for our purposes in previous papers [26]. The intestinal wall integrity score from the previous study was adjusted for a defective model on the large intestine. Together with the rest of the involved assessment methods, it forms the most robust and complex evaluation system of anastomotic healing in similar experiments according to our knowledge and literature search.

The above-mentioned results all suggest possible contribution to AL prevention by our material only indirectly. To obtain more distinguishable results, a model with more compromised anastomotic healing with high risk of AL manifestation would be necessary. This is certainly a limitation of this study.

Because the material was washed out during the histological processing, we cannot evaluate the level of biodegradation. However, this was studied earlier for PCL in other forms [44].

The material seems to be an ideal version for use in combination with active substances like anti-inflammatory drugs, antibacterial agents or antibiotics as an anastomotic patch. Polycaprolactone was identified as a good medium for regulated drug release [33,45]; there is a broad spectrum of active molecules that could be beneficial for either AL prevention or prevention of excessive PA formation [39,46–49]. Therefore, we intend to perfect the material using these substances and to study their impact on anastomotic healing and complications further to finally offer a perfect anastomotic patch for patients with high risk of AL. Possible clinical studies will be planned afterwards.

5. Conclusions

We succeeded in creating a unique ultrafine polycaprolactone electrospun material and in applying it in a model of complicated anastomotic healing on the pig colon. The planar PCL layer was fabricated via needleless electrospinning technique, a method suitable for eventual large-scale production. The material is easy to use without any need for further fixation. The presence of the material did not cause any adverse effects in vivo. The PCL layer showed good cytocompatibility and biocompatibility and was well tolerated during the whole animal study. The material is also not pro-adhesive and did not cause anastomotic strictures or other complications. The anastomotic specimens showed significantly higher levels of collagen after the 3 weeks of observation, which is an indirect sign of higher mechanical strength. Impact on the risk of AL was not observed directly as no AL appeared in either group. We intend to develop new versions of the material with active agents and study them further in adjusted experimental settings to obtain more distinguishable results before moving to clinical studies on colorectal surgical patients.

Supplementary Materials: The following are available online at https://www.mdpi.com/2227-9059/9/2/102/s1, Figure S1: Nanospider scheme, Figure S2: Perianastomotic adhesions amount scoring system, Table S1: Leukocytosis development, Document S1: power analysis.

Author Contributions: Conceptualization, J.R., V.L., J.H., methodology, M.K., A.K., R.P. (Richard Palek); software, P.H., M.K.; validation, P.H.; formal analysis, L.C.; investigation, L.C., R.P. (Robert Polak); resources, J.H.; data curation P.H.; writing—original draft preparation, J.R., M.K.; writing—review and editing, J.R., P.H.; visualization, J.S.; supervision, V.L., V.T., J.C.; project administration J.H., V.L.; funding acquisition, J.H., V.L. All authors have read and agreed to the published version of the manuscript.

Funding: This research was funded by the project Czech Health Research Council project AZV NU20J-08-00009 Prevention of intestinal anastomotic leakage and postoperative adhesions by using nanofibrous biodegradable materials, and by the Centrum of Clinical and Experimental Liver Surgery project UNCE/MED/006 and from European Regional Development Fund-Project Application of Modern Technologies in Medicine and Industry project CZ.02.1.01/0.0/0.0/17_048/0007280.

Institutional Review Board Statement: Work with animals: All experimental procedures with the use of piglets were certified by the Commission of Work with Experimental Animals at the Medical Faculty of Pilsen (project code: MSMT-26570/2017-2), Charles University, and were under control of the Ministry of Agriculture of the Czech Republic. All procedures were performed in compliance with the law of the Czech Republic, which is compatible with the legislation of the European Union.

Informed Consent Statement: Not applicable.

Data Availability Statement: All data included in the article or supplementary materials.

Conflicts of Interest: The authors declare no conflict of interest. The funders had no role in the design of the study; in the collection, analyses, or interpretation of data; in the writing of the manuscript, or in the decision to publish the results.

Appendix A

Table A1. Process parameters of the needless electrospinning via Nanospider™.

Distance between the electrodes [mm]	175
Voltage Electrode 1 [kV]	−10
Voltage Electrode 2 [kV]	40
Rewinding speed [mm/min]	60
Cartridge movement speed [mm/s]	450–500
Temperature [°C]	22
Relative humidity [%]	50

Appendix B

Table A2. Intestinal Wall Integrity Score.

Layer	Points	Finding
Mucosa	1/4	Completely re-epithelized
	0/4	Incompletely re-epithelized
Submucosa	1/4	Completely healed
	0/4	Purulent infiltration, necrosis
Muscularis *	3/12	No distance (≤0.09 mm)
	2/12	Distance 0.1 to 1.99 mm
	1/12	Distance 2 to 3.99 mm
	0/12	Distance over 4 mm
Serosa	3/12	No purulent infiltration and necrosis
	2/12	Purulent infiltration and/or necrosis from the muscular layer to area of nanomaterial **
	1/12	Purulent infiltration and/or necrosis from the area of nanomaterial to the peritoneum ***
	0/12	Purulent infiltration and/or necrosis passes to the peritoneum

* Distance between the two anastomosed muscle layers. ** 2/12 points for purulent infiltration and/or necrosis from muscular layer to half thickness of the serosa in the Control group. *** 1/12 points for purulent infiltration and/or necrosis from half thickness of the serosa to the peritoneum in the Control group.

Appendix C

Table A3. Weight profile of experimental animals.

Animal	POD 0 Weight (kg)	POD 3 Weight (kg)	POD 7 Weight (kg)	POD 14 Weight (kg)	POD 21 Weight (kg)
Control group					
cg 01	34	31.6	31.4	33.8	33
cg 02	31	30.1	29.4	30.7	30.7
cg 03	37	33.8	33.7	34.5	34.5
cg 04	45.5	41.3	41.1	42	42.1
cg 05	48.4	43.6	42.8	44	43.8
cg 06	30.6	30	30.7	29.5	32.5
cg 07	30	29	29.8	33.6	32.1
cg 08	27.8	25.9	27.2	30.5	30.5
Experimental group					
eg 01	28.7	28.3	29.2	29.4	29.4
eg 02	29.9	29.3	28.2	29	30.3
eg 03	35.8	35.2	35.2	39	37.9
eg 04	37.3	36.8	36	41	41
eg 05	41.7	41.5	41.3	43.4	45.2
eg 06	42.9	42.2	42.2	43.8	45.1
eg 07	27.9	27.4	26.3	29.4	30
eg 08	27.2	26.8	25.8	29.1	29

References

1. Rahbari, N.N.; Weitz, J.; Hohenberger, W.; Heald, R.J.; Moran, B.; Ulrich, A.; Holm, T.; Wong, W.D.; Tiret, E.; Moriya, Y.; et al. Definition and grading of anastomotic leakage following anterior resection of the rectum: A proposal by the International Study Group of Rectal Cancer. *Surgery* **2010**, *147*, 339–351. [CrossRef] [PubMed]
2. Gessler, B.; Eriksson, O.; Angenete, E. Diagnosis, treatment, and consequences of anastomotic leakage in colorectal surgery. *Int. J. Color. Dis.* **2017**, *32*, 549–556. [CrossRef] [PubMed]
3. Vasiliu, E.C.Z.; Zarnescu, N.O.; Costea, R.; Neagu, S. Review of Risk Factors for Anastomotic Leakage in Colorectal Surgery. *Chirurgia (Buchar. Rom. 1990)* **2015**, *110*, 26305194.
4. Iversen, H.; Ahlberg, M.; Lindqvist, M.; Buchli, C. Changes in Clinical Practice Reduce the Rate of Anastomotic Leakage after Colorectal Resections. *World J. Surg.* **2018**, *42*, 2234–2241. [CrossRef] [PubMed]
5. Kasi, P.M.; Shahjehan, F.; Cochuyt, J.J.; Li, Z.; Colibaseanu, D.T.; Merchea, A. Rising Proportion of Young Individuals with Rectal and Colon Cancer. *Clin. Color. Cancer* **2019**, *18*, e87–e95. [CrossRef] [PubMed]
6. Tsai, Y.-Y.; Chen, W.T.-L. Management of anastomotic leakage after rectal surgery: A review article. *J. Gastrointest. Oncol.* **2019**, *10*, 1229–1237. [CrossRef]
7. Fukada, M.; Matsuhashi, N.; Takahashi, T.; Imai, H.; Tanaka, Y.; Yamaguchi, K.; Yoshida, K. Risk and early predictive factors of anastomotic leakage in laparoscopic low anterior resection for rectal cancer. *World J. Surg. Oncol.* **2019**, *17*, 1–10. [CrossRef]
8. Räsänen, M.; Renkonen-Sinisalo, L.; Carpelan-Holmström, M.; Lepistö, A. Low anterior resection combined with a covering stoma in the treatment of rectal cancer reduces the risk of permanent anastomotic failure. *Int. J. Color. Dis.* **2015**, *30*, 1323–1328. [CrossRef]
9. Van Rooijen, S.; Huisman, D.; Stuijvenberg, M.; Stens, J.; Roumen, R.; Daams, F.; Slooter, G. Intraoperative modifiable risk factors of colorectal anastomotic leakage: Why surgeons and anesthesiologists should act together. *Int. J. Surg.* **2016**, *36*, 183–200. [CrossRef]
10. Sciuto, A.; Merola, G.; De Palma, G.D.; Sodo, M.; Pirozzi, F.; Bracale, U. Predictive factors for anastomotic leakage after laparoscopic colorectal surgery. *World J. Gastroenterol.* **2018**, *24*, 2247–2260. [CrossRef]
11. Kawada, K.; Sakai, Y. Preoperative, intraoperative and postoperative risk factors for anastomotic leakage after laparoscopic low anterior resection with double stapling technique anastomosis. *World J. Gastroenterol.* **2016**, *22*, 5718–5727. [CrossRef] [PubMed]

12. La Regina, D.; Di Giuseppe, M.; Lucchelli, M.; Saporito, A.; Boni, L.; Efthymiou, C.; Cafarotti, S.; Marengo, M.; Mongelli, F. Financial Impact of Anastomotic Leakage in Colorectal Surgery. *J. Gastrointest. Surg.* **2018**, *23*, 580–586. [CrossRef] [PubMed]
13. Lee, S.W.; Gregory, D.; Cool, C.L. Clinical and economic burden of colorectal and bariatric anastomotic leaks. *Surg. Endosc.* **2020**, *34*, 1–8. [CrossRef] [PubMed]
14. Ha, G.W.; Lee, M.R.; Kim, J.H. Adhesive small bowel obstruction after laparoscopic and open colorectal surgery: A systematic review and meta-analysis. *Am. J. Surg.* **2016**, *212*, 527–536. [CrossRef]
15. Trotter, J.; Onos, L.; McNaught, C.; Peter, M.; Gatt, M.; Maude, K.; MacFie, J. The use of a novel adhesive tissue patch as an aid to anastomotic healing. *Ann. R. Coll. Surg. Engl.* **2018**, *100*, 230–234. [CrossRef]
16. Testini, M.; Gurrado, A.; Portincasa, P.; Scacco, S.; Marzullo, A.; Piccinni, G.; Lissidini, G.; Greco, L.; De Salvia, M.A.; Bonfrate, L.; et al. Bovine Pericardium Patch Wrapping Intestinal Anastomosis Improves Healing Process and Prevents Leakage in a Pig Model. *PLoS ONE* **2014**, *9*, e86627. [CrossRef]
17. Yaita, A.; Nakamura, T.; Sugimachi, K.; Inokuchi, K. Use of free peritoneal patch in reenforcing alimentary tract anastomosis. *Surg. Today* **1975**, *5*, 56–63. [CrossRef]
18. Zhong, W.; Xing, M.M.; Maibach, H.I. Nanofibrous materials for wound care. *Cutan. Ocul. Toxicol.* **2010**, *29*, 143–152. [CrossRef]
19. Fu, X.; Gao, W.; Fu, X.; Shi, M.; Xie, W.; Zhang, W.; Zhao, F.; Chen, X. Enhanced wound healing in diabetic rats by nanofibrous scaffolds mimicking the basketweave pattern of collagen fibrils in native skin. *Biomater. Sci.* **2018**, *6*, 340–349. [CrossRef]
20. Adeli, H.; Khorasani, M.T.; Parvazinia, M. Wound dressing based on electrospun PVA/chitosan/starch nanofibrous mats: Fabrication, antibacterial and cytocompatibility evaluation and in vitro healing assay. *Int. J. Biol. Macromol.* **2019**, *122*, 238–254. [CrossRef]
21. Gunatillake, P.A. Biodegradable synthetic polymers for tissue engineering. *Eur. Cells Mater.* **2003**, *5*, 1–16. [CrossRef] [PubMed]
22. Luo, L.; He, Y.; Chang, Q.; Xie, G.; Zhan, W.; Wang, X.; Zhou, T.; Xing, M.; Lu, F. Polycaprolactone nanofibrous mesh reduces foreign body reaction and induces adipose flap expansion in tissue engineering chamber. *Int. J. Nanomed.* **2016**, *11*, 6471–6483. [CrossRef] [PubMed]
23. Townsend, J.M.; Ott, L.M.; Salash, J.R.; Fung, K.-M.; Easley, J.T.; Seim, H.B.; Johnson, J.K.; Weatherly, R.A.; Detamore, M.S. Reinforced Electrospun Polycaprolactone Nanofibers for Tracheal Repair in an In Vivo Ovine Model. *Tissue Eng. Part A* **2018**, *24*, 1301–1308. [CrossRef] [PubMed]
24. Fuchs, J.; Mueller, M.; Daxböck, C.; Stückler, M.; Lang, I.; Leitinger, G.; Bock, E.; El-Heliebi, A.; Moser, G.; Glasmacher, B.; et al. Histological processing of un-/cellularized thermosensitive electrospun scaffolds. *Histochem. Cell Biol.* **2018**, *151*, 343–356. [CrossRef] [PubMed]
25. Vasita, R.; Katti, D.S. Nanofibers and their applications in tissue engineering. *Int. J. Nanomed.* **2006**, *1*, 15–30. [CrossRef] [PubMed]
26. Rosendorf, J.; Horakova, J.; Klicova, M.; Palek, R.; Cervenkova, L.; Kural, T.; Hošek, P.; Kriz, T.; Tegl, V.; Moulisova, V.; et al. Experimental fortification of intestinal anastomoses with nanofibrous materials in a large animal model. *Sci. Rep.* **2020**, *10*, 1–12. [CrossRef] [PubMed]
27. Horakova, J.; Klicova, M.; Erben, J.; Klapstova, A.; Novotny, V.; Behalek, L.; Chvojka, J. Impact of Various Sterilization and Disinfection Techniques on Electrospun Poly-ε-caprolactone. *ACS Omega* **2020**, *5*, 8885–8892. [CrossRef]
28. Childs, D.R.; Murthy, A.S. Overview of Wound Healing and Management. *Surg. Clin. N. Am.* **2017**, *97*, 189–207. [CrossRef]
29. Mehrotra, R.; Devuyst, O.; Davies, S.J.; Johnson, D.W. The Current State of Peritoneal Dialysis. *J. Am. Soc. Nephrol.* **2016**, *27*, 3238–3252. [CrossRef]
30. Giffin, D.M.; Gow, K.W.; Warriner, C.B.; Walley, K.R.; Phang, P.T. Oxygen uptake during peritoneal ventilation in a porcine model of hypoxemia. *Crit. Care Med.* **1998**, *26*, 1564–1568. [CrossRef]
31. Cai, E.Z.; Teo, E.Y.; Jing, L.; Koh, Y.P.; Qian, T.S.; Wen, F.; Lee, J.W.K.; Hing, E.C.H.; Yap, Y.L.; Lee, H.; et al. Bio-Conjugated Polycaprolactone Membranes: A Novel Wound Dressing. *Arch. Plast. Surg.* **2014**, *41*, 638–646. [CrossRef] [PubMed]
32. Hashemi, H.; Asgari, S.; Shahhoseini, S.; Mahbod, M.; Atyabi, F.; Bakhshandeh, H.; Beheshtnejad, A.H. Application of polycaprolactone nanofibers as patch graft in ophthalmology. *Indian J. Ophthalmol.* **2018**, *66*, 225–228.
33. García-Salinas, S.; Evangelopoulos, M.; Gámez-Herrera, E.; Arruebo, M.; Irusta, S.; Taraballi, F.; Mendoza, G.; Tasciotti, E. Electrospun anti-inflammatory patch loaded with essential oils for wound healing. *Int. J. Pharm.* **2020**, *577*, 119067. [CrossRef] [PubMed]
34. Ricciardi, R.; Roberts, P.L.; Marcello, P.W.; Hall, J.F.; Read, T.E.; Schoetz, D.J. Anastomotic Leak Testing After Colorectal Resection. *Arch. Surg.* **2009**, *144*, 407–411. [CrossRef] [PubMed]
35. Bsc, C.L.S.; Van Groningen, J.T.; Lingsma, H.; Wouters, M.W.; Menon, A.G.; Kleinrensink, G.-J.; Jeekel, J.; Lange, J.F. Different Risk Factors for Early and Late Colorectal Anastomotic Leakage in a Nationwide Audit. *Dis. Colon Rectum* **2018**, *61*, 1258–1266. [CrossRef]
36. Marchant-Forde, J.N.; Herskin, M.S. Pigs as laboratory animals. In *Advances in Pig Welfare*; Elsevier: Amsterdam, The Netherlands, 2018; pp. 445–475.
37. Bertocchi, E.; Barugola, G.; Benini, M.; Bocus, P.; Rossini, R.; Ceccaroni, M.; Ruffo, G. Colorectal Anastomotic Stenosis: Lessons Learned after 1643 Colorectal Resections for Deep Infiltrating Endometriosis. *J. Minim. Invasive Gynecol.* **2019**, *26*, 100–104. [CrossRef]
38. Ergul, E.; Korukluoglu, B. Peritoneal adhesions: Facing the enemy. *Int. J. Surg.* **2008**, *6*, 253–260. [CrossRef]

39. Braun, K.M.; Diamond, M.P. The biology of adhesion formation in the peritoneal cavity. *Semin. Pediatr. Surg.* **2014**, *23*, 336–343. [CrossRef]
40. Williams, D.L.; Browder, I.W. Murine Models of Intestinal Anastomoses. In *Wound Healing: Methods and Protocols*, 1st ed.; Di Pietro, L.A., Burns, A.L., Eds.; Humana Press Inc.: Totowa, NJ, USA, 2010; pp. 133–140.
41. Shogan, B.D.; Belogortseva, N.; Luong, P.M.; Zaborin, A.; Lax, S.; Bethel, C.; Ward, M.; Muldoon, J.P.; Singer, M.; Alexander, Z.; et al. Collagen degradation and MMP9 activation byEnterococcus faecaliscontribute to intestinal anastomotic leak. *Sci. Transl. Med.* **2015**, *7*, 286ra68. [CrossRef]
42. Krarup, P.; Eld, M.; Jorgensen, L.; Hansen, M.B.; Ågren, M.S. Selective matrix metalloproteinase inhibition increases breaking strength and reduces anastomotic leakage in experimentally obstructed colon. *Int. J. Color. Dis.* **2017**, *32*, 1277–1284. [CrossRef] [PubMed]
43. Guyton, K.L.; Levine, Z.C.; Lowry, A.C.; Lambert, L.; Gribovskaja-Rupp, I.; Hyman, N.; Zaborina, O.; Alverdy, J.C. Identification of Collagenolytic Bacteria in Human Samples. *Dis. Colon Rectum* **2019**, *62*, 972–979. [CrossRef]
44. Li, Y.; Xia, X.; Zou, Q.; Ma, J.; Jin, S.; Li, J.; Zuo, Y.; Li, Y. The long-term behaviors and differences in bone reconstruction of three polymer-based scaffolds with different degradability. *J. Mater. Chem. B* **2019**, *7*, 7690–7703. [CrossRef]
45. Ranjbar-Mohammadi, M.; Bahrami, S.H. Electrospun curcumin loaded poly(ε-caprolactone)/gum tragacanth nanofibers for biomedical application. *Int. J. Biol. Macromol.* **2016**, *84*, 448–456. [CrossRef]
46. Wirth, U.; Rogers, S.; Haubensak, K.; Schopf, S.; Von Ahnen, T.; Schardey, H.M. Local antibiotic decontamination to prevent anastomotic leakage short-term outcome in rectal cancer surgery. *Int. J. Color. Dis.* **2017**, *33*, 53–60. [CrossRef]
47. Oh, J.; Kuan, K.G.; Tiong, L.U.; Trochsler, M.; Jay, G.; Schmidt, T.A.; Barnett, H.; Maddern, G.J. Recombinant human lubricin for prevention of postoperative intra-abdominal adhesions in a rat model. *J. Surg. Res.* **2017**, *208*, 20–25. [CrossRef]
48. Hirai, K.; Tabata, Y.; Hasegawa, S.; Sakai, Y. Enhanced intestinal anastomotic healing with gelatin hydrogel incorporating basic fibroblast growth factor. *J. Tissue Eng. Regen. Med.* **2016**, *10*, E433–E442. [CrossRef]
49. Landes, L.C.; Drescher, D.; Tagkalos, E.; Grimminger, P.; Thieme, R.; Jansen-Winkeln, B.; Lang, H.; Gockel, I. Upregulation of VEGFR1 in a rat model of esophagogastric anastomotic healing. *Acta Chir. Belg.* **2017**, *118*, 161–166. [CrossRef]